ABSTRACTS FOR

THE INTERNATIONAL CONFERENCE ON ASTEROIDS, COMETS, METEORS 1991

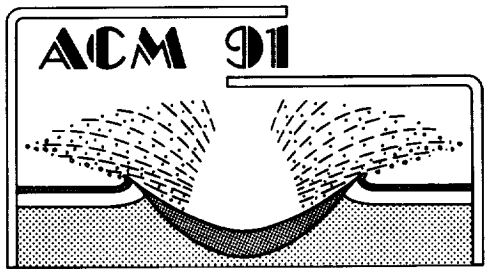

Flagstaff, Arizona

June 24-28, 1991

Sponsored by
Barringer Crater Company
Lunar and Planetary Institute
Lowell Observatory
Meteor Crater Enterprises, Inc.
National Aeronautics and Space Administration (NASA)
Northern Arizona University
U.S. Geological Survey

ABSTRACTS FOR THE INTERNATIONAL CONFERENCE ON ASTEROIDS, COMETS, METEORS 1991

Flagstaff, Arizona

June 24-28, 1991

Sponsored by

Barringer Crater Company

Lunar and Planetary Institute

Lowell Observatory

Meteor Crater Enterprises, Inc.

National Aeronautics and Space Administration (NASA)

Northern Arizona University

U.S. Geological Survey

Compiled in 1991 by

Lunar and Planetary Institute
3303 NASA Road 1
Houston TX 77058-4399

LPI Contribution No. 765

Compiled in 1991 by

Lunar and Planetary Institute
3303 NASA Road 1
Houston TX 77058-4399

The Lunar and Planetary Institute is operated by the Universities Space Research Association under Contract No. NASW-4574 with the National Aeronautics and Space Administration.

PREFACE

This volume contains abstracts that have been accepted for presentation at the International Conference on Asteroids, Comets, Meteors 1991 in Flagstaff, Arizona, June 24-28, 1991. All abstracts accepted as of May 10, 1991 are included in alphabetical order of first authors. No distinctions have been made between invited papers, contributed papers, and poster papers. Late abstracts, if any, will be provided at the time of registration.

Responsible for the program are Michael A'Hearn, University of Maryland; Edward Bowell, Lowell Observatory; Clark Chapman, Planetary Science Institute; Michel Festou, Observatoire Midi-Pyrénées; Alan Harris, Jet Propulsion Laboratory; Pamela Jones, Lunar and Planetary Institute; and Eugene Shoemaker, U.S. Geological Survey, Flagstaff.

Logistics and administrative support were provided by the Program Services Department at the Lunar and Planetary Institute. The abstract volume was prepared by the Publications Services Department at the Lunar and Planetary Institute.

Table of Contents

Evolutionary Effects in Cometary Chemical Abundances

Michael F. A'Hearn (UMD), Robert L. Millis, David G. Schleicher, David J. Osip (Lowell Obs), and Peter V. Birch (Perth Obs)

Our large data base of molecular production rates in comets has been searched for effects that can be associated with the secular evolution of comets. Chemical differences in dynamically new comets can tell us about the irradiation processes in the Oort cloud, differences as a function of reciprocal semi-major axis (statistically the dynamical age) can tell us about the initial stratification of chemicals within cometary nuclei, and changes from one apparition to the next of short-period comets can tell us about the evolution of comets into asteroids.

Periodic comets in stable orbits and observed at multiple apparitions, with one possible exception, show no evidence for secular changes in the production of gas or dust whereas two periodic comets which exhibit significant orbital changes also showed significant changes in outgassing fora given heliocentric distance. Comparison of OH with other species for inbound, dynamically new comets suggests that the grains in the comae of these comets are relatively pure H_2O and that the other species normally seen in comets must be part of a more volatile matrix in the irradiated outer layers. Differences in the asymmetries about perihelion between short-period and other comets suggest, although the statistics are not good enough to be conclusive, that the asymmetries for short-period comets are due primarily to seasonal effects coupled with localized outgassing whereas the asymmetries for new and long-period comets have a different origin. No systematic differences are found for comets known to be heavily mantled although, at certain heliocentric distances, there is systematically increased scatter in the abundance ratios for dynamically older comets.

Imaging Small Bodies with the Faint-Object Camera

Rudolf Albrecht, Space Telescope European Coordinating Facility,
Karl-Schwarzschild-Str 2, D-8046 Garching, Germany

NO ABSTRACT AVAILABLE

Qualitative Researches of Evolution of Outer Part of Asteroidal Belt.

E.V.Alfimova, I.A.Gerasimov

In the planar case of the restricted three-body problem It was consided the evolution of resonant orbits of outer part of asteroidal belt. It was shown, in the case the change of circular problem to elliptic problem the splitting of separatrix separate the different types orbits on the fase plane took place. However, for the Gilda's groop of asteroids (correlation 2:3) the type orbits survived near the stationary solution and avoid the approaching with Jupiter (type of stationary orbits), is survived.

For other asteroids nearly the Jupiter, begining since the 5:6 resonanse, it was noticed the crossing of resonant zones and, therefore, orbits of asteroids in that zones are none-stationary.

For the Hecuba's groop of asteroids (correlation 1:2) near the stationary solution e, there is the more fast motion of apsid line, therefore, probability of their collition with other asteroids for one oder higher as the none-resinant zone.

N91-25983

CHARACTERIZING WATER/ROCK INTERACTIONS IN SIMULATED COMET NUCLEI VIA CALORIMETRY: TOOL FOR *IN-SITU* SCIENCE, LABORATORY ANALYSIS, AND SAMPLE PRESERVATION.

Judith H. Allton[1] and James L. Gooding[2] [1]C23/Lockheed Engineering & Sciences Co., Houston, TX, 77058 USA. [2]SN21/Planetary Science Branch, NASA/Johnson Space Center, Houston, TX 77058 USA.

Introduction. Although results from the *Giotto* and *Vega* spacecraft flybys of comet P/Halley indicate a complex chemistry for both the ices and dust in the nucleus [1], carbonaceous chondrite meteorites are still regarded as useful analogs for the rocky component [2]. Carbonaceous chondrites mixed with water enable us to simulate water/rock interactions which may occur in cometary nuclei. Three general types of interactions can be expected between water and minerals at sub-freezing temperatures: (a) heterogeneous nucleation of ice by insoluble minerals; (b) adsorption of water vapor by hygroscopic phases; and (c) freezing- and melting-point depression of liquid water sustained by soluble minerals.

Samples and Methods. Two series of experiments were performed in a differential scanning calorimeter (DSC) with homogenized powders of the following whole-rock meteorites and comparison samples: Allende (CV3), Murchison (CM2), Orgueil (CI), Holbrook (L6), and Pasamonte (eucrite) meteorites as well as on peridotite (PCC-1, U.S.G.S.), saponite (SapCa-1, CMS), montmorillonite (STx-1, CMS), and serpentine (Franciscan Formation, California)[3,4]. In Series 1 experiments, approximately equal masses of mineral/rock powder and deionized water were blended into mud at room temperature and crimp-sealed in an aluminum container; a physically separate droplet of deionized water, overhanging the mud, served as an internal standard. Series 2 used the same procedure except that a dry mineral/rock sample was exposed only to water vapor from the overhanging droplet. Each sample container was placed in a Perkin-Elmer DSC-2 instrument and cooled at 10 K/min to $\leq$ 200 K, followed by re-heating at 10 K/min, under a continuous argon gas purge of 20 cm^3/min. DSC heat-flow data were acquired during multiple freeze/thaw cycles.

Results. Series 1 experiments indicate that the freezing of water in water/rock mud mixtures is heavily influenced by heterogeneous nucleation. Because the aluminum container is a relatively poor nucleator, liquid water undercools substantially before freezing in the absence of minerals. Only Orgueil deviated from a nucleation trend-line, consistent with the additional influence of freezing- and melting-point depression by dissolved salts, which are more abundant in CI chondrites [5]. Whereas freeze/thaw cycling of Series 1 samples revealed little, if any, systematic change with time, data for Series 2 samples showed pronounced changes with successive thermal cycles. Freezing and melting peaks controlled by mineral/rock samples grow during successive freeze/thaw cycles, presumably as water vapor is progressively adsorbed and condensed on the initially dry samples. Mineralogical effects on condensation and freezing are seen in all three carbonaceous chondrites but are most pronounced for Orgueil, probably as a consequence of its more abundant hygroscopic phyllosilicates and sulfates [5]. Individual melting peaks in Orgueil appear to correlate with peaks in pure-substance comparison samples, but further work is needed for confirmation.

Implications for in-situ cometary analyzers, laboratory analysis, and sample preservation. Besides identification of volatile ices, DSC-type experiments could help diagnose the rocky component of a comet nucleus. Based on our freezing/melting data, we could expect (at the minimum) eucrites could be distinguished from ordinary and carbonaceous chondrites and that CI chondrites could be distinguished from other chondrites. Additional experimental work would be necessary to establish the nucleation, dissolved species, and adsorption effects or other interactions of carbon dioxide, ammonia, and methane ices, additional minerals, and organic matter. DSC data taken *in-situ* can be compared with laboratory measurements on returned samples to check the quality of sample preservation. Current mission planning for sample preservation requirements leans heavily on phase transition temperatures of pure substances [6]. To assure sample preservation, transition temperatures for mixtures should be experimentally determined.

References: [1] Kissel J. et al (1986) *Nature, 321,* 280-282. [2] McSween H. Y. Jr. and Weissman P. R. (1989) *Geochim. Cosmochim Acta, 53,* 3263-3271. [3] Gooding J. L. and Allton J. H. (1991) In *Lunar Planet. Sci. XXII,* Lunar and Planetary Institute, Houston, TX, 459-460. [4] Gooding J. L. and Allton J. H. (1991) In *Reports of the Planetary Geo. & Geophys. Program - 1990,* NASA Tech. Memo., Washington, D. C. [5] Zolensky M. and McSween H. Y. Jr. (1988) In *Meteorites and the Early Solar System,* (J. F. Kerridge and M. S. Matthews, eds.), 114-143. [6] T. J. Ahrens et al. (1987) *Rosetta - The comet nucleus sample return mission.* SCI (87)3, European Space Res. & Tech. Centre.

ABOUT DISTRIBUTION AND ORIGIN OF THE PECULIAR GROUP OF SPORADIC METEORS; V.V.ANDREEV, Kazan University, Engelhardt Astronomical Observatory, 422526, USSR.

The group of the peculiar meteors are picked out from analysis of meteor catalogues obtained from radar observations in Mogadisho and Kharkov. For these meteors inclinations of orbits i are equal or more than 90^0 and

$$T = a^{-1} + 2 A_J^{-3/2} \sqrt{a (1 - e^2)} \quad \text{Cos } i \geqslant 0.5767,$$

where A_J is the Jupiter's semi-major axis.

Semi-major axises of the meteor orbits are equal or more than 1.73 AU for these conditions. Distributions of radiants, velocities and elements of orbits were derived. A possible source of meteor bodies of this peculiar group is the long-period comets, in particular, the comets of the Kreutz's group.

PHOBOS AND DEIMOS ARE SOURSES OF METEOROIDS. ANDREEV V.V., BELKOVICH O.I. Kazan University, Engelhardt Astronomical Observatory, 422526, USSR.

Data of Pioneer IO meteoroid penetration detectors were revised taking into account the orientation of detectors and the spacecraft velocity relative of the sporadic meteor flux. The meteor flux density increases exponentially to the orbit of Mars for six times and then decreases after the orbit. Ejections of secondary meteoroid particles are the plossible explanation of the increase of the meteoroid flux.

FROM C/MRKOS TO P/HALLEY : 30 YEARS OF COMETARY SPECTROSCOPY

C. Arpigny, F. Dossin
Université de Liège, Belgium
A. Woszczyk
Copernicus University, Torun, Poland
B. Donn
NASA, Goddard Space Flight Center, USA
J. Rahe
NASA Headquarters, USA
S. Wyckoff
State University of Arizona, USA

An **Atlas of Cometary Spectra** has been compiled, as a sequel to the well-known Atlas published by Swings and Haser in 1956. The new atlas comprises some 400 reproductions of cometary spectra secured in the world's largest observatories during the three decades or so from the passage of comet Mrkos 1957 V, for which the very first high-dispersion spectrum was obtained, to the return of Halley's comet. The illustrations refer to 40 different comet apparitions; they are grouped into a set of 186 loose 11" x 14" plates, while the texts, comments and relevant data are given in a separate booklet.

The main purpose of this atlas is to show in detail the tremendous progress which was achieved in cometary spectroscopy during the period covered, essentially thanks to the use of high-resolution coudé spectrographs and large telescopes, the considerable extension of the observed wavelength range, and the advent of electronic detectors. It is divided in two parts. Part I, which contains about two thirds of the selected material, presents photographic spectra, while electronically recorded spectra covering the vacuum ultraviolet, through the optical, infrared and radio regions appear in Part II.

The table of contents as well as reproductions of a few atlas plates are shown in the display.

ROSETTA, the Comet Nucleus Sample Return Mission

by

A. ATZEI (ESA) - R. MITCHELL (JPL)

Rosetta is a cornerstone mission of the science programme of the European Space Agency (ESA) and it is being studied as a collaborative project with NASA. Since 1986, ESA and NASA have been jointly defining the science objectives and conducting mission design and engineering studies. ESA is also developing most of the new technologies required by the mission.

The major scientific objective of Rosetta is to return cometary nucleus samples to earth, while preserving their fundamental chemical, isotopic and structural properties. Rosetta will provide information important to planetary scientists, astrophysicists and life scientists. It will investigate the nature of the raw material of the solar system (interstellar dust and organic compounds) and address the presolar processes in stars and the interstellar medium that created this raw material. The analysis of the most primitive condensed organic material could establish an essential link with the prebiotic environment that preceeded the beginning of life.

The proposed mission is based on a Titan/Centaur launcher and on a spacecraft assembly of three modules: a cruiser, a lander and an earth re-entry capsule. The cruiser is in charge of the overall mission control; the lander contains anchoring, sampling, and manipulation mechanisms; the earth re-entry capsule is in charge of preserving the samples until their recovery on earth. The mission will be controlled via the DSN.

The spacecraft would be launched in December 2002 into a delta vega trajectory; in January 2008, it will approach a short period comet (Hartley-2 is the current target) near its aphelion, at about 5 AU. It will spend about 100 days in near-comet orbits, performing a global comet characterisation and detailed mapping of suitable landing sites by means of active and passive optical and microwave instruments. It will eventually synchronize its motion with that of a selected landing site and initiate an autonomous slow vertical descent using laser mapping techniques for position control. After touch down, it will perform sounding to identify the subsurface properties of the sampling site. It will then anchor to the nucleus by means of penetrating devices fired into the soil, for compensating torques and forces generated during sampling in a milligravity environment. Sampling operations will begin with the deployment of a container attached to a robot arm, to collect and compress pieces of loose material from the cometary surface. Subsequently, a drill facility will collect core samples 1 to 3 meters from below the surface in 4 cylindrical 60 cm long and 10 cm diameter pieces. A manipulator arm will store the samples inside the aerocapsule in a super isolated container, in which a hermetically sealed compartment will prevent loss of the volatile components preserved in the deapest core sample. Inside this container, the samples will be kept around 130 K until recovery. The sampling operations, which may last up to 15 days, will be autonomous to a great extent and will be performed according to pre-determined sequences loaded on board and adjustable as function of the local soil properties. Once the sampling operations are completed, the cruiser and the aerocapsule will re-launch toward Earth, leaving the lander behind. Two years later, in November 2010, while the spacecraft approaches Earth, the aerocapsule will separate from the cruiser, and it will accomplish a ballistic atmospheric re-entry. After a parachute assisted final descent, the aerocapsule will touch-down on the Pacific Ocean, where it will be recovered by ship-based helicopters and the sample container delivered to the receiving laboratory.

FRAGMENTATION AND DENSITY OF METEOROIDS; P.B.Babadzhanov
Institute of Astrophysics, Dushanbe, 734670 USSR

Photographic observations of meteors carried out in Dushanbe by the method of instantaneous exposure (0.00056 s) have shown clearly that meteoroids entering the Earth's Atmosphere are subjected to different types of fragmentation (Babadzhanov 1983) The main forms of fragmentation are:

1) the decay of a meteoroid into comparable large nonfragmentating debris;

2) the progressive disintegration of the original meteoroid into fragments, at which each fragment continue to disintegrate into smaller fragments;

3) the quasi-continuous fragmentation - a gradual release of smallest fragments from the surface of a parent meteoroid and their subsequent evaporation;

4) the instantaneous spray of a large number of small particles that gives rise to flares on meteor light curve.

Observations show that the quasi-continuous fragmentation of meteoroids is mostly spread. Using the physical theory of meteors which takes into account the quasi-continuous fragmentation based on light curves of meteors both the density of meteoroids of different streams and the sizes of separated fragments have been determined. The results enable to conclude that the densities of meteoroids are of over magnitude higher than they had been assumed before. Moreover they are close to the densities of carbonaceous and ordinary chondrites.

REFERENCE:

Babadzhanov P.B. 1983, in Asteroids, Comets, Meteors, eds. C.I. Lagerkvist and H.Rickman, Reprocentralen HSC,Uppsala,pp;439-445

P/MACHHOLZ 1986 VW AND QUADRANTID METEOROID STREAM. ORBITAL EVOLUTION AND INTERRELATION; P.B.Babadzhanov, Yu.V.Obrubov, Institute of Astrophysics, Dushanbe, 734670 USSR

The Quadrantids are the most interesting major meteor shower.However, a search for the hypothetical parent comet has been unsuccessful since long. In 1986 D.Machholz discovered a comet, which would have been a progenitor for the Quadrantids, in spite of a significant difference between the present comet's orbit and the observed orbits of the Quadrantids (B.McIntosh, 1990, Icarus, 86, p.299). The investigations of the P/Machholz and the Quadrantids orbital evolution show the similarity in their dynamical behavior although a certain shift in time. This shift is obvious from Fig., which presents the evolution of orbital inclinations i of the P/Machholz comet (curve 1) and a modelled Quadrantid meteoroid (curve 2). However, due to the closeness to the Jupiter's orbit the period of variation of i depends strongly on the initial position of a body in its orbit. Moreover, in long time intervals the element determining the body's position in the Keplerian orbit is calculated rather roughly. Thus, it is necessary to study the motion of the comet or a meteoroid under different starting positions. Curve 3 in Fig. denotes the variation in orbital inclination of a modelled Quadrantid meteoroid, that coincides in phase with variation of P/Machholz up to 500 A.D. It is necessary to note that curves 2 and 3 were obtained for the meteoroids of the same initial orbit, although their starting positions differed by 180 . Thus, it is evident that the observed difference between the orbits of the P/Machholz comet and the Quadrantid meteor shower may be resulted from the planetary perturbations.

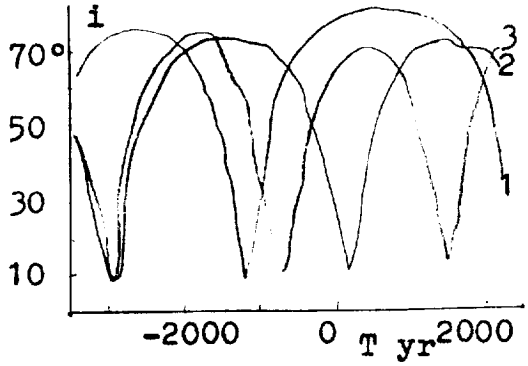

Six of eight near-earth or earth-crossing orbits of the P/Machholz comet are given below. These orbits are the theoretical (T) orbits of possible meteor showers of the P/Machholz. Here also given the observed (O) mean orbits of the meteor showers which can be produced by the same meteoroid stream (P.B. & Yu.O., 1989, Highlights of Astron., v.8, p.287).

	Quadrantids					Ursids				
	e	q	i	Ω	w	e	q	i	Ω	w
T	0.746	0.78	74°	280°	171°	0.758	0.73	73°	278°	189°
O	0.682	0.97	70	282	168	0.761	0.97	63	281	195
	S. δ-Aquarids					N. δ-Aquarids				
T	0.985	0.05	22	130	327	0.989	0.03	19	312	147
O	0.970	0.07	23	154	307	0.960	0.08	21	331	128
	Daytime Arietids					α -Cetids				
T	0.988	0.04	23	71	32	0.985	0.05	19	248	213
O	.0940	0.09	21	77	29	0.950	0.06	20	258	202

So, a satisfactory similarity of the theoretical and observed meteor shower orbits points to the fact that these showers could have been resulted from the decay of P/Machholz nuclear.

RADAR METEOR ORBITAL STRUCTURE OF SOUTHERN HEMISPHERE COMETARY DUST STREAMS; W.J. Baggaley, A.D. Taylor, Physics Department, University of Canterbury, Christchurch, New Zealand.

The Christchurch, New Zealand meteor orbit radar (AMOR) with its high precision and sensitivity, permits studies of the orbital fine structure of cometary streams. PC generated graphics will be presented of data on Southern Hemisphere Streams. Such structure can be related to the formation phase and subsequent dynamical processes of dust streams.

A SOUTHERN HEMISPHERE RADAR METEOR ORBIT SURVEY; W.J. Baggaley, D. I. Steel†, A.D. Taylor, Physics Department, University of Canterbury, Christchurch, New Zealand.

A meteor radar system has been operating on a routine basis in Christchurch, New Zealand, to determine the orbits of earth-impacting solar system dust particles. The system sensitivity is +13 visual magnitude corresponding to 100 micron size particles. With an orbital precision of 2^0 in angular elements and 10% in 1/a, the operation yields an average 1500 orbits daily with $> 10^5$ to date.

The use of PC's and automated data reduction permit large data sets to be routinely reduced.

Illustrative examples will be presented using comprehensive graphics of the signal processing and orbit reduction. Current studies include the solar system dust orbital distribution; the influx of dust associated with NEA's and the orbital structure existing in cometary streams.

† Now at Anglo-Australian Observatory, Coonabarabroon, NSW 2357, Australia.

Diffusion of gas through porous dust layers formed in comet simulation experiments (KOSI)

MICHAEL BAGUHL, EBERHARD GRÜN AND HARALD KOHL
Max-Planck-Institut für Kernphysik, Heidelberg, Germany

The thermodynamic behaviour of cometary nuclei is difficult to determine in situ. In the comet simulation experiments (KOSI) conducted at the space simulator at DLR in Köln, Germany, a sample of some tents of cm composed of porous ices of H_2O and CO_2, minerals and carbon simulating the comet nucleus is irradiated by an artificial sun.

The temperatures and the pressures within the samples are measured in various depths. The pressure within porous cometary nuclei plays an important role in heat conduction via the gas phase into the nucleus, in gas and in dust emission mechanisms. Two processes are responsible for the actual value of the pressure. The first is gas sublimation and recondensation controlled by th amount of heat conducted into the nucleus. The second is diffusion of the gases through the porous texture of the sample. After some hours of irradiation a dust mantle builds up on the sample surface. The diffusion constant of such porous dust layers have been studied in detail.

The measurement of the diffusion constant was performed by directing a constant flow of N_2 gas through a sample of known size and measuring the pressure differentials between both sides with capacitive pressure gauges. The diffusion constant was found to vary between 1 and $3 \cdot 10^{-3}$ m^2/s with different species of dust.

ON THE VALIDITY OF MARKOV CHAIN METHODS FOR MODELLING OF ORBITAL EVOLUTION.

Philippe Baille, Dave Hamburger
Royal Military College of Canada,Kingston,Ontario,Canada

Studies of the origin and evolution of comets or asteroids require the exact solution of their long term dynamical evolution. Such a solution is still computationally unattainable for a statistically significant number of small bodies. Therefore, these diffusions are frequently approximated by Monte Carlo methods. Essentially, these methods replace the exact diffusion mapping by a stochastic Monte Carlo mapping. A further efficient simplification involves representing the diffusion by a probability matrix, itself a by-product of the Monte Carlo method. This is the Markov chain formalism from which the asymptotic behaviour is readily extracted. We know of three such applications to cometary and asteroid dynamics. Here we present an independent test of the Markov method where we assert its efficiency and reliability using a discrete dynamical system (a mapping), as in our previous test of the Monte Carlo method.

SOME EXPERIMENTS RELEVANT TO THE FORMATION OF A COMETARY ORGANIC CRUST; G.A.Baratta, Osservatorio Astrofisico di Catania; G.Strazzulla, Istituto di Astronomia di Catania

For several years many experimental results have been obtained on the chemical and physical changes induced by ion and electron irradiation of materials with a view to their Astrophysical relevance[1-4]. Among the studied effects one of particular interest is the formation of an organic refractory residue left over after ion irradiation and warming-up at room temperature; we call this residue IPHAC (Ion Produced Hydrogenated Amorphous Carbon). Although "in situ" infrared spectroscopy has pointed out both the formation of new molecular species during irradiation, as well as the presence of features even observed in the organic residue at room temperature, it is not clear if IPHAC is already formed or if its formation is triggered by temperature increase during warming-up of the irradiated target.

Being Raman spectroscopy a technique particularly suitable in providing valuable evidence to the structural properties of carbonaceous material[5], we have thought and build up an experimental apparatus to obtain Raman Spectra of frozen Hydrocarbons during ion irradiation[6]. The present experimental results point out to the formation of IPHAC already at low T (10K) during ion irradiation.

These results may have relevant astrophysical applications, in particular for cometary physics, indeed they support the hypothesis that the cometary organic crust can be already formed during the long stay (4.6×10^9 years) in the Oort cloud and its development does not requires a first passage (heating) in the inner Solar System.

REFERENCES

1. Strazzulla, G. & Johnson, R.E. in Comets in the Post-Halley Era, (eds. Newburn, R. Jr, Neugebauer, M. & Rahe, J.) in press (Kluwer, Dordrecht 1991).
2. Andronico, G., Baratta, G.A., Spinella, F. & Strazzulla, G.: Astron. Astrophys. **184**, 333 (1987).
3. Foti, G., Calcagno, L., Sheng, K.L. & Strazzulla, G.: Nature **310**, 126 (1984).
4. Lanzerotti, L.J., Brown, W.L. & Marcantonio, K.J.: Astrophys.J. **313**, 910 (1987).
5. Robertson, J.: Adv. in Phys. **35**, 317 (1986).
6. Spinella, F., Baratta, G.A., Strazzulla, G.: Rew. Sc. Instr. (1991 in press).

Comets Formation and their Contribution to the Volatiles on the Terrestrial Planets

Akiva Bar-Nun, Dept. of Geophysics and Planetary Sciences, Tel Aviv University, Tel Aviv 69978, Israel

NO ABSTRACT AVAILABLE

DOES EXIST A "NATURAL BREAK" IN THE SPIN DISTRIBUTION OF SMALL ASTEROIDS? A. Barucci, Observatoire de Paris; M. Di Martino, Osservatorio Astronomico di Torino; and M. Fulchignoni, Istituto Astronomico, Universita' La Sapienza, Roma.

The spin rate distribution of more than 500 asteroids (shown here below), having reliability codes larger than 2, have been examined.

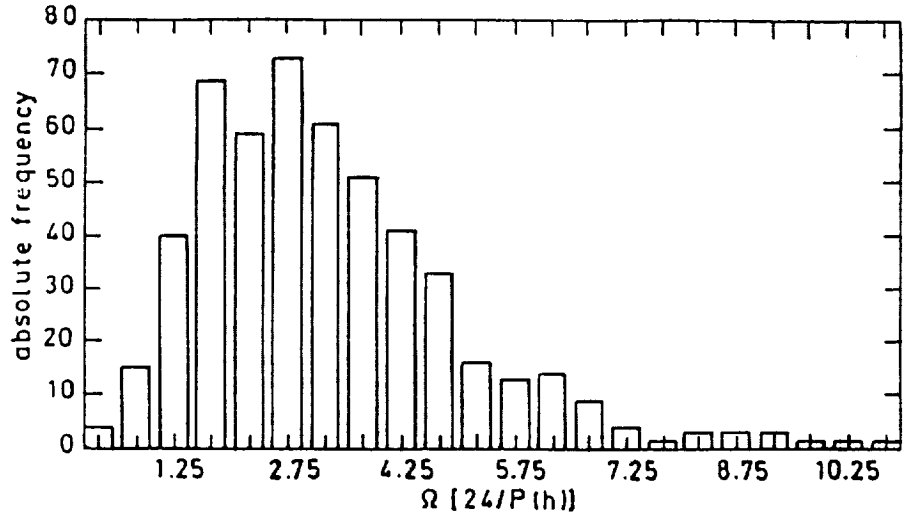

A gap corresponding to 2 rev./day is evident. The gap is enhanced in all the subsamples of objects with diameter lesser or equal to 55 km and disappears in the subsample of objects with diameter larger than 55 km.

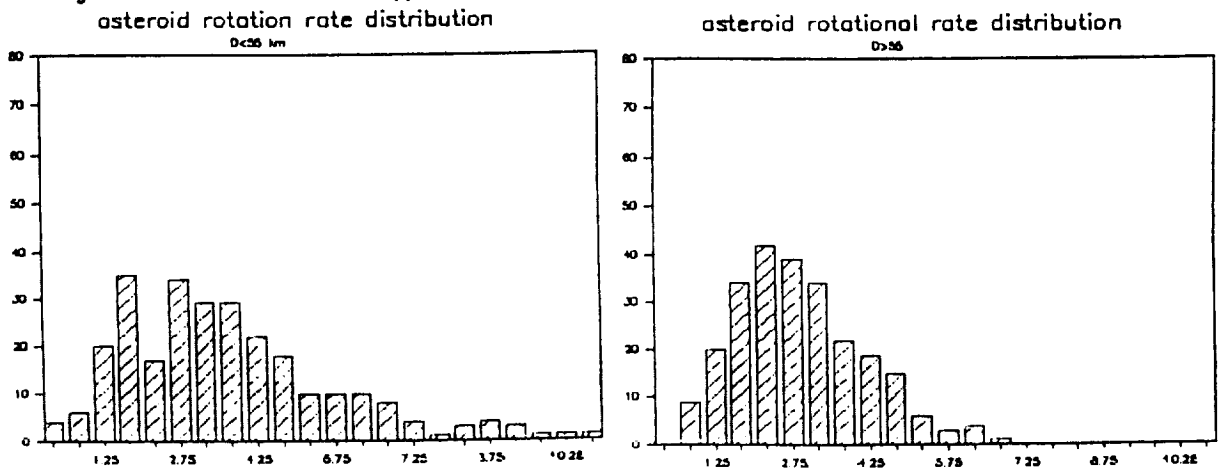

Binzel (1984, Icarus 57, 294) found in his sample of asteroids with diameter less or equal 30 km the same gap, and he refers to it as "a natural break" in the spin distribution. This gap is not due to selection effects in the determination of the rotational period or in the graphical representation.

We discuss the possible meaning of this confirmed "natural break" in terms of collisional evolution of the asteroid population.

THE NATURE OF 951 GASPRA A. Barucci, Observatoire de Paris; M. Coradini, ESA Hdq, Paris; M. Di Martino, Osservatorio Astronomico di Torino; M. Fulchignoni, C. De Sanctis and A. Rotundi, Istituto Astronomico, Universita' La Sapienza, Roma.

The Galileo spacecraft will fly-by the asteroid 951 Gaspra on October 29, 1991. The results of an international observation campaign carried out in the past years have been utilized to precalibrate and define the sequence of observations by the Galileo Spacecraft Instruments. This will be the first close approach of an asteroid by a man-made spacecraft. 951 Gaspra will be observed by several instruments that will provide us with a unique set of measurements. The information obtained during the Galileo fly-by, besides their intrinsic value, will represent a formidable "ground-truth" to calibrate the methods developed to infer asteroid properties out of ground based observations.

In May 22, 1991 the last opposition before the encounter will occur. We obtained observating time at the ESO (La Silla) 2.2 meter telescope (April, June, July, August) to perform CCD photometry and observing time at 1 meter telescope (May and June) IR + photoelectric photometry. We will report on the preliminary results obtained during the above mentioned campaign. Our aim is to refine and/or determine with the best possible accuracy the asteroid pole orientation, phase function, shape and morphology. We are confident will come up with a sound model of 951 Gaspra before Galileo spacecraft will encounter it.

ON THE POSSIBILITY OF DETERMINING THE MASS OF SOME MINOR PLANETS OF THE HIPPARCOS PROGRAMME; A. Bec-Borsenberger, Service des calculs et de Mécanique céleste du Bureau des Longitudes, Unité Associée au CNRS 00707, 77 avenue Denfert-Rochereau, F-75014 Paris, France

A systematic study of the close approaches of the minor planets of the Hipparcos programme is carried out, mainly during the periods of the observations realised for and by the satellite Hipparcos, in order to determine, when this is possible, the mass of the minor planets concerned.

DETERMINATION OF METEOR FLUX DENSITY DISTRIBUTION OVER THE CELESTIAL SPHERE. O.I.BELKOVICH, Engelhardt Astronomical Observatory, T.K.FILIMONOVA, V.V.SIDOROV, Kazan University.

A new method of determination of meteor flux density distribution over the celestial sphere from observations by radar with measurements of arrival angles of radio waves reflected from meteor trails is discussed. The rôle of small meteor showers over the sporadic background is shown.

THE S-TYPE ASTEROID CONTROVERSY. Jeffrey F. Bell (Dept. of Geology and Geophysics, SOEST, Univ. of Hawaii, Honolulu HI 96822)

The longest running argument in asteroid science concerns the mineral composition and meteoritical association of the asteroids assigned to taxonomic type S. The approaching flyby of the S-type asteroid Gaspra by the Galileo spacecraft will drag an even larger section of the space science community into this turgid debate. Below are summarized the various proposed S asteroid surface compositions in roughly the order in which they appeared.

A) ORDINARY CHONDRITES: It was known long before asteroid spectroscopy began that ordinary chondrites (OCs) make up more than 75% of observed meteorite falls. Thus when the first asteroid colors and albedos were obtained in the early 1970s there was a strong expectation that many asteroids would resemble OCs. Indeed, the spectral class "S" originally was intended to stand for "silicaceous" as "M=metal" and "C=carbonaceous". Thus the original 3 asteroid types neatly accounted for ordinary chondrites, irons, and carbonaceous chondrites.

B) STONY-IRONS: Later, when spectra of ordinary chondrites were measured in the lab it became apparent that they actually had little similarity to S asteroids. The asteroids have a steep red continuum totally unlike that of the OCs, and the details of the silicate bands vary wildly, implying mineralogies usually far outside the OC range. To explain these facts it was suggested that most S-type surfaces are differentiated assemblages of metal, orthopyroxene, and olivine, similar to stony-iron meteorites.

C) WEATHERED ORDINARY CHONDRITES: Upon discovery of the continnuum slope problem, advocates of interpretation A) proposed that the red continuum of S asteroids is created by some "space weathering" process which alters the spectrum of the uppermost regolith. This proposal has inspired investigations of both synthetic metal-rich regoliths derived from OCs and natural OC parent body regolith material preserved in some meteorite breccias. All these studies demonstrate that "weathered" OC material does not redden, but rather becomes spectrally flatter and in extreme cases approximates a C-type spectrum, never an S-type.

D) CARBONLESS CARBONACEOUS CHONDRITES: When the first near-IR spectra of S asteroids revealed that most had higher ol/pyx than any OC, it was proposed that they represented unknown types of chondrites, specifically material with the silicate composition of carbonaceous chondrites but no carbon. But since no such meteorites have ever fallen on Earth, this hypothesis requires its advocates to abandon the very fall-statistics argument that had originally inspired the chondritic interpretation of S-types in the first place. Furthermore, the asteroid Flora which was cited as the most OC-like of the S-types was later shown to have large variations in silicate mineralogy between different regions of its surface, far outside the range of OCs.

E) EVERYTHING: The mounting spectral evidence for wild variations in composition between different S asteroids and even across the surface of individual ones leads some workers to wonder if both schools might be right. It is impossible to rule out some chondritic areas on the surfaces of S asteroids with the current data, if one allows the other areas to be made of extreme differentiated mineralogies (e.g. pure metal or pure olivine). Since we observe an entire "hemisphere" at once with Earth-based telescopes the chondritic areas could not be separated from the differentiated areas. The fatal objection to this theory is that the actual OC breccias do not contain differentiated clasts, which would be sure to exist in the regolith of a "patchwork asteroid".

F) NOTHING: Alternatively one may take the wide variety of S spectra to indicate that there is really no such thing as a unified "S-type asteroid", but a variety of different objects with different origins and histories which we have not yet properly distinguished. For instance, the Eos asteroid family contains objects formally classified S in most systems, but with IR spectra that closely match those of CO or CV chondrites. A new class "K" was recently created to contain these objects. But there does seem to be a hard core of well observed objects with classical S properties that will always remain even if some of the fainter objects which have only incomplete spectral data later turn out to be something else.

THE CURRENT POSITION: At present almost all scientists actively involved in research on asteroid composition appear to hold some version of interpretation B. In fact, no full journal article defending any other view has appeared for at least 10 years. Yet some of them (especially C) continue to be defended vigorously in less formal situations, and none can be rigourously excluded on the basis of current data.

ASTEROIDS WITH UNUSUAL LIGHTCURVES: 14 IRENE AND 51 NEMAUSA; I.N.Belskaya, Astronomical Observatory of Kharkov University, and A.N.Dovgopol, Main Astronomical Observatory of the Ukraine Academy of Sciences, Kiev, USSR

New photometric observations of 14 Irene and 51 Nemausa received in 1989 and 1990 are presented. Irene's rotation period of 28.06 hours which three times longer than previously reported is the most suitable to our observations. Composite lightcurves of both asteroids display very irregular shape with at least three pairs of extrema. We applied different methods including Fourier analysis and numerical modelling to interpret all available data of these asteroids. Obtained results and their reliability are discussed.

LOW COST MISSIONS TO EXPLORE THE DIVERSITY OF NEAR EARTH COMETARY NUCLEI.

Michael J.S. Belton, Kitt Peak National Observatory, Tucson AZ 85719.

A scientific rationale is presented for undertaking a series of low absolute cost flyby/flythrough missions to near-Earth cometary nuclei. The primary scientific goal is to study the *diversity* in cometary nuclei and builds on the results of VEGA/GIOTTO missions to Halley and the ICE mission to Giacobini-Zinner. It is shown how such a program would naturally complement future "approved" missions like CRAF and ROSETTA. An attempt is made to define a rational concept of diversity for the purpose of mission planning and groups of specific measurement goals are proposed. The concept can easily be extended to an international program in which budgetary and technical interdependencies are minimized but for which scientific productivity is optimized. The mission concept is based on the availability of low cost launchers (Pegasus) and fully integrated spacecraft/instument development. Mission costs (based on class C/D quality assurance guidelines) are expected to be well below $100M per mission.

DISTRIBUTION OF ACTIVE AREAS ON THE NUCLEUS OF COMET P/HALLEY: EVIDENCE FOR INHOMOGENEITY.

Michael J.S. Belton, Kitt Peak National Observatory, Tucson AZ 85719, William H. Julian, New Mexico State University, Las Cruces, NM 88003, and Beatrice E.A. Mueller, Kitt Peak National Observatory, Tucson AZ 85719

A new model for the spin state of the nucleus of comet P/Halley (Belton *et al.* 1991, submitted to *Icarus*), which satisfies a wide range of ground-based, earth-orbital, and spacecraft data, is used to explore the distribution of active areas on the surface of comet Halley. The model is an axially symmetric rotator with the shape of a prolate spheroid. The spin vector is inclined to the (fixed) angular momentum vector by 21°.4 and precesses around it with a period of 3.69 days. The total spin period is 2.84 days. Most of the activity seen from the ground is found to originate in five specific locations on the nucleus and one of these regions (located near the waist of the nucleus) appears to have properties that are different from those of the others. In particular there is evidence that it was active at large heliocentric distances (>5 AU) on approach to the Sun. We discuss the possibility that this area represents a large-scale chemical inhomogeneity in the nucleus.

SIMULATED FAMILIES: A TEST OF DIFFERENT METHODS OF FAMILIES IDENTIFICATION

P. Bendjoya (1), A. Cellino (2), Cl. Froeschle' (1), and V. Zappala' (2)

(1) Observatoire de la Cote d'Azur
B.P. 139
F-06003 Nice cedex (France)
(2) Osservatorio Astronomico di Torino
Strada Osservatorio 20
I-10025 Pino Torinese (TO) (Italy)

A set of families generated in fictitious impact events (leading to a wide range of "structures" in the orbital elements space) have been superimposed to various backgrounds of different densities in order to investigate the efficiency and the limitations of the methods by Zappala' et al. (Astron.J., 100, 2030, 1990) and Bendjoya et al. (Submitted to Astron. and Astrophys., 1991) for identifying asteroid families. In addition, an evaluation of the expected interlopers at different significance levels, the possible apparent splitting of families characterized by very high ejection velocities, the possibility of improving the definition of the level of maximum significance of a given family, etc., were analyzed.

THE USE OF THE WAVELET CLUSTER ANALYSIS FOR ASTEROID FAMILY DETERMINATION.

Bendjoya Ph., Slezak E., Froeschlé Cl.

Observatoire de la Côte d'Azur
B.P. 139
F-06003 Nice cedex (France)

Abstract:

The asteroid family determination has been for a longtime analysis method dependent. A new cluster analysis based on the wavelet transform has allowed an automatic definition of families with a degree of significance versus randomness. Actually this method is rather general an can be applied to any kind of structural analysis. We will rather concentrate on the main features of the method. The analysis has been performed on the set of 4100 asteroid proper elements computed by Milani and Knézévic (Celestial Mechanics submited1990). Twenty one families have been found and influence of the chosen metric has been tested. The results have been compared with Zappala et al.'s ones (Astronomy and Astrophysic submited 1990) obtained by the use of a completely different method applied on the same set of data. For the first time, a good overlapping has been found between the both method results, not only for the big well known families but also for the smallest ones.

STOCHASTICITY OF COMET P/SLAUGHTER-BURNHAM; D.Benest and R.Gonczi, O.C.A. Observatoire de Nice

Three comets are now known to be at or near the 1/1 resonance with Jupiter: P/Slaughter-Burnham, P/Boethin and the newly discovered P/Ge-Wang. Although details of the individual orbits differ, the three comets have very similar general dynamical behaviour: their orbits show many transitions between the different types of resonant motion (satellite libration, anti-satellite libration and circulating motion) [1].

The stochastic character of such cometary orbits, mainly due to encounters with Jupiter, is investigated. For each comet of the group, we study the influences of initial eccentricity, inclination, longitude of node and $l - l_J$ (mean longitude of comet minus mean longitude of Jupiter).

We present here our first results for P/Slaughter-Burnham.

Reference:

[1] D.Benest, 1990, Celes.Mech. 47,361

LIFETIME AND CRATERING RECORD FOR GASPRA: A PRE-GALILEO ESTIMATE

Richard P. Binzel
Noriyuki Namiki
Department of Earth, Atmospheric, and Planetary Sciences
Massachusetts Institute of Technology
Cambridge, MA 02139

We attempt to quantitatively model the collisional environment and surface evolution of asteroid 951 Gaspra prior to the flyby of the Galileo spacecraft later this year. We compute Gaspra's average intrinsic collisional probability to be 5.4×10^{-18} km^{-2} yr^{-1} with a root mean square impact velocity of 5.0 km sec^{-1}. The impacting population is highly uncertain and we consider three cases for high, intermediate, and low fluxes. Based on these models, Gaspra is unlikely to be a primordial object surviving from the beginning of the solar system. It is most likely a second or multiple generation fragment forming ~10^8 yr ago. For an age <10^9 yr and a constant intermediate impacting population, we predict Gaspra's surface is not in a state of crater equilibrium. For this case the crater size distribution directly reveals the size distribution of the impacting population. In the figure below we present isochrons assuming an intermediate impactor population as proposed by Greenberg and Chapman (1983, *Icarus* **55,** 455). If an equilibrium surface is found, our model sets lower limits for the age (~10^9 yr) and flux for Gaspra.

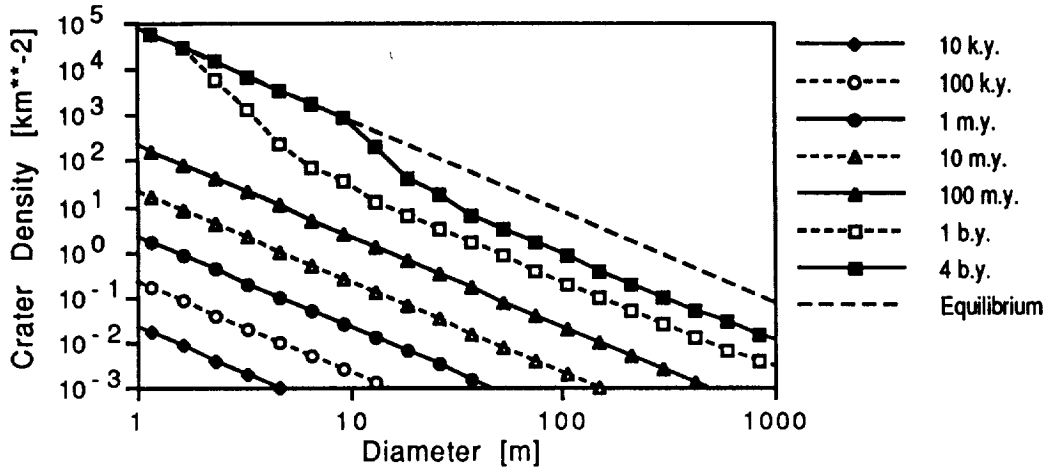

TROJAN, HILDA, AND CYBELE ASTEROIDS: ARE THEY *REALLY* MORE ELONGATED THAN MAIN-BELT OBJECTS?

Richard P. Binzel
Linda M. Sauter
Department of Earth, Atmospheric, and Planetary Sciences
Massachusetts Institute of Technology
Cambridge, MA 02139

Previous researchers (French 1987, *Icarus* **72**, 325; Hartmann et al. 1988, *Icarus* **73**, 487) have proposed that Trojan asteroids (and perhaps Hildas and Cybeles) have higher mean lightcurve amplitudes than their similar-diameter counterparts in the main belt, possibly due to differences in their formation or subsequent collisional evolution. We have obtained new lightcurve observations of 23 Trojan, Hilda, and Cybele asteroids using the University of Texas McDonald Observatory 2.1- and 0.9-m telescopes over the interval 1987-1990. Because this new data set significantly increases the sample size and because many of the newly observed objects display low lightcurve amplitudes, we are performing a new and rigorous analysis to test the higher amplitude hypothesis.

Of particular importance to this new analysis is a correction for bias effects. These arise in at least two ways. First, large amplitude lightcurves are easier to detect and are more likely to lead to publishable and tabulated results. Second, previous analyses have used the tabulated value for the *maximum* observed amplitude. This presents a bias toward higher amplitudes for objects that have been observed over multiple apparitions, as is the case for many Trojans.

We seek to overcome these biases in the following ways. First we include all data, even those that yield no rotation period information and give only a lower limit for the lightcurve amplitude. Second, we apply a geometric correction factor to multiply observed asteroids in order to estimate the lightcurve amplitude which would most likely be observed at a single random polar aspect angle. For randomly oriented spin vectors, this corresponds to an aspect angle of 60 degrees.

N91-25985

Low-pressure clathrate-hydrate formation in amorphous astrophysical ice analogs

D.F. Blake,[1] L.J. Allamandola,[2] S. Sandford,[2] D. Hudgins[2] and F. Freund[1]

[1] Planetary Biology Branch, MS 239-4 and [2] Astrophysics Branch, MS 245-6, NASA/Ames Research Center, Moffett Field, CA 94035-1000

In modeling cometary ice, some researchers have called upon the properties of clathrate hydrates to explain anomalous gas release at large radial distances from the sun, and the retention of particular gas inventories at elevated temperatures.[1] Clathrates may also have been important early in solar system history.[2] However, there has never been a reasonable mechanism proposed for clathrate formation under the low pressures typical of these environments. We show for the first time that clathrate hydrates can be formed by warming and annealing amorphous mixed molecular ices at low pressures. The complex microstructures which occur as a result of clathrate formation from the solid state may provide an explanation for a variety of heretofore unexplained phenomena.

We have modified the vacuum and imaging systems of an Hitachi H-500H Analytical Electron Microscope to study mixed molecular ices at temperatures between 12 K and 373 K.[3] The resulting ices are characterized by low-electron dose Transmission Electron Microscopy (TEM) and Selected Area Electron Diffraction (SAED). Amorphous H_2O-CH_3OH ices are prepared by vapor-deposition of a 2:1 H_2O:CH_3OH gas mixture onto a thin (<10 nm) carbon film substrate maintained at a temperature of 85 K inside the TEM. On stepwise heating at ~1 K per minute, the 2:1 H_2O:CH_3OH sample remains in the amorphous state until about 120 K at which time a series of powder diffraction rings begin to appear in the SAED pattern. Bright field TEM micrographs in the 120-130 K temperature range reveal the development of a tightly intergrown microstructure of two components, of which one is crystalline. By the time the sample temperature has reached 130 K, 7-8 powder diffraction rings are observed which can be indexed to the clathrate II hydrate structure (space group Fd3m)[4,5] using an a -parameter of 16.28 Å.[6] All of the diffraction maxima present fit the clathrate II hydrate structure reasonably well, though some maxima are absent. This slight mismatch is likely due to hydrogen bonding between the guest molecules and the H_2O of the clathrate cages.[6] As the temperature of the ice reaches ~145 K, the amorphous component sublimes away leaving a microporous architecture. The powder diffraction rings in the SAED pattern from the remaining material can be indexed as hexagonal H_2O ice. Laboratory IR spectra from these ices show temperature-dependent band changes consistent with the above interpretation.

The implications of these results for the mechanical and gas release properties of comets will be discussed. Laboratory IR data from similar ices will be presented which suggest the possibility of remotely observing and identifying clathrates in astrophysical objects.

1. A.H. Delsemme and P. Swings, *Ann. d'Ap.***15**, 1 (1952).
2. S. Engle, J. I. Lunine and J.S. Lewis, *Icarus* **85**, 380 (1990).
3. D.F. Blake et al., *Proc. XII Intl. Cong. E.M.*, **I**, 594 (1990).
4. T.C.W. Mak and R.K. McMullan, *J. Chem. Phys.* **42**(8), 2732 (1965).
5. J.E. Bertie and S.M. Jacobs, *J. Chem. Phys.* **69**(9), 4105 (1978).
6. P. Boutron and A. Kaufmann, *J. Chem. Phys.* **68**(11), 5032 (1978).
7. D.F. Blake et al., *Science*, in submission.

OBSERVATIONS OF OH IN COMET LEVY (1990c) WITH THE NANCAY RADIO TELESCOPE; D. Bockelée-Morvan, P. Colom, J. Crovisier, E. Gérard, and G. Bourgois (Observatoire de Paris-Meudon).

From mid-June to September 1991, the radio lines of OH were monitored in comet Levy (1990c) with the Nançay radio telescope. The signal was strong, due to favourable excitation of the OH radical, a gas production rate exceeding 10^{29} s^{-1}, and a small earth-comet distance. At the beginning of September, the signal was still enhanced when the comet was observed against the continuum of the galactic centre region; at that moment, the OH lines exceeded 1.5 K in antenna temperature and were the strongest ever recorded in a comet.

The exceptionally good signal-to-noise ratio of these observations allows us to make an analysis of the following topics:

a) Line shapes and study of the kinematics of the cometary atmosphere: expansion velocity and anisotropic outgassing.

b) Spatial variation of the line shapes and intensities, in relation with anisotropic outgassing, scalelength of the OH radical, and collisional quenching of the OH maser.

c) Relative intensities of the four hyperfine components of the OH lines and test of the excitation model.

d) Zeeman effect in the OH main lines and corresponding limits on the magnetic field averaged over the line of sight in the cometary atmosphere.

Coma Imaging of Comet P/Brorsen-Metcalf at Calar Alto in Late July to Mid August 1989

H. Boehnhardt (mbp Software&Systems, Dortmund)
V. Vanysek (Charles Univerity, Prague)
K. Birkle, (Max-Planck-Institut für Astronomie,
U. Hopp Heidelberg)

The coma of the periodic comet P/Brorsen-Metcalf was monitored from late July to mid August 1989 at the Calar Alto Observatory/Spain. On 1989/07/28+30 broad-band B and R filter CCD images of the inner coma were obtained with the 3.5m telescope. Large-scale phenomena were observed on 1989/08/04+12+14 with the 80cm Schmidt telescope in B and R filter exposures as well as in integral light. The coma regions of the Schmidt plates were digitized (pixel size 0.86x0.86 arcsec) and calibrated using intensity spots on the plates. In that way they can be directly compared with the calibrated CCD observations (pixel size 0.25x0.25 arcsec). To all CCD frames and to the calibrated scans of a R filter plate on 1989/08/04 and of a B filter plate on 1989/08/12 further image processing (radial renormalisation of the coma brightness distribution) was applied in order to enhance faint structures in the cometary coma.

A narrow ion tail, pointing into anti-solar direction, can be clearly identified in the calibrated and in the processed images. It is particulary prominent in the R filter exposures which might be due to the H2O+ ion emission in this spectral region. While on 1989/07/28 and on 1989/08/04+12+14 a single ion tail of about 5 deg opening angle originated from the cometary nucleus, the triplicate tail of in total about 20 deg opening angle on 1989/07/30 may resemble the convolution of cometary tail rays. A fan-like brightness core of about 7000 km extension is located in the tail vertex on the anti-solar side of the coma.

The CCD images and the B filter Schmidt plate on 1989/08/12 show prominent asymmetries in the isophote patterns of the coma. Radial renormalization of the coma images reveals a broad brightness enhancement (slightly asymmetric in North/South) in the sunward coma region on 1989/07/28 and 1989/08/12. A strong curved jet feature was detected in the coma on 1989/07/30. The brighter sunward coma hemisphere may indicate the higher nuclear activity of gas and dust emission because of the solar illumination. The coma jet (extending at least 30000 km into the coma) may arise from a temporarily, but highly active emission source releasing a significant amount of gas and dust into the coma. The jet curvature can be interpreted as due to the rotation motion of the cometary nucleus. More coma structure observations and jet feature modelling are needed to derive the characteristics (period, axis orientation) of the nuclear rotation of P/Brorsen-Metcalf.

N91-25986

MODELING THE COMA OF 2060 CHIRON ; D.C. Boice[1], I. Konno[1], S. Alan Stern[1,2], and W.F. Huebner[1], [1]Southwest Research Institute, San Antonio, TX 78228, and [2]Visiting Scientist, SwRI

There has been much interest in 2060 Chiron since observations of comet-like activity and a resolved coma established that it is a comet. Determinations of its radius range from 65 to 200 km. This unusually large size for a comet suggests that the atmosphere of Chiron is intermediate to the tightly bound, thin atmospheres typical of planets and satellites and the greatly extended atmospheres in free expansion typical of cometary comae. Under certain conditions it may gravitationally bind an atmosphere that is thick compared to its size (depending on molecular weight, temperature, heliocentric distance, and the size and mass of Chiron) while a significant amount of gas escapes to an extensive exosphere. These attributes coupled with reports of sporadic outbursts at large heliocentric distances (> 12 AU) and the identification of CN in the coma make Chiron a challenging object to model. Simple models of gas production and the dusty coma have been recently presented by several investigators (see, e.g., 1-3) but a general concensus on many basic features has not emerged. We have begun development of a more complete coma model of Chiron (4). The objectives of this paper will be to report progress on this model and give preliminary results for understanding Chiron.

Throughout its orbit, Chiron remains too far from the Sun for direct sublimation of water to be important, but CO, N_2, and CH_4 ices exhibit activity during its complete orbit (1,4). CO_2 production "turns on" only about 10 years prior to perihelion. At perihelion, on the order of a Mg/s of CO can be released even if only a small amount (few %) of Chiron's surface is active. At these activity levels, the mean free path of a CO molecule at the surface is on the order of 100 m, much smaller than the flow scale length, so the sublimating gas is collisionally coupled and the fluid dynamic approach is required.

The sublimation of a volatile like CO leads to a gas temperature close to 30 K throughout Chiron's orbit (2), far below that of a blackbody. This results in a thermal velocity that is comparable to the escape velocity (4), given uncertainities in the size and mass of Chiron, and may lead to a bound atmosphere with extensive exosphere. Other processes can heat and cool the gas (4), including photo reactions (heating), radiative cooling, collisions with grains that are hotter than the gas (heating), sublimation from icy grains, and expansion cooling of the gas. In the case of photo destruction of CO, typical rates (5) at 10 AU yield a lifetime of 4.5 years, making this a minor source of energy and ions on smaller timescales. Charge exchange with the solar wind may be an important ion source at Chiron.

The sublimating gas entrains dust particles as it leaves the surface. The dust dynamics is also influenced by the gravity and rotation of Chiron within a sphere of influence, $R_{GS} \approx 1500 R_{Chiron}$ (4). The maximum particle size that can be lifted by gas drag has been estimated to be on the order of 100 μm with CO sublimation (2). In a typical comet, once lifted off the nucleus, these particles will escape. However, considering gas production from restricted active areas and the effects of gravity on the gas, the gas density will decrease more rapidly than R^{-2} and larger particles may decouple from the gas before escape, traveling in bound orbits that may eventually fall back to the surface. The extent of the gas–dust interaction region depends on particle size and density. Based on our preliminary model, we estimate the size of this region to be on the order of a few tens of Chiron radii for 1 to 10 μm particles.

In this preliminary model of Chiron, based on one-dimensional fluid dynamics with dust (6), CO was assumed to be the only volatile. Other model parameters were $r_{hel} = 10.5$ AU, $R_{Chiron} = 120$ km, $A = 0.03$, $\rho_{Chiron} = 1$. The dust-to-gas mass ratio was 1 and two sizes of dust ($a = 1, 10\mu$m) were considered. The inclusion of dust had two important effects on the gas flow. The first was an initial mass-loading of the gas, reducing the gas velocity to subsonic values close to the surface. The second effect was a strong coupling of the gas and dust temperatures near the nucleus. Upon release, the dust heats rapidly to its radiative equilibrium value of 85 K. Collisions of molecules with dust particles heat the gas (initially at 30 K) to 75 K within a Chiron radius. This results in a terminal gas velocity about 20% higher than that calculated from a pure gas model. Additional features of the dusty coma model (including a CO_2 coma) will be discussed.

Acknowledgements. This study was supported by the NASA Planetary Atmospheres Program.

References. (1) Stern SA (1989) *PASP* **101**, 126. (2) Luu JX and Jewitt DC (1990) *Astron. J.* **100**, 913. (3) Meech KJ and Belton MJS (1990) *Astron. J.* **100**, 1323. (4) Boice DC et al. (1991) *LPSC* **XXII**, 121. (5) Schmidt HU et al. (1988) *Comp. Phys. Comm.* **49**, 17. (6) Konno I and Huebner WF (1991) *IAU Colloquium* **126**, in press.

CHAOTIC BEHAVIOR OF COMET NUCLEI by Eric Bois, Pascal Gherti, and Claude Froeschle; Observatoire de la Cafe d' Azur, Dept. CERGA, Ave. Copernic, France

Abstract:

Numerical experiments of the rotational behaviour of comet nuclei have been performed, including the Sun and Jupiter's disturbing torques in the models. In stable position, the solar torque induces great librations on comet nuclei, and Jupiter's close approach leads to a limited change on the rotational motion compared to the orbital one. But, because of the motion sensitivity to initial conditions, the rotational features can be largely perturbed. Moreover, the comet rotational behaviour is suspected to be chaotic for particular initial conditions. This phenomenon may be important when studying non-gravitational effects. The unstable configuration is characterized by great librations of the nutation angle, and the existence of a possibly large chaotic zone in the phase space.

H_2O^+ STRUCTURES IN THE INNER PLASMA TAIL OF COMET AUSTIN

T. Bonev, Max-Planck-Institut für Aeronomie, D-W-3411 Katlenburg-Lindau, Germany,
on leave from Department of Astronomy, Bulgarian Acad. Sci.

K. Jockers, Max-Planck-Institut für Aeronomie, D-W-3411 Katlenburg-Lindau, Germany

E.H. Geyer, Observatorium Hoher List, D-W-5568 Daun, Germany

To study the spatial distribution and temporal behaviour of water ions in the inner coma, comet Austin $1989c_1$ was observed with a focal reducer and tunable Fabry-Perot interferometer (FPI) at the 1m Cassagrain telescope of the Hoher List Observatory in the period Apr 30 - May 7 1990. The piezoelectrically controlled FPI has a spectral resolution of 3.7Å. Images were taken at wavelengths of 6203 and at 6199Å to register continuum and the line doublet at 6198.747 and 6200.030 Å of the 0-8-0 transition of the $\tilde{A}^2A_1 - \tilde{X}^2B_1$ electronic system of H_2O^+. At the 1m telescope the angular size of one image element is 1.6 arcsec which corresponds to approximately 600 km at the comet. The exposure time was 20 min and the time difference between individual images was 22 - 23 min.

A special formalism was applied to correct the spatial modulation of the monochromatic signal introduced by the FPI and to completely remove the continuum. The doublet structure of the emission was explicitly taken into account. The images were absolutely calibrated and converted to column densities. After the full processing cycle a portion of approximately 2×10^5 km of the cometary images remains usable. These images will be presented and discussed.

The column densities in the inner parts of these images are varying from 1×10^{11} cm^{-2} to 3×10^{11} cm^{-2} without significant correlation to the changing heliocentric distance. Sometimes the maximum of the H_2O^+ column density is offset tailwards from the optical center of the continuum emission by as much as 5000 km. Associated with the column density variations are morphological changes in the plasma distribution near the nucleus. The development of tail rays can be observed starting at a distance of 5000 km from the nucleus. By integrating the column densities across the tail at 5×10^4 km tailwards, we obtained for the number of ions per unit tail length a mean value of 3×10^{20} cm^{-1}. With an assumed outflow velocity of 35 km s^{-1} this yields a water ion production rate of 1×10^{27} s^{-1}. The mean value of the total ion content up to 5×10^5 km into the tail is 3.5×10^{30} ions. It varies from night to night, again without any significant correlation to the heliocentric distance.

A (semi-)analytical method was developed for calculating number densities from the observed column densities under assumption of axial symmetry with respect to an arbitrary axis in the image plane. During the observations the comet-Sun line was very close to the image plane, so it was possible with this method to derive densities under the assumption of axial symmetry with respect to the comet-Sun axis. This assumption is clearly not correct at the tail side of the nucleus. Model calculations found in the literature indicate, however, that it may be valid sunward of the nucleus. Using this method, we obtain on May 3 an H_2O^+ density of 200 ions cm^{-3} at a distance of 2000 km from the nucleus in the direction perpendicular to the comet-Sun line.

Probable causes for the temporal variation of the column densities and their possible relation to the observed morphological changes will be discussed.

Initial Overview of Disconnection Events in Halley's Comet 1986

J. C. Brandt, C. E. Randall, and Y. Yi
(U. Colorado/LASP)

The most spectacular of all plasma tail phenomena is the disconnection event or DE, in which the plasma tail is severed from the cometary head. Several individual DEs have been analyzed in comet Halley in order to understand the physical mechanisms involved. The number of analyzed DEs is sufficient to begin considering them in groups.

As a test of the front-side magnetic reconnection mechanism (Niedner and Brandt 1978), we can consider a specific area of the calculated heliospheric current sheet, which is projected into interplanetary space from potential models giving the magnetic field at approximately 2 $R_{\odot}$. The projected positions of the heliospheric current sheet can be checked against the direct measurements from spacecraft such as IMP-8, ICE, and PVO. We find that while the heliospheric current sheet for January through April 1986 had a complex shape which changed with the solar rotation, the gross, qualitative features remained relatively constant during this period.

Thus, we calculate that the same area of the heliospheric current sheet or sector boundary encountered comet Halley on 9 January, ~ 21 February, 15 March, and 10 April. On all four of these crossings, we find the corresponding DEs. At the times of these DEs, the solar-wind speeds were average to somewhat elevated, and the solar-wind densities were normal with the possible exception of the 10 April DE. Therefore, we conclude that the occurrence of DEs caused by front-side magnetic reconnection is a general phenomenon in cometary plasma tail dynamics.

Reference

Niedner, M. B., Jr. and J. C. Brandt, *Astrophys. J.*, 223, 655-670 (1978).

ASTEROID CLASSIFICATION WITH FIVE ECAS COLORS. D.T. Britt and L.A. Lebofsky. Lunar and Planetary Laboratory, University of Arizona, Tucson, AZ 85721.

Observations of asteroids have progressed so that many of the larger/brighter asteroids in the main belt have at least some spectral data available. These data have lead to the spectral classification of a large number of asteroids in several classification systems [1,2,3]. But a major limitation on spectral observation is the brightness of the target asteroid. Observations in the near-infrared and the blue/ultraviolet wavelengths often require long integration times because of either low solar flux or strong atmospheric attenuation. In the case of the ECAS filters the integration time required for the ultraviolet u-filter can be many times longer than the visible wavelength v-filter. This has tended to limit spectral observations to those objects that are brighter, or larger, or both. However, some major questions in asteroidal science concern compositional relationships between small and large asteroids, and between the typically small planet-crossing asteroids and main belt asteroids [4,5]. One way to address these questions is to extend the asteroid spectral classification system to smaller and/or darker (ie lower magnitude) objects such as planet-crossing asteroids. But the difficulties of observing these low magnitude objects often result in limited spectral coverage. In the case of a number of planet-crossing asteroids spectral data is only available in five colors [6]. A primary question to address is can asteroids with only five color spectral data be classified in the Tholen (1984) classification system which is based on eight color data?

The Tholen (1984) asteroid classification system used principal components analysis to quantify the spectral similarities and differences in the ECAS data set [7] and defined a system of 14 single-letter spectral classes. Shown in **Figure 1** are the first two principal components of the 8-color spectral data from 412 single letter class asteroids. The domains in statistical space occupied by each asteroid class are outlined. Most asteroid classes can be defined in terms of occupying a unique zone in statistical space. The exceptions are the E, M, and P classes which are very spectrally similar so occupy the same statistical zone, but can be recognized by strong differences in albedo. Shown in **Figure 2** are the results of the same principal components analysis using only five of the eight ECAS colors. The filters on the wavelength extremes of the ECAS system, the ultraviolet s and u-filters and the IR z-filter, have been dropped. The result of the reduced spectral information is to shift the domains of the asteroid classes and blur the distinctions between some of the classes. The A, D, Q, R, S, T, and V-classes are still well-defined by occupying unique areas in statistical space. The low-albedo B, C, G, and G-classes were close to each other in the 8-color statistics and the reduced filter set moves these classes into overlaping zones in statistical space. The E, M, and P-classes also overlap the domain the the C-class. Another limitation of this reduced spectral data set would be increased difficulties in determining the olivine/pryoxene ratio in S-type asteroids. The five-color asteroid spectral data can be used to uniquely classify objects into seven of the fourteen asteroid spectral classes. For the other classes this limited spectral data can be used to narrow the possible classifications and identify interesting objects for more intensive observations.

References: [1] Tholen D.J. (1984) Ph.D. Thesis, Univ. of Ariz. [2] Barucci M.A. et al. (1987) *Icarus 70*, 304. [3] Tedesco E.F. et al. (1989) *Astron. J.* 97, 580. [4] Bell J.F. et al. (1989) *Asteroids II*, 921. [5] McFadden L.A. et al. (1989) *Asteroids II*, 442. [6] Cruikshank D.P. et al. (1991) *Icarus 89*, 1 [7] Zellner D.J. et al. (1985) *Icarus 61*, 355.

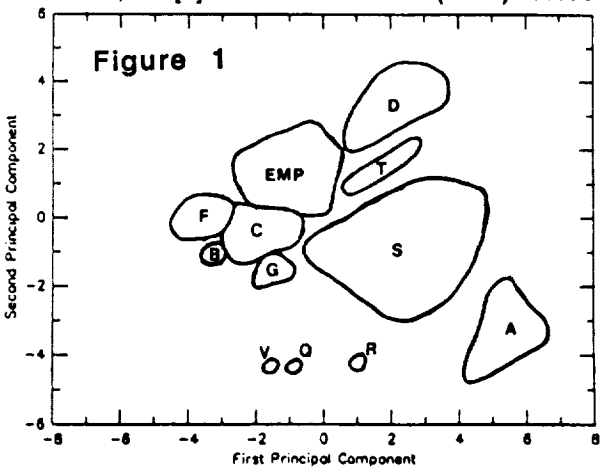

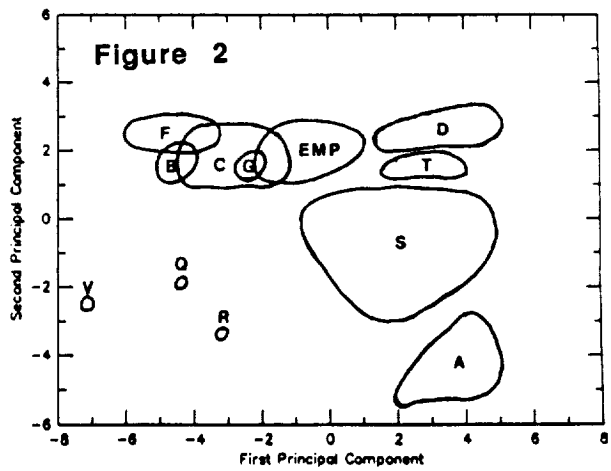

OBSERVATIONS OF THE VELOCITY AND SPATIAL DISTRIBUTIONS OF HYDROGEN IN COMETS AUSTIN AND LEVY

M.E. Brown and H. Spinrad, Univ. of Cal. at Berkeley

We have obtained high resolution ($\sim$ 0.05Å) long-slit spectra of Hα 6562Å emission in comets Austin and Levy. Hα is excited by solar Lyβ emission and provides direct information about the spatial and velocity distribution of hydrogen, a probable daughter and grand-daughter product of H_2O. We model the hydrogen velocity distribution assuming simple radial outflow with velocity contributions from 20 km/sec (product of $H_2O + \gamma \rightarrow H + OH$ reaction), 8 km/sec (from $OH + \gamma \rightarrow H + O$), and 4 km/sec (from collisional thermalization in the dense nuclear region) components. Previous observations of cometary Hα have not had sufficient spectral resolution to disentangle the different velocity components of the hydrogen (Magee-Sauer, Ph.D. thesis, 1988). Our observations are of sufficient quality to show that all three velocity components are important: The velocity profile from our Austin spectrum of 14 May 1990 (UT) contains a narrow core that cannot be fit without some contribution from a slow thermal component. In addition, the profile has distinct high velocity wings that require a substantial fraction of gas to be at a minimum of 20 km/sec. The Levy velocity profile, observed on 12 September 1990 (UT), shows a similar distribution in the central 200 km, but on the sunward side, from about 200 km to 2500 km, the emission is dominated by even faster hydrogen with a velocity of approximately 35 km/sec. Possible causes for this unusual and unexpected fast component will be discussed. Comets Austin and Levy also differed in their spatial distribution of hydrogen. Austin showed an unusual distribution: the gas emission was confined to a spatial region that was even narrower than the region of dust emission. The peak of hydrogen emission was also observed to be shifted 150 km to the tail side of the peak of dust emission. Levy showed a different distribution: the hydrogen was more widely distributed than the dust, consistent with the large-scale distributions observed in Lyα images of previous comets.

Implementation of Moving-Target Programs

Marc W. Buie, Space Telescope Science Institute, 3700 San Martin Drive, Baltimore MD 20771

NO ABSTRACT AVAILABLE

N91-25987

CCD Photometry of 2060 Chiron, 1991 January

B.J. Buratti, R.L. Marcialis (JPL/Caltech)
E.S. Howell, M.C. Nolan (LPL/U. Arizona)

2060 Chiron was observed on UT 1991 January 07–08 with the Mt. Palomar 1.52-m telescope in the Gunn-R passband. On-chip field stars were used to perform differential reductions. The repeatability of the 5.9-hour light curve was excellent, both within a night and from night to night. No evidence for short-term (~day) secular variations similar to those seen last year by both Luu and Jewitt (1990) and Buratti and Dunbar (1991) is seen in the new light curve.

Chiron's rotational light curve appears strikingly similar to that obtained a year earlier by Luu and Jewitt (1990), both in amplitude (0.04 mag) and shape. Both light curves show strongly correlated changes over a timescale of perhaps 15 minutes (*e.g.* UT 10.4 and 11.2, below). These same features were marginally visible in the 1986 light curve (Bus *et al.* 1987). We believe such behavior is evidence that Chiron may be more aspherical than the 4% intensity variation might otherwise indicate, and favors a viewing geometry where the subearth latitude is rather low. Chiron was much fainter in 1985, when a partial light curve was obtained by Marcialis. Due to the lower sampling rate of these early data, no conclusions can be made regarding the high-frequency lightcurve structure back then. All three of these light curves differ significantly from that obtained by Buratti and Dunbar (1991), one week before the observations of Luu and Jewitt. The difference may be attributed to the fact that the Buratti and Dunbar data were obtained at the end of a short-term outburst, when the nucleus was most obscured by coma.

The Chiron field was calibrated using Landolt standards on UT 1991 March 15. We find a mean R-magnitude of 15.6 ± 0.1 (preliminary result). This is somewhat brighter than expected, based upon a "smooth" fit to the object's recent "nonasteroidal" variations.

Variability of 2060 Chiron has been demonstrated over timescales of minutes, hours, years, and as shown by the accompanying paper of Bus *et al.*, even several decades. We encourage an intense campaign to monitor the photometric behavior of Chiron throughout the 1990's, and can state that the only "secular" trends seen so far is that Chiron becomes both more interesting and more perplexing with time. (Work performed under contract to NASA).

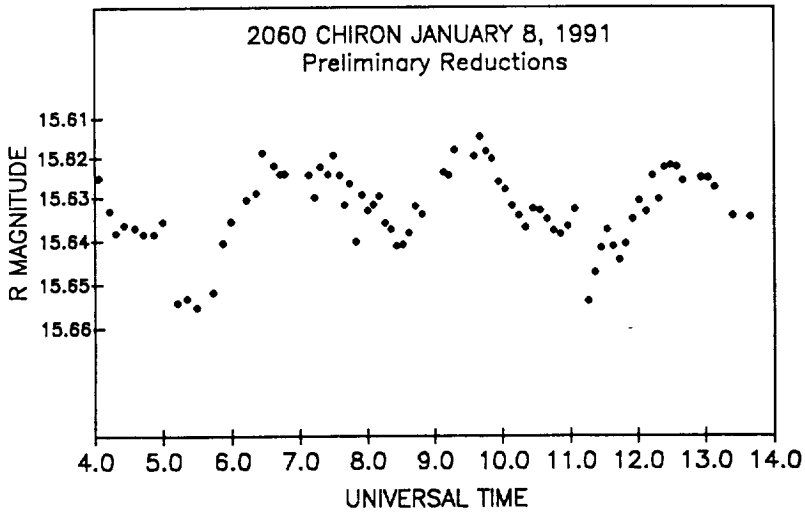

References:

Buratti, B.J. and Dunbar, R.S. (1991) *Astrophys. Jour.* **366**, L47–L49.
Bus, S.J., Bowell, E., Harris, A.W., and Hewitt, A.V. (1989) *Icarus* **78**, 211.
Luu, J.X. and Jewitt, D.C. (1990) *Astron. Jour.* **100**, 913.
Marcialis, R.L. (1989) *Bull. Amer. Astron. Soc.* **21**, 965.

CHIRON: EVIDENCE FOR HISTORIC COMETARY ACTIVITY

Schelte J. Bus and Edward Bowell (Lowell Observatory),
S. Alan Stern (University of Colorado),
Michael F. A'Hearn (University of Maryland)

The non-asteroidal brightening of (2060) Chiron, first noted by Tholen in 1988 (*IAUC* 4554), is now ascribed to cometary activity. Photometry since 1988 has revealed a broad surge in brightness that peaked in 1989 about 1.0 mag above the brightness in the mid-1980s. The surge is evidently due to the sporadic formation of a dust coma, which is itself driven by the presence of extremely volatile ices at or near the surface. We note that CN emission has recently been reported (Bus *et al., Science* **251**, 774–777, 1991; see also Cochran and Cochran, *Icarus* **90**, 172–175, 1991). Since Chiron is now nearing perihelion (at 8.5 AU heliocentric distance), there is interest in determining whether it has exhibited anomalous brightening in the past, particularly at greater heliocentric distances. It should thereby be possible to refine our understanding of the surface processes occurring on Chiron and the mechanisms generating comatic activity.

Photographic plates dating back to 1895 are known to contain images of Chiron. Using some of this archival material, we present the initial results of a project to determine Chiron's brightness history over orbital timescales. Because of excessive trailing and poor quality of the emulsions, some of the oldest plates are amenable only to rough photographic photometry, but they may still be valuable in placing useful limits on Chiron's historical cometary activity. We have so far examined a particularly homogeneous and high-quality set of plates taken prior to and around the time of Chiron's discovery in October 1977 at the 1.2-m Oschin Schmidt telescope at Palomar Mountain Observatory. Images of Chiron have been identified and digitized using a PDS microdensitometer, and images of field stars around Chiron have been both similarly digitized and photometrically calibrated using recently acquired B- and V-band CCD frames. Plotted below is the V-band absolute magnitude H_V of Chiron versus date and heliocentric distance. Points shown between 1978 and 1989 are from the tabulation by Hartmann *et al.* (*Icarus* **83**, 1–15, 1990). As a result of the present work, eleven new data, including estimated errors, have been added between 1969 and 1977. They indicate Chiron to have been as bright or brighter in the early 1970s—at a heliocentric distance of 18.9 AU and very close to aphelion—than during the current outburst. The implication that Chiron can be active at any heliocentric distance in its present orbit suggests that the active volatile is either N_2, CH_4 or CO, and that a substantial degree of mantling may have developed (cf. Stern, *Publ. Astron. Soc. Pacific* **101**, 126–132, 1989). We will present further historical data, discuss the error bars, and suggest possible mechanisms for the observed activity.

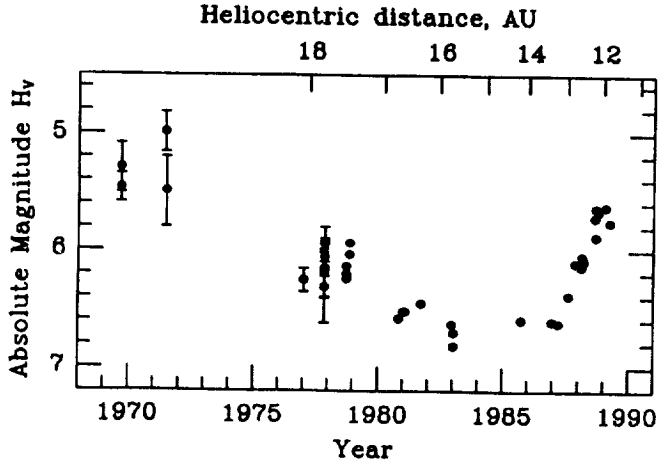

Research supported, in part, by NASA grant NAGW-1470.

N91-25989

The Dust Coma of Comet Austin (1989c1)

H. Campins, S. C. Tegler (University of Florida),
C. M. Telesco and C. Benson (NASA-MSFC)

Thermal-infrared (10 and 20 micron) images of Comet Austin were obtained on UT April 30.6, May 1.8, 2.8, and 3.6, 1990. We used the NASA-Marshall Space Flight Center 20-pixel bolometer array at the NASA 3-meter Infrared Telescope Facility in Hawaii. We obtained 10.8 micron (FWHM = 5.3 microns) maps with maximum dimensions of 113 arcsec (57,5000 km.) in R.A. and 45 arcsec (23,000 km.) in Declination, with a pixel size of 4.2x4.2 arcsec. A smaller, 45x18 arcsec,map was obtained in the 19.2 micron (FWHM = 5.2 microns) bandpass. At the time of these observations Comet Austin's heliocentric and geocentric distances were 0.7 AU and 0.5 AU respectively. The peak flux density (within the brightest pixel) was 23 ± 2 Janskys for the first three dates and only marginally lower the last day; i.e., within the observational uncertainties we found no evidence for day-to-day variability like that observed in Comet Halley.A dynamical analysis of the morphology of the extended dust emission is used to constrain the size distribution and production rate of the dust particles. The results of this analysis are compared with similar studies carried out on comets P/Giacobini-Zinner, P/Brorsen-Metcalf, P/Halley, P/Tempel 2, and Wilson (1987l).

THE SIZE DISTRIBUTION OF ASTEROIDS FROM IRAS DATA

A. Cellino (1), P. Farinella (2), and V. Zappala' (1)

(1) Osservatorio Astronomico di Torino
strada Osservatorio 20
I-10025 Pino Torinese (TO) (Italy)
(2) Dipartimento di Matematica
Universita' di Pisa
via Buonarroti 2
I-56127 Pisa (Italy)

Taking profit of the whole IRAS data base on asteroid diameters and albedos, we have analyzed the overall size distribution of asteroids, on the basis of different statistical methods aimed to derive reliable diameter estimates for the objects lacking an individual IRAS observation. We find that asteroids belonging to dynamical families and to the Flora region show a different behavior with respect to the rest of the asteroid population. In fact, apart from the Flora region, non-family asteroids have always size distributions characterized by a strong change in slope at diameters around 150 km, with the differential power-law distribution exponent passing from values around 3 or more at large sizes, to about 1 at smaller ones. On the other hand, in the Flora region, as well as for family asteroids, a steep slope is observed also at small sizes. We stress the importance of the present results for further studies of the process of collisional evolution of asteroids.

GROSS-FRAGMENTATION OF METEOROIDS AND BULK DENSITY OF GEMINIDS FROM PHOTOGRAPHIC FIREBALL RECORDS; Z.Ceplecha, Astronomical Institute, Czechoslovak Academy of Sciences, 251 65 Ondrejov, Czechoslovakia; R.E.McCrosky, Smithsonian Astrophysical Observatory, 02138 Cambridge, USA.

The explicit solution of the drag and ablation equations of a single non-fragmenting meteoroid moving in any actual atmosphere was generalized by allowing for one or more points, where a sudden gross fragmentation can occur. Using this generalized solution, the distances along the meteoroid trajectory can be computed for any choice of input parameters and compared with the observed distances flown by the meteoroid. For the most precise and long fireball trajectories, the least--squares solution can thus yield the initial velocities, the ablation coefficients, the positions of gross-fragmentation points and the terminal mass. At a gross-fragmentation point, the ratio of the main mass to all the remaining fragments can be computed. The photometricly-determined meteoroid mass can be compared with the dynamic mass determined from our gross-fragmentation model and thus the meteoroid bulk density can be evaluated.

This gross-fragmentation model was used for computation of bulk densities of the Geminid meteoroids. From all the Prairie Network (PN) Geminids, only two (G15 and G54) have enough long and deep trajectories, enough observed change of velocity and enough precise heights and lengths measured for individual time-marks, that they allow the complete application of our gross-fragmentation model. If the previous non-gross-fragmentation model was used for G15 and G54, the time sequence of residua of the solutions exhibited a prevailing systematic part ($\doteq$ 80%) and the bulk densities came out close to 1.0 g/cm^3. If the new gross-fragmentation model was applied to the same observational data, the systematic part of the time sequence of residua was completely gone and the bulk densities resulted in 3 to 4 gr/cm^3. Thus the value of the bulk density of Geminids, 1 g/cm^3, advocated for a long time and determined by indirect methods, may have been caused by neglect of the gross-fragmentation effects on the meteoroid motion. This may, of course, hold also for about 25% of PN fireballs, which exhibit a systematic part in the time sequence of residua of the non--gross-fragmentation solutions. The gross-fragmentation model should be applied to all suitable PN fireballs with such systematic residua in non-gross-fragmentation solutions.

We applied the same gross-fragmentation model to the terminal part of the Lost City fireball data. The bulk density, the rough position of the fragmentation point, the shape coefficient and the terminal mass are known in this case and since their values computed from our gross-fragmentation model came out quite close to this reality, the bulk densities of G15 and G54 Geminids are about 3 or 4 times greater than densities of the Geminid meteoroids postulated so far.

Why use Space Telescope?

Clark R. Chapman, Planetary Science Institute, 2421 E. Sixth Street, Tucson AZ 85719

NO ABSTRACT AVAILABLE

GASPRA: THE SCIENTIFIC ISSUES

Clark R. Chapman and Donald R. Davis, Planetary Science Inst., 2421 E. 6th St., Tucson, AZ 85719

As we write, *Galileo*'s final Gaspra encounter parameters have not been determined nor is the spacecraft even healthy. Here we outline some scientific issues about main belt asteroids (especially S types) that can be addressed if the prime objectives for the camera (SSI) and NIMS instruments are met this October. They include: (a) one high resolution (full frame) picture at ~90 phase; (b) multi-filter images at moderate resolution; (c) resolved imaging throughout a rotation period; and (d) low phase angle IR spectral mapping by NIMS (few dozen resolved nimsels).

Calibration of Ground-based Observations. As the first asteroid to be studied closely by spacecraft, it is important to learn how well our pre-encounter inferences about Gaspra represent reality. In a 7 December 1990 *Galileo* Project memo prepared by one of us (CRC), various physical parameters were proposed for adoption as "nominal." These include the oft-quoted, but highly uncertain, 16 km diameter (it is more likely to be smaller than larger), values for spin period, axis orientation, and body shape. Groundbased observers may improve on these estimates during Gaspra's current apparition. We need to assess how well we have done and where we went wrong so we can understand how reliably we can trust groundbased results for *other* asteroids, which is all we will ever have for most of them.

Compositional Nature of S-Types. Gaspra appears (from 8-color photometry) to be an olivine-rich S-type, which contrasts with pyroxene-rich Ida (*Galileo*'s second asteroid target). The two objects should roughly bracket the range of S-types. If Gaspra is geochemically differentiated, most models suggest that it could well show prominent mineralogical variations reflecting the differentiation process. SSI multispectral images should reveal and distinguish units that are metal-rich, pyroxene-rich, and olivine-rich; if units are of large enough spatial scale, NIMS can obtain refined and mineralogically diagnostic spectra of them. Silicate variations can be interpreted in terms of differentiation using the interpretational approach that Gaffey (1984, *Icarus*, **60**, 83) first applied to hemispheric data of Flora. Conceivably, Gaspra either (a) is a monomineralic fragment or (b) has compositional variations on a scale of less than a few 100 meters, in which case the issue of primitive vs. differentiated nature may go unresolved.

Collisional/Cratering History. Gaspra is almost certainly a fragment of a larger body according to standard calculations of collisional lifetimes; it may be a "Flora family" member. Its highly irregular shape (compatible with 1989 PB-like duplicity or "rubble-pile" structure) may, at high resolution, reveal much about the fragmentation process. For a wide variety of possible projectile populations, and independent of whether Gaspra is a "fresh" fragment or overdue for collisional disruption, the observed crater population (including degradation states and density variations) should be interpretable in terms of the as-yet-unknown production function. Gaspra must be in a state of quasi-saturation equilibrium. It is not clear that the age of the body or its inherent strength can be determined from *Galileo* data.

Surface Morphology. Gaspra is the first case for studying questions of regolith retention, development, and character on a small, heliocentric body (it is near the threshold size for a strong body to retain regolith according to Housen *et al.*, 1979, *Icarus*, **39**, 317). Surface morphology on an iron-rich object, which Gaspra may be, is particularly uncertain.

THE LIFETIME OF BINARY ASTEROIDS VS. GRAVITATIONAL ENCOUNTERS AND COLLISIONS

B. Chauvineau (1), P. Farinella (2), and F. Mignard (1)

(1) Observatoire de la Côte d'Azur, Avenue Copernic, 06130 Grasse, France
(2) Dipartimento di Matematica, Università di Pisa, via Buonarroti 2, I-56127 Pisa, Italy

Abstract. In this paper we investigate the effect on the dynamics of a binary asteroid of the near encounter with a third body. The dynamics of the binary is modelled by the two-body problem perturbed by an approaching body in the following ways: either direct collisions with a component of the binary or near encounters. In the case of collisions, two sub-cases are examined: collisional ejection and collisional disruption. In the case of gravitational encounters, three sub-cases are considered: very close, close and far encounters. In each case, the typical value of the two-body energy variation is estimated, and a random walk for the cumulative effect is assumed. The results are applied to the cases of 146 Lucina, 216 Kleopatra, 532 Herculina and 1220 Crocus which are binary candidates. The main conclusion is that the collisional disruption is the dominant effect, giving lifetimes comparable with the age of the solar system.

ON THE EFFECTS OF THE OBSERVATIONAL SELECTION IN THE MODERN DISCOVERIES OF ASTEROIDS

N.S.Chernykh, Crimean Astrophysical Observatory

The sample of the numbered minor planets discovered at the Crimean Astrophysical Observatory is discussed and compared with the asteroid "collections" of some other observatories. The statistical features of the examined samples are found to be similar despite of the variety of the observational conditions depending on the geographical positions of the observatories, used telescopes and techniques, etc. It follows that the selection effects must be here the same for all considered samples.

Sincerely N.Chernykh

THE TRIPLET $d^3\Delta - a^3\Pi_r$ AND ASUNDI $a'^3\Sigma^+ - a^3\Pi_r$ BANDS OF THE NEUTRAL CO IN THE COMET SCORICHENKO-GEORGE($1989e_1$) SPECTRUM.
K. I. CHURYUMOV, ASTRONOMICAL OBSERVATORY OF KIEV SHEVCHENKO UNIVERSITY

The comet Scorichenko-George ($1989e_1$) spectrum obtained by V. L. Afanas'ev, A. I. Shapovalova and the author with the help of a TV spectral scanner of the 6-m reflector (BTA) at the Spectral Astrophysical Observatory of the USSR Academy of Sciences (Pastukhov's Mount) shows to have the emission bands of the triplet and Asundi systems of the neutral CO. This leads to suggest the comet nucleus includes the formaldehyde H_2CO or polyformaldehyde $(H_2CO)_5$ which gives birth to HCO^+-ions which if recombined and photodissociated result in CO-radicals at $d^3\Delta$ and $a'^3\Sigma^+$ levels necessary to exite the CO-emissions in the triplet and Asundi system bands. The peculiarities of the rate production of CO-gas and the lightcurve of Comet Scorichenko-George ($1989e_1$) are discussed.

SOLAR ACTIVITY INFLUENCE UPON THE LIGHT CURVE OF COMETS P/HALLEY (1986 III) AND P/CHURYUMOV-GERASIMENKO (1982 VIII).
K. I. Churyumov, Astronomical Observatory of Kiev Shevchenko University, V. S. Filonenko, Astronomical Observatory of Khar'kov University

It is shown that despite the negative results obtained by Prof. S. V. Orlov about the absence of a correlation between the total brightness variations of Comet P/Halley (1910 II) and solar activity (Wolf number) Comet P/Halley (1986 III) total brightness correlates with changes in the solar activity indices and the solar wind velocity.

A statistically reliable correlation between the outbursts of brightness and brightness variations of the shortperiodic Comet Churyumov-Gerasimenko (1982 VIII) and the level of the solar activity have been found out.

DUST AND GAS JETS. EVIDENCE FOR A DIFFUSE SOURCE IN HALLEY'S COMA

J. Clairemidi , P. Rousselot , F. Vernotte , G. Moreels, Observatoire de Besançon, BP 1615, 25010 Besançon Cedex, France

Monochromatic images constructed in using the data obtained with the Vega 2 three-channel spectrometer provide the spatial distributions of molecular and dust-scattered intensities inside the field of view scanned by the instrument, which is an angular sector centered on the nucleus having an aperture of 50° and an extension of 40 000 km. Two well-contrasted jets appear in the monochromatic images at the wavelengths of molecular emissions : OH, NH, CN, C_2, C_3. At the same locations, dust jets are also present. Dust jets are less apparent because the dust solar-scattered intensity decreases with cometocentric distance as $r^{-\alpha}$ with $1<\alpha<1.6$ and is very weak at r= 20000 to 40000 km, if compared to the intensity close to the nucleus. The spatial distributions and radial profiles of the solar-scattered intensity at 377, 482 and 607 nm are presented. A pixel-to-pixel ratio of these images shows that the intensity of continuum is slightly colored : bluer close to the jets in the 20000-30000 km region and redder between the jets in a region called "valley" at distances smaller than 30000 km.

Present observations provide a good evidence for the existence of a diffuse source responsible for the release of molecules that build the gas jets and form the CO extended source measured by the Giotto NMS experiment. Following a Mie calculation, the coloration of the continuum shows that the dust grains have a submicronic size. They constitute a population of tiny grains which was detected by the dust-impact analysers of Giotto and Vega at distances of 20000 to 40000 km. In this range, on the sunlit part of the coma, dust models predicted a cut-off at the lower mass end of the particle mass distribution function which was not observed. The figure below gives two log-log intensity distributions of dust-scattered continuum at 482 nm along two radii in the more contrasted jet (C) and in the valley (D). The distributions of OH (A) and CN (B) at their maximum has also been plotted.

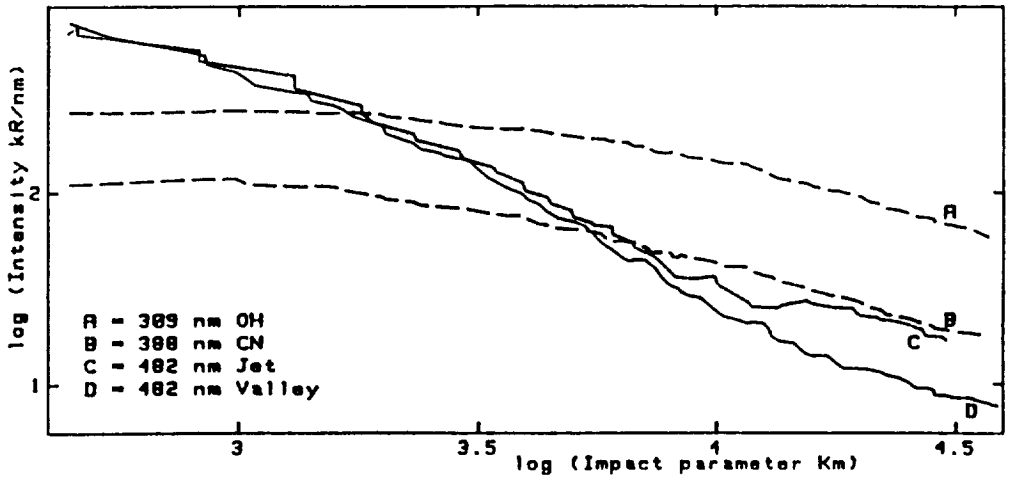

The Coma of Comet P/Schwassmann-Wachmann 1

Anita L. Cochran and William D. Cochran
Astronomy Department and McDonald Observatory
The University of Texas
Austin, TX 78712

We have obtained spectra of comet P/Scwhassmann-Wachmann 1 (SW1) during observing runs in December 1989 and December 1990. The data were obtained using the Large Cass Spectrograph (LCS) on the 2.7 m telescope of McDonald Observatory. The LCS has a long slit and images onto a TI 800 × 800 CCD detector. During both runs, the comet was extended and a CO^+ coma was detected. In addition, we detected emission due to CN and an unknown species during the December 1989 observations but *not* during the December 1990 observations.

During December 1990, we observed the strengthening of the CO^+ emissions by a factor of 2.5 in the course of one day. However, during this time, the continuum magnitude remained unchanged.

We will present these data and discuss the implications for formation of the CO^+. We can rule out photoionization of CO to form the observed CO^+ in SW1. We will also demonstrate evidence for non-equilibrium conditions in the CO^+ coma of this comet.

OBSERVATIONS OF COMETARY PARENT MOLECULES WITH THE IRAM RADIO ELESCOPE; P. Colom, (Observatoire de Paris-Meudon), D. Despois (Observatoire e Bordeaux), G. Paubert (IRAM, Granada), D. Bockelee-Morvan and J. Crovisier Observatoire de Paris-Meudon).

Spectroscopic observations at millimetre wavelengths of comets /Brorsen-Metcalf 1989 X, Austin 1989c1 and Levy 1990c were conducted at he IRAM 30-m radio telescope. Hydrogen cyanide (HCN), already detected in /Halley, was observed through two transitions. Formaldehyde (H2CO) was nambiguously identified. Hydrogen sulfide (H2S) and methanol (CH3OH) were etected for the first time in comets, through several transitions. In ddition, observations of the transitions of several other molecular species HC3N, H2CS, SO2, OCS...) were unsuccessful, but yielded significant upper imits.

The possibility to observe several transitions of the same species t a time (up to 12 transitions of CH3OH were observed) gives stringent onstraints on their excitation conditions. The observed molecules appear o be rotationally relaxed, as expected from excitation models.

HCN and H2S are minor species, with production rates relative to ater of 0.3 to 1.8 10^-3 for HCN (depending on the comet), of 2 10^-3 for 2S. H2CO, if one assumes it is a parent molecule, has a production rate of .4 to 4 10^-3 that of water (depending on the comet), which is at least one rder of magnitude smaller than the production rates of H2CO in comet Halley nferred from infrared and centimetric radio observations. CH3OH is a more bundant species with a production rate about 10^-2 that of water; this mplies that the vibrational bands of CH3OH should significantly contribute o the cometary 3.2-3.6 micron emission.

The existence of these interstellar molecules in cometary nuclei, he absence of others (SO2, OCS...), the cold storage implied by the resence of species with low sublimation temperatures (such as H2S) are onstraints which will have to be taken into account in order to achieve a onsistent scenario of the formation of cometary material and cometary uclei.

The Appearance of the 7.4-day Periodic Variation in the Spatial Profiles of C_2, CN, NH_2 and $O(^1D)$ in Comet Halley

Michael R. Combi[1] and Uwe Fink[2]

[1] Space Physics Research Laboratory, University of Michigan
Ann Arbor, MI, USA
[2] Lunar and Planetary Laboratory, University of Arizona
Tucson, AZ, USA

Spatial profiles of C_2, CN, NH_2 and $O(^1D)$ in comet P/Halley taken on April 14.3 and 15.3, 1986 show clear evidence of the effects of the 7.4-day periodic variation seen in photometric observations. The profiles show unusually large changes in shape between the two nights. Analysis with the usual steady-state models would require unphysically large changes in scale lengths. However, a time-dependent model for the spatial distributions of neutral species in comets does show that the unusual shapes are caused by the 7.4-day periodic variation in gas production seen in photometry. The time-dependent production rate at the source was adapted from the "C_2 light curve" of Schleicher, et al. (1990, *Astron. J.* **100**, 896-912). Variations in the profile shapes are directly accounted for by the periodic variations in gas production. Furthermore, we are able to reproduce the highly variable profiles with a model that uses only standard scale lengths reduced to the appropriate heliocentric distance (1.38 AU) and adopted from observations of Halley and other comets. There is a small phase lag of about 6 hours between the photometric light curve and the actual source rate time dependence. This expected phase lag is attributable to the filling time of the gas in the photometric aperture. An amplitude for the variation in gas production, which is 20% larger than that present in the photometry, is also required. This is quite consistent with the photometric aperture time smear. Although CN, C_2, OH and dust continuum seem to show the same variations, this is the first demonstration that NH_2, which is the likely dissociation product of NH_3, and $O(^1D)$, which is a direct tracer of H_2O in the inner coma, also follow the same time dependence.

Asteroids, Comets, Meteors 1991: Flagstaff, Arizona, June 24-28, 1991

RADIO SPECTROSCOPY OF COMETS: RECENT RESULTS AND FUTURE PROSPECTS; J. Crovisier (Observatoire de Paris-Meudon).

After the P/Halley observing campaign, cometary radio astronomy entered a new phase recently with the observations of P/Brorsen-Metcalf 1989 X, Austin 1989c1 and Levy 1990c. Successful spectroscopic observations were conducted at millimeter and submillimeter wavelengths with three different instruments (Institut de Radio Astronomie Millimetrique, Caltech Submillimeter Observatory and Swedish-ESO Submillimetre Telescope).

Hydrogen cyanide (previously detected in comets Kohoutek 1973 XII and P/Halley) and formaldehyde (previously tentatively identified in P/Halley) were observed in the three comets. Two new cometary molecules were identified in comets Austin and Levy: hydrogen sulfide and methanol. to test excitation models. They significantly increase the credibility of the molecular production rate determinations.

The abundances relative to water of these molecules are of the order of 10^-3 for HCN and H2S, of a few 10^-3 for H2CO, of 10^-2 for CH3OH. Radio spectroscopy has thus access to relatively minor constituents as well as to relatively complex species such as methanol. This technique appears to be a powerful tool for studying the chemical composition of the coma. It seems probable that several other molecular species (or ions) could still be observed. The future prospect of cometary radio spectroscopy, at centimetric, millimetric and submillimetric (for both ground-based and space instruments) wavelengths, will be reviewed.

THE GREAT ASTEROID NOMENCLATURE CONTROVERSY OF 1801

Clifford J. Cunningham
250 Frederick St., Apt. 1707
Kitchener, Ontario
Canada N2H 2N1

In 1801 the first asteroid was regarded by most astronomers as the eighth planet of the solar system. The name to be assigned to such an important object thus assumed great significance. Its discoverer, Giuseppe Piazzi, fought hard for his right to name the object Ceres Ferdinandea. Pitted against him were German astronomers who had assigned the name Hera to the object before it had even been discovered, and French astronomers backed by none other than Napoleon, who took an active interest in the discovery. Even the popular press of the day was used to promote alternate names. The presentation of the development of this controversy is based on the original publications and letters of Europe's foremost astronomers.

THE MINOR PLANET INDEX TO SCIENTIFIC PAPERS

Clifford Cunningham
250 Frederick St., Apt. 1707
Kitchener, Ontario
Canada N2H 2N1

DESCRIPTION

For the first time, a comprehensive index is available to minor planet researchers. The Minor Planet Index to Scientific Papers includes virtually every paper published on the subject of minor planets in the 20th century. Several hundred references from the 19th century are also included.

In all, there are nearly 12,000 entries in the Index. It is updated frequently, ensuring the most timely list available at the time of purchase. Each entry contains the following data (as applicable): name of journal, book, magazine or newspaper; title of paper, article or dissertation; author(s); date; volume number or circular number; page number. Additional fields being added are a keyword field and one containing the numbers of all the asteroids under study in each paper.

The Index has a wide scope. In addition to papers specifically dealing with asteroids, papers on related topics are included. These include the extinction (impact) theory, meteorites and comets. All doctoral theses, books, and magazine articles are included, as well as the New York Times and Times of London database. This Index is far more comprehensive than Astronomy & Astrophysics Abstracts.

AVAILABILITY

Order forms for the Index are available from the author. With the use of a database management program purchasers may search or sort the database on any field or combination of fields. Since the database exceeds two megabytes, it is compressed and placed on one 1.2 Meg IBM-compatible 5.25-inch floppy disk. Formats available include ASCII, dBASE, WordPerfect and Lotus. A bound, laser-printed version is also available. It includes the entire index sorted three ways: alphabetically by author, alphabetically by journal, and chronologically. The laser print version costs U.S. $100, versus U.S. $40 for the floppy disk version.

Orbital evolution studies of asteroids near the 4:1 mean motion resonance with Jupiter

M.Dahlgren †, *G.Hahn* ‡, *C.-I.Lagerkvist* †, *M.Lundström* †

† *Astronomiska Observatoriet, Box 515, S-75120 Uppsala, Sweden.*
‡ *Dept. of Astronomy, The University, Manchester M13 9PL, U.K.*

The orbits for ten asteroids with their present osculating semimajor axises near the 4:1 mean motion resonance with Jupiter have been integrated 200 000 years into the future. The integrations were made with the 15th order RADAU integrator and perturbations due to all planets from Venus to Neptune were taken into account. The integrated asteroids are all close to the resonance at a=2.065 AU, including two Amor- and five Mars-crossing asteroids.

The aim of this investigation is to study the evolution of asteroids in the neighbourhood of the 4:1 resonance and the timescales of the removal of the asteroids from the resonance. To what extent the resonance is a source region of the Athen-, Apollo- and Amor asteroids and on what timescales the transitions between the different classes occur is also an interesting aspect to be considered in this study. Comparison will also be made with our earlier investigation of the 5:2 resonance.

OBSERVATIONS OF COMET LEVY 1990c IN THE [OI] 6300Å LINE WITH AN IMAGING FABRY-PEROT

C. Debi-Prasad, K. Jockers, H. Rauer, Max-Planck-Institut für Aeronomie,
D-W-3411 Katlenburg-Lindau, Germany

E.H. Geyer, Observatorium Hoher List, D-W-5568 Daun, Germany

We have observed the comet Levy 1990c during 16-25 August 1990 using the MPAE focal reducer system based Fabry-Perot etalon coupled with the 1 meter telescope of Observatory of Hoher List. The free spectral range and resolution limit of the interferometer was $\sim$ 2.18 Å and $\sim$ 0.171 Å respectively. Classical Fabry-Perot fringes were recorded on a CCD in the cometary [OI] 6300 Å line. They are well resolved from telluric air glow and cometary NH_2 emission. Our observations indicate that the [OI] is distributed asymmetrically with respect to the center of the comet, extending further into the tail direction. We report the spatial distribution of [OI] emission and its line width in the coma of comet Levy and an estimate of the H_2O production rate. We also address the question of parent molecule of $_1D$ O at regions far away from the nucleus.

INTERPLANETARY MAGNETIC FIELD CHANGES AND CONDENSATIONS IN COMET HALLEY'S PLASMA TAIL

M. Delva, H. Lichtenegger, K. Schwingenschuh,
Institut fuer Weltraumforschung, Graz, Austria

In a time-dependant 3 dimensional MHD simulation for cometary plasmas, Schmidt-Voigt (1988) could observe the formation of condensations in the plasma tail after a 90 degree change in the interplanetary magnetic field (IMF) sweeping over the comet. From the Vega-SC, IMF measurements are available in high resolution in the vicinity of the comet. We here investigate these data for 90 degree changes in the direction and study the relation between them and optical observations of condensations in the plasma tail of Comet Halley.

THE ORIGIN AND EVOLUTION OF THE ZODIACAL DUST CLOUD.

S. F. Dermott, D. Durda, R. S. Gomes, B. Gustafson, S. Jayaraman, and Y-L Xu, Department of Astronomy, University of Florida, Gainesville, FL 32611

P. D. Nicholson, Department of Astronomy, Cornell University, Ithaca, NY 14853.

We have now analysed a substantial fraction of the IRAS observations of the zodiacal cloud. We have also developed a numerical model, the SIMUL model, that allows us to calculate the distribution of night-sky brightness that would be produced by any particular distribution of dust particle orbits. This model includes the effects of orbital perturbations by the planets and solar radiation, it reproduces the exact viewing geometry of the IRAS telescope, and allows for the eccentricity of the Earth's orbit. The result is a model for the variation with ecliptic latitude of the brightness observed in a given waveband as the line of sight of the telescope sweeps through the model distribution of orbits at a constant elongation angle (Dermott and Nicholson, 1989). We are now using SIMUL to model not just the solar system dust bands discovered by IRAS but the whole zodiacal cloud. Our model is based on (a) the observed distribution of asteroidal orbits, and (b) the calculated distributions of orbital elements of the dust particles after allowance for the secular perturbation of these orbits by the planets, light pressure, and Poynting-Robertson light drag.

Our main achievement this year has been the development of a new secular perturbation theory that describes the variations of the eccentricities, inclinations and semimajor axes of dust particle orbits and incorporates the effects of gravitational forces due to the planets and those due to solar radiation. In our new theory (Gomes and Dermott, 1991), the classical concepts of forced and proper elements still hold good, but the magnitudes of the forced elements no longer depend on the semimajor axes of the dust particle orbits alone, they also depend on the drag rates of the particles and thus on their sizes and orbital histories. With this new theory, we have been able to: (1) Account for the observed inclination of the background zodiacal cloud; (2) Relate the distribution of orbital elements of asteroids in the Hirayama families to the observed shapes of the IRAS solar system dustbands; (3) Show that there is clear ***observational*** evidence in the IRAS data for the transport of dust particles from the asteroid belt to the Earth.

Dermott, S.F., and Nicholson, P.D. Highlights of Astronomy, **8**, 259–266, 1989.

Gomes, R.S., and Dermott, S.F. To be submitted to Icarus, 1991.

A PHOTOMETRIC SURVEY OF OUTER BELT ASTEROIDS [1]

M. Di Martino *, M. Gonano-Beurer ‡, S. Mottola ‡, and G. Neukum ‡;
*Osservatorio Astronomico di Torino, I-10025 Pino Torinese, Italy
‡DLR German Aerospace Research Establishment, D-8031 Oberpfaffenhofen,

Some recent studies have shown the fundamental role that the rotational properties can play for understanding the evolution of the asteroids belonging to the main belt and to other peculiar groups (Binzel et al., 1989; Zappalà et al.,1989). Much promising for a study of the physical features of the original planetesimals is the analysis of the Trojan asteroids and of the dinamically isolated objects (Hilda and Cybele groups), which, due to their dynamical characteristics, may have undergone less fragmentation due to collisions. In fact, both compositional studies (Vilas and Smith, 1985; Jewitt and Luu, 1990) and dynamical models (Milani and Nobili, 1985) suggest that they may have experienced an evolutionary history which may be significantly different from that of the main belt asteroids. A comparison of the rotational properties of these "primordial" objects with those of the collisionally evolved main belt asteroids could solve several problems connected with the evolution of asteroids and of the whole solar system.
Since 1988 we have been carrying out an observational survey of the asteroids belonging to the Trojan, Hilda, and Cybele groups, to determine their physical properties in terms of spin periods, lightcurve amplitudes and magnitudes. At present our data set includes new photoelectric and CCD lightcurves of 21 outer belt asteroids collected at different observatories in Italy, Germany, USA, and Chile (see Table 1). No previous information on the rotational properties was available for most of the program objects.

Table 1. List of the observed outer belt asteroids

Asteroid	Group	Asteroid	Group	Asteroid	Group
617 Patroclus	Tro	3564 Talthybius	Tro	1989 CK1	Tro
1143 Odysseus	Tro	3596 Meriones	Tro	1180 Rita	Hil
2207 Antenor	Tro	3708 1974 FV1	Tro	1748 Mauderli	Hil
2893 Peiroos	Tro	3709 Polypoites	Tro	1902 Shaposhnikov	Hil
2895 Memnon	Tro	4035 1986 WD	Tro	87 Sylvia	Cyb
3317 Paris	Tro	4348 1988 RU	Tro	909 Ulla	Cyb
3540 Protesilaos	Tro	4709 1988 TU2	Tro	1280 Baillauda	Cyb

The rotational properties that we have determined for the listed objects, represent a sensible enlargement of the existing data set. The high photometric accuracy of the collected data and their good time-sampling allowed us to compute reliable amplitudes, periods and Fourier coefficients for most of the lightcurves. It was then possible to perform a statistically significant analysis of the amplitude and of the rotational period distributions of the Trojans and study the coefficients obtained by the Fourier expansion of the lightcurves, comparing all these results with those determined for a sample of main belt asteroids in a comparable size range. A similar comparison has been performed also with the distributions obtained for the fragments produced in laboratory hypervelocity impact experiments. Preliminary results of this analysis are presented.

REFERENCES

Binzel R.P., P. Farinella, V. Zappalà, and A. Cellino (1989). In "Asteroids II" (Binzel R.P., Gehrels T., Matthews M.S., eds.). The University of Arizona Press, Tucson, p. 416.
Jewitt D.C. and J.X. Luu (1990). Astron. J. 100, 933-944.
Milani A., and A.M. Nobili (1985). Astron. Astrophys. 144, 261-274.
Vilas F., and B.A. Smith (1985). Icarus 64, 503-516.
Zappalà V., M. Di Martino, A. Cellino, P. Farinella, G. De Sanctis, and W. Ferreri (1989). Icarus 82, 354-368.

[1] Based in part on observations collected at the European Southern Observatory, La Silla (Chile)

ON THE STABILITY OF THE ASTEROIDAL BELT

C. Dinev and V. Shkodrov

Department of Astronomy, Bulgarian Academy of Sciences, 1784 Sofia, 72 Lenin blvd.

This paper treats a simplified model of the asteriodal belt. A secular stability criterion is obtained by varying the equation of motion. The criterion is very simple and in accordance with the available observational data. The aim of this criterion is to explane the distribution of the asteroids in the belt.

A Search for CO (1 –> 0) Emission in Comet Austin (1989c1)

M. DiSanti, M. Mumma, S. Hoban (*GSFC*), J. Lacy and R. Parmar (*U. Texas*)

High-resolution ($\lambda/\Delta\lambda \approx 2 \times 10^4$) observations of comet Austin, conducted UT 1990 May 16 and 18 with the University of Texas Infrared Echelle Spectrometer (IRSHELL) on the IRTF, were used to search for emission lines comprising the CO (1–>0) vibration-rotation band. The instrument used a Si-As impurity band array detector with 10 spatial elements, each 1″ on the sky, and 64 spectral channels per spatial element. The grating was set so that the central spectral channel was midway between the P3 and P2 lines, at $\nu \approx 2133.8$ cm^{-1}.

We detected an emission at the correct Doppler-shifted position of the P3 line, at roughly the 5–σ confidence level, which filled two spectral channels and (at least) three pixels in the spatial dimension. The feature was present, however, for only the first 45 minutes of actual clock time (~15 min of on-source integration time) on 16 May, and was not seen in subsequent data obtained either night.

The measured P3 line flux was found to be consistent with a production rate $Q_{CO} = (8.3 \pm 2.0) \times 10^{27}$ s^{-1}, or roughly 10% that of water. This value of Q_{CO} is nearly five times larger than that reported by Budzien *et al.* (BAAS 22, 1095, 1990) based upon 09 May observations with IUE. We interpret our observations as being consistent with an outburst of duration at least ~3000 s. The P3 flux expected, based on the quiescent $Q_{CO} \approx 1.7 \times 10^{27}$ s^{-1}, was found to be well below the 3–σ limits obtained from our data.

Furthermore, P2 emission was not detected in any of the data. The ratio of measured P3 line flux to the 3–σ upper limit for P2 was found to be consistent with a beam-averaged coma temperature of at least ~30 K.

COMETARY PROGENITORS FOR SATURN-LIKE RING SYSTEMS;

L. Dones, CITA/University of Toronto

Recent work (Dones 1991) has shown that tidal disruption of a large comet or asteroid during a close passage to a planet can result in the formation of a Saturn-like ring system at the present epoch. If the encounter is parabolic or weakly hyperbolic, up to $\approx 40\%$ of the mass of the stray body can be captured, even assuming no dissipation. For instance, 2060 Chiron presently crosses the orbits of Saturn and Uranus, and has a mass $M_{\rm Chiron} = (0.01\text{–}2)\ M_{\rm rings}$, where the mass of Saturn's ring system $M_{\rm rings} = 3 \times 10^{22}$ g, and I have assumed that Chiron's radius is between 90 and 186 km (Lebofsky et al. 1984; Sykes and Walker 1991), and its density $\rho_{\rm comet}$ is between 0.1 and 2 g/cm^3. Based on an Öpik-type calculation, the characteristic time for a body in a Chiron-like orbit ($v_\infty = 3.1$ km/s with respect to Saturn) to pass within a distance p of Saturn's surface is $t_{\rm enc} = 3 \times 10^7 (R_{\rm S}/p)$ years, where $R_{\rm S}$ is Saturn's radius.

The criterion for tidal disruption of a body with material strength is that the body pass within a distance q of Saturn's center, such that $q/R_{\rm S} < c(\rho_{\rm S}/\rho_{\rm comet})^{1/3}$, where Saturn's density $\rho_{\rm S} = 0.7$ g/cm^3 and the value of the coefficient c depends on the failure mode (Boss 1991). The classical Roche criterion for a fluid body is $c < c_{\rm crit} = 2.45$; analytic work by Dobrovolskis (1990) implies that $c_{\rm crit} \approx 1.34\,(a/200\ {\rm km})^{2/3}(\rho_{\rm comet}/1\ {\rm g\ cm^{-3}})^{2/3}$ for an icy, non-rotating, stray body of radius a which fails by shear fracture; and a model based on smoothed-particle hydrodynamics simulations by Boss et al. (1991) gives $c_{\rm crit} \approx 1$. The frequency of events in which bound debris is captured by the planet is not very sensitive to the exact value of $c_{\rm crit}$, as long as $c_{\rm crit} \geq 1$, for two reasons. (1) Because of gravitational focusing by Saturn, encounter probabilities per unit impact parameter are nearly independent of distance from the planet. (2) Because of the steep radial dependence of the tidal force, much more mass is captured in encounters with periapses very close to the planet's surface. From Monte Carlo simulations, I find that the rate of mass capture is only lower by a factor of two if I require $q < 1.2R_{\rm S}$ for disruption, compared with $q < 2.2R_{\rm S}$, the Roche criterion for a comet of unit density.

After disintegrative capture occurs, collisions among the fragments lead to a flat, equatorial ring, while collisions with inner satellites, which occur at a comparable rate, produce a population of craters with a sharp upper size cutoff and a density which declines with distance from the planet. These properties are similar to those observed for the Population II craters on the inner Saturnian satellites.

Assuming a nominal flux of Saturn-crossers, 10–100 passages within the Roche limit occur in 4.5 Gyr. Most close passages leave no bound debris, so that approximately one ring capture event occurs in the age of the solar system. However, the flux of Saturn-crossers is highly uncertain. Most such objects probably originate in a Kuiper comet belt beyond the orbit of Neptune; ongoing searches for outer solar-system planetesimals (Levison and Duncan 1990) will help determine the rate of tidal events.

REFERENCES

Boss, A. P. 1991. Abstract, Lunar and Planetary Science Conference.

Boss, A. P., Cameron, A. G. W., and Benz, W. 1991. *Icarus*, submitted.

Dobrovolskis, A. R. 1990. *Icarus* **88**, 24-38.

Dones, L. 1991. *Icarus*, in press.

Lebofsky, L., Tholen, D. J., Rieke, G. H., and Lebofsky, M. J. 1984. *Icarus* **60**, 532-537.

Levison, H. F., and Duncan, M. J. 1990. *Astron. J.* **100**, 1669-1675.

Sykes, M. V., and Walker, R. G. 1991. *Science* **251**, 777-780.

ERUPTIVE COSMOGONY OF MINOR BODIES AND THEIR INTERRELATIONS; E.M.Drobyshevski (A.F.Ioffe Phys.-Tech.Inst., 194021 Leningrad)

The problem of the origin and evolution of minor bodies - comets, asteroids, Trojans, planetary rings, Jovian irregular and Martian satellites - is usually treated for each group from different standpoints and can hardly be considered as solved.

Nearly all the relevant questions can be answered in terms of the eruptive cosmogony if one assumes the possibility of bulk electrolysis in thick ($\sim 10^3$ km) ice envelopes of bodies like Ganymede or Callisto /1/. Electric currents of up to 10^8 A were generated as the magnetized plasma of planetary magnetospheres or solar wind flowed around them. The ices contain impurities (silicates and metal oxides, carbon-rich substances etc.) identical to carbonaceous chondrites and exhibiting electronic conduction. Therefore the current produces solid state electrolysis in ice. At pressures $\sim 10^3$ atm the electrolysis products $2H_2+O_2$ are accumulated in ice in the form of a solid solution. At concentrations of 12-15% such a solution is capable of detonation /2/.

An exploding body of $M \lesssim 0.5M_\zeta$ breaks up completely, which apparently created ~ 3.9 Byr ago the main asteroidal belt. The specific features of a noncentral explosion may account for the distribution of the S, M, and C type objects in solar distance.

The explosion of a body with $M > 1M_\zeta$ removes only a part of its material in the form of vapors of water and organics present in ices, mineral grains and large ice fragments of the outermost cold layers which also contain $2H_2+O_2$. These are cometary nuclei, their material also being capable of detonation or combustion under certain conditions. It is the combustion initiated by solar radiation in the sublimation products of ice saturated by $2H_2+O_2$ that can account for the P/Halley near-nuclear energetics and chemistry /3/. This approach is capable of explaining also the explosive capture and properties of the Martian satellites and making certain predictions concerning their structure /4/.

The explosions of the ices of the Galilean satellites and of their fragments can account for many of their properties (differences in their ice content, in the topography of Ganymede which underwent one explosion, and of Callisto whose ices did not yet explode /5/, etc.), as well as for the origin and properties of the irregular satellites and the Trojans /6/.

As follows from the peculiar orbital distribution of the LP comets of Saturn's family, a sizable fraction of them appeared $\lesssim 10^4$ yrs ago escaping from deep in Saturn's sphere of action. This allows the dating of the possible explosion of the ices of Titan which created its atmosphere and Saturn's rings, as well as the reservoir of cometary nuclei between the orbits of Jupiter and Saturn which presently replenishes the Jovian family /7/. Some of the predictions made on this basis have already been confirmed, the others awaiting confirmation.

/1/ E.M.Drobyshevski, Moon & Planets 23,339,1980; /2/ E.M.Drobyshevski, Earth,Moon,& Planets 34,213,1986; /3/ E.M.Drobyshevski, ibid.,43,87,1988; /4/ E.M.Drobyshevski, ibid.,40,1,1988; /5/ E.M.Drobyshevski,ibid.,44,7,1989; /6/ I.I.Agafonova, E.M.Drobyshevski, ibid.,33,1,11,1985; /7/ E.M.Drobyshevski, ibid.,24,13,1981.

THE SIZES AND SHAPES OF (4) VESTA, (216) KLEOPATRA, AND (381) MYRRHA FROM OCCULTATIONS OBSERVED DURING JANUARY 1991

David W. Dunham, Computer Sci. Corp. and Internat'l Occultation Timing Assoc.; Wayne Osborn & Glen Williams, Physics Dept., Central Michigan Univ.; Jack Brisbin, Andreas Gada, Toshio Hirose, Paul Maley, Harold Povenmire, James Stamm, and Jeff Thrush, Internat'l Occultation Timing Assoc. Chris Aikman and Murray Fletcher, Dom. Astrophys. Obs., Victoria, B.C.; Mitsuru Soma, National Observatory, Mitaka, Tokyo, Japan; and Wang Sichao, Purple Mountain Observatory, Nanjing, China

(4) Vesta: On January 4th, Vesta occulted the 7.3-mag. star SAO 93228 as seen from the Great Lakes region. Photoelectric and video recordings were made at 8 sites in Michigan and one in Ohio; at least 11 visual observers obtained additional useful timings as far east as Toronto. Our preliminary analysis shows that the observations are fit well by an ellipse of dimensions 520 km by 482 km. The photoelectric data suggest irregularities departing from the elliptical shape by 15 km or more. If the 1989 August occultation result is considered, the mean diameter of Vesta is probably about 547 km. This value will be refined as lightcurve and pole position data are taken into account.

(381) Myrrha: On January 13th, Myrrha occulted 1.9-mag. Gamma Geminorum, the brightest star yet to be seen covered by an asteroid. The path unexpectedly shifted north, passing directly over the Tokyo region, where the event was monitored photoelectrically at one site, videotaped at two sites, photographed at two more sites, and timed visually at 14 other locations. A preliminary analysis indicates an elliptical outline, 80 km by 120 km, for Myrrha. Those with larger telescopes reported seeing a close companion of Gamma reappear while the bright star was covered. The companion was yellowish and about 8th magnitude; it must have been about 0".04 from the primary. In China, a nationwide campaign was organized, perhaps one of the largest in astronomical history. Over 5000 observers watched the star. The occultation was seen from at least 4 locations in Shandong province.

(216) Kleopatra: On January 19th, Kleopatra occulted 9.1-mag. SAO 115296 across the northern U.S.A. and southwestern Canada. The event was videotaped by Dunham using portable equipment in central New Jersey, and a photoelectric record was obtained with the 1.22-m telescope at the Dominion Astrophysical Observatory in Victoria. Six observers at other locations made visual timings. All of these chords are projected onto the sky plane in the figure below, which shows that Kleopatra's outline was about 55 km wide and about 230 km long! The occultation occurred near the maximum of Kleopatra's large-amplitude lightcurve. Care will be needed to combine this result with the 93 km x 125 km outline obtained during a 1980 October occultation that occurred near minimum light.

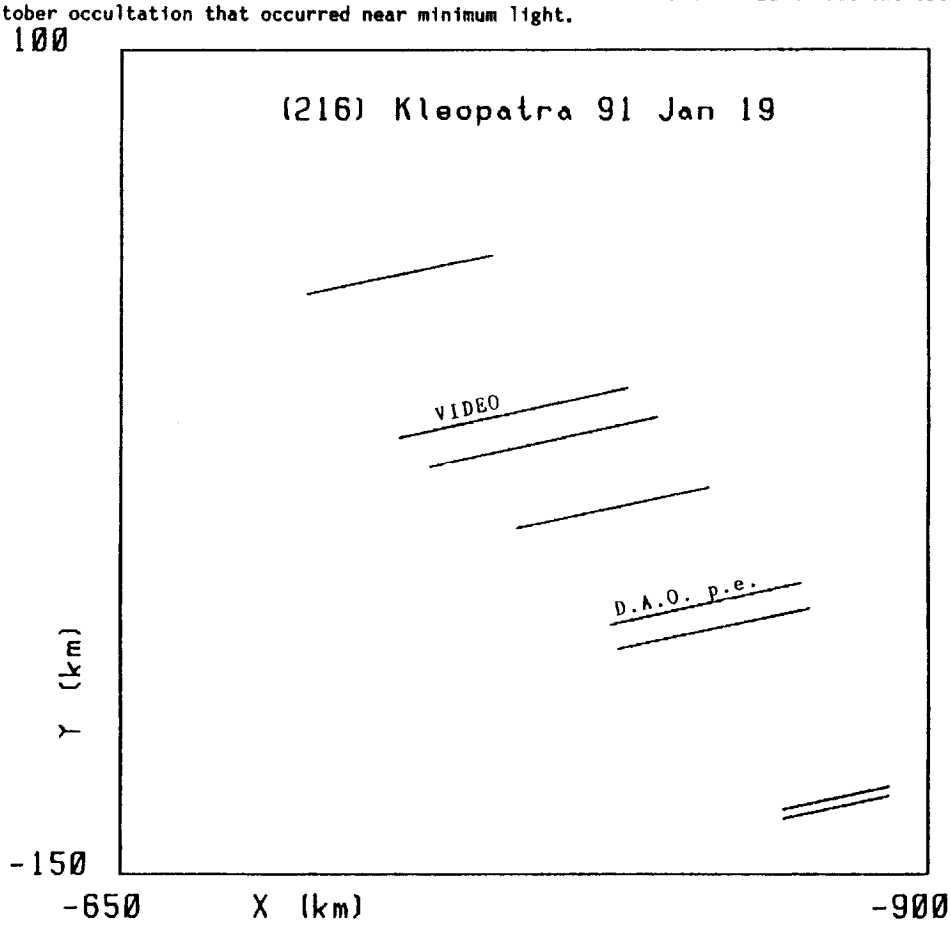

CALIBRATION OF ASTEROIDAL DUST PRODUCTION RATES THROUGH OBSERVATIONS OF THE HIRAYAMA FAMILIES AND THEIR ASSOCIATED IRAS DUST BANDS

D. D. Durda and S. F. Dermott (Department of Astronomy, University of Florida)

We determine the contribution of asteroidal collisions to the zodiacal cloud using the dust known to be associated with the Hirayama families as a calibrator. The ratio of the dust production rate associated with the prominent Hirayama families to that associated with the background asteroids is modeled. By working with ratios, we avoid the uncertainties inherent in specifying model dependent parameters (such as impact strength and energy partitioning) which strongly affect collisional outcomes. The observed ratio of the area of the dust associated with the families to that of the dust in the zodiacal background is found by analysis of IRAS data. We compare this ratio to the modeled ratio of family to background dust production rates and comment on whether mutual asteroidal collisions alone are sufficient to supply the zodiacal background.

Väisälä revisited

Eric W. Elst, Royal Observatory at Uccle, Belgium

The method of perihelion orbit of Väisälä (1939) is revisited. It shows that it is still an outstanding method for calculating preliminary orbits, based on only two nights. By taken in account all the astrometric positions of the two nights, it is possible to obtain an even much better orbit. Further, we were able to derive a meaningful orbit from positions that lie less than one hour away from each other.

PRECURSOR MATERIAL FOR COMET FORMATION; S. Engel and J. I. Lunine (LPL/ U of Arizona)

Comet nucleus composition, if formed in the outer solar system, could inherit interstellar as well as solar nebula material. Hence the evolution of precursor material after entering the outer solar nebula disk and before comet accretion was investigated in more detail. Chemical and physical alteration of interstellar material is enhanced in the inner regions, whereas further out some of this material may survive in its initial molecular composition. Physical processes which affect the heating of the particle during entry into the accretion disk are radiation and sublimation. Prior to cometary accretion grain surface reactions could contribute to a change in chemical composition.

The initial conditions for a collapsing molecular cloud and final formation of a accretion disk was taken from calculations by Wood (1984). The decoupled grains in the disk get heated up by drag through the surrounding gas. As test particles we used the Greenberg model of an interstellar grain which consists of a refractory core, covered by organics and overlied by volatile ices. Sublimation rates of different molecules (volatiles and organics) as a function of infall velocities were calculated. The recondensation of the vapor onto left over grain cores could lead to a core-mantle structure different from the interstellar one. Here the layered structure of organic and volatile material disappears and a mixture of these two components in a homogeneous mantle can be seen. Recondensation under nebula conditions could also avoid some of the kinetic problems associated with clathrate formation. Hence fractionation of gases such as CH_4 and CO will occur as they are co-deposited in the clathrate and amorphous ice structure.

In the above mentioned processes differences could be expected between molecular abundances in the gas phase and the solid phase. Interstellar ices could be chemically different from solar nebula ices.

Wood J.A. (1984) Smithson. Astrophys. Obs. Spec. Rep. 394.

THERMAL EVOLUTION AND PHYSICAL DIFFERENTIATION OF THE SUBSURFACE LAYERS OF SHORT PERIOD COMETS. CRUST FORMATION; S. Espinasse, A. Coradini, C. Federico, and F. Capaccioni, IAS-Reparto Planetologia, Viale dell' Universitâ, 11 00185 ROMA ITALY

The evolution of the subsurface layers of a short period comet has been studied. Particular attention was given to the variations of porosity and changes of composition of the superficial layers due to sublimation-recondensation phenomena, to gas diffusion processes through the pore system and to the sputtering of dust particles. Our nucleus model is composed of a water ice, CO2 ice and dust mixture in specified proportions. The icy matrix is assumed to be porous and crystalline.

The model is based on the resolution of two symmetric diffusion equations through the whole nucleus, one describing the transport of matter and the other the transport of heat. These equations are linked by the source term which accounts for production or loss of gas in terms of matter or of latent heat under two assumptions. First, we assume that the water vapor present in the pore system acts as a perfect gas. Second, we consider that sublimation and recondensation are instantaneous in order to maintain locally the thermodynamic equilibrium between the solid phase and its vapor. Under these assumptions, the source term depends on the variation of the pressure due to vapor diffusion and on the variation of the saturation pressure of the vapor due to the evolution of the temperature. The diffusion regime, Knudsen or viscous, depends on the mean free path of the molecules of gas through the pore network considered as a system of cylindrical pipes. The possibility is given to the dust particles to be ejected from the surface of the nucleus according to the force balance between gases fluxes, gravity and centrifugal forces and to the dust particles size distribution.

The calculations are performed for a nucleus on the orbit of P/Dutoit - Hartley because it is one of the possible targets for the Rosetta/CNSR mission. Different nucleus compositions with different CO2/H2O ice ratios and different dust/ice ratios are investigated. Results are presented on the evolution of the stratigraphy of the nucleus and of the production rates of CO2, H2O and dust particles as a function of the heliocentric distance. Several phenomena are evidenced, such as the depletion of CO2 ice in the subsurface layers and the possible presence of a dust layer at the nucleus surface.

INJECTING ASTEROID FRAGMENTS INTO RESONANCES

P. Farinella (Univ. di Pisa, Italy); R. Gonczi, Ch. Froeschle'
& Cl. Froeschle'(OCA - Observatoire de Nice, France)

Most meteorites and near-Earth asteroids (NEAs) are widely believed to be asteroidal fragments, coming from the asteroid belt through chaotic dynamical routes, associated with mean motion and secular resonances. We have tried to model and assess in a quantitative way the first part of this process, namely the ejection of fragments from cratering or break-up events undergone by the existing asteroids as a consequence of impacts, and the chance insertion of the escaping fragments into the "dangerous" regions of the phase space close to the 3:1 (mean motion) and g=g6 (nu6) (secular) resonances. For every parent asteroid, the efficiency of this process depends on several factors: (i) the amount of ejected material per unit time; (ii) the mass vs. ejection velocity distribution of the fragments; (iii) the escape velocity of the parent body; (iv) the delta-V required to approach a resonance surface; (v) the width of the strip surrounding the resonance surfaces where chaotic eccentricity increases are possible. By varying some model parameters, we have estimated the fraction of ejected fragments falling in the two resonances from all the existing asteroids larger than 50 km and orbiting inside 2.8 AU. The results show that most meteorites and NEAs can be generated by a small fraction of the overall asteroid population, mostly located in the vicinity of resonances. Both resonances are probably effective channels for fragment collection and delivery, although they sample in a different way the orbital elements and the physical properties (size and taxonomic type) of the parent objects.

IUE Observations of Comet P/Tempel-2 During 1988

P. D. Feldman

Department of Physics and Astronomy
The Johns Hopkins University
Baltimore, MD 21218, USA

M. C. Festou

Observatoire Midi-Pyrenees
31400 Toulouse, France

We summarize the results of observations made between 10 June and 18 December 1988 with the *International Ultraviolet Explorer* (*IUE*) of comet P/Tempel-2 during its 1988 apparation. The derived water production rate (c.f. Roettger *et al.*, Icarus, **86**, 100, 1990) and relative gas/dust ratio are compared with those of P/Halley, observed with *IUE* in 1985-86, and other potential CRAF target comets, P/Kopff and P/Tempel-1, both observed with *IUE* in 1983.

HUT Observations of Carbon Monoxide in the Coma of Comet Levy (1990c)

P. D. Feldman, A. F. Davidsen, W. P. Blair, C. W. Bowers, W. V. Dixon, S. T. Durrance, R. C. Henry, G. A. Kriss, J. Kruk, H. W. Moos, O. Vancura
Department of Physics and Astronomy
The Johns Hopkins University
Baltimore, MD 21218, USA

H. C. Ferguson
Institute of Astronomy, Cambridge University
Cambridge CB3 0HA, England

K. S. Long
Space Telescope Science Institute
Baltimore, MD 21218, USA

R. A. Kimble and T. R. Gull
Laboratory for Astronomy and Solar Physics
NASA Goddard Space Flight Center
Greenbelt, MD 20771, USA

Observations of comet Levy (1990c) were made with the Hopkins Ultraviolet Telescope during the Astro-1 Space Shuttle mission on 1990 December 10. The spectrum, covering the wavelength range 415 - 1850 Å at a spectral resolution of 3 Å (in first order), shows the presence of carbon monoxide and atomic hydrogen, carbon and sulfur in the coma. Aside from H I Lyman-β, no cometary features are detected below 1200 Å, although cometary O I and O II would be masked by the same emissions present in the day airglow spectrum. The 9.4 $\times$ 116 arcsecond aperture corresponds to 12000 $\times$ 148000 km at the comet. The derived production rate of CO relative to water, 0.13 $\pm$ 0.02, compared with the same ratio derived from *IUE* observations (made in September 1990) which sample a much smaller region of the coma, 0.04 $\pm$ 0.01, suggests the presence of an extended source of CO, as was found in comet Halley. Upper limits on Ne and Ar abundance are within an order of magnitude of solar abundances.

The Hopkins Ultraviolet Telescope Project is supported by NASA contract NAS 5-27000 to the Johns Hopkins University.

Ultraviolet and Visible Variability of the Coma of Comet Levy (1990c)

P. D. Feldman, S. A. Budzien
Department of Physics and Astronomy
The Johns Hopkins University
Baltimore, MD 21218, USA

M. F. A'Hearn
Astronomy Program, University of Maryland
College Park, MD 20742, USA

M. C. Festou
Observatoire Midi-Pyrenees
31400 Toulouse, France

G. P. Tozzi
Osservatorio Astrofisico di Arcetri
50125 Florence, Italy

Short-term variability of the coma of comet Levy (1990c) was detected and monitored (c.f. IAU Circular 5081) with the *International Ultraviolet Explorer* (*IUE*) satellite observatory during August and September 1990 including 24 hours of continuous observation on 18 September. The visible light curve obtained on this date with the *IUE* Fine Error Sensor (FES) shows two distinct maxima separated by 17.1 $\pm$ 0.2 hours. However, this period cannot properly match in phase the FES data obtained during eight-hour shifts on 11 and 13 September, and suggests a decrease in apparent period of $\sim$0.5 % per day. A similar decrease is derived from a comparison with the period derived from ground-based data taken in late August (Schleicher *et al.*). The variation in the ultraviolet emissions of OH, CS, and CO_2^+ was also determined from 18 consecutive long-wavelength *IUE* spectra taken on 18 September. From the shape of the ultraviolet and visible light curves it is possible to determine the ratio of gas to dust outflow velocities. A sharp change in CO_2^+ brightness suggests that a sub-surface region of volatiles, including CO_2, may be responsible for the observed variability, although the origin of the decrease in period remains unexplained. CO was also observed, with a production rate=0.04 $\pm$ 0.01 that of H_2O, but the long exposure time required for this measurement precluded any determination of CO variability. *IUE* observations made post-perihelion on 9-10 January 1991 showed no variability.

" BULK DENSITIES AND MASSES OF COMETARY NUCLEI ". Ignacio Ferrin, Astrophysics Group, Departament of Physics, UNIVERSITY OF THE ANDES, Merida 5101-A, VENEZUELA.

We have devised a method to derive bulk densities of comets from the observed values of the period of rotation, P_{rot}, and oblateness, $A = a/(a-b)$, where a and b, are the semi-axis of the nuclear ellipsoid.

For five planets and one comet the following law is capable of predicting the density with a mean error of only 8%:

$$\rho\ (+-8\%\ m.e.) = 0.33\ .\ A^{0.58}\ .\ P^{-0.17}$$

This means that we have identified the main physical variables that determine the oblateness (period of rotation and density).

We have applied this law to 9 comets for which we have periods of rotation an oblateness: Halley, Encke, Neujmin 1, Arend Rigaux, Giacobinni-Zinner, Temple 2, Iras-Araki-Alcock, Comas Sola and Kopff.

It is strongly concluded that comets are low density objects. For 9 comets in our data base, we obtain a mean density of 0.35 +- $0.11 g/cm^3$, and a mean mass of 2.5×10^{17} g.

A plot of Mass versus Total absolute magnitude, gives a poor fit to the data. However, a plot of mass versus nuclear absolute magnitudes $V_N(1,1,0)$ gives a rather good fit, with the following equation:

$$Log\ M = 25.9 - 0.6 \cdot V_N(1,1,0)$$

Our result implies that the total mass of the Oort Cloud may have to be revised upwards, since 8 comets in our data set are periodic, and thus should have a mass smaller than that of new comets.

Our result also implies that we now have an accurate (+-8%) method to obtain the density of a comet, if we know the period of rotation and the oblateness of its nucleus. Both parameters can be easily obtained from nuclear observations at large distances from the Sun.

COMPARISON OF A MULTI-GENERATIONAL MONTE CARLO COMETARY MODEL WITH OBSERVATIONS.

Anthony J. Ferro
Arizona State University

A steady-state, multi-generational Monte Carlo model has been developed to examine the distribution of neutral coma species. The model follows the photodissociation steps through several generations of parent-daughter reactions.

Specifically, we look at the production of NH by the sequence:

$$NH_3 \rightarrow NH_2 \rightarrow NH \rightarrow N.$$

The model is compared with narrow band images of C/Austin, obtained at the MDM 1.3-m telescope on Kitt Peak.

Other model features include predictions of distributions due to a distributed source in the form of grains ejected from the comet nucleus, and subsequent photodissociation of the sublimated molecules. Also included, for specific molecules, is acceleration due to solar radiation pressure, and anisotropic ejection of the parent molecules from the nucleus.

WATER AND DUST PRODUCTION RATES IN COMET P/HALLEY (1986 III) FROM ULTRAVIOLET AND OPTICAL OBSERVATIONS:

M.C. FESTOU, Soutwest Research Institute, San Antonio, TX, 78228, USA and Observatoire Midi-Pyrénées, 14 avenue E. Belin, F-31400 Toulouse, France.

Comet P/Halley was observed from September 1985 until July 1986 with the International Ultraviolet Explorer. The long wavelength spectrograph was used to monitor and measure the water production (via the OH emission) and the dust production (via its scattered light in the 2920-3020Å window) rates of the comet. The Fine Error Sensor camera was primarily used to acquire the comet in the instrumental fields of view; it also provided optical measurements of the brightness of the central coma at a time resolution far superior to that of the spectrocopic observations. One of the interesting aspects of those measurements if that, since the fields of view are small, of order 10 arc sec, the signals that were measured never integrated the activity of the nucleus over time periods larger than one to three hours. The two sets of observations are combined to derive a comprehensive picture of the evolution of the activity of the nucleus during the above-mentioned 10 month period. When necessary, visual magnitudes are used to complement the information given by our data sets. The short and long (secular) terms of the activity curves are separated. The contributions of the gaseous and the continuum emissions to the optical measurements are separated too. It is found that most of the time, the activity of the nucleus was smoothly varying. However, there are two well documented cases, namely on 18 March and on 10 April 1986, during which the nucleus activity was of 'explosive' nature, but of small amplitude, though. Water and dust production rates, the dust to gas ratio and the evolution of those parameters with heliocentric distance are given.

WATER PRODUCTION RATE OF COMET P/d'ARREST (1982 VII) AT ITS 1982 APPARITION: M.C. Festou[1], P.D. Feldman[2], M.F. A'Hearn[3]. 1: Soutwest Research Institute, San Antonio, TX, 78228, USA and Observatoire Midi-Pyrénées, F-31400 Toulouse, France; 2: Department of Physics and Astronomy, The Johns Hopkins University, Baltimore, MD, 21218, USA; 3: Astronomy Program, University of Maryland, MD 20742, USA.

Comet P/d'Arrest (1982 VII) was observed with the International Ultraviolet Explorer during the first 30 days following its passage through perihelion in 1982. During this long period, both the heliocentric and geocentric distance varied very little, allowing thus a quasi model independent comparison of the observations. As is well known from past visual observations, the gas production of that comet does not decrease immediately when the comet receedes from the sun. From our data set, it is possible to state that the water production was still increasing five weeks after perihelion passage. Since the visual data indicate a very sharp increase of the visual brightness during the last few weeks before perihelion passage, the light curve of that comet is exceptionally asymmetric. The continuum emission was only detected during the second part of the observations, still at a very low level. CS and CO_2^+ emissions were never detected. The short wavelength spectra only revealed the expected HI Lyman alpha emission. Water production rates and upper limits for the CS and SI production rates are given. A comparison of the dustiness of the comet with other periodic comets observed in nearly similar conditions is made. The water production measured in 1982, after the comet was back on its 1.30 AU perihelion orbit, was about ten times smaller than in 1976, when the perihelion distance was only 1.16 AU. Since the visual light curves in 1976 and 1982 did not differ much, it is inferred that the insolating conditions as a function of time were the same, except for the absolute values that were larger in 1976. In the light of those measurements, the change of the temperature of the nucleus with distance to the sun is discussed.

A CCD spectrum and production rates for Comet P/Temple 2

Uwe Fink and Michael Hicks

Lunar and Planetary Laboratory, University of Arizona, Tucson, AZ 85721

Abstract

Now that comet P/Temple 2 has been resurrected as the primary target for the CRAF mission we wish to present an analysis of a 20 minute exposure taken 1988 Oct. 09. The comet displays a typical spectrum with no unusual omissions or additions. The comet therefore appears to be quite suitable for detailed spacecraft study as a representative object. Strong emissions by C_2, NH_2, CN and OI ^1D are exhibited. Compared to the emissions, the continuum is moderately strong but appears somewhat weaker than for P/Halley. Production rates for H_2O (from OI ^1D) and the parent of C_2, NH_2, and CN will be presented and compared to P/Halley.

This research was supported by NASA grant NAGW 1549.

P/Halley: Spatial distribution and scale lengths for C_2, CN, NH_2, and H_2O

Uwe Fink[1], Michael Combi[2] and Michael A. DiSanti[3]
Lunar and Planetary Laboratory, University of Arizona

Abstract

From P/Halley long slit spectroscopic exposures on 12 dates, extending form 1985 Oct. to 1986 May, spatial profiles were obtained for emissions by C_2, CN, NH_2, and OI (^{1}D). Haser model scale lengths were fitted to these data. The extended time coverage allowed us to check for consistency between the various dates. Not unexpectedly, the time varying production rate of P/Halley severely affected the profiles after perihelion, which is nicely demonstrated in two profile sequences on adjacent dates, March 01/02 and April 14/15. Because of the time varying production rate, it was not possible to obtain reliable Haser model scale lengths after perihelion. Our pre-perihelion analysis yielded Haser model scale lengths of sufficient consistency that they can be used for production rate determinations, whenever it is necessary to extrapolate from observed column densities within finite observing aperatures. Results of scale lengths reduced to 1 AU are as follows:

	parent (10^3 km)	daughter (10^3 km)
C_2	58±20	58±20
CN	28±15	320+200/-100
NH_2	4.9±1.5	62±20
H_2O	74±60	--

For C_2 a slight flattening of the profile close to the nucleus could not be fitted with a two step Haser model but can be accommodated with a CHON halo model (Combi and Fink 1991). If the inner region is excluded from the fit, the daughter/parent scale length ratio changes from near one to about 6. However, when production rates are sought using a two step Haser algorithm only an equal scale length model comes close to providing an acceptable fit. Only three observations yielded a CN daughter scale lengths because our profiles did not extend sufficiently far. The long daughter of CN also makes this emission very sensitive to production rate variations causing greater scatter in the parent values. A curios asymmetry of the scale lengths for NH_2 was found with the post-perihelion parent being about twice the pre-perihelion value, but the daughter being about half the pre-perihelion number. We have as yet not found a ready explanation for this behavior. Most of the OI ^{1}D profiles, which effectively map out the comet's H_2O distribution, deviated very little from a $^1/_r$ fall off so that it was not possible to obtain a reliable H_2O parent scale length, although consistency with the nominal lifetime of $80x10^3$ seconds is quite clearly demonstrated.

This research was supported by NASA grant NAGW 1549.

[1] Uwe Fink: Lunar and Planetary Laboratory, University of Arizona, Tucson, AZ 85721
[2] Michael R. Combi: Space Research Building, University of Michigan, Ann Arbor, MI 48109-2143
[3] Michael A. DiSanti: Infrared & Radio Astronomy Branch, NASA-Goddard, Code 693, Greenbelt, MD 20771

LOW-RESOLUTION SPECTROSCOPY OF D-TYPE ASTEROIDS

A. Fitzsimmons, Queen's University Belfast
P. Magnusson and I.P. Williams, Queen Mary and Westfield College, London
M. Dahlgren and C.-I. Lagerkvist, Uppsala Observatory

We have obtained reflectance spectra of 19 D-type asteroids using the 4.2 m William Herschel Telescope on La Plama. The wavelength coverage of 370 nm to 950 nm has allowed us to measure accurate reflectance slopes for all of these low-albedo objects. A simultaneous search for absorption and emission features has been performed. An initial result is that we have been unable to confirm the existance of absorption bands in 279 Thule as reported by us previously. Preliminary results will be presented and discussed.

LARGE MICROMETEORITES: ATMOSPHERIC ENTRY SURVIVAL, RELATION TO MAIN-BELT ASTEROIDS, AND IMPLICATIONS FOR THE COMETARY DUST FLUX. G. J. Flynn, SUNY-Plattsburgh, Plattsburgh, NY 12901.

Micrometeors and micrometeorites 50 μm to 1 mm in diameter constitute 80% of all the meteoritic mass (excluding rare, large impactors > 10^{14} grams) accreting onto the Earth [Hughes 1978]. Although small micrometeorites ($\leq$ 50 μm in diameter) have been collected from the Earth's stratosphere since the early-1970's, micrometeorites larger than 100 μm were expected to vaporize on atmospheric entry. Large micrometeorites (>100 μm), partially melted and unmelted, have recently been recovered from the sea floor [Brownlee 1981] and polar ices [Maurette et al. 1986]. IDENTIFICATION AS MICROMETEORITES: High Ne concentrations in several large micrometeorites confirm their extraterrestrial origin, and establish they were individually irradiated by the solar wind as small objects, thus they are not ablation debris or interior parts of a much larger body [Olinger et al. 1989]. Cosmogenic nuclei, ^{10}Be and ^{26}Al, in large micrometeorites also indicate small body or surface exposure [Nishiizumi et al. 1991]. ENTRY HEATING SOURCE IMPLICATIONS: Computer simulations of the atmospheric entry of large micrometeorites show only those with very low geocentric velocities survive without vaporization, indicating the large micrometeorites arrive at Earth by Poynting-Robertson (P-R) orbital evolution from main-belt asteroids [Flynn 1990, 1991; Love and Brownlee 1991] or comets in low inclination, near-circular orbits, like Schwassman-Wachmann 1 [Flynn 1989]. RELATIONSHIPS TO METEORITES AND ASTEROIDS: The most common large micrometeorites are partially melted spheres consisting of olivine grains with minor amounts of magnetite. They have "chondritic" (or solar) abundances of Mg, Al, Si, Mn, and Fe [Maurette et al. 1986]. Sutton et al. [1988] suggest the elemental abundance patterns observed in 3 of 9 melted spheres are more consistent with ordinary chondrite than carbonaceous chondrite composition. Thus S and C type asteroids seem the most likely parent bodies. But high carbon abundances, >10% in 1/3rd of particles examined [Maurette et al. 1987], leave open P or D asteroid parent bodies. IMPLICATIONS FOR FLUX OF COMETARY DUST: The contribution of main-belt asteroids to the flux of large micrometeorites at Earth has previously been assumed to be small [eg, Flynn 1989] because the calculated catastrophic collision lifetimes of these particles (~10^4 to 10^5 years) were substantially shorter than the times required for P-R orbital evolution from the main-belt to Earth (~10^6 years)[eg, Dohanyi 1978]. The space exposure ages of large micrometeorites (10^5 to 10^7 years) measured by Nishiizumi et al. [1991] are consistent with the calculated P-R lifetimes, suggesting the true collisional lifetimes are much longer than those calculated by Dohanyi [Flynn 1990; Nishiizumi et al. 1991]. Since the collisional lifetimes are calculated to be dominated by smaller cometary particles, suggesting the cometary contribution to the interplanetary dust cloud in the 1 μm to 20 μm diameter range (responsible for the fragmentation of the larger particles) is significantly less than previously assumed, consistent with the conclusion that much of the 10 to 20 μm cosmic dust collected at earth is asteroidal [Flynn 1989; Sandford and Bradley 1990].

REFERENCES: Brownlee, D. E. (1981) in The Sea, vol. 7, Wiley, 733-762. Dohanyi, J.S. (1978) in Cosmic Dust (ed. J.A.M. McDonnell) Wiley, 527-605. Flynn, G.J. (1989) Icarus, 77, 287-310. Flynn, G. J. (1990) Meteoritics, 25, 365. Flynn, G. J. (1991) Lunar & Planet. Sci. XXII, 393-394. Hughes, D.W. (1978) in Cosmic Dust (ed. J.A.M. McDonnell), Wiley, 123-185. Love, S.G. and Brownlee, D.E. (1991) Icarus, 89, 26-43. Maurette, M. et al. (1986) Science, 233, 869-872. Maurette, M. et al. (1987) Nature, 328, 699-702. Nishiizumi, K. et al. (1991) Exposure History of Individual Cosmic Particles, Earth Planet. Sci. Lett. (in press). Olinger et al. (1989) Meteoritics, 24, 312. Sandford, S. and Bradley, J.(1990) Icarus, 82, 146-166. Sutton, S.R. et al. (1988) Meteoritics, 23, 304.

C-2

Bulk abundances of the main rock-forming element in the P/Halley dust component

Fomenkova M.N., Evlanov E.N., Mukhin L.M., Prilutsky O.F. (Space Research Insitute, Profsoyuznaya 84/32, Moscow 117810, USSR)

The main data on the chemical composition of P/Halley dust component were obtained after Vega missions from PUMA-1,2 dust-impact mass-spectrometers. Ion ratios of a "compound bulk comet" obtained by different authors (1-3) as the average of the individual grins spectra differ greatly from elemental abundances in carbonaceous chondrites of type CI even for the main rock-forming elements.However, taking into account mass of dust particles brings about a quite satisfactory coincidence of the average ionic composition of comet dust with the solar abundances of these elements.

The procedure of averaging was as follows. First, the sum of all the ions of the main elements in an individual spectrum was assumed to be 100% and the percentage of every element in this spectrum was calculated. The next step was to average the obtained values in all spectra with weighting factors equalling the independently derived mass of dust particles (4). This procedure enables to eliminate uncertainities due to the variations of the ion signal in the spectra of particles of similar mass.

To determine abundances of minor elements as Al, K, Ca, Ti, Cr, Ni we used selected spectra of higher quality, where these elements are surely identified. It is necessary, because noise pulses caused by impacts of very small dust grains can be confused with peaks of minor elements. Results are given in the table for both instruments and for different modes of functioning. Errors have been estimated assuming that individual error of every peak is a square root of its amplitude.

	PUMA1, wide	PUMA1, narrow	PUMA2, wide	PUMA2, narrow
Na	40.8 ± 17.2	29.3 ± 1.7	69.7 ± 5.7	48.2 ± 3.7
Mg	107.7 ±39.6	168.4 ± 5.9	138.7 ± 8.6	177.0 ± 10.8
Al	18.9 ± 6.3	9.0 ± 0.8	23.6 ± 1.6	23.3 ± 1.6
Si	100	100	100	100
S	67.3 ± 23.5	50.3 ± 2.5	74.7 ± 5.3	85.6 ± 5.9
Cl	34.9 ± 10.2	22.1 ± 1.2	3.6 ± 0.2	0.2 ± 0.01
K	0.4 ± 0.2	1.2 ± 0.3	2..6 ± 0.3	2..3 ± 0.2
Ca	7.4 ± 3.0	5.3 ± 0.6	11.6 ± 1.2	12.5 ± 1.1
Ti	0.3 ± 0.15	0.9 ± 0.2	1.1 ± 0.1	0.9 ± 0.1
Cr	1.3 ± 0.6	1.7 ± 0.4	3.0 ± 0.2	3.8 ± 0.3
Fe	92.7 ± 33.4	54.7 ± 3.0	70.9 ± 5.1	49.9 ± 3.2
Ni	4.8 ± 1.5	2..5 ± 0.4	0.6 ± 0.1	< 0.1

REFERENCES

1. Sagdeev, R.Z. et al. Space Research 25, 840-848 (1987).
2. Langevin, Y. et al. Astron. Astrophys. 187, 761-766 (1987).
3. Jessberger, E.K. et al. Nature 332, 691-695 (1988).
4. Fomenkova M.N. et al. Lunar Planet Sci. Conf. 22, 397-398 (1991).

Synthetic mapping for long range integration of Hamiltonian system

Cl. Froeschlé and J.M. Petit

Different types of interpolation are proposed and tested for transforming a non linear differential system, and more particulary Hamitonians one with 2 and three degrees of freedom into maps without having to integrate the whole orbit as in the well known Poincaré return map technique. We construct piecewise polynomial maps by coarse-graining the phase surface of section into parallelograms using values of the Poincaré maps at the vertices to define a polynomial approximation within each cell. The numerical experiments are in good agreement with both the real symplectic and Poincaré maps. The agreement is better when the number of vertices and the order of the polynomial fit increase.

The effect of secular resonances in the asteroid region between 2.1 and 2.4 AU

Ch. Froeschlé, H.Scholl
Observatoire de la Côte d'Azur, Nice, France

The asteroid region between 2.1 and 2.4 AU at inclinations between 10° and 20° is anormally depopulated. This region is surrounded by the principal secular resonances ν_5, ν_6 and ν_{16} and it is crossed by higher order secular resonances. Our aim is to investigate the effect of secular resonances on the orbital evolutions of asteroids in this region. We integrate in the frame of the four-body problem Sun-Jupiter-Saturn-asteroid the orbits of twenty fictitious asteroids with the same initial eccentricity of $e = 0.14$, initial semimajor axes in the range $2.1 \leq a \leq 2.4AU$, and initial inclinations between $12° \leq i \leq 20°$.

N91-25993

VARIATIONS IN MAGMATIC PROCESSES AMONG IGNEOUS ASTEROIDS; M.J. Gaffey, Geology Dept., Rensselaer Polytechnic Institute, Troy, New York 12181 USA

Six asteroid classes [types V,E,A,R,M,S] are composed primarily of differentiated assemblages produced by igneous processes within their parent planetesimals. These are identified by surface materials which deviate from a chondritic composition to a degree that requires igneous chemical fractionation processes. There are significant variations among these igneous asteroids in the peak temperatures attained, in the efficiency of magmatic phase separation, and in the depth within the original parent body exposed at the present surface. These variations provide important constraints on the nature of asteroidal heating events, on the differentiation processes within small planetary bodies, and on the disruption of those parent bodies.

Variations due to depth within the parent body: The assemblages exposed on igneous asteroid surfaces formed at a range of depths in their parent bodies. For example, the basaltic assemblage of 4 Vesta [type V] are surface flows and shallow intrusives on a nearly intact body. The metallic surface of 16 Psyche [type M] represents a fragment of the iron core of a disrupted parent body. A-type (e.g. 446 Aeternitas) and olivine-dominated S-type asteroids (e.g. 113 Amalthea) represent mantle fragments, while many S-asteroids appear to represent the core-mantle boundary region, with the core enclosed. Some igneous asteroids (e.g. 15 Eunomia [S] and 349 Dembowska [R]) sample a range of depths within their parent planetesimals from the crust to the core-mantle boundary. Differences in mechanical properties between metal-poor mantles and metal-rich cores seems to have been important in the rarity and small size of mantle fragments relative to core-dominated objects.

Variations due to degree of magmatic differentiation: The largest igneous group (type S) exhibits a wide diversity in the mafic silicate assemblage (dunite to basalt), mafic mineral composition, and metal abundance. This variety appears to reflect differing degrees of magmatic segregation within the parent bodies. Although the relationships are complex and non-linear, in general separation of different phases (e.g. metal from silicates, silicate melt from matrix) should be more efficient for larger planetesimals (stronger internal gravitational fields) and for those which achieved higher peak temperatures (greater melt fraction). A significant subset of the S-asteroids attained temperatures ($1000C \leq T \leq 1200C$) sufficient to melt a major portion of the metallic phases (NiFe and/or FeS) but not sufficient to extensively melt the silicate fraction or were located within parent bodies which were too small to allow efficient segregation of the silicate phases. Although these have approximately chondritic silicates, they are enriched to varying degrees in metal, perhaps representing deeper zones to which descending Fe-FeS melts were added. Other S-asteroids (e.g. 113 Amalthea) with nearly pure olivine silicate fractions require very high degrees of partial melting ($T \geq 1600C$) in their parent planetesimals.

The igneous asteroids exhibit the full range of differentiation from low degrees of partial melting and/or low melt extraction through complete melting and full phase separation. Most igneous asteroids are consistent with moderately oxidized (H,L,LL,CV,CO) parent materials. However, some such as the E-asteroid 44 Nysa must have derived either from a very reduced parent material or from one with a substantial initial inventory of reductant. The decreasing relative abundance of igneous asteroids with heliocentric distance is probably the signature of a sun-centered heating mechanism.

This work was supported in part by NASA Planetary Geology and Geophysics Grant NAGW-642 and by NSF Solar System Astronomy Grant AST-9012180.

THE MILLMAN METEOR SPECTRA ARCHIVE; M.J. Gaffey, K.L. Reed, Geology Dept., Rensselaer Polytechnic Institute, Troy, New York 12181, USA; P.A. Feldman, I. Halliday, Herzberg Institute of Astrophysics, National Research Council of Canada, 100 Sussex Drive, Ottawa, Ontario K1A OR6 Canada

A working archive of meteor spectra is being established at the Rensselaer Polytechnic Institute in order to preserve the data set obtained and collected by Dr. Peter M. Millman during his long career prior to his unexpected demise in December, 1990. This archive will maintain and catalog the collection and will provide access and supporting documentation to potential users. We are also interested in additional data sets from other sources.

Potential users or contributors should contact Dr. Michael Gaffey [Geology Department, Rensselaer Polytechnic Institute, Troy, New York 12181 USA; Phone 518-276-6300; FAX 518-276-6003; e-mail (BITNET) USEREMUN@RPITSMTS] for further information or to be placed on our mailing list for further announcements.

Observations of Bolide Spectra with a Fish Eye Camera

V.S. Getman, Astrophysical Institute of the Tajik Academy of Science, 734670, Dushanbe, USSR

A new method of observationing the spectrum of bolides in the higher orders with the objective Fish eye lens (f/3.5, focal length 30 mm, 180° field of view) is described. The method was developed at the Arecibo Observatory during the AIDA (Arecibo Initiative in Dynamics of the Atmosphere) campaign. The Lunar (first quarter) spectrum and the the sodium lidar beam, directed towards the zenith, were photographed simultaneously. The continuous spectrum of the Moon and 6 orders of the sodium doublet were obtained. Additionally, observations of bolides from two points – the Sanglock and HIssar observatories – were organized in Dushanbe. Three Fish eye cameras – one for direct photography and two with 300 line/mm gratings fixed mutually perpendicular were placed at each location. A total of 257 hours of observations yielded 22 meteors and bolides and 7 spectra, 3 of which have been processed and will be presented. Two Fish eye cameras with diffraction gratings at 45°, to yield bolide spectra optimally, are to be used for future observations.

Bolide AIDA: Orbital and Physical Characteristics

V. S. Getman[1], J. D. Mathews[2], Y. T. Morton[2], Q. Zhou[2], and R. G. Roper[3]

1. Astrophysical Institute of the Tajik Academy of Science, 734670, Dushanbe, USSR
2. Communications and Space Sciences Laboratory, The Pennsylvania State University, University Park, Pennsylvania 16802, USA
3. School of Geophysical Sciences, Georgia Institute of Technology, Atlanta, Georgia 30332, USA

The preliminary results of our investigation of Bolide AIDA, which was observed on April 8, 1989 at 0526 UT from three locations in Puerto Rico, are given. The observations were made as part of the AIDA '89 (Arecibo Initiative in Dynamics of the Atmosphere) campaign which involved about 20 separate instruments. This array of instruments serendipitously, and perhaps uniquely, allowed observation of this bright bolide by six methods simultaneously – visually, by All-Sky camera, by video camera system, by CCD Infrared Imager, by imaging narrow band spectrometer (MORTI), and by IDI (Imaging Doppler Interferometer) radar – resulting in a variety of data. Preliminary calculations indicate that the Bolide entered the atmosphere on a steep trajectory, about 33° from vertical, which was followed from 72 km altitude and 20 km/s velocity down to 27.5 km altitude and 2-3 km/s velocity. The time of occurrence, the radiant (α_R = 189.3°; δ_R= -7.9°), and the orbit show that the bolide belongs to the χ-Virginid stream, which is connected with the Apollo Group asteroids. Towards the end of the observed trajectory the Bolide exploded into at least four large fragments which were observed by the All-Sky camera and the Video camera system.

PHOTOMETRY OF 243 IDA: RESULTS FOR THE 1990 OPPOSITION [1]

M. Gonano-Beurer ‡, M. Di Martino *, S. Mottola ‡, and G. Neukum ‡;
‡DLR German Aerospace Research Establishment, D-8031 Oberpfaffenhofen,
*Osservatorio Astronomico di Torino, I-10025 Pino Torinese, Italy

243 Ida is the second main belt asteroid which is planned to be flown-by by the Galileo spacecraft. In the framework of our program of observations of space mission targets, we have undertaken CCD and photoelectric measurements of 243 Ida from the observatories of Loiano (Italy) and ESO (La Silla, Chile) during the 1990 apparition.
Lightcurves in the V Johnson band spanning three months in time and covering the phase angle range from 3 to 20 degrees are presented. From these measurements we have obtained for the first time the magnitude-phase relation of this asteroid. The good quality of these data allowed a substantial improvement in the determination of the synodic rotational period. U-B and B-V color indices have been also derived.

[1]Based in part on observations collected at the European Southern Observatory, La Silla (Chile)

TESTING THE ASTEROID FAMILY PARADIGM. **James C. Granahan and Jeffrey F. Bell (Planetary Geosciences Division, Dept. of Geology and Geophysics, SOEST, University of Hawaii, 2525 Correa Rd., Honolulu, HI 96822)**

Many main belt asteroids have a tendency to cluster around certain principle orbital elements (a, i, and e). This was first noticed by Hirayama in 1918, who named these clumps "asteroid families" to emphasize his belief that they were the product of the disruption of a large proto-asteroid.

There are two major ways in which asteroid families are defined. The first method (e.g. Williams, 1989) is to plot asteroids according to their proper orbital elements and visually designate an asteroid family by the apparent clusters seen on the plots. The second method (e.g. Zappala et al, 1990) is to apply cluster statistical analysis to the proper element data to define family membership. Visual workers tend to produce more families (117 Williams families) than those using clustering statistics (21 Zappala families).

We applied a geologic analysis to test the asteroid family paradigm of Hirayama (1918) to the recently proposed asteroid family taxonomies of Williams (1989) and Zappala (1990). Utilizing the spectra database and asteroid classification of Tholen (1984) with some comparisons of similar databases (Barucci,1987 and Tedesco,1989) one can derive asteroid mineralogies of observed asteroid family members. The mineralogic interpretations of Bell (1989) were used to turn asteroid taxonomic types into geologic material types.

An asteroid family is thought to result from a catastrophic collision of the parent body. In most cases the impactor is disintegrated in the collision and is therfore not detected by telescopic observation. The parent body breaks up after impact and its larger fragments become an asteroid family. Hence, an asteroid family should be able to be reconstructed into a geologically sensible parent body.

Families chiefly composed of one taxonomic type can be readily interpreted as fragments of homogeneous parent bodies. Asteroid families of mixed taxonomic types can also be produced by fragmentation, provided the parent bodies were differentiated. However, there some mixtures, like a family composed of igneous (S) and primitive (C) type asteroids, that are nearly impossible. It appears unlikely that many asteroid parent bodies could contain significant amounts of thermally unaltered chondritic material in combination with extensive magmatic differentiation.

The following are key results of the above analysis:
(1) Themis, Eos, Koronis, and Maria families are nearly identical in both family classifications. They also are geologically consistent with the common parent body model. (2) The Williams Nysa family, which is geologically consistent (provided that Nysa is omitted), virtually disappears in the Zappala classification. (3) Most of the geologically questionable Williams families do not directly correspond to Zappala families. 80 of the Williams families have no correspondence to any of the Zappala families. (4) Many of the Williams Families can not be derived from a common parent body. Most Zappala families can be. (5) Some interloping asteroids may be present in the Zappala Eos and Themis families.

The general conclusion of this study is that the Zappala et al (1990) analysis appears to be closer to "reality" than that of Williams in terms of number of families and fraction of asteroids belonging to families, but the assignment of a particular asteroid to a given parent body is somewhat uncertain.

References: [1]Hirayama, K. (1918), Proc. Phys.-Math. Soc. Japan, Ser. 2 9, pp. 354-361. [2]Williams, J.G. (1989), in Asteroids II, pp. 1034-1072. [3]Carusi,A. and Massaro,E. (1978), Astron. Astrophs. Suppl. 34, pp. 81-90. [4]Zappala,V., et al (1990), The Astron. J. Vol. 100, No.6 pp 2030-2046. [5]Tholen,D.J. (1984), PhD Thesis, University of Arizona. [6]Barucci,M.A., et al (1987), Icarus 72, pp. 304-324. [7]Tedesco, E.F., et al (1989), The Astron. J. Vol. 97, No. 2, pp. 580-606. [8]Bell, J.F., et al (1989), in Asteroids II, pp. 921-945.

Giotto - Spaceprobe to Visit Two Comets

by: Manfred G. Grensemann

Project Manager Giotto Extended Mission
Scientific Directorate, European Space Agency

The European Spacecraft Giotto was launched on 2 July 1985 and encountered Comet Halley on 13/14 March 1986, passing the comet Halley at a distance of 596 Km.

On 2 April 1986 the spacecraft was put into hibernation, to be reactivated after 46 months on 19 February 1990. Spacecraft System were then checked out, so were the experiments on board.

It was determined that all systems had survived encounter and hibernation with exception of the Star Mapper, which Sun-baffle had been perforated, and the redundancy in the antenna despin system had been lost, although the main system was still fully functional. It was also found that the thermal surfaces had been severely affected by the Halley encounter, resulting in high temperatures on the spacecraft units measured at the time of reactivation.

After the status of the spacecraft systems was established, all experiments aboard were switched on and tested. Out of the 11 experiments on board, 7 had survived encounter and hibernation, and it was concluded that this payload could provide valuable scientific data during a next encounter with a second comet.

Giotto was retargeted to comet P/Grigg Skjellerup and hibernated again on 23 July 1990.

The next reactivation will occur in the first week of May 1992 using the NASA Deep Space Network. The closest encounter with comet P/Grigg Skjellerup will then occur on 10 July 1992.

INTERPLANETARY DUST NEAR 1 AU; E. Grün, M. Baguhl, H. Fechtig, J. Kissel, D. Linkert, G. Linkert and N. Siddique, Max-Planck-Institut für Kernphysik, 6900 Heidelberg, Germany; M. S. Hanner, Jet Propulsion Laboratory, Pasadena, CA91103, U.S.A.; B.A. Lindblad, Lund Observatory, 221 Lund, Sweden; J. A. M. McDonnell, University of Kent, Canterbury, CT2 7NR, U.K.; G. E. Morfill, Max-Planck-Institut für Extraterrestrische Physik, 8046 Garching, Germany; G. Schwehm, ESA ESTEC, 2200 AG Noordwijk, The Netherlands; and H. A. Zook, NASA Johnson Space Center, TX 77058, Houston, U.S.A.

The Galileo and Ulysses spaceprobes carry two similar dust detectors. Both instruments have geometric factors of 0.14 m^2 sr. The Galileo is mounted at an angle of 55 deg. with respect to the positive spacecraft spin axis wich points away from the Sun. The Ulysses detector is mounted at an angle of 95 deg. with respect to the positive spin axis which points away from the Earth. We report here on accumulated data of big impacts which correspond to dust particles above a mass threshold of 10^{-13} g at impact speeds of 20 km/s. Between December 28, 1989 and March 25, 1991 Galileo traversed repeatedly interplanetary space between 0.7 and 1.3 AU and detected 344 big impacts. The observed impact rates ranged from 0.1 to about 3 impacts per day. At the same heliocentric distance the impact rates were different by up to an order of magnitude depending on whether the spacecraft moved towards or away from the Sun. From October 27, 1990 to January 1, 1991 the Ulysses spacecraft had reached a distance of 1.6 AU from the Sun and had recorded 9 big impacts. The observed flux was very low, comparable to the lowest fluxes recorded by the Galileo detector at the same distances. Both observed fluxes are compatible with a population of interplanetary dust particles moving on low-eccentricity (e = 0 to 0.3) and low-inclination (i = 0 to 30 deg.) orbits with semi-major axes between 0.5 and 1.9 AU.

N91-25994

DEIMOS: A FEATURELESS ASTEROID-LIKE SPECTRUM; W. M. Grundy and U. Fink, Lunar and Planetary Laboratory, University of Arizona, Tucson, AZ 85721.

We obtained high quality CCD spectra of Deimos from 0.5 to 1.0 μm at a spectral resolution of 15 Å at the time of the 1988 Mars opposition. Our data acquisition and reduction methods allowed us to quantitatively prevent scattered light from Mars from contaminating the spectra. Solar analog stars BS560, BS2007, and BS8931 were observed the same night to allow removal of telluric absorptions. The ratio spectrum of Deimos has a red slope, increasing in reflectance by a factor of ~50% over the one-octave wavelength interval observed. Other than this slope, the spectrum is remarkably featureless. The absence of absorption bands in the spectrum of Deimos is in marked contrast with the spectra of Martian surface materials. No trace of the Fe^{2+} charge transfer absorption band around 1 μm is observed, which rules out the presence of significant quantities of minerals such as the pyroxenes or olivines at the surface of Deimos. The featureless red spectrum of Deimos appears to be consistent with a surface composition of fine grained carbonaceous chondrite type material. We will present an analysis of the spectrum of Deimos which makes use of the Hapke scattering surface model.

This work was supported by NASA grants NAGW 1549 and NGT 50661.

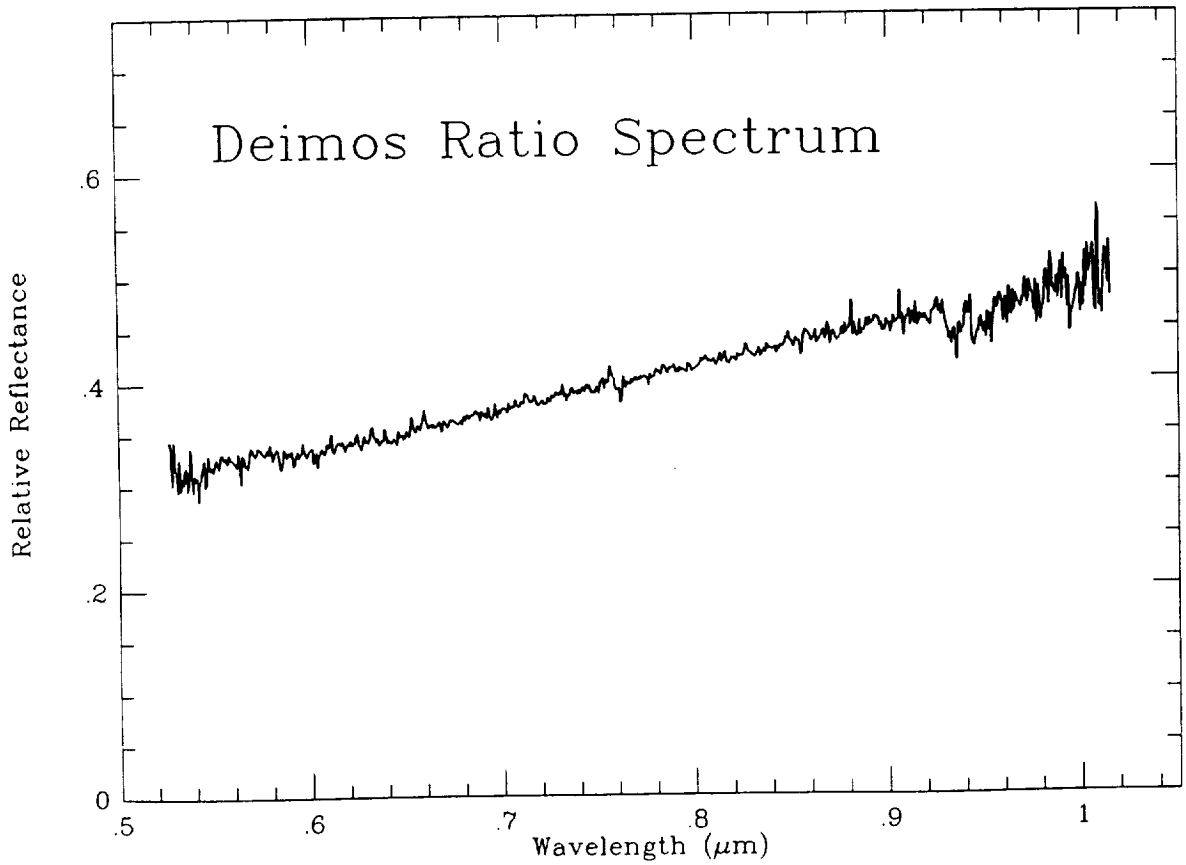

ON THE COMMON GENETIC CONNECTION AND MUTUAL CONDITIONALITY OF THE FORMING OF STABLE STRUCTURES IN CENTRAL GRAVITATING SYSTEMS

Yu.K.Gulak
Pedagogical Institute, 314000 Poltava, USSR

1) Mathematical uniformity of gravitational interaction in planetary systems (PS) of Sun, solitary planets, its massive satellites (S);

2) non-zero central bodies (CB) sizes $r_0 \neq 0$ and mutual restriction $r_g \neq \infty$ of each PS $\Delta r = r_g - r_0$;

3) the in force field of CB energy and angular momentum conservation laws, those are obligatory for every S, which mutually perturb their radial, azimuthal, and latitudal components of motion;

4) sufficiently large number of different masses (fractions) in the system;

5) the natural selection of the permanent S and their separation into the fractions (into degrees of pliability to mutual perturbations), i.e. relaxation, transition to stable state of spatially limited oscillating systems with many degrees of freedom;

6) these obvious from a classical physics' positions theses

a) secure a structuring of PS: forming within them "continuous-discrete" radial, azimuthal, and latitudal standing waves in superposition of which every satellites introduces its own deposit as a bearer of its spatial continuous force field. Such waves really exist and show (is observed) in PS as a system of mutually limiting and shepherding rings (belts), along which move these separated fractions of S. Analogous by nature waves are reproduced easy in laboratory tests;

b) permit to obtain the equation, which is mathematically identical with Schrödinger equation, but (in contrast to the latter) to have physically clear in classical physics' spirit interpretation of each from membering functions, values, and obtained solutions. The direct connection between a CB mass and constant, which takes the place of Planck's constant, is determinad theoretically. Here a misterious nature of this constant as well as connected with it quantum phenomena also acquire a sense of the wellknown images of classical physics: in particular the mathematical "density waves of probability", quantum regularities of radiation and absorption, spin phenomena etc..

Thus, genetic unity of structural formating in the large and small bodies-satellites medium is determined in cosmic planetary systems. It is difficult not to conclude in this a deep analogy between the mechanics of the cosmic and atomic systems, if one remembers the mathematical closeness of the laws of Newton and Coulomb.

REGULARITIES OF THE ORBITAL DISTRIBUTION OF ASTEROIDS, COMETS AND METEORS

Yu.K.Gulak, I.A.Dichko
Gravimetric Observatory of Ukrainian Acad.Sc.314000 Poltava,USSR

Regularities of the orbits of gravitating matter's radial distribution in the Solar system (planets, asteroids, comets, and meteoric bodies, satellites and meteoric matter in planetary systems) are discussed in this report. The orbits of the bodies-satellites tend to group themselves in commensurable (quantum) distances from the attractive centre according to the proposed theory (see report by Gulak), so that their semi-major axes a_n may be shown by an all common gravitational systems formula: $a_n = n a_o/2$, where: n- natural series number, a_o- commensurability element, which is determined singly by the central body mass M of the system: $a_o = \beta M^{7/9}$. Empiric determination of the integration constant β showed, that it doesn't differ practically within a huge range(which exceeds seven powers of ten) of the values M in the Solar system.

Mean semi-major axes within annular systems of asteroids clearly separated by gaps conform well to theoretical calculations using the above formula. 26 orbits between Mars and Jupiter were predicted in 1959 using this theory. In 1959 only 6 of these orbits were found to be occupied by asteroids. In 1969, in connection with the discovery of new asteroids, 8 more of the 26 orbits were found to be occupied, and in 1979 9 more of the original 26 were found to be occupied, leaving 3 orbits yet to be verified.

As regards to comets nuclei (cometoids) then the works by E.I.Kazimirchak-Polonskaya and Yu.K.Gulak showed that they have a property to be in a stable condition based on the pre-calculated orbits of our theory. It is implied in favour with this that whole comet body belts (which are sorces of short-period comets) may be there between giant planets, not only in Oort cloud.

Graundbased observations and calculations of the hundreds of thousands of meteoric bodies'orbits show that its distribution is "formed under the potent influence of macroquantum phenomena" (Yu.I.Voloshchuk, B.L.Kashcheev). These authors draw a conclusion that Gulak's theory gives the best correspondence under comparison of cited observations with the theories by Gulak, Quiroga and Chechelnicky.

The planetary rings including the recently discovered Uranian and Neptunian rings give a good correspondence with this theory, as well as dusty belts around the Earth and Moon (spacecrafts Electron 1-3, Geos-2, Luna-10, Pioneer-9, 10).

The report is illustrated by the tables of gravitating matter's distributions in the systems of Sun, Earth, Jupiter, Saturn, Uranus, and Neptune.

THE SHAPE OF METEOR STREAMS IN ORBITAL PARAMETER SPACE FROM INDEPENDENT METEOR SURVEYS.

B.Å.S. Gustafson

Astronomy Department, University of Florida 211 SSRB, 32611 Florida, USA.

A measure of meteoroid number density based on Drummond's (1981, *Icarus* **47**, p. 545-553) measure of orbital similarity is used to chart the meteoric complex and the extent of major meteor streams in orbital parameter space. Bias correction reveals both narrow congregations and extended structures that may be related to streams. The measure of meteoroid number density can help discriminate between meteor streams. The Tisserand quantity and a set of other "quasi-stationary parameters" were tested on actual meteor streams as an additional discriminant.

SIZE DISTRIBUTION DEPENDANCE OF INFRARED EMISSION FROM MODELS OF ASTEROIDAL AND COMETARY DUST.

B.Å.S. Gustafson

Astronomy Department, University of Florida 211 SSRB, 32611 Florida, USA

Emission efficiencies from near-infrared to far-infrared wavelengths are calculated for two models of asteroid comminute particles and compared with those for a model of cometary dust. The asteroid dust models have higher efficiencies than the cometary dust model of dimensions smaller than the wavelength; but the comet dust model produces more thermal radiation per unit mass. Particles smaller than 10 μm in size dominate the brightness from asteroid dust in the collisional equilibrium size distribution. However, particles in the 10 to 100 μm size range dominate in populations of the cometary and asteroidal dust when the empirical interplanetary size distribution by Grün *et al.* (1985, *Icarus,* **62,** p. 244-272) is applied. While the temperatures of large cometary and asteroidal particles of all concave shapes are within approximately 6% of the black-body equilibrium temperature, the temperatures of the brightest particles deviate substantially from that of a black-body. Cometary dust appear hotter, while asteroid produced dust may appear colder depending on the size distribution below 100μm.

MODELLING OF LONG TERM EVOLUTION AND EQUILIBRIUM STATE OF A DUST COMPONENT FROM THE ASTEROID BELT

B.Å.S. Gustafson[1], E. Grün[2]

1) Astronomy Department, University of Florida 211 SSRB, 32611 Florida, USA.
2) Max-Planck Institut für Kernphysik, Postfach 10 39 80, D-6900 Heidelberg 1, FRG.

The size distribution of collisional debris from an asteroid in the main belt is modeled over time periods of millions of years. The dust is allowed to collide with a background population of dust and meteoroids as they spiral toward the Sun under the action of Poynting-Robertson drag. The background population is modelled using the empirical interplanetary size distribution by Grün *et al.* (1985, *Icarus,* **62,** p. 244-272). The resulting time dependent size distribution at 1 AU is presented along with the heliocentric particle number density distribution as a function of particle mass. As an equilibrium state is approached, deviations from the equilibrium size distribution based on "particles in a box" -model is described.

A SEARCH FOR STREAMS ASSOCIATED WITH EARTH-APPROACHING ASTEROIDS 3551, 3908, AND 4055.

B.Å.S. Gustafson[1] and I.P. Williams[2]

1) Astronomy Department, University of Florida 211 SSRB, 32611 Florida, USA.
2) School of Mathematical Sciences, Queen Mary and Westfield College, University of London, Mile End Road, London E1 4NS, England.

Based on spectral similarity Cruikshank *et al.* (1991, *Icarus* **89,** p. 1-13) suggested that a set of basaltic Earth-approaching asteroids (3551, 3908, 4055, and possibly Vesta) are fragments produced in a collision that may also have generated a stream of basaltic meteoroids. They argue that the stream might be producing Eucrites, Howardites, and Diogenites (HED meteorites) with similar spectra.

This article presents a search for meteor orbits near these asteroids in twelve independent photographic and RADAR surveys. A procedure to search for streams in a wider range of orbital parameter space is presented and used on the 1968-1969 synoptic year Harvard RADAR survey (Sekanina and Southworth, 1975, NASA CR-2615) and graphically reduced Super Schmidt orbits (McCrosky and Posen, 1961, *Smithsonian Contr. Astrophys.*, **4,** No.2). The relatively small set of graphically reduced fireball orbits by McCrosky *et al.* (1976, *Meteoritica,* **37,** p.44-59) are also searched, as the survey was specifically aimed at detecting meteorite dropping fireballs. These survey's were corrected for some of their bias and an attempt made to judge the significance of the meteor associations.

LIGHT SCATTERING BY OPEN-STRUCTURED, FILAMENTARY, COMET DUST MODELS

B.Å.S. Gustafson[1], R.H. Zerull[2], K. Schulz[2] and E. Corbach[2]

1) Astronomy Department, University of Florida 211 SSRB, 32611 Florida, USA.
2) Ruhr-Universität, Fakultät für Physik und Astronomie, Bochum, F.R.G.

A simulation experiment of the light scattering by comet dust was performed at the microwave analogue scattering facility of the Ruhr-Universität Bochum in the Federal Republic of Germany. The scattering targets are designed to approximate the morphology of cosmic dust including cometary and nebular dust. The models can be described as open-structured aggregates of submicron silicate spheres with or without an absorbing mantle. Whether the models are fractal or not is a matter of terminology. They encompass a range of fractal dimensions near 1 to approximately 3. Efficiency factors for extinction, absorption, scattering and radiation pressure will be presented. The angular dependence of scattered intensity and polarization is also shown.

LONG-TERM EVOLUTION OF 1991 DA: A DYNAMICALLY EVOLVED EXTINCT HALLEY-TYPE COMET? G. Hahn & M.E. Bailey, Department of Astronomy, The University, Manchester M13 9PL, England, U.K.

The long-term dynamical evolution of the recently discovered intermediate-period asteroid 1991 DA and a bundle of similar orbits has been followed for $\pm 100,000$ years in a model solar system including the Earth through Neptune. The orbit of 1991 DA is close to the 2:7 resonance with Jupiter; it avoids close encounters ($\Delta < 1$ AU) for at least the past 30,000 years even at the node crossing. This is due to libration of the critical argument σ. Apart from small perturbations due to close encounters with Mars and Uranus in the recent past ($t \simeq -2000$ yr), the orbit evolves mainly through perturbations by Saturn; the time between node crossings with Jupiter or Saturn is $\approx 3 \times 10^4$ yr. Strong secular evolution about 5×10^4 yr ago causes changes in the perihelion distance to $q < 1$ AU and large-amplitude variations in the eccentricity and inclination ($25° \lesssim i \lesssim 75°$). These are similar, for example, to those found in P/Machholz. The long-term orbital evolution of 1991 DA is illustrated, while the connexion between high-inclination, intermediate-period, small q orbits and those of observed Halley-type comets is emphasized. If 1991 DA was indeed a comet, it is not surprising that it is now extinct; searches for residual, low-level cometary activity and associated dust streams should be encouraged.

Dynamical Constraints on Material Orbiting Asteroids

D. P. Hamilton and J. A. Burns (Cornell University)

As Galileo's Gaspra flyby draws near, questions of the quantity and spatial distribution of material which might be found in its vicinity become critically importance to spacecraft mission planners who are making final decisions on how closely to approach this small asteroid. Obviously, in the absence of any perturbations, particles can move on Keplerian orbits at any distance from an asteroid. In reality, however, gravitational perturbations from the Sun and planets, and solar radiation pressure will limit the zone in which particles can stably orbit. Following many other studies, we discuss elsewhere (Hamilton and Burns, Icarus in press) the size and three-dimensional shape of the stability zone for an asteroid that moves along a circular heliocentric orbit, ignoring solar radiation pressure and perturbations from Jupiter. We find that the stability zone scales like the radius of Hill's sphere and that orbits are stable out to lesser distances over the orbital pole than in the asteroid's orbital plane. Chauvineau and Mignard (Icarus 1990, 87, 377) consider how Jupiter perturbs planar orbits about the asteroid and show that the consequent diffusion of the Jacobi constant leads to additional escapes. Here we discuss two further perturbation effects: the influence of the asteroid's orbital eccentricity and the contribution of solar radiation pressure.

We find numerically that the relatively large eccentricity of Galileo's target Gaspra significantly reduces the size of the stability zone for test particles that are followed for five orbits of the asteroid around the Sun. The figure shows the maximum height (measured in asteroid radii) attained for a series of test cases as a function of initial inclination off the asteroid's orbital plane. The solid circles are for an asteroid moving on a circular orbit and the crosses are for one with Gaspra's eccentricity (e=0.17). We see that orbits around an asteroid with sizable eccentricity rise to lesser heights than those around an asteroid with zero eccentricity.

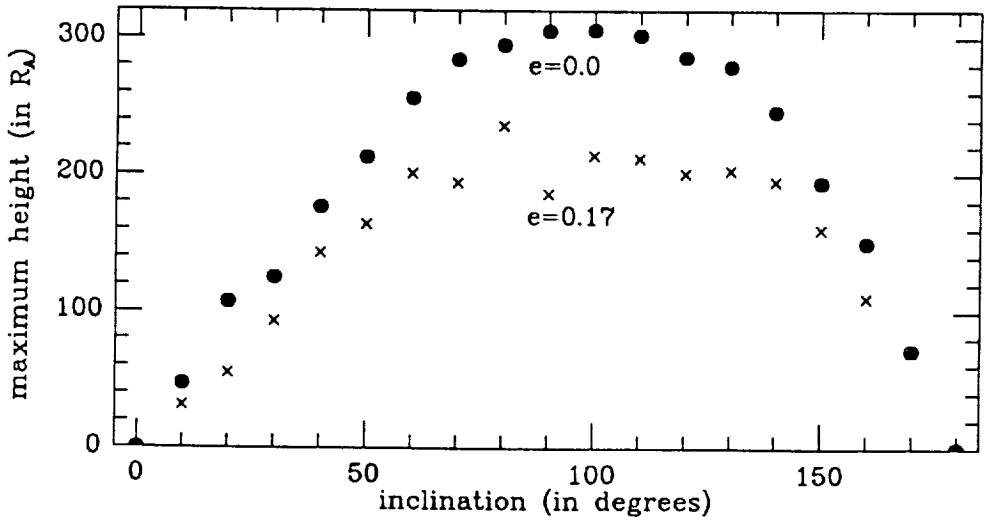

Radiation pressure is found to be surprisingly effective in removing mm and cm sized particles from circum-asteroidal orbits. For such large particles in orbit around the Sun or the planets, radiation pressure can be safely ignored, but in the shallow gravitational well of an asteroid it is a strong perturbation. We find that particles satisfying the following inequality are forced to crash into the asteroid:

$$s(cm) < 1.7\left(\frac{r(km)}{1000}\right)\left(\frac{2.2}{a(AU)}\right)\left(\frac{M_{Gaspra}}{M_{Asteroid}}\right)\left(\frac{Q_{pr}}{1.0}\right)\left(\frac{2.5}{\rho(g/cm^3)}\right);$$

these collisions occur in timescales shorter than the asteroid's orbital period. Here s is the particle's radius, r is its distance from the asteroid, a is the asteroid's distance from the Sun, the M's are masses, Q_{pr} is a radiation efficiency coefficient with an expected value near unity and ρ is the particle's density. Coincidentally, a size distribution consisting of solely mm and cm sized particles is the most dangerous to a spacecraft for a given amount of mass in orbit around the asteroid. Combining observational constraints on the optical depth with the changes in the size distribution from orbital evolution induced by radiation pressure, the worst-case probability for a crippling collision should be reduced.

HIGH PRECISION PHASE RELATIONS OF DARK, LIGHT, AND INTERMEDIATE ASTEROIDS

A.W. Harris, Jet Propulsion Laboratory

A fundamental hypothesis in the formulation of the H-G magnitude system is that all phase curves can be represented as a linear combination (in intensity space) of two phase curves. The physical motivation is the assumption that the singly scattered and multiply scattered components have the same phase dependance for any surface; thus the resultant phase curve is a linear sum of the two components, with the ratio of each loosely related to the albedo of the surface. To test this hypothesis, it is not necessary to "observe" the pure single-scattered and multiple-scattered phase relations. Any two phase relations, sufficiently different from one another, should be able to match any other phase relation as a linear combination (in intensity space) of the first two. A simple corollary is that if any two phase curves (normalized at zero phase angle) cross over at another phase angle, then all phase curves must pass through that point. In the figure below, we present three high precision phase curves: 44 Nysa, one of the highest albedo asteroids known (These data are from Harris, et al., Icarus 81, 365-374, 1989); 47 Aglaja, a moderately dark C Class asteroid (Harris, et al., this conference); and 113 Amalthea (previously unpublished data). Amalthea is higher than average albedo, but about intermediate between 44 and 47. All three curves have been adjusted to the same level at zero phase angle. Each curve crosses over the other two, none at the same phase angle, thus violating the above stated corollary. (The corollary applies in either magnitude or intensity space.) Thus it is clear that the fundamental postulate of the H-G system is not valid, and a more complete theory must be sought.

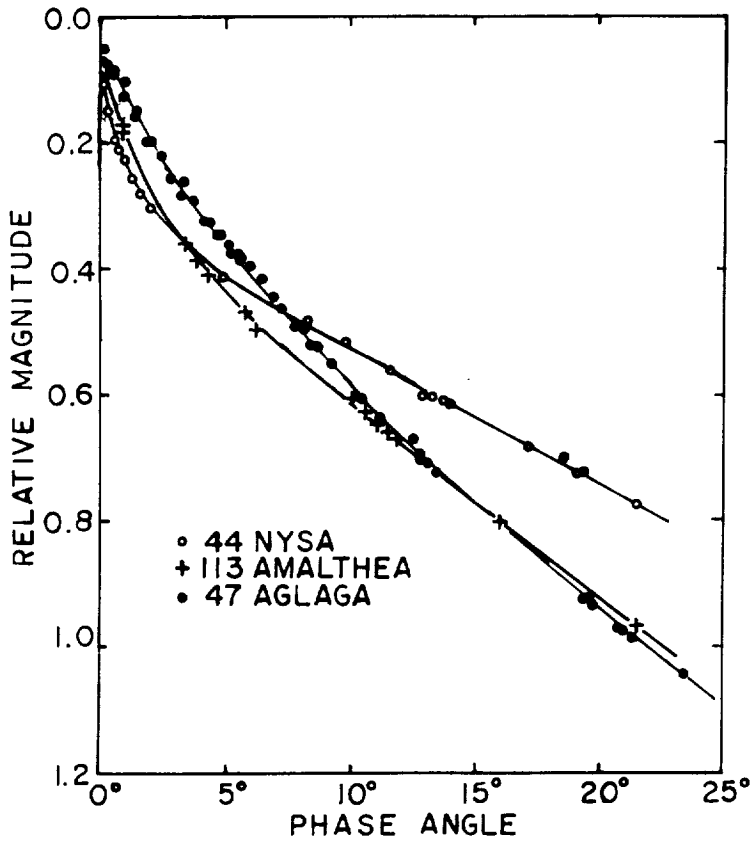

PHOTOELECTRIC LIGHTCURVE AND PHASE RELATION OF 47 AGLAJA

A.W. Harris, G.P. Chernova, D.F. Lupishko, J.W. Young, N.N. Kiselev, L.V. Jones, and B.J. Wallace

Millis, et al. (Icarus 81, 375-385, 1989) present occultation and photometric results for 47 Aglaja which indicate that it is a fairly dark asteroid (albedo = 0.071 on the H-G system). The phase curve presented shows considerable variation in intrinsic brightness with different aspects, but coverage at any one opposition was insufficient to fully define G, and allow accurate assessment of the relative light levels each year. Furthermore, there was some indication that Aglaja might be substantially deficient in opposition effect with respect to the H-G model, as had been found for several other dark asteroids (cf., Harris and Young, Icarus 81, 314-364, 1989). We embarked on an international observing campaign in 1989 in order to resolve some of these issues. The resulting data set, from 4 observatories in the USSR, USA, and Columbia, is the largest data set ever obtained on a single asteroid at one apparition, consisting of over 2000 individual observations on about 50 nights. The period was determined unambiguously, P = 13.176 $\pm$0.001 hours, and the phase curve was sampled thoroughly from phase angle 23^{o} down to 0^{o}.10. The phase relation is indeed less curved (less opposition effect) than predicted by the H-G model. By drawing a smooth curve through the phase data, and assuming the same curve at other oppositions, it was possible to define the relative light levels at 5 other observed apparitions. These results confirm the conclusion of Millis, et al. (1989) that Aglaja was observed nearly pole-on in 1979, at ecliptic longitude 330^{o}.

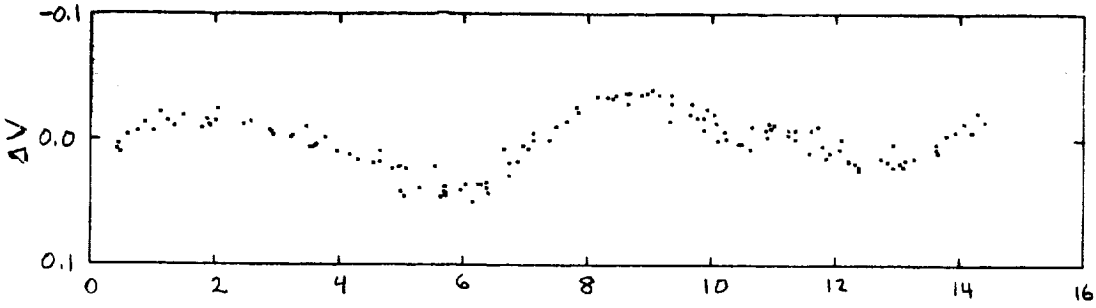

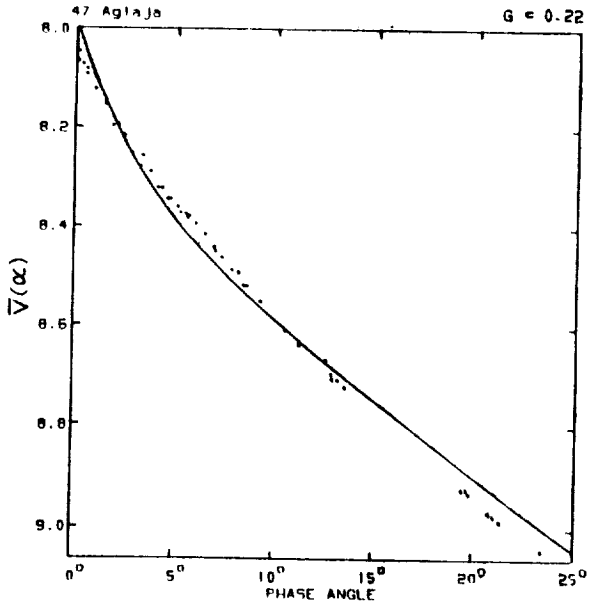

The data used in the composite lightcurve (above) have been heavily averaged to reduce clutter of plotted points. The vertical scale is 0.1 mag. per tick, and the horizontal scale is 2 hr per tick. The phase plot (left) shows the deviation of the best-fit H-G relation (solid line) from the observed phase relation (dots).

A CORVID METEOR SHOWER IS PREDICTED FOR 2003 OR 2006

Jack B. Hartung, Max-Planck-Institute für Kernphysik, 6900 Heidelberg, Germany.

The Corvid meteor stream was observed only once, from June 25 to July 2 in 1937. Its observed radiant is given by a right ascension of 192° and a declination of -19°. The direction of motion of Corvid meteoroids, which is just opposite to their radiant, is given by a right ascension of 12° (192° - 180°) and declination of +19°.

The formation of the lunar crater, Giordano Bruno (GB), was observed on the evening of June 25, 1178 (Gregorian calendar). On that evening the phase of the Moon was 19.5° past new moon, the ecliptic longitude of the Sun was 93°, and the optical libration in longitude was 1.5°. The location of GB is lunar latitude, 36° N., and lunar longitude, 103° E. With these data one can determine the ecliptic longitudes of the lunar prime meridian, 294° (93° + 19.5° + 1.5° + 180°), and the zenith direction at GB, 37° (294° + 103° - 360°). The ecliptic latitude of the zenith direction is approximately +36°. By transforming from ecliptic to equatorial coordinates we obtain the right ascension, 18°, and declination, 47°, of the zenith direction at GB at the time of the impact.

By solving a spherical triangle we find the angle between the zenith direction at GB and the direction of motion of Corvid meteoroids to be 28°. Laboratory experiments show that for ejection velocities of 2.4 km/sec, the lunar escape velocity, the angle between the ejecta direction and the local vertical (zenith) is also 28°! It seems beyond coincidence that the observed direction of motion of Corvid meteoroids and one independently expected direction of ejecta motion based on experiments are identical.

If ejecta from the GB impact is to be seen in late June many years later at the Earth, an integer number of ejecta orbits must be executed during exactly the time required for the Earth-Moon system to complete an integer number of orbits. The year of the GB impact, 1178, differs from the only year Corvid meteors were observed, 1937, by 759 years. If a connection between these two events exists, then 759 must be the product of two integers, one representing the number of years, or Earth orbits, between Earth-Corvid encounters, and the second integer representing the number of such encounters that have occurred through 1937. Integer factors of 759 are: 3, 11, 23, 33, 69, and 253. The period of the Corvid orbit is limited to those numbers which, when divided into any of these factors, yield integer quotients, the integer quotients representing the number of Corvid orbits between each Earth-Corvid encounter. Therefore, for each integer factor we can state unequivocally which years could yield observable Corvid meteors.

Factors 3 and 11 can probably be ruled out because encounters would be expected every 3 or 11 years, respectively. Encounters so often should have been observed, although 1992 (1937 + (5 x 11)) should not be ignored. It is possible that appropriate observations were not made in late June of 1948, 1959, 1970, or 1981. The next possible opportunity to observe Corvid meteoroids, if they were, in fact, produced by the GB impact in 1178, will be in late June of 2003 (1937 + (2 x 33)). Another opportunity will occur in 2006 (1937 + (3 x 23)). Accordingly, I predict that another Corvid meteor shower will occur in late June and early July of 2003 or 2006.

LIGHTCURVE OF COMET AUSTIN(1989C1) AND ITS DUST MANTLE DEVELOPMENT; H. Hasegawa, ASTEC, Inc. and J. Watanabe, National Astronomical Observatory

Brightness variation of comet Austin(1989c1) was investigated in terms of the variations of water production rate. We used Newburn's semi-empirical law to translate the visual brightness data into water production rates. The curve of the water production rates as a function of heliocentric distance was compared with the model calculations that were assumed energy balance between solar incident and vaporization of water. Thermal flow in a dust mantle at a surface of the nucleus is also included in the model. The model calculations including the dust mantle are more favorable to the observed rate than the non-dust mantle cases. It is also expected that the dust mantle would have been developed when the comet was at a large heliocentric distance before the perihelion passage. Dust tail analysis of the comet showed such dust release. And the extinction after the perihelion passage suggests that the dust mantle was developed gradually.

COMET CHARACTERISATION AND LANDING: STATUS OF ESA STUDIES FOR ROSETTA

M. Hechler, J. de Lafontaine
European Space Agency

The Rosetta mission, one of the cornerstones of the ESA Space Science programme, has the objective of returning a comet nucleus sample to Earth laboratories, preserving its fundamental chemical and physical properties. It is believed that the analysis of cometary material will provide answers to questions related to the origin and early evolution of the solar system. The mission design and the spacecraft system have been studied jointly by NASA and ESA. A description of the baseline mission scenario is presented by A. Atzei and R. Mitchell at this Conference. In parallel to the mission definition activities, a series of technology studies sponsored by ESA have been addressing the critical elements of the mission which are mainly related to its near-comet phases. An overview of the current Rosetta mission planning in the near-comet phases before landing is presented here, as it is currently foreseen in the studies carried out within ESA and in Industry under ESA sponsorship.

The near-comet phases until landing include: (1) the Approach Phase, (2) the Observation Phase, and (3) the Descent and Landing Phase. The Approach Phase begins with comet acquisition by the on-board camera. With a sequence of orbital manoeuvres commanded from the ground, the spacecraft velocity is progressively reduced. For safety, the spacecraft trajectory is never directed at the comet but the fly-by distance is also gradually decreased to perform an orbital rendez-vous with the comet, a few hundreds of kilometers above it. During the approach, a preliminary identification of the comet kinematic and geometrical characteristics is obtained, using ground processing of on-board and ground-based observables.

After entering the gravitational field of the comet (some 30 to 1300 km above it, depending on the comet mass), the spacecraft acquires a succession of remote-sensing orbits around the nucleus. The Observation Phase activities begin with a global mapping of the illuminated part of the comet. Near-circular polar orbits are selected to maximize the coverage while satisfying the requirements of constant communication link with the ground stations. Based on these data, three to five candidate landing sites are selected by the ground and subsequently analyzed in more detail from eccentric orbits which overfly these locations at about 5 km altitude. Detailed maps of the candidate landing areas (500 m x 500 m) in the visible, the infrared and the thermal infrared spectra are acquired to determine their suitability from safety and scientific interest points of view. The site safety assessment is also supported by a laser ranging instrument that provides a detailed topographic map of the area in terms of altitude profiles. In addition, subsurface radar sounding may support the landing site selection. During the observation activities, on-board measurements and tracking data from ground are processed to estimate the comet kinematics, its gravitational field and the spacecraft orbit to an accuracy required for the safe navigation and guidance of the spacecraft to the desired landing point. Once these parameters are uplinked from ground, the autonomous Descent and Landing Phase towards the selected landing site is initiated from an approach orbit at a few kilometers above the surface.

Two descent scenarios, a primary and a back-up, are foreseen for the Rosetta mission. In the nominal case, the spacecraft autonomous navigation relies on the laser range finder. Elevation maps are built in real time with the scanning instrument and are compared with on-board maps stored earlier, at the end of the Observation Phase. Accurate information on the spacecraft horizontal position are thus derived. In the alternate case where the laser may have failed, the spacecraft horizontal position is predicted by on-board models but a microwave radar ensures landing safety by searching and locking on a detected flat area. In both scenarios, precise altitude, velocity and attitude measurements are available from the radar system. Numerical simulations have demonstrated that landing accuracies of the order of 20 m in the baseline scenario and 200 m in the second one (3 sigmas) can be achieved.

Further refinements to these strategies are currently being performed in the ESA studies. More detailed analyses are also conducted to design and test the ground-based and on-board algorithms required for spacecraft navigation, guidance and control. Microprocessor implementation of some of the on-board algorithms is foreseen by the end of 1992.

N91-25995

Near-Earth Asteroid Discovery Rate Review, Eleanor F. Helin, Jet Propulsion Laboratory

Fifteen to twenty years ago the discovery of 1-2 Near-Earth Asteroids (NEA's) per year was typical from one systematic search program, Palomar Planet-Crossing Asteroid Survey (PCAS), and the incidental discovery from a variety of other astronomical programs. Sky coverage and magnitude were both limited by slower emulsions, requiring longer exposures. The 1970's sky coverage of 15,000 to 25,000 sq. deg. per year led to about one NEA discovery every 13,000 sq. deg.

Looking at the years from 1987 through 1990, we find that by comparing 1987/1988 and 1989/1990 the worldwide discovery rate of NEA's went from 20 to 43, a little more than a twofold increase from the first two year period to the latter two years. More specifically, PCAS' results when grouped into the two year periods, show an increase from 5 discoveries in 1987/1988 to 20 in the 1989/1990 time period, a fourfold increase. Also, that our discoveries went from representing about 25 percent of the worldwide total to contributing roughly 50 percent of the discoveries worldwide in the 1989/1990 period. This trend continues into 1991, whereby PCAS is discovering about a NEA per month. As the discovery rate continues to spiral up, with significant contributions coming from McNaught/Steel in Australia and Gehrels, Scotti and Rabinowitch in Arizona, I anticipate a doubling again in discoveries in the 1991/1992 period. Of course, an important aspect of these more recent discoveries is the inclusion of fainter than magnitude 20-21 objects extending out as faint as H magnitude 28 (1991 BA). At the same time several very bright asteroids have been discovered which indicates that in the NEA population not all of the objects to magnitude 13-14 have been discovered. The PCAS discovery of the 1990 SQ at H magnitude 12.5 surpasses (1627) Ivar as the brightest known asteroid in the NEA population. It is rather remarkable that our most recent NEA discoveries in 1990/1991 include the brightest (1990 SQ) and the faintest (1991BA) on record, certainly suggesting that a wide range of undetected objects still roam in earth-approaching and crossing orbits. The surge of discoveries enjoyed by PCAS in particular is attributed to new fine grain sensitive emulsions, film hypering, more uniformity in the quality of the photograph, more equitable scheduling, better weather, excellent team members and coordination of efforts. Although one hopes that more improvements and fine tuning may be possible, it seems that we have just about attained our maximum output for the discovery of NEA's using current techniques at the 0.46 M Palomar Schmidt. I anticipate working diligently to maintain our current rate of discovery. Significant increase in discoveries in the next two year period will most likely come from elsewhere (the southern hemisphere and fainter, smaller objects found by CCD - electronic sensor detector-facilities). With the stunning increase in the last 2 year period over the previous two years, an order of magnitude, if not greater, increase in the discovery rate of NEA's can be anticipated by the end of the decade with the advent of CCD Schmidt Telescopes distributed around the world.

I wish to thank Palomar Observatory for observing time and necessary support. This research was carried out in the Planetary/Astronomy programs at Jet Propulsion Laboratory, California Institute of Technology, under contract with National Aeronautics and Space Administration.

SPECTROSCOPIC OBSERVATIONS OF COMET AUSTIN (1989c)

Rod Heyd, Susan Wyckoff and Peter Wehinger, Arizona State University
Terry Rettig, University of Notre Dame
Peter Mack, Michigan-Dartmouth-MIT Observatory

Longslit CCD spectra($\lambda = 5100-6400$ Å, $\Delta\lambda \sim 3$ Å) were obtained with the Michigan-Dartmouth-MIT 1.3 meter telescope in May 1990($r = 0.74$ AU, $\Delta = 0.50$ AU). The spectra have been reduced with IRAF. Spectral extractions offset sunward and tailward from the nucleus were analyzed. Species observed in the spectra include: C_2, NH_2, H_2O^+, CO^+, and several unidentified features. Spatial extractions of rotational lines in the NH_2(10-0) band extend $\sim 10^{4.5}$ km from the nucleus. A fit of the vectorial model to the NH_2(10-0) spatial profile is consistent with an NH_3 parent molecule. The NH_2 production rate and an ammonia to water abundance ratio have been derived.

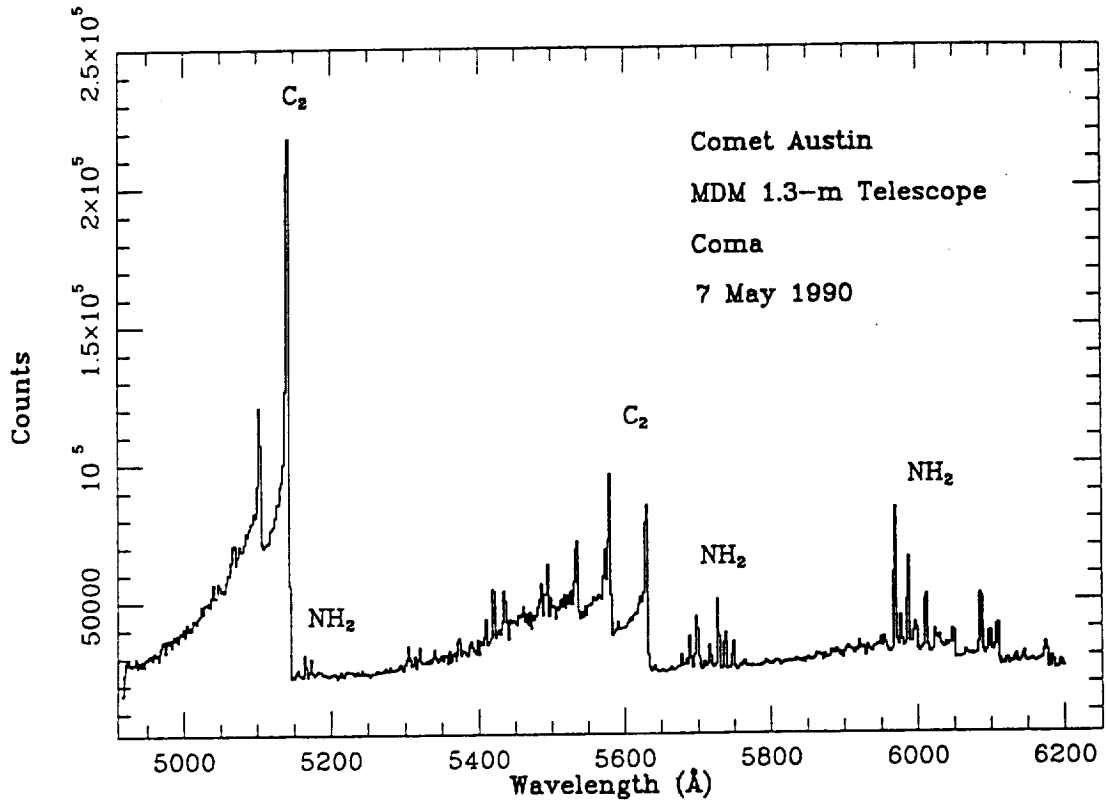

IR Spectroscopy of Comets: Methanol at 3.52 μm

S. Hoban, M. Mumma, D. Reuter, M. DiSanti *(NASA/GSCF)*,
R. Joyce *(NOAO)* and A. Storrs*(U. Texas)*

As part of an ongoing program to use infrared spectroscopy to search for molecular species which are directly sublimated from cometary nuclei, we present medium resolution ($\lambda/\Delta\lambda \approx 10^3$) long-slit spectra of several recent comets in the 3-μm region. In the 3.44-3.64 μm spectral region, we detect the red wing of the broad "organic" feature which is centered at 3.36 μm, and a narrower feature is apparent which peaks at 3.52 μm, which we tentatively identify with methanol. We find that the spatial profile of the 3.52-μm emission is consistent with that of a directly sublimated species. We will compare our results with the detections of methanol and formaldehyde in comets at millimeter wavelengths. We will report upper limits for formaldehyde retrieved from our spectra, and we will discuss the implications of a possible extended source of H_2CO on our results.

LIGHT CURVE DERIVATIVES AS A TOOL FOR THE ANALYSIS OF ASTEROID REFLECTION PROPERTIES, M. Hoffmann, Observatorium Hoher List, Universitäts-Sternwarte Bonn, Daun, F. R. Germany

Signatures of the collisional origin, subsequent cratering, and of albedo variegation show up in the light curves of asteroids, but it is impossible to separate these effects by a light curve inversion uniquely. For smooth ellipsoidal and multifractal surface models as well as for several aspects of the asteroid 7 Iris some characteristic properties of their rotation light curves are shown by a spectral analysis of their derivatives. Contrary to light curve analysis techniques involving spherical harmonics the high frequencies of their brightness changes are utilized by this method.

U.S. GEOLOGICAL SURVEY-LOWELL OBSERVATORY ASTEROID SURVEY: FIRST RESULTS; H.E. Holt, USGS, Flagstaff, Ariz., E. Bowell, Lowell Observatory, Flagstaff, Ariz., C.S. Shoemaker and E.M. Shoemaker, USGS, Flagstaff, Ariz.

Each year during the course of the asteroid and comet survey conducted by us at Palomar, about 1,000 fields, 8.75 degrees in diameter, are photographed with multiple exposures on hypered Kodak 4415 film. Under favorable conditions of observing, the detection threshold for main belt asteroids is about B = 18.5. Single fields near opposition may contain more than 100 asteroids, most of which are new. Altogether, several thousand asteroids are found and marked on the films each year. Until recently, because of limited manpower, astrometry was carried out only for a modest number of objects, chiefly planet-crossing asteroids, Trojans, high inclination asteroids, and comets.

A systematic effort was begun in the fall of 1990 to complete astrometry for the majority of asteroids observed in selected months. The immediate objectives of this pilot effort are to update the orbits of numbered asteroids, to extend the orbital arcs of previously designated objects and search for linkages, and to determine orbital elements for numerous new asteroids. To date, asteroids observed in 50 fields have been measured on 2 to 3 pairs of films separated by 2 to 6 days during a single dark run. More than 2,000 asteroids have been measured; among those, 820 objects were initially regarded as new asteroids. We are attempting to obtain at least one-month arc orbits for as many of the new objects as possible. So far, updated orbits have resulted for about 200 numbered asteroids; improved orbits have been obtained for about 100 unnumbered asteroids, of which about 20 have now been numbered. New short arc orbits were derived for about 300 asteroids from our observations; in many cases it has permitted the linkage of previously designated asteroids, resulting in multiple opposition orbits. A few of the new objects have already been numbered.

Our principal objective in this investigation is to substantially increase the rate of discovery and of numbering of main belt asteroids. Our long range goal is to double or triple the number of main belt asteroids with high precision orbits in order to resolve questions concerning the dynamical structure of the belt. In particular, we are interested in the identification of collisional families. The present statistics of proper elements are sufficient to recognize only large families with high confidence. Greatly expanded knowledge of the asteroid belt is required to demonstrate the reality of small families and thereby document many specific events in the collisional history of the belt.

ORIGIN OF ASTEROIDS AND COMETS

Zhong-wei Hu, Er-kang Wang, Nanjing University, China

The physico-chemical conditions of the nebular disk around the sun,especially the temperature profile, caused the asteroid region to be a transition region between non-condensation and condensation of ice-matter, resulting in a discontinuity in the projected surface density of solid acrretable matter. Because the ice-matter can condense in the Jupiter region and there was more acrretable matter, large planetesimals formed very early and grew rapidly. The mutual perturbation and encounders of these planetesimals changed their orbits,making some of them pass through the asteroid region. At that time, the planetesimals in the asteroid region were still small, so the interlopers accreted and took away with them the local accretable matter, causing the local planetesimals to stop at the "half-finished product" stage, forming only asteroids and not major planets. Perturbation by interlopers also increased the random velocity of the local remant planetesimals and their break-up through mutual collision gave rise to the great orbital veriety of asteroids and their mass spectrum. this basic view is proved by quantitative analysis, including accretion of Jet streams.

The structure in the outer region of the nebular disk is analysed and no formation zone of comets can exist there. Our view is that the comets evolved from the residual ice-planetesimals in the zone between Jupiter and Nepture.

ANALYSIS OF MEI VILLAGE FALLEN ICE

Zhong-wei Hu,Zhao-lin Li,Ru-liang Li,Hao-shen Jiang,Er-kang Wang
Nanjing University,China
Xi-yuan Xu,Science and Technology Commitee of Wu-Xi county,China

A piece of ice fell down from the sky into a field near cottage Chen Shan Fang of Mei village,Wu-Xi county in China,on 17 november 1984. By investigating the scene of the fallen ice and witnesses and departments of meteorology and aviation, possibilities that the ice was of artificial or meteorological or airplane origins was excluded. A few samples of the ice were submitted to serious experimental analysis, and preliminary results show that there are some differences between the ice and terrestrial matter. It is in favour of the viewpoint that the ice originated from extraterrestrail space, maybe from a small comet. Further researching fallen ice might be of great significance for understanding nature of comets and water resource on the earth as well as relevant problems of meteorology, geology and astronomy.

METALLIC ATOMS AND IONS IN COMETS

S. Ibadov
Institute of Astrophysics, Dushanbe 734670, USSR

Investigation of metallic component in comets is important in different aspects. Emissions of refractory metallic atoms (Fe, Ni, Si, etc.) have usually been detected in Sun-grazing comets at heliocentric distances R $\simeq$ 0.01 AU. Meanwhile, in situ measurements carried out withing the coma of comet Halley 1986 III by VEGA and GIOTTO spacecraft near R=1 AU led to the discovery of metal ions of the Fe^+ type.

Anomalous distribution of the Na D-line emissions in the head of the bright comet Mrkos was detected by 200-inch Palomar telescope in 1957, the origin of which is the puzzle in the physics of comets.

Metallic atoms have the low ionization potentials and in this connection the short photoionization time scale ($\sim 10^4$ sec at R=1 AU) so that generation mechanisms of metal atoms may also by important in the problem of the ionization of the cometary matter, particularly of the inner coma.

Theoretical considerations of the different mechanisms of generation of metal atoms and ions in the cometary comae led to the following conclusions. Depression of the temperature of the cometary dust - of the potential source of cometary coma metallic component - by the outflowing cryogenic gas from the cometary nucleus may occur in the near-nuclear region of bright comets and therefore the gas production rate of such comets may be determined on the basis of anomalous distribution of the sodium D-line emissions.

Ions of refractory elements (Fe^+, Si^+, etc.) in the cometary coma at large heliocentric distances will be effectively produced by high velocity ($\geq$10 km/s) collisions of cometary and zodiacal dust particles and therefore such metallic ions may serve as indicators of the passage of dusty comets of the Halley type through interplanetary dust clouds.

1990 MB: THE FIRST MARS TROJAN

Kimmo A. Innanen (York University), Seppo Mikkola (University of Turku),
Edward Bowell (Lowell Observatory), Karri Muinonen (Lowell Observatory),
Eugene M. Shoemaker (U.S. Geological Survey, Flagstaff)

Asteroid 1990 MB was discovered by D. H. Levy and H. E. Holt on 20 June 1990 during the course of the Mars and Earth–Crossing Asteroid and Comet Survey conducted by E. M. and C. S. Shoemaker. An orbit based on a 9–day arc and the asteroid's location near Mars' L5 (trailing Lagrangean) longitude led E. Bowell to speculate that it might be in 1:1 resonance with Mars, analogous to the Trojan asteroids of Jupiter. Subsequent observations strengthened the possibility (IAUC 5067), and later calculations by M. Yoshikawa and B. G. Marsden (IAUC 5075) confirmed it. Thus 1990 MB is the first known asteroid in 1:1 resonance with a planet other than Jupiter. The most recent orbit, from observations in 1979 and 1990, shows that the asteroid's semimajor axis (1.5235591 ± 0.0000003 AU, epoch 10 December 1990) is very similar to that of Mars (1.5235830 AU, same epoch).

The existence of 1990 MB—a small body most likely between 2 and 4 km in diameter—provides remarkable confirmation of computer simulations performed by S. Mikkola and K. A. Innanen (IAU Colloquium 123, in press). Their self–consistent n–body simulations have demonstrated just this sort of stability for Trojans of all the terrestrial planets over at least a 2–million–year time base. In the case of Mars Trojans, it was initially thought that stable–looking orbits must have semimajor axes that depart from Mars' by less than $\Delta a/a = 0.003$ and angular excursions from L5 that are less than 2°. Such a small region of stability led Bowell *et al.* (*Bull. Amer. Astron. Soc.* **22**, 1357, 1990) to speculate that 1990 MB was captured from a free orbit fairly late in solar system history, since it is not likely to have survived the heavy bombardment known to have occurred in the region of the terrestrial planets. Additional evidence came from the existence of (3800) Karayusuf, an asteroid having a semimajor axis of 1.578 AU, which suggests that multiple encounters with Mars could lead to orbits rather close to the 1:1 resonance. However, more recent integrations of the motion of 1990 MB by Mikkola and Innanen show that stable excursions about L5 as large as 80° occur on timescales of millions of years. Thus, the question of whether 1990 MB is a primeval Mars Trojan remains open. Clearly, it is desirable to investigate the size and nature of the region of Mars–Trojan stability, and to examine possible implantation mechanisms.

The discovery of 1990 MB suggests that others of similar or smaller diameter may be found. Using hypothetical populations of Mars Trojans, we have modeled their possible sky–plane distributions as a first step in undertaking a systematic observational search of Mars' L4 and L5 libration regions.

Research supported, in part, by NASA grant NAGW–1470.

DUST EMISSION FROM 2060 CHIRON

W.-H. Ip, Max-Planck-Institut fuer Aeronomie, D-3411 Katlenburg-Lindau, Germany

Recent photometric observations of (2060) Chiron have shown that a coma of submicrom dust particles is developed around this distant object. In the present report we shall consider the volatile sublimation process on Chiron's surface and the resultant ejection of small dust particles via gas drag. The dependence of the morphology of the dust cloud on the surface gravity and nucleus rotation will also be investigated. The merits of other possible dust emission mechanisms such as electrostatic charging will be compared with the gas sublimation effect.

THE PRODUCTION OF HOT IONS AND ENERGETIC NEUTRAL ATOMS IN COMETARY COMAS.

W.-H. Ip, Max-Planck-Institut fuer Aeronomie, D-3411 Katlenburg-Lindau, Germany

A burst of hot ions with energies up to a few hundred eV was observed by the Giotto probe as it passed through the contact surface of the cometary ionosphere. The origin of these hot ions in the inner coma has not been satisfactoriy explained. The collisional re-ionization of energetic neutral atoms created in the outer coma was found to be problematic, for example. In the present report we shall assess the possible contribution of particle acceleration by reconnection process in the ion tail. The potential "internal" ionization effect from such auroral process will be estimated as well.

ASTEROID–TYPE ORBIT EVOLUTION NEAR THE 5:2 RESONANCE. **S.I. Ipatov,** *M.V.Keldysh Institute of Applied Mathematics, Moscow, USSR*

In the case of the 5:2 commensurability with the motion of Jupiter the asteroid can reach the orbits of Mars, Earth and Venus when eccentricity **e** is greater than 0.41, 0.65 and 0.74, respectively. For individual fictitious asteroids Ipatov [1] obtained the growth of **e** from 0.15 to 0.74–0.76. Rates of changes of orbital orientations are different for Mars, Earth, Venus and asteroid. Therefore, for corresponding values of **e** the asteroid could encounter these planets and leave the gap due to those encounters. In order to investigate this hypothesis of the 5:2 Kirkwood gap formation Ipatov [2] studied the regions of initial data for which the eccentricities of asteroids located near the 5:2 commensurability exceeded 0.41 during evolution. The orbit evolution for 500 fictitious asteroids was investigated by numerical integration of the complete (unaveraged) equations of motion for the three–body problem (Sun–Jupiter–asteroid). Variations in **e** for most of these asteroids were quasiperiodic. The equations of motion were integrated in the time interval $\Delta t \geq 5 \cdot 10^3 t_J$ (t_J is the heliocentric orbital period of Jupiter) in the two–dimensional case and $\Delta t \geq 10^4 t_J$ in the three–dimensional case. Various initial orientations of the orbit of the asteroid and its location in orbit were considered in the case when initial value of asteroidal semimajor axis *a* was equal to the resonance value. For the initial asteroidal eccentricity $e_o=0.15$ it was obtained that maximum value of asteroidal eccentricity exceeded 0.41 for 2/3 of all investigated asteroids. We defined the maximum region of the initial values of *a* and **e** for which fictitious asteroids penetrated within the orbit of Mars during their evolution. It was shown that the outer boundaries of this region coincided with the boundaries of the 5:2 Kirkwood gap. For $e_o \leq 0.2$ and initial inclination $i_o \leq 20^o$ the regions of initial data for which fictitious asteroids reached the orbits of Earth and Mars are close to each other. Asteroids reached the orbits of Mars and Venus as a rule for certain types of relationships between variations in eccentricity and longitude of perihelium. For $e_o \leq 0.15$ and $5^o \leq i_o \leq 10^o$ resonant relationships were obtained in some cases between the periods of variations in eccentricity, inclination **i**, argument of perihelium and longitude of the ascending node. In the case $i_o=40^o$ the equations of motion were integrated in a time interval equal to $5 \cdot 10^4 t_J$ or $10^5 t_J$ because in this case for the majority of runs maximum values of **e** and **i** were reached in the time $\Delta t > 2 \cdot 10^4 t_J$. When $i_o=40^o$ and $e_o=0.15$ it was obtained for all investigated asteroids that the maximum values of eccentricity $e_{max}>0.6$, and for most of the asteroids $e_{max}>0.99$ while the maximum value of inclination $i_{max} \geq 89^o$.

References: [1] Ipatov S.I. (1988) *Kinematics Phys. Celest. Bodies.* **4**, *N* 4, 49. [2] Ipatov S.I. (1989) *Sov. Astron. Lett.* **15**, 324

PHOTOMETRY OF COMET AUSTIN AROUND CN 0-0 BAND

V. Ivanova, B. Komitov,
S. Vladimirov and V. Shkodrov

Department of Astronomy, Bulgarian Academy
of Sciences, 1784 Sofia, 72 Lenin blvd.

Photographic observations of Comet Austin 1989c1 were taken with the 50/70cm Schmidt telescope of the Bulgarian National Observatory - Rozhen through an interference filter transmiting the CN band around 382nm. The observations were carried out on 18 and 27 of May 1990, when the comet has been at heliocentric distances r=1AU and r=1.2AU and geocentric distances of 0.28AU and 0.24AU respectively.

The radial profiles of relative intensities are derived. For the both observations they are very similar. In the both cases the CN 0-0 emission is generated by photodissociative excitation during the decomposition of CN parent molecules. The possible parent compounds are discussed.

Dust Particles from Comets and Asteroids Collected at the Earth's Orbit: Parent-Daughter Relationships

A. A. Jackson
Lockheed Engineering and Sciences Company, Houston Texas

H. A. Zook National Aeronautics and Space Administration, Houston, Texas

The relative contributions of comets and asteroids to the reservoir of dust in the interplanetary medium is not well known. There are direct observations of dust released from comets and there is evidence to associate the IRAS dust bands with possible collisions of Asteroids in the main belt (1). A means towards identifying the parent sources has been proposed in the establishment of a dust collector on the Freedom Space Station, the CDCF (Cosmic Dust Collection Facility) Horz (2). The purpose of such a facility would be to collect not only cosmic dust particles intact but also the state vectors they have as they arrive at the detector. The idea being that one may combine analytical laboratory analysis of the physics and chemistry of the captured particles with orbital data in order to identify comet and asteroid parent bodies.

It is possible to use the collected orbits of the dust to connect with its source in two ways. One is to consider the long time orbit evolution of the dust under Poynting-Robertson drag. The other is to look at the prompt orbit change of dust from comets onto trajectories that intersects the earth's orbit.

The orbital motion of dust when radiation forces alone are acting is well understood, Burns, et. al. (3) When gravitational forces due to the planets are included the motion can become quite complex, Gonczi, Froeschle and Froeschle (4), Gustafson and Misconi (4) Jackson and Zook (5). In order to characterize the orbits of dust particles evolved over a long period of time a study of its orbital evolution was undertaken. We have considered various parameters associated with these dust orbits as they cross the Earth's orbit to see if one may in a general way discriminate between particles evolved from comets and asteroids.

In the study we considered the dust particles as ideal black bodies,of density of 1 gm/cc, and spherical with radii between 10 to 100 microns. Particles of this size are effected by radiation forces, photon pressure and Poynting-Robertson drag. Account was also taken of solar wind drag which amounts to about 30 percent of the Poynting-Robertson drag. For particles of these sizes radial solar wind pressure and Lorentz forces are negligible. The gravitational forces due to the planets are included, with the planets propagated in two body Keplerian orbits only. Our method was to calculate explicitly by a numerical procedure the orbits of dust particles after they left their parent bodies.

In general dust from comets and asteroids follow complicated orbital evolutional histories as they decay into the sun. Scatterings ,exterior and interior mean motion resonances traps with the planets occur. It appears , however, that as the particles pass the earth's orbit asteroidal grains and cometary grains can be differentiated on the basis or their measured orbital eccentricities even after much planetary perturbation. Broad parent-daughter associations can be made on this basis from measurement of their trajectories intercepted in earth orbit.

Secondly for comets with perihelia close to the earth dust ejecta may have their orbital elements altered is such a way that their ascending or descending node will be promptly at the earth's orbit. Interception of these particles could lead to a clear cut identification of the cometary source body. It can also be shown using a discriminate criterion this association can retain identity over long periods of time.

REFERENCES:Dermot,S.F.,Nicholson,P.D.,and Houck,J.R.,1984,Nature,312,505-509. (2)Horz, F. (1190) NASA TM - 102160. (3)Burns, J.A.,Lamay,P.L., and Soter,S.(1979),Icarus,40,1-48. (4) Gonczi,R.,Froeschle,Ch.and Froeschle,Cl.,Icarus,51,1982, 633-654. (5)Gustafson, B. and Misconi, N., (1986),Icarus,66,280-287. (6) Jackson, A. and Zook, H., Nature,337,629-631.

N91-25998

COMETARY IMPLICATIONS OF THE INTERNAL ENERGY DISTRIBUTIONS OF THE C_2 AND C_3 RADICALS PRODUCED IN THE PHOTOLYSIS OF THE C_2H AND C_3H_2 RADICALS; William M. Jackson, Yihan Bao, Randall S. Urdahl, Xueyu Song, Jai Gosine, and Chi Luu, Department of Chemistry, University of California, Davis, Ca. 95616

The C_2 and C_3 radicals are prominent emission in the visible region of cometary spectra. Observational evidence exist that suggest these radicals are formed as granddaughter fragments in the photolysis of more stable molecules. Likely candidates for these parent molecules are C_2H_2, C_3H_4 (allene) and CH_3C_2H (propyne). Recent laboratory studies have been done on all of these parent molecules and they indicate that they can indeed produce the observed cometary radicals. In the case of C_2H_2 the laboratory evidence suggest that C_2 is formed via that the following mechanism;

$$C_2H_2 + h\nu_{193nm} \rightarrow C_2H + H \qquad (1)$$

$$C_2H + h\nu_{193nm} \rightarrow C_2 + H \qquad (2)$$

Evidence will be presented to show that the C_2 radical produced in the second reaction occurs in a variety of electronic, vibrational and rotational states. It will be argued that this is a result of conical intersections in the potential energy curves and the density of states associated with these curves. Since this is a property of the C_2H radical similar initial product state distributions are expected to occur in comets. This means that any models of the C_2 emission may have to start off with rotationally excited C_2 radicals in both the singlet and the triplet manifolds.

When C_3H_4 (allene) and CH_3C_2H (propyne) were photolyzed the C_3 radical is formed. In the allene case laboratory evidence shows that the C_3 radical is formed via the following mechanism;

$$C_3H_4 + h\nu_{193nm} \rightarrow C_3H_2 + H_2 \qquad (3)$$

$$C_3H_2 + h\nu_{193nm} \rightarrow C_3 + H_2 \qquad (4)$$

More C_3 is formed in the case of allene than in the propyne case, even though the absorption cross section for propyne is a factor of 2 larger. This suggest that competing dissociation pathways are present during the photolysis of propyne that are not available to allene. The observed quantum state distributions of the C_3 product was the same for both parent molecules, indicating that the same intermediate state is involved. These observations can be understood if the excited propyne formed in the initial absorption step isomerizes to excited allene before it dissociates to the same daughter compound. This postulate has been tested by comparing RRKM calculations of the rate of isomerization of excited propyne versus the rate of decomposition to other products such as $CH_3 + C_2H$, and $H + C_3H_3$.

Acknowledgements: The authors gratefully acknowledge the support of NASA under grant NAGW- 903.

N91-25999

FORMATION OF IONS AND RADICALS FROM ICY GRAINS IN COMETS; William M. Jackson, Christopher Gerth, Chemistry Department, University of California, Davis, California 95616 and Charles Hendricks, Lawerence Livermore National Laboratories, Livermore, California 94550

Ion and radical formation in comets are thought to occur primarily by photodissociation of gas phase molecules. In this paper experimental evidence and theoretical calculations will be presented that show that some of the radical and ions can come directly from ice grains. The experimental evidence suggest that if the frozen molecules on the surface of grains undergo direct dissociation then they may be able to release radicals directly in the gas phase. If the molecules undergo predissociation it is unlikely that they will release radicals in the gas phase since they should be quenched. Calculations of this direct photodissociation mechanism further indicate that even if the parent molecule undergoes direct dissociation the yield will not be high not to explain the rays structure in comets unless the radicals are stored in the grains and then released when the grain evaporates.

Calculations were also preformed to determine the maximum number of ions that can be stored in an icy grain it's radius. This number is compared with the ratio of the ion to neutral molecular density. From the comparison, it is suggested that some of the ions observed near the nucleus of the comet could have originally been present in the cometary nucleus. It is also pointed out that the presence of these ions in icy grains could lead to radical formation via electron recombination. Finally an avalanche process has been evaluated as another means of producing ions in comets.

Acknowledgements: William M. Jackson and Christopher Gerth gratefully acknowledge the support of NASA under grant number NAGW-1144.

Interstellar origin of CHON particles

Peter Jenniskens, Menno de Groot, J. Mayo Greenberg
Laboratory Astrophysics, P.O. Box 9513, NL–2300 RA Leiden.

The organic component of cometary dust, known as CHON particles, is of interstellar origin. The organics are nitrogen poor and contain saturated and unsaturated compounds with no, one or two oxygen atoms (Korth et al., 1989). The particles that were detected, have sizes from 0.05 μm radius up to 0.5 μm, with a trend for an increase in mean density with size (Maas et al., 1989).

Unsaturated organic matter is found in space as the product of carbon rich outflows of red giant stars, or as the product of the UV photolysis of small gas phase molecules frozen on dust grains. The lifetime of organic grains is very short due to the sensitivity to errosion by chemical sputtering and shock destruction. The in–situ formation mechanism by UV photolysis is therefore a potentially important mechanism and is studied in laboratory analogue experiments (i.e. De Groot et al. 1988).

We have found that the UV photolysis of second generation molecules on a cold substrate in vacuum leads to the formation of small complex polymeric materials, that have in common that they show a more or less linear increase in extinction between $\lambda^{-1} = 2\mu\text{m}^{-1}$ and $\lambda^{-1} = 5\mu\text{m}^{-1}$. Such a linear increase is a feature of the interstellar extinction curve (Fitzpatrick and Massa, 1988). In order to absorb efficiently in the UV, part of the organic mantles of grains should be shattered by grain–grain collisions into small (a$< 0.02\mu$m) pieces.

In spite of early hopes, it is not possible to form the tiny graphitic grains thought to be responsible for the bump absorption at 220 nm, in this way in the laboratory. In space the necessary carbonisation may occur by pyrolysis of the smallest of the fragments, which obtain high temperatures after absorption of a single photon. In order not to evaporate, the third generation organic material should still contain a significant amount of oxygen. This generic picture qualitatively agrees with the correlations found between big grain size and both linear rise and bump absorption.

The generic picture implies that the pre–solar system dust exists as of core–mantle grains and pieces of mantle material. Both kinds grow due to accretion in the dense pre–solar cloud. Coaggulation of the small (a$\sim$0.01 μm) organic grains leads to small (a= 0.05 μm) low density fluffy CHON particles and accretion on larger pieces to large (a = 0.5 μm) higher density CHONs. The core–mantle particles and large CHONs grow into the fluffy Greenberg–Hage particles, needed to explain the infrared emission bands of cometary dust (Greenberg and Hage, 1990).

Fitzpatrick E.L., Massa D.: 1988, *Astroph. J.*, **328**, 734

Greenberg J.M., Hage J.I.: 1990, *Astroph. J.*, **361**, 260

de Groot M.S., van der Zwet G.P., Jenniskens P.M.M., Bauer R., Baas F., Greenberg J.M.: 1988 in *Dust in the Universe*, 265

Korth A., Krueger F.R., Mendis D.A., Mitchell D.L.: 1989 *Asteroids Comets Meteors III*, 373

Maas D., Krueger F.R., Kissel J.: 1989 in *Asteroids Comets Meteors III*, 389

New Geminid meteor orbits

Peter Jenniskens, Marc de Lignie, Casper ter Kuile, Hans Betlem
Dutch Meteor Society, Lederkarper 4, NL–2311 NB Leiden

The most likely candidate for an extinct cometary nucleus is the asteroidal object 3200 Phaeton. The object is associated with the Geminid meteor stream. From a numerical integration back in time of a number of Geminid meteoroids, Gustafson (1989) found that the meteoroids had been ejected at perihelium, not at aphelium, which favours a cometary origin.

For further research, he expressed the wish for data on meteoroids with both well determined orbits and an estimate of the surface to mass ratio. Between 1990, december 11–15, we obtained over 100 geminid meteoroid orbits from a small camera network campaign, conducted under ideal circumstances in the south of France. At least part of the data are expected to provide also estimates of surface to mass ratios, needed to improve the quality and statistics of the numerical calculations.

Gustafson B.A.S.: 1989, *Astron. Astrophys.*, **225**, 533

THE EVOLUTION OF THE QUADRANTID METEOR STREAM; J. Jones, Physics Dept. University of Western Ontario, London, Ontario, Canada, N6A 3K7 and W. Jones, Physics Dept., University of Sheffield, S3 7RH, U.K.

According to the orbital calculations of Babjahnov and Obrubov (1987) the last close approach of the Quadrantid stream with Jupiter occurred about 3200 years ago which may have been the occasion when the parent comet of the Quadrantid stream was captured into its "present" orbit. If this is the case the stream may be only a few thousand years old. We have modelled the evolution of the stream to determine if the observed features of the Quadrantid/Arietid/δ-Aquarid complex are consistent with such a short time scale. Two starting dates were chosen 4000 years and 2400 years ago for a detailed modelling of the stream with 500 test particles including the gravitational perturbations of 6 planets as well as the likely spread in initial orbits elements resulting from the ejection process of the grains from the comet. The calculations show that although gravitational perturbations alone are unable to account for the observed features of the complex much better agreement is possible when the effects of the differential ejection velocities are included.

FORWARD-SCATTER RADIO-METEOR STUDIES; J. Jones, Physics Dept. University of Western Ontario, London, Ontario, Canada, N6A 3K7 and A.R. Webster, Department of Electrical Engineering, University of Western Ontario, London, Ontario, Canada. N6A 5B9.

Forward-scatter systems have been much neglected for the study of meteors and meteor streams. Much of this neglect stems from the complicated geometry which has made the interpretation of results difficult in the past. This no longer presents a problem because the of the computer power now available. There are practical advantages in using forward-scatter in that low-power transmitters are much easier to handle than the high-power ones used in pulsed back-scatter radars. The data reduction of the CW signals is significantly simpler than the pulsed signals usually associated with back-scatter meteor radars. Also the reflection geometry causes the duration of the echoes to the somewhat longer than for back-scatter geometry which partially alleviates the problem of the under-dense echo ceiling.

We have built a "short hop" forward-scatter system between Ottawa and London (Ont) for which the transmitter and receivers are separated by about 500 km. With it we are able to measure unambiguously the directions of arrival of the echoes using a 5-antenna interferometer of novel design. The directional errors are of the order of 0.5 degree. We describe this system and discuss its performance.

Jones (1977, BAC, 28, 272) and Morton & Jones (1982, MN, 198, 737) have shown how the echo direction distribution can be deconvolved to yield the meteor radiant distribution for back-scatter data. We extend that technique here to the forward-scatter case and present some preliminary meteor radiant distribution maps.

EFFECT OF THE GEOMAGNETIC FIELD ON THE DIFFUSION OF METEOR TRAINS; W Jones, Department of Physics, University of Sheffield, Sheffield S3 7RH, UK and J Jones, University of Western Ontario, London, Ontario N6A 3K7, Canada

The solution to the problem of the diffusion of a meteor train in the geomagnetic field from an initial line density may be written in closed form in terms of effective diffusion coefficients depending on direction. The solution is essentially exact within the quasi-neutrality approxdmation, and enables detailed calculations across the entire range of angle of train to field and relevant heights.

For heights of 95km and above the diffusion is severely inhibited by the field if θ, the angle between train axis and the field lines, is close to zero. This effect diminishes very rapidly as θ is increased to about 2°, in accordance with previous suggestions based on considerations of a planar plasma irregularity. The completely new element of our results is that while the effective diffusion coefficient in the plane of train and field then remains close to the zero field ambipolar value right up to 90° the effective coefficient in the direction of the normal to plane of train and field drops steadily to its $\theta = 0$ value at $\theta = 90°$. Even for a height as low as 95km the magnetic field can reduce the diffusion in the normal direction by a factor of two below the zero field value. This corresponds to a change of almost 5km in "diffusion height", that is, the height of an underdense meteor calculated on the basis of the exponential decay of its radar echo. We estimate the consequent changes in the expected distribution of diffusion heights for various orientations of radar antenna.

OBSERVATION OF METEORS BY MST RADAR: W Jones, Department of Physics, University of Sheffield, Sheffield S3 7RH, UK and S P Kingsley, Department of Electronic and Electrical Engineering, University of Sheffield, Sheffield S1 3JD, UK

The vast majority of meteors give appreciable back scatter radar echoes only from a region near the "reflection point" on the perpendicular from the train to the receiver. This implies trains observed with the vertical beam of an MST radar to be horizontal; thus relatively few meteors will be observed, the majority having burned up before reaching the reflection point. There are advantages to using an MST radar in the observation of meteors, nevertheless, in particular that the height resolution is very good and that the zenith angle is known.

We have used the Aberystwyth MST radar to observe the Geminid meteor shower of December 1990, recording heights and the rate of decay of the echo.

The heights of underdense meteors are commonly estimated on the basis of diffusion theory. This theory predicts that the exponential decay time of the radar echo will be inversely proportional to the diffusion coefficient D and thus directly proportional to the air density. However, because of the difficulty of estimating the meteor height by other means, confirmation of this procedure has in the past been largely statistical and not completely satisfactory. The MST radar provides us with accurate heights for individual meteors, and in the range for which the echoes occur shows the average of the "diffusion heights" to be in fair agreement with the true height, but also that the diffusion height of an individual meteor can differ from the true height by to 4 km.

Since the zenith angle is known, we can use the true heights to estimate the size of the individual particles from the usual ablation theory, suitably modified to take account of the curvature of the Earth. The true heights are almost entirely confined to the range 86.5 - 91km, and are interesting in indicating a fairly sharp cutoff in the size distribution at the upper end. However, the absence of echoes above 91km, is to be attributed to the fact that the radar returns data every 1/12th of a second, so that if a signal decays in less time we are unable to determine it as a meteor.

THE CORRELATION BETWEEN WATER PRODUCTION RATES AND VISUAL MAGNITUDES IN COMETS; L. Jorda (Observatoire de Paris-Meudon and European Southern Observatory), J. Crovisier (Observatoire de Paris-Meudon), and D.W.E. Green (Smithsonian Astrophysical Observatory).

We have studied the correlation between the water production rate and the visual magnitude in a dozen of recent comets with heliocentric distances ranging from 0.32 to 2.8 AU. The visual magnitudes are taken from the International Comet Quarterly data base. The water production rates are evaluated in a consistent way from the OH 18-cm lines measured with the Nançay radio telescope, following the method of Bockelée-Morvan *et al* (1990, *Astron. Astrophys.* **238**, 382). There is a strong correlation between the heliocentric magnitude m_h and the water production $Q[H_2O]$. The empirical law deduced from the whole set of data is:

$$\log Q[H_2O] = 30.76 - 0.25\ m_h.$$

Surprisingly, there is no strong deviations from this law for individual comets. In a first inspection, dusty and non-dusty comets behave in the same way. This law may be used for gas production rate estimations when no spectroscopic observations are available.

Inversion Methods for the Interpretation of Asteroid Lightcurves

M. Kaasalainen, L. Lamberg, and K. Lumme (University of Helsinki)

We have developed methods of inversion that can be used in determining the three-dimensional shape or the albedo distribution of the surface of an asteroid from lightcurve observations, assuming the shape to be strictly convex (*Bull. Amer. Astron. Soc.* **22**, 1113, 1990; *Asteroids, Comets, Meteors III*, pp. 115-118, 1990). Although in theory it is sometimes possible to obtain separate solutions describing both the shape and the albedo distribution of an object, the present quantity and quality of observational data of asteroids are not sufficient for this in practice. Thus one must decide in each case whether the result obtained in the inversion is taken to describe shape rather than albedo features, or if the surface is not convex on a global scale; fortunately, there are some indicators for this. A solution ascribed to shape is less sensitive to errors in lightcurve data than one ascribed to albedo variegation.

Since small errors in the data may have large effects on the results, we discuss the influence of various observational factors on the inversion. Of these factors, the most important ones are the number and range of the observing geometries (primarily concerning the solar phase angle and the aspect angle) and the accuracies of the lightcurve measurements and the pole position used for the asteroid. We also present results obtained using real asteroid lightcurve data and discuss the possible interpretations.

CYCLOTRON IRRADIATION SIMULATION OF COSMIC RAY MODIFICATION OF ORGANIC MATTER

R. Kaiser, K. Roessler

Institut für Chemie 1 (Nuklearchemie), Forschungszentrum Jülich, D-5170 Jülich, FRG

Frozen CH_4 and CH_4/Ar mixtures are irradiated at 15 K with 10 to 20 MeV p and $^3He^{2+}$ ions from the Jülich compact cyclotron CV28 in order to simulate the effect of cosmic rays on solid organic matter in comets. The products both gaseous and solid, in particular non volatile residues, were analyzed by a multiplicity of analytical methods including MS, REM, RBS, ERDA, ^{1}H-NMR, HPLC, GC/FID, GC/MS, FTIR und RAMAN. It could be shown that non volatile residues consisted of a mixture of long chained aliphatic and olefinic compounds and polycyclic aromatic substances (PAH and related). The formation of cyclic compounds is due to a multicenter reaction within the collision cascades induced by the cyclotron (cosmic ray) ions and their secondaries and depends in particular on energy density. Critical L_T values for the formation of PAHs for solid CH_4 are between $2 \cdot 10^3$ and 10^4 eV/μm. He-ions and heavier components of solar or cosmic rays are very effective in processing organic matter. There is a distinct difference between solids closed into cuvettes compared to those condensed in μm layers onto cold fingers in vacuum. The first are representative for reactions in the interior of comets or icy planets and yield more PAHs. The latter are representative for thin layers on dust grains, ring material or cometary, planetary or asteroidal surfaces and yield preferentially aliphatic compounds, and solid carbon. Carbon formation is a consequence of stronger H-elimination in the open targets.

METEOR FIREBALL SOUNDS IDENTIFIED

Colin Keay, Physics Department, University of Newcastle, NSW.

Sounds heard simultaneously with the flight of large meteor fireballs are electrical in origin. Confirmation that Extra/Very Low Frequency (ELF/VLF) electromagnetic radiation is generated by the fireball has been obtained by Japanese researchers. Although the generation mechanism is not fully understood, studies of MORP and other fireball data indicate that interaction with the atmosphere is definitely responsible and the cut-off magnitude of -9 found by Astapovich for sustained electrophonic sounds is supported by theory. Brief brief bursts of ELF/VLF radiation may accompany flares or explosions of smaller fireballs, producing transient sounds near favourably placed observers.
Laboratory studies show that mundane physical objects can respond to electrical excitation and produce audible sounds.
Reports of electrophonic sounds should no longer be discarded. A catalog of over 300 reports relating to electrophonic phenomena associated with meteor fireballs, aurorae and lightning has been assembled. Many other reports have been catalogued in Russian by Bronshten. These may assist the full solution of the similar long-standing and contentious mystery of audible auroral displays.

HIGH RESOLUTION SPECTRA OF CH, CO_2^+, C_3 AND NH_2 IN COMET AUSTIN;

S.J. Kim and M.F. A'Hearn (University of Maryland, College Park), M. Brown and H. Spinrad (University of California, Berkeley)

We analyzed high resolution (~ 0.05 A) spectra of the nuclear regions of comet Austin (1989c1) in the 3800 - 8000 A range, which were obtained at the Lick Observatory on May 13, 1990 (UT) (Brown and Spinrad, BAAS, 22, 1100, 1990). The purpose of this analysis is to construct molecular band models of CH, CO_2^+, C_3, NH_2 and S_2 in order to compare the models with observed emission lines and to identify molecular lines in the spectra. The constructed models of the CH, CO_2^+, C_3, and NH_2 bands are preliminary. We could, however, indentify numerous lines of the CO_2^+, C_3, and NH_2 bands, and of the 0-0 band of CH. In particular, some of the individual lines of the CH band are clearly resolved, which have not been previously resolved with relatively low resolution spectroscopy (Arpigny, C. et al., Symposium on the Diversity and Similarity of Comets, pp. 607-612, April 1987, Brussels, Belgium, ESA SP-278). We could not find any S_2 lines in the Austin spectra. We will present rotational temperatures derived from the molecular band structures of these molecules, and discuss their implications on the collisional and fluorescence processes in the coma of comet Austin.

SIMILARITY AND DIFFERENCE OF POLARIMETRIC CHARACTERISTICS OF DUST PARTICLES OF COMETARY ATMOSPHERES AND THE SURFACE LAYERS OF ASTEROIDS. N.N.Kiselev, G.P.Chernova, Institute of Astrophysics, Dushanbe 734042, USSR

Phase dependences of polarization of dust particles of comets and asteroids are being compared. The "asteroid like" negative branch of polarization of comets is a good evidence of aggregate structure of particles of cometary atmospheres and the identity of scattering processes of sun light on the grains of comets and asteroids. The phase dependence of polarization of comets are similar to C-type asteroids in the region of small angles ($\alpha<25°$). It is shown that comets with a considerable continuum have more stable parameters P(min), α(inv), h(slope) in comparison with asteroids of any types. Their constancy is interpreted as the result of homogeneous composition of dust particles in atmospheres of different comets. Parameters of the positive polarization P(max), α(max) of comets and asteroids are badly known. The few observations of comets and near-Earth asteroids of S-type permit us to state their considerable differences: for comets - P(max)$\approx$25%, α(max)=90°; for asteroids - P(max)$\approx$8.5% and α(max)$\approx$110°. The parameters of the positive polarization of comets are explained by the considerable contribution of the quasi-Rayleigh polarization component arising from the effective scattering of light on small particles of cometary atmospheres.

POLARIMETRY OF ASTEROIDS IN THE USSR. N.N.Kiselev[1], D.F. Lupishko[2], G.P.Chernova[1]

1) Institute of Astrophysics, Dushanbe, 734042, USSR
2) Astronomical Observatory of Kharkov University, Kharkov, 310022, USSR

The review is given of the results of the polarimetric observations of asteroids obtaining according to the following programmes: the polarimetry of the CMEU-asteroids with the aim of classifying them to types, distinguishing and studying the M-type asteroids; the investigation of spectral dependence of polarization; the polarimetry of near-Earth asteroids; the polarimetry of individual asteroids (4 Vesta, 16 Psyche and others).

The results show the polarimetry is an effective method of investigation and should be used more widely, especially combined with photometry.

The following perspective directions of investigations are noted:

a) determining the parameters of phase curves of polarization of asteroids of all types, groups and sizes;
b) studying the spectral dependences of P(min), inversion angle α(inv) and slope h and determining their diagnostic significance for the study of structural and mineralogical properties of asteroid surfaces;
c) the polarimetry of near-Earth asteroids with the aim of obtaining the maximum complete phase dependence, the study of regoliths of several kilometer bodies, the distinction of minor planets - probable extinct cometary nuclei;
d) the polarimetry of individual asteroids for studying the photometric heterogeneous of their surfaces.

ASTEROID FAMILIES AND DIFFERENTIAL MASS INDEX; J. Klačka, Department of Astronomy, MFF UK, Mlynská dolina, 842 15 Bratislava, Czecho-Slovakia

The basic results and consequences of the existence of asteroid groups with differential mass index $k > 2$ are reviewed. This result is practically independent on various classifications of asteroid families. The only groups with such value of k are situated in the inner and outer part of the asteroid belt. The total mass is dominated by the small-particle end of the range of masses. So, the total mass of such groups could have been much higher than it is at present and also much higher as to be initially concentrated in one body and disrupted by collision (generally accepted explanation of the origin of asteroid families). Since the collision mean-life $\propto D^{3k-5}$, we do not have $\propto D^{1/2}$ as it is generally accepted but $\propto D^{2}$ (approximately). This explains why the present total mass of investigated groups of asteroids corresponds to values generally accepted. The greater part of asteroids with $D \lesssim 1$ km is depleted from given groups due to collisions. This conclusion about the critical point where the size-frequency curve of small objects departs from that extrapolated from known asteroids should be verified in future. Some other consequences (histogram distributions of rotation rates for the Koronis and Eos families and a set of nonfamily asteroids; the presence of dust bands in Themis, Eos, Koronis families and not in Flora family) can be also explained by this interpretation.

ASTEROIDAL JET-STREAM FLORA A; J. Klačka, Department of Astronomy, Komenský University, Bratislava, Czecho-Slovakia

Problem of the existence of the most significant jet-stream Flora A is analysed. On the basis of the data analysis it is shown that Flora A consists mostly of very faint asteroids with oppositions falling on the autumn months and with very low inclinations. Due to the favourable observing conditions just during September, the concentration of proper perihelion longitudes is explained as a consequence of the observational selection effects. The low inclinations explain the concentration in proper longitudes of nodes just in the area corresponding to that of the jet--stream Flora A. Thus the most important asteroidal jet-stream Flora A is fully explained as a consequence of observational selection effects.

Comet Levy Images at 3.36μm

James Jay Klavetter (UMD) and Susan Hoban (GSFC)

We observed comet Levy (1990c) with the ProtoCAM through a 1.4% CVF centered at 3.36μm at the IRTF on 1990 August 8 and 10. After subtracting the continuum, we find the spatial profile of the unidentified 3.36μm emission feature to be indistinguishable from the continuum out to 1225 km from the optocenter. Our measurements of the ratio of the flux at 3.36μm to that of the continuum in comet Levy is consistent with values reported by Brooke *et al.* (1991) of P/Halley at comparable heliocentric distance. Since the average value of the dust-to-gas ratio in P/Halley (25.4, by Brooke *et al.*(1990)) is similar to that of comet Levy measured on 1990 August 25-27 (25.6, D. Schleicher, private communication), our measurements of the feature-to-continuum ratio in comet Levy strengthen the conclusions of Brooke *et al.* (1990) that the abundance of the progenitor of the 3.36μm feature relative to water is comparable for all comets observed to date. For the August 10 data, we find the integrated band flux at 3.36 ± 0.014 μm in a 2.7" aperture to be 1.45×10^{-17} W/m^2 (±10%).

THE CARBON ISOTOPE ABUNDANCE RATIO IN COMETS HALLEY AND LEVY

M. Kleine, S. Wyckoff, P. A. Wehinger, *Department of Physics and Astronomy, Arizona State University*, and B. A. Peterson, *Mount Stromlo and Siding Spring Observatories.*

High resolution spectra of the R-Branch (0-0) band of the CN $B^2\Sigma^+ - X^2\Sigma^+$ transitions have been observed using the Mount Stromlo Observatory 1.9 *m* telescope and coudé echelle spectrograph of comets Halley(1986 III) and Levy(1990c). The observed rotational spectra is very sensitive to the comet's heliocentric velocity. New fluorescence calculations to model the Swings effect have been developed so that the $^{12}C/^{13}C$ abundance ratio could be determined from the observed line intensities. The abundance ratio for P/Halley is a reanalysis of the data (cf. Wyckoff *et al.* 1989, *Ap. J.*, **339**, 488) utilizing these new fluorescence efficiencies. The carbon isotope abundance ratios for comets Halley and Levy will be presented.

IMPROVED ASTEROID PROPER ELEMENTS AND THEIR ACCURACY

Z. Knežević, Astron. Obs., Belgrade, and A. Milani, Univ. Pisa

We have computed a new set of proper elements for 4537 numbered asteroids by a fully analytical iterative theory extending the one described in Milani and Knežević, 1990, *Cel. Mech.*, in press. The main improvements with respect to the previous version are: (i) a more accurate computation of the Laplace coefficients; (ii) the effects of all four outer planets being accounted for at the level of the linear theory; (iii) the effects of Saturn being included up to degree four in eccentricity/inclination and to order two in the mass of Saturn; (iv) a correction to the secular frequency due to the inner planets is applied; (v) possible secular resonance cases are identified and separately reported.

The advantages of this type of proper elements are that they can be computed efficiently; this allows not only to process large catalogues of orbits, but also to test their accuracy and long term stability by a conceptually simple procedure. We have performed an extensive set of numerical integrations of representative asteroid orbits (by chosing one example for almost each family identified by Zappalà et al., 1990, *Astron. J.*); then proper elements have been computed and their changes with time used as an estimate of the accuracy. The results show a significantly better accuracy with respect to the previously distributed version; apart from some dynamically peculiar regions (e.g. near the Kirkwood gaps, near the main secular resonances, and the ω-libration region), for most of the asteroid main belt and for an overwhelming majority of asteroids, the accuracy is more than enough for the identification of fragments of catastrophic disruptions. The error estimate can be used for statistical tests of the reliability of family identifications.

Laboratory Studies Of The Gas-Particle-Interaction On Comets; H. Kochan [1] and Markiewicz, W.J. [2].1) Institut für Raumsimulation, DLR-Köln, P.O.Box 906058, D-5000 Köln 90, FRG., 2) Max-Planck-Institut für Aeronomie, P.O.Box 20, D-3411 Katlenburg-Lindau, FRG.

The in situ observation of insolated ice/mineral mixtures in the DLR Space-Simulator opened some insights e.g. in the emission processes of ice-/dust-particles from the surface [1,2,3]. The cited results may be shortly reviewed by the statements: 1)The particles are bonded to their neighbors. Before the individual particles can be emitted at first their interlinking bonds have to be "eroded" by the outstreaming gas, originating from the sublimation of volatiles. 2) The extricated particles are entrained into the gas flow, rather than ejected from the surface.
In the last experiments KOSI (= Kometen-Simulation) 5, 6, and 7 dating from 1989 to 1991 the ice-/dust-particle emission was monitored with three high-speed shutter CCD-video-cameras. In the experiments KOSI 5 and KOSI 6 the same cylindrical sample container 15 cm high and 30 cm in diameter was used. The gas-particle interaction investigated and published so far is based on the experiments that used this sample container. KOSI 7 (Jan.`91) was performed with the new larger sample container 30 cm high and 60 cm in diameter, requiring 80 litres of the icy material.
The gas-particle-interaction, i.e. the exchange of momentum depends on the gas flux (velocity, density) and on the nature (density, structure, cross section) of the ice-/dust-particles. The particle collectors developed and operated by KOSI team members [4], define the portion of volatiles in the emitted particles. At the beginning of the experiment when a fresh sample surface is insolated, particles with a high amount of volatiles are emitted. The "ice-load"-factor of the emitted ice-/dust-particles decreases with increasing insolation time. To get a better understanding of the drag-coefficient, during KOSI 7 cryogenized collectors were introduced, to preserve the emitted particles for a later inspection. At the end of the same experiment glass-spheres (drag-coefficient known) of different diameters, all in the micron area, were dropped down on the sample surface. The glass spheres also were entrained into the gas flow. Emission angle and -velocity were defined via the video observation.
The video records of the ice-/dust-particle trajectories crossing the new, large sample container are under evaluation. These trajectories are controlled by the momentum transfer from the gas flow to the particles. The region of decoupling is determined for the different experimental conditions, large and smaller sample. The particle trajectories markedly differ from the ballistic parabolas calculated with the first observable values of emission angle and velocity. The gas-particle-interaction derived from the different experiments will be discussed.

References: **[1]** Kochan, H., Ratke, L., Thiel, K., and Grün, E., (1990) Particle emission From Artificial Cometary Surfaces: Material Science Aspects. Proc.Lunar Planet. Sci. Conf. 20th, pp. 401-411. Lunar and Planetary Institute, Houston. **[2]** Kochan, H., Seidensticker, K., and Koerver, W., (1990) Angular Distribution And Velocities Of Dust Emissions Observed At Artificial Comets; In Lunar and Planetary Science XXI, pp.641-642. Lunar and Planetary Institute, Houston. **[3]** Kochan, H., Markiewicz, W.J., and Keller, H.U., (1991).KOSI: Gas Drag Derived From Ice/Dust-Particle Trajectories. Geophysical Research Letters, Vol., 18, No. 2., pp. 273-276. **[4]** Mauersberger, K., Michel, H.-J., Krankowsky, D., Lämmerzahl, P., and Hesselbarth, P., (1991) Measurement Of The Volatile Component In Particles Emitted From An Ice/Dust Mixture. Geophysical Research Letters, Vol., 18, No. 2., pp. 277-280.

INTEGRATED SOFTWARE PACKAGE "STAMP" FOR MINOR PLANETS;
O. M. Kochetova, V. A. Shor, Institute of Theoretical Astronomy, USSR Academy of Sciences.

The package STAMP is designed for rapid and precise reproducing the tables of the annual "Ephemerides of Minor Planets" with the help of PC XT/AT. STAMP makes it possible to reproduce any table from the current volume of the EMP, to print it or to write it in a file. Then, the package enables to select the data from the tables complying with a condition or combination of some conditions. Finally, it provides a means for calculation of some often used functions of the orbital elements, for sorting the results of selection and/or calculations, for drawing the histograms and for interpolating the tabular data. In addition, STAMP makes it possible to solve the routine problems such as the comparison of the observed positions with ephemerides, the identification of minor planets, the determination of the planets which can be seen at a given moment within the limited sky region.

Thus, STAMP is of great utility in solution of varied problems related to minor planets. Dealing with the package is accomplished through the multistage menu. It is useful tool for professional astronomers and amateurs.

Laser Characterization of Small Particles Ejected from Cometary Analogue Samples

HARALD KOHL AND EBERHARD GRÜN
Max-Planck-Institut für Kernphysik, Heidelberg, FRG

Particle ejection is one of the basic physical processes which occur at the surfaces of cometary nuclei. This has already been confirmed by different laboratory simulation experiments of the KOSI project. They proofed that even in the terrestrial gravitational environment dust and ice particles may be lifted from the surface of sublimating ice-dust-samples. However, there had been no possibility to characterize even small particle ($<100\mu$m).

For this reason we developed, calibrated and applicated a laser particle detector for the large space simulator in the KOSI experiments. The beam of a 7 mW He-Ne-laser has been chopped by a high frequency crystal deflector in order to open a few cm wide detection area. Reflected light signals of the passing particles are observed by a optical photomultiplier system. Main experimental problem was the background light suppression within the space simulator. Calibration measurements and results of the instrument are presented.

We present the results from the KOSI 7 experiment. It has been shown that size distribution of the emitted particles changes with duration of irradiation time significantly. While a large number of the smaller particles have been emitted during the first hours of irradiation the distribution shows a significant lack of the small ones in later phases. A simple model for this behaviour will be presented.

The emission activity decreases in the free sublimation experiment down to about fifty percent. Single particle evaluation by analyzing the light scattering signals shows a distinct correlation between speed and size. The results are discussed taking calibration measurements into account. They are compared with results of other diagnostic instruments of KOSI.

PARTICLE EMISSION FROM COMETARY MATERIALS; G. Kölzer, Abteilung Nuklearchemie, Universität zu Köln, Zülpicher Str. 47, D-5000 Köln 1, FRG, H. Kochan, WB-RS, DLR, Postfach 906058, D-5000 Köln 90, FRG, K. Thiel, Abteilung Nuklearchemie, Universität zu Köln, Zülpicher Str. 47, D-5000 Köln 1, FRG

During KOSI (comet simulation) experiments mineral-/ice mixtures are observed in laboratory simulated space conditions. Here we refer to the KOSI 5 experiment where the sample consisted of 70 weight % H_2O-, 17 weight % CO_2- and 4 weight % CH_3OH-ices and 9 weight % minerals (olivine:montmorillonite = 9:1). This mixture was insolated with xenon lamps to simulate solar radiation. The intensity of insolation was nearly 1.2 solar constants for about 12 hours. The pressure in the space simulation chamber was about 10^{-4} Pa.

Emission of ice-/dust particles from the sample surface is observed by different devices. The particles trajectories are recorded with a video system. The recorded tapes are evaluated with an image processing system. The two parameters that were extracted are the elevation angle and the particle velocity near the sample surface. To study the time dependence of the emission process we looked at definite time intervals covering the total insolation period. Time dependent measurements are also possible by rotating particle collectors. The dust residues of the particles in a selected collector are investigated by optical microscopy in transmitted light. Then the sizes of the particles are measured via an image processing system. So the size distributions can be determined as a function of time. The volatile component of the collected particles is measured by a particle detector with ionization gauge. All these detectors are mounted on a frame in front of the sample together with 264 passive dust collectors. By these collectors a spatial distribution of dust particles is determined. In a distance of about 1 m several piezo acoustic impact detectors are arranged azimuthally on this frame. The signals from the particles hitting the detectors give the size and the velocity of the individual particles.

The particle emission activity decays exponentially with time. The emission rate of ice particles reaches its maximum immediately after the sun is switched on and levels off within less than one hour. Mineral type particles with slowly sublimating volatiles reach their maximum emission rate about 30 minutes after the beginning of insolation. At this time the maximum emission rate of particles is also observed on the video tapes. The particle velocities near the sample surface range from 0.4 to 2.4 m/s, with a mean around 1.1 m/s. The mean elevation angle of the velocity vector decreases with time. The size distributions of particles measured by piezo detectors (≥ 200 μm) and collected in rotating collectors (≥ 40 μm) are nearly constant with time.

These results are correlated to the gas flux density and the temperature on the sample surface during the insolation period. The data are interpreted in terms of phenomena on the sample surface, e. g. formation of a dust mantle and mechanisms of particle emission and are related to processes on real comet surfaces.

ENERGY BALANCE OF COMETARY SURFACE LAYERS

N.I.Kömle and G. Steiner
Space Research Institute, Austrian Academy of Sciences,
Lustbühel Observatory, Graz, Austria

Abstract

It is likely that large parts of a typical cometary surface consist of porous ice which is covered by a thin layer of non–volatile material. In order to study the thermal behavior of such a system we have performed both systematic laboratory experiments and theoretical investigations. The energy balance of such a crust/ice system, the ice temperature as a function of the flow resistance of the overlying crust, and the gas pressure in the interior of the porous ice is discussed in detail. It is found that a non-volatile porous crust has a strong influence both on the ice temperature and on the gas loss rate of a comet.

Disturbances of Both Cometary and Earth's Magnetospheres Excited by Single Solar Flares

I. Konno[1], T. Saito[2], Y. Kozuka[2], K. Nishioka[3], M. Saito[4], and T. Takahashi[2]

1. SwRI, Texas, USA 2. Tohoku Univ., Japan 3. Olympus Optical Co. Ltd., Japan 4. Saito Astronomical Obs., Japan

Comets P/Brorsen-Matcalf and C/Okazaki-Levy-Rudenko appeared successively in 1989 and displayed marvellous disturbances of the magnetospheres. A comet is generally like a windvane moving three-dimensionally in the heliomagnetosphere. The recent period of the sunspot maximum phase is important for the study of comets, because the neutral sheet of the heliosphere is nearly perpendicular to the ecliptic plane and intense solar flares occur very frequently.

We found two cases of a phenomenon in which outstanding disconnection event of the cometary plasma tail (on August 13 and November 16, 1989) was followed by geomagnetic storms (on August 14 and November 17). A survey of solar flares clarified that the identical solar flare excited successively the earth's magnetosphere and the cometary magnetosphere.

The velocities of the shock front in the interplanetary space were calculated by using the onset times of the disturbances of both the comets and the earth. The results suggest that the propagation of the shock front associated with the flare is not symmetric around the radial axis from the flare region of the sun.

A NEW MEASUREMENT OF THERMAL CONDUCTIVITY OF AMORPHOUS ICE: RELEVANCE TO COMET EVOLUTION

A. Kouchi[1], J.M. Greenberg[1], T. Yamamoto[2] & T. Mukai[3]

[1]: Lab. Astrophys., Univ. of Leiden, Leiden, The Netherlands
[2]: Inst. of Space & Astronautical Sci., Sagamihara, Japan
[3]: Dept. of Earth Sci., Kobe Univ., Kobe, Japan

Although the importance of knowing the thermal conductivity of amorphous ice (a-H_2O) for predicting the thermal evolution of comets has been widely realized. There has been no previous direct measurement available. Until now, all the discussions on comet evolution have been based on a theoretical estimation of the thermal conductivity by Klinger[1]. On the basis of our new experimental results, we have arrived at a new estimate of the thermal conductivity of a-H_2O.

A thin film of H_2O ice was prepared at 125-135 K by the condensation of water vapor onto a metal substrate in a vacuum chamber (5×10^{-7} Pa). The structural change of thin ice film was examined in-situ by reflection electron diffraction. When the ice film is thin the deposited ice is amorphous. On the other hand, when the thickness of the ice exceeds the critical value, Xc, the diffraction pattern has been changed to ice Ic. This observation shows that the surface temperature of an a-H_2O film exceed the transition temperature (Tx=140 K) at the critical thickness, Xc.

To calculate the thermal conductivity using above data we have solved the equation of thermal conduction in the ice film. We also considered the net rate of radiation input from the external radiation field and heat of condensation as a boundary condition. We have found that the thermal conductivity of a-H_2O ranges from at least one to four or more orders of magnitude smaller than that estimated by Klinger[1] and depends strongly on its formation conditions.

Our results have very important implications for the thermal evolution of comets. Since the cometary nucleus itself is very porous, the thermal conductivity of the comet nucleus may be an additional four orders of magnitude smaller than that of the constituent icy grains. This suggests that the net thermal conductivity of the comet nucleus is smaller than 10^{-8} W m^{-1} K^{-1} ! The major mechanism of heat transfer in the comet nucleus can not be by conduction. Although we considered the heat transfer either by radiation or by diffusion of water molecules, both effects are negligible. Consequently, it appears unlikely taht the heating of a comet at depths larger than 10 cm (conservatively) has ever occurred.

Reference

[1] Klinger J. (1980) Science 209, 271-272.

The Solar Wind Structure that Caused a Large-scale Disturbance of the Plasma Tail of Comet Austin

Y. Kozuka[1], I. Konno[2], T. Saito[1], and S. Numazawa[3]

1. Tohoku Univ., Japan 2. SwRI, Texas, USA
3. Japan Planetarium Lab., Japan

The study of disturbances of cometary plasma tails or cometary magnetospheres provides us very valuable information on the solar wind and the solar magnetosphere. From the last half of 1989, five bright comets appeared within a year and many disturbance phenomena of the plasma tails were observed. Since it was a period of the active sun, more disturbances were observed in these comets than in comet Halley which appeared at the solar minimum. From the analyses of these phenomena, various results have been obtained. In this study we report the results of the analysis and the fact obtained from the very distinct phenomenon observed in comet Austin on April 29, 1990.

A series of photographs shows the movement and variation of two kinds of very peculiar structures. One structure is of many arcades with a scale of $\sim 10^6$ km. The other is a large wave structure of the order of 10^7 km. A multi-arcade structure is interpreted as the structure of the magnetic field lines which passed through the cometary plasmapause around the nucleus. The travel speeds of these structures are found to increase with the distance from the nucleus. It is proposed that the large wave structure was caused by a change of the non-radial component of the solar wind flow. A computer simulation of the deformation of the plasma tail was performed by changing the speed and the direction of the solar wind flow. The result agrees quite well with the observation. It is concluded that this non-radial flow was caused by an interaction between a high-speed flow from a coronal hole and a low-speed flow from the western region of the sun.

Early and unidentified apparitions of short-period comets

Ľ. Kresák and M. Kresáková
Astronomical Institute of the Slovak Academy of Sciences, Bratislava, CSFR

Comets listed in Marsden's Catalogue (1989) with parabolic orbits were examined to find how many, and which of them, had in fact revolution periods shorter than 20 years. Two statistical approaches were applied to estimate their number : evaluation of the relative distributions of extreme apparent magnitudes of long- and short-period comets, and of the distributions of their orbital inclinations. The conclusion was that there are about 15 unrecognized short-period comets observed before 1759, but only very few observed later.

For the identification of these comets, a combination of 7 criteria was developed, basing on the compatibility of the positional data with a short-period orbit, the orbital inclination, perihelion latitude, perihelion distance, absolute magnitude, apparent magnitudes, angular tail lengths, and observing geometry. 25 candidates selected in this way were divided into five groups according to the probability P' that they were actually of short period :

P' = 99% : comets 1678, 1702, 1743 I, 1949 III and 1963 IX
P' = 95% : comets 1230, 1345, 1351, 1457 I, 1491 II, 1499, 1539, 1577 II, 1585 and 1833. P' = 80% : comets 568, 1080 and 1457 II. P' = 50% : comets 1245, 1293, 1618 I and 1618 III. P' = 20% : comets 390, 1757 and 1860 IV. The sum of these objects weighted by P' - 16 before 1759 and 3 thereafter - agrees very well with the statistical estimates.

Comet 1678 was already identified with certainty with periodic comet d'Arrest by Carusi et al. (1991). Other identities with the known short-period comets appear possible. Pairs of similar orbits include comet 1457 II and P/Finlay or P/Denning-Fujikawa, comet 1230 and P/Biela, comet 568 and P/d'Arrest, comet 1618 III and P/Barnard 3, comet 1491 II and P/Denning. Unambiguous identifications are difficult mainly due to the unknown operation of nongravitational effects over long time spans, with many planetary encounters. However, as illustrated by the linkage of comet 1678 with P/d'Arrest, they could provide important information on the active lifetimes, progressive fading, behaviour of nongravitational forces, and orbital evolutions over periods much longer than those for which observations are available at present.

On the ecliptical concentration of long-period comets

Ľ. Kresák and M. Kresáková
Astronomical Institute of the Slovak Academy of Sciences,
Bratislava, CSFR

The distribution of comets in orbital inclination as a function of their revolution periods (or aphelion distances) provides the principal distinction between their subsystems of different dynamical evolution, and perhaps also of different origin. While the separation of the Jupiter family from the comets of Halley type is sharp, the transition between the latter group and the old long-period comets is rather smooth. The question at which aphelion distance the prevalence of direct orbits disappears entirely, is relevant both to their sources and evolutionary mechanisms : the possible flattening of the inner Oort cloud, the dependence of planetary perturbations on the encounter geometry, and the active lifetimes of comets.

While the present database on cometary orbits is extensive enough for statistical studies, it is strongly affected by observational biases. Even the answer to the question whether prograde or retrograde orbits prevail, depends on the limiting accuracy of the orbit determination adopted for the investigated sample. This reflects the dependence of the discovery probability and of the duration of observability on the orbital geometry. A simple illustration : the median duration of the observation of long-period and parabolic comets is 65 days for $i > 150^{\circ}$, but 90 days for $i < 30^{\circ}$. When those parabolic comets which were in fact of short period are discarded, the latter figure even increases to 120 days. At the same time, the number of comets observed longer is essentially the same in both samples : 21 and 23 for $D > 120$ days, and 7 and 6 for $D > 1$ year. In the present paper we attempt to evaluate the impact of the various selection effects involved, and to determine the limits within which direct orbits actually prevail.

The result is a limiting aphelion distance of about 120 AU corresponding to revolution periods between 450 and 500 years for the comets which can be detected Beyond this limit, the excess of retrograde motions among all orbits, the excess of prograde orbits among those of higher accuracy, and the lack of orbital planes perpendicular to the ecliptic, are produced by the interaction of a number of selection effects.

E. Kuehrt, B. Giese, and H. U. Keller

"Interpretation of Infrared Measurements of Small Solar System Bodies"

Atmosphereless bodies like asteroids, comets, and small moons show strong small-scale temperature inhomogeneities due to their surface roughness. This effect has to be taken into account in interpretations of any infrared measurements. A model for thermal radiation from rough surfaces is described and some results of the analysis of spacecraft based measurements of Phobos and ground based measurements of Deimos are given.

SPIN VECTOR AND SHAPE OF 532 HERCULINA; T.Kwiatkowski, and T.Michałowski, Astronomical Observatory, Adam Mickiewicz University, ul. Słoneczna 36, 60-286 Poznań, Poland

Some oppositions of 532 Herculina show two maxima and two minima per rotational cycle, while the others only one maximum and one minimum. Thermal lightcurves lead to conclusion that the light variations of this asteroid are due primarily to shape rather than to surface albedo variegation.

We have obtained the spin vector of Herculina, and try to explain both the reflected and thermal lightcurves by non-ellipsoidal shape of this asteroid.

Second Update of the Asteroid Photometric Catalogue

C.-I.Lagerkvist †, *M.A.Barucci* ‡, *M.T.Capria* •, *M.Dahlgren* †,
M.Fulchignoni ◇, *P.Magnusson* ⋆

† *Astronomiska Observatoriet, Box 515, S-75120 Uppsala, Sweden.*
‡ *Observatoire de Paris, 92195 Meudon Principal Cedex, France.*
• *Instituto di Astrofisica Spaziale, CNR, Viale dell'Università, 11-00185 Roma, Italy.*
◇ *Istituto Astronomico, Università 'La Sapienza', Via Lancisi, 29-00161 Roma, Italy.*
⋆ *School of Mathematical Sciences, Queen Mary and Westfield College, U.K.*

A new update of the Asteroid Photometric Catalogue is now beeing prepared. It contains asteroid lightcurve observations published during the period 1988-90. All observations have been reduced to unit distance and corrected for light-time, if applicable. For easy comparison, they are plotted in diagrams with the same scale for all curves of the same asteroid. Information on the observing site, photometric system and aspect data are also provided.
In addition, a digital version containing the same information is available. It also includes the data in the original catalogue and its first update, making a total of about 4000 lightcurves for more than 560 different asteroids.
An order form for both versions will be available at the poster.

CHANGING PROPERTIES OF THE DUST COMA OF P/HALLEY: IMPLICATIONS FOR AN INHOMOGENEOUS NUCLEUS

P. LAMY, C. COSMOVICI, G. SCHWARZ

High-resolution maps of the color and polarization of the coma of comet Halley derived from CCD images obtained during the first half of March 1986 reveal considerable temporal as well as spatial variations. They remain however restricted to the inner coma and are well correlated with the activity of the comet. The varying reddening and polarization are best explained by a population of organic grains which do not survive beyond a few 10000 km. Color and polarization do not exhibit a unique correspondance. Taking into account the rotation of the nucleus, this implies an inhomogeneous nucleus. The maps of the color, the polarization and the jet structures as revealed by unsharp masking are correlated to delineate the physical properties of the dust grains in the jets and in the background coma.

N91-26000

EVALUATING SOME COMPUTER ENHANCEMENT ALGORITHMS THAT IMPROVE THE VISIBILITY OF COMETARY MORPHOLOGY;

S. M. Larson, Lunar and Planetary Laboratory, University of Arizona, Tucson, AZ. 85721, and
C. D. Slaughter, Photometrics Ltd., 3440 Brittania Dr., Tucson, AZ. 85706.

The observed morphology of cometary comae is determined by ejection circumstances and the interaction of the ejected material with the local environment. Anisotropic emission can provide useful information on such things as orientation of the nucleus, location of active areas on the nucleus, and the formation of ion structure near the nucleus. However, discrete coma features are usually diffuse, of low amplitude, and superimposed on a steep intensity gradient radial to the nucleus. To improve the visibility of these features, a variety of digital enhancement algorithms have been employed with varying degrees of success. They usually produce some degree of spatial filtering, and are chosen to optimize visibility of certain detail. Since information in the image is altered, it is important to understand the effects of parameter selection and processing artifacts can have on subsequent interpretation. Using the criteria that the ideal algorithm must enhance low contrast features while not introducing misleading artifacts (or features that cannot be seen in the stretched, unprocessed image), we assess the suitability of various algorithms that aid cometary studies of. The strong and weak points of each are identified in the context of maintaining positional integrity of features at the expense of photometric information.

The simplest operation is to alter the intensity scale by some non-linear relation (such as the base 10 logarithm) that suppresses the steep intensity peak near the photocenter. This helps bring the brightness of the faint outer regions of the coma closer to those in the inner coma. No artifacts are introduced, but there is only a modest improvement in visibility of low contrast features.

Spatial derivative, or "shift-difference" algorithms enhance intensity discontinuities, but only in the direction of the shift. The simple linear shift-difference is very effective for bringing out ion tail structure when the shift is perpendicular to the tail axis. The degree of shift is a compromise between showing the smallest detail and enhancing the noise. The most serious problems with this method is that the results are directionally dependent, and are not easily interpretable. The resulting features, showing the rate of change of intensity, locate the edges of jets and shells. The radial plus rotational (with respect to the photocenter) shift difference algorithm reduces the directional dependency, but still requires care in interpretation since it enhances the edges of features. Finding the best combination of rotational and radial shifts can be difficult and enhances only a limited spatial frequency range.

Temporal derivative images are projected velocity maps that (among other things) make it easy to distinguish rapidly varying ion features from the slower moving dust structures. Successful short-term difference images bring out ion features which are normally a minor component of a broad-band image. This method places great demands upon sets of images with nearly identical quality and very precise registration. Variations in seeing and guiding can complicate the result. This method will be particularly useful in extracting ion features in the consistent quality images produced by the Hubble Space Telescope. Interpretation must be made with care, since the result is an image of moving feature edges.

Azimuthal function algorithms reduce the radial gradient by either subtracting the average value in the annulus of constant distance from the photocenter, or by subtracting a best-fit, low-order function to the annulus. Averaging and function fitting is more easily done after a polar to rectangular coordinate transformation (with the photocenter at the origin). This method is very efficient in eliminating the radial gradient, does not have any directional dependencies, and interpretation is straight-forward. The photocenter must be determined very carefully, especially for undersampled data, or spurious features close to the nucleus may be produced.

Traditional spatial filtering algorithms reduce the radial gradient by eliminating the low spatial frequency domain in the image. A "high-pass" gaussian deconvolution retains features in the image smaller than the gaussian, and by eliminating the broad radial gradient, the contrast of the smaller features can be increased. There is no directional dependency, but "ringing" artifacts can be seen around stars and the central condensation of the comet. Selecting the optimum size gaussian usually depends upon the characteristic size of the features of interest.

Since cometary features typically become larger farther from the nucleus, spatially selective spatial filtering might be desirable. One method is to subtract a synthetic image based on a generalized model of particle outflow. This assumes some *a priori* knowledge of the ejection function. A simple isotropic r^{-1} distribution might work well for a rapidly rotating nucleus, but not for a slow rotator emitting on the illuminated hemisphere. If there is enough data, subtraction of a mask produced by the median of many images over time.may also work (note that this is similar to a temporal derivative). We have recently developed a variable kernel deconvolution routine that passes increasingly higher frequencies closer to the photocenter. This enhances a larger spatial range of coma features which often exist in an image.

This work is supported by NASA grant NAGW 1974.

HELIOCENTRIC DISTANCE DEPENDENCIES OF THE C_2 LIFETIME AND C_2 PARENT PRODUCTION RATE IN COMET P/BRORSEN-METCALF (1989o); M. Lazzarin, *Dipartimento di Astronomia, Università di Padova (I)*, G.P. Tozzi, *Osservatorio Astrofisico di Arcetri - Firenze (I)*, C. Barbieri, *Osservatorio Astronomico and Dipartimento di Astronomia - Padova (I)*, and M.C. Festou, *Observatoire Midi-Pyrénées - Toulouse (F)*

Comet p/Brorsen-Metcalf (1989o) has been spectroscopically observed during July and August 1989 when its heliocentric distance ranged from 1.1 to 0.65 AU. From long-slit spectra covering the 4000–7000 Å region, brightness profiles for the C_2 Swan bands $\Delta v = +1, 0, -1$ have been obtained. This large data set allows both the determination of the lifetimes of the C_2 radical and its parent and the study of their evolution with heliocentric distance, Rh.

The data were analyzed assuming a parent molecule velocity varying as 0.85 $R_h^{-0.5}$ km s^{-1}. The C_2 lifetime was found to vary as R_h^2, wich is consistent with the fact that its main production path is a single photodissociation of a parent molecule. The production of the C_2 radical and its parent molecule were found to vary as R_h^4 in agreement with the water production rate variation derived from IUE observations.

EVOLUTION OF COMETARY DUST : SOME CLUES DERIVED FROM POLARIMETRIC OBSERVATIONS OF LEVY 1990 c AND OTHER COMETS

A.C. LEVASSEUR-REGOURD, J.B. RENARD, A. HADAMCIK
Université Paris 6/Service d'Aéronomie
BP 3 91371 Verrières, France

Numerous measurements of normalized intensity and polarization of solar light scattered by comet Halley dust particles have been performed during the 1985/1986 return, in the 0° to 73° phase angle (α) range. Compilations of the data already published or transferred to IHW archives are available (1). Typically, the polarization was found to be negative (direction of polarization in the scattering plane) at small phase angles, to change sign for $\alpha = (21 \pm 1)°$ and to increase almost linearly (0.3 % per degree near $\lambda = 500$ nm).

Recent accurate polarimetric cometary observations (e.g. Austin 1989 c_1, Levy 1990 c) allow us to derive synthetic polarization curves. No significant differences are found between old periodic comets and new comets near the inversion point (where the polarization changes sign). However a significant spreading of the data is detected i) for small apertures observations and ii) at large phase angles.

The analysis of the polarimetric maps (2) we derived from observations performed in August 1990 at Pic du Midi Observatory (2 m telescope + CCD 510 x 320) suggests that the former result can be interpreted in terms of jet activity in the inner coma. The comparison between the polarimetric properties of comets and those of interplanetary dust grains (3, 4), which depend upon their solar distance and the inclination of their orbit upon the ecliptic, suggests that the latter result can be interpreted in terms of evolution of the optical properties of the cometary dust with surface temperature and ageing of the cometary nucleus.

References :

(1) Dollfus A, Bastien P, Le Borgne J.F., Levasseur-Regourd A.C. and Mukai T., 1988, Astron. Astrophys., 206, 348-356.
(2) Renard J.B., Levasseur-Regourd A.C. and Dollfus A., 1991, Ann. Geophys., Vol. 9, Supp., C385.
(3) Levasseur-Regourd A.C., Dumont R and Renard J.B., 1990, Icarus, 86, 264-272.
(4) Levasseur-Regourd A.C., Renard J.B. and Dumont R., 1991, in "Origin and evolution of interplanetary dust", Kluwer, 131-138.

The LONG–TERM DYNAMICAL BEHAVIOR OF SMALL BODIES IN THE KUIPER BELT

H.F. Levison, U.S. Naval Observatory, Washington, D.C. 20392

Recent numerical calculations [1, 2] have shown that short-period comets, which are on low inclination orbits, cannot originate from the gravitational scatter of long-period comets. Work by Duncan, Quinn, & Tremaine [1] shows that objects originally on low inclination, Neptune-crossing orbits will evolve into a population of objects with orbital parameters consistent with those of short-period comets. However, they point out that the timescale to deplete this initial population of planet-crossing objects is short. Therefore, they conclude, that there must be a system of objects that are evolving into planet-crossers on the timescale of the age of the solar system. The most likely source of these objects is a region just beyond the orbit of Neptune, the *Kuiper belt*.

In order to complete this theory, it is still necessary to show that objects that formed in the Kuiper belt can become Neptune-crossers and to determine the timescale for this process. For if the length of time to deplete the Kuiper belt is too short, then it can no longer be the source for the short-period comets seen today. If the length of time is too long, then it will be difficult to reproduce a large enough flux of new comets to explain the number of observed short-period comets. Unfortunately, because the timescales involved must be on the order of the age of the solar system, it is not possible to determine them through the use of direct numerical integration of orbits with current computer technology. In this paper we calculate the timescales of the evolution of objects in the Kuiper belt using a new technique that treats the evolution of orbits in integral space as a diffusion problem.

The details of our results depend on what region of the solar system is studied. Here we define the Kuiper belt as the region of integral space such that $q \geq 30AU$ and $a \leq 100AU$. Objects tend to diffuse through this region on timescales that are on the order of the age of the solar system. These diffusion times imply that it is very unlikely to find an object near to where it formed. The diffusion process can be viewed as a random-walk where the q and a slowly change as a function of time. Surprisingly, the tendency is for objects to diffuse outward in the solar system. Although this trend is significant, objects are free to migrate in either direction.

A large fraction of integral space is covered with orbits whose lifetimes are on the order of the age of the solar system. Here, *lifetime* is defined as the statistically mean length of time it takes for an object to evolve out of the Kuiper belt ($q < 30AU$ or $a > 100AU$). For a large fraction of integral space ($Q \lesssim 100AU$), the expected lifetime of an object is approximately dependent only on its initial perihelion distance. The region of the Kuiper belt where objects formed and are still present in the Kuiper belt has an inner edge at approximately $45AU$. Although it is possible to find such a region, the objects that formed there have most likely evolved to fill the entire Kuiper belt because the diffusion rates are significant. The longest mean expected time for an object to remain in the Kuiper belt is 1.8×10^{10} years. It occurs for an object that formed in circular orbit at $a = 75AU$. Approximately 30% of these objects become Neptune-crossers and thus provide a source for short-period comets. The rest are stored in orbits further out in the solar-system.

Even objects that form close to the orbit of Neptune have a significant chance to evolve to orbits with $a > 100AU$. For example, objects that formed in circular orbits at $45AU$ have a 50% chance of evolving to orbits with $a > 100AU$. However, objects stored in this region of the solar system are not precluded from becoming short-period comets. It is possible that after being stored for some time that they can diffuse back through the system to become Neptune-crossers. Indeed, a significant fraction of objects follow this evolutionary track. They formed near the orbit of Neptune and slowly evolved to orbits with $a > 100AU$. After being stored there for some time (say approximately 5×10^9 years), they can diffuse back through the Kupier belt and become Neptune-crossers. Thus, a significant fraction of objects that formed near the orbit of Neptune can currently be evolving into short-period comets.

Determining these timescales was the last remaining hurdle in the development of a complete theory of the formation of short-period comets. Our work shows that the timescales for objects leaving the Kuiper belt are consistent with it being the source for short-period comets.

References:

[1] Duncan, M., Quinn, T.,& Tremaine, S. (1988). *Ap.J. Lett.* **328**, L69.
[2] Joss, P.C. (1973). *Astron. Astrophy.* **25**, 271.

MAPPING THE STABILITY FIELD OF TROJAN ORBITS IN THE OUTER SOLAR SYSTEM. H.F. Levison, U.S. Naval Observatory, Washington, D.C. 20392, E.M. Shoemaker and R.F. Wolfe, U.S. Geological Survey, Flagstaff, AZ 86001

Trojan orbits are stable or quasistable orbits that librate about the 1 : 1 resonance with the mean motion about the Sun of their co-orbital planet. Objects currently found on these orbits are remnants of solar system planetesimals. Studying these objects may provide important insights into the physical conditions that existed in the region near their co-orbital planet at the time of planetary formation, provided the dynamical history of these objects can be understood. The only outer planet with an observed ensemble of Trojan asteroids is Jupiter. Trojans associated with the other giant planets, if they do indeed exist, have yet to be discovered. In order to determine whether these objects should theoretically exist, we have undertaken to map the stability field of Trojans about Jupiter, Saturn, and Neptune in terms of the variables proper eccentricity, e_p, and libration amplitude, D. In the case of Jupiter, this mapping is intended to aid in our understanding of the dynamical evolution of the observed Trojan swarms. For Saturn and Neptune, it was carried out to determine if the Trojans should be present and, if so, where they can be found.

To accomplish the mapping for a particular planet, we integrated numerically the orbits of 110 particles with e_p in the range 0 to 0.8 and D in the range 0° to 140°. Orbits of the Sun and the four Jovian planets were integrated as a full N-body system, in a barycentric frame. The orbits of the test particles were calculated under the gravitational influence of these 5 bodies, but were not self-gravitating. The equations of motion for all the objects were integrated using a fourth order symplectic scheme [1, 2]. Test particles were started with orbits in the orbital plane of the planet being studied. We did perform a preliminary series of integrations of Jupiter Trojans carried out to 178 000 years, where the initial inclination of the orbits was 10°, we found no significant difference in the limit of the stability field from that obtained with $i = 0$. Test particles were considered to be on Trojan orbits until they either experienced a close approach with their co-orbital planet, or visited all four quadrants of a coordinate system moving with the co-orbital planet.

We first discuss the results for Jupiter. In a preliminary study of highly eccentric orbits we found that the longitude of the libration point is not fixed at ±60° from the mean longitude of Jupiter but is a function of e_p and can be as large as 110° for orbits with $e_p = 0.8$. Initially the stability field is quite large. After only 18 000 years it contains orbits with D as large as 110° and orbits with e_p as large as 0.7. With increasing time, however, the stability field shrinks in both e_p and D. At the end of our $18 Myr$ integration, the stability field did not contain any orbit with $D \gtrsim 90°$ or $e_p \gtrsim 0.25$. It is important to note that this is much larger than that limit of the main field of observed Jupiter Trojans ($D \lesssim 70°$, $e_p \lesssim 0.15$). Thus, we think that if we continued our integrations, the stability field would continue to shrink and that the current limit of the main field of observed Jupiter Trojans probably represents the approximate limit of stability for a time interval of 4.5 billion years. One recently discovered Jupiter Trojan, 1989 BQ, lies well outside the main Trojan field ($e_p = 0.22$, $D = 17°$) and is close to our stability limit at $18 Myr$. We suggest that the dynamical lifetime of 1989 BQ may be of order 10^8 years and that it has been captured late in solar system history.

Mapping of Saturn Trojan orbits shows that both small and large libration amplitude orbits are unstable on very short timescales. After only 30 000 years all orbits with $D \lesssim 40°$, $D \gtrsim 95°$, or $e_p \gtrsim 0.1$ have disappeared. Again, with increasing time the stability field shrinks in both e_p and D. After $30 Myr$ the stability field is quite small, containing only orbits with $50° \lesssim D \lesssim 80°$ and $e_p \lesssim 0.06$. It has been suggested that these orbits may be long-lived because their libration periods are close to a commensurability with the period of the *great inequality* between Jupiter and Saturn [3]. At the end of our integration, the limit of stability was still shrinking. We think that it is unlikely that any Saturn Trojan orbit will be stable for the age of the solar system.

A preliminary study of Neptune Trojan orbits shows that orbits with small libration amplitudes, $D \lesssim 35°$, do not exist. Any particle placed initially in an orbit with a semi-major axis the same as Neptune will begin to librate independent of its initial longitude or its initial velocity with respect to Neptune. After $3 Myr$, the mapping shows a stability field containing only orbits with $35° \lesssim D \lesssim 85°$ and $e_p \lesssim 0.1$. As was the case with Saturn, the limit of stability was still shrinking at the end of the integration. Since the region of stability is so small after $3 Myr$, we think that all the Neptune Trojan orbits will be unstable after 4.5 billion years.

References:

[1] Gladman, B., and Duncan, M., 1990, *Astron. Jour.*, **100**, p. 1680–1693.
[2] Gladman, B., Duncan, M., and Candy, J., 1991, To appear in *Celest. Mech.*
[3] Innanen, K.A., and Mikkola, S., 1989, *Astron. Jour.*, **97**, p. 900–908.

Numerical Simulations of Cometary Gas and Dust

David J. Lien

Bucknell University

Most observations of comets are done photometrically or spectrophotometrically. The interpretation of the aperature–averaged flux is relatively simple for an isotropic, radially expanding coma. However, the interpretation of the observations is not so clear when the the motion of the gas and dust is affected by radiation pressure, or when the emission is time–varying and anisotropic. Additionally, both the gas and dust have problems specific to themselves: the gas is created and destroyed via photo–processes, with non–radial velocities imparted to the photo–products, and the dust is characterized by a size distribution, with size dependencies on the expansion velocity, the scattered and thermal radiation, the response to radiation pressure, and probably the density. How good then are the approximations normally used in determining the production rates of the gas and dust when these effects are present?

As part of a program to better understand the dynamics of cometary dust and gas, a computer program has been developed which numerically simulates the emission of both dust and gas from the nucleus of a tilted rotating nucleus. The gas coma simulation includes the effects of the lifetime of the parent and daughter products, non–radial velocities upon dissociation, and radiation pressure. The dust coma simulation includes the effects of the size dependencies on the expansion velocity, and scattering or thermal emissivity (based on either approximations or Mie theory calculations using measured optical constants) and on the response to radiation pressure. Anisotropic emission is approximated by a gaussian jet centered at any latitude and longitude on a rotating nucleus of arbitrary rotation rate and obliquity.

The "image" of the gas or dust coma can be generated, as well as aperture– or annulus–averaged fluxes. An example of the annulus–averaged flux is presented below for P/Halley on 15 March 1986. Figure 1 shows isotropic dust emission for 14 days at $v = 0.05\,km/s$ with $\beta = 0$ along with the analytical result for the same input parameters. In Figure 2, the effects of a distribution of sizes (approximated here by a distribution in β which is rectangular in $\log(\beta)$ on the interval $[-4, -2]$, and where the scattered radiation is $\propto \beta^{-2}$ and the expansion velocities are in the range $[0.016, 0.16]\,km/s$). Clearly, the assumption of isotropic expansion is not justified. Aperture photometry would show a decrease in flux as the aperture increases.

A series of models will be presented which show the effects of radiation pressure, anisotropic emission, and rotation on the aperture– and annulus–averaged fluxes. These models will be analyzed by assuming isotropic, radial expansion to determine production rates, and compared with the production rates used in the simulations.

Figure 1

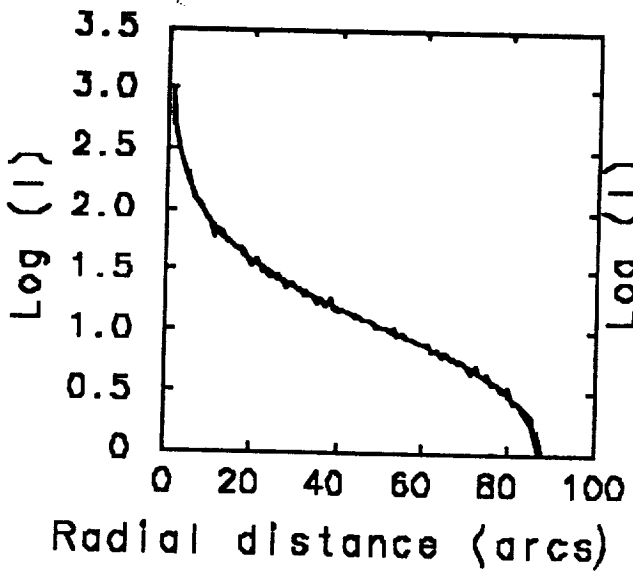

Figure 2

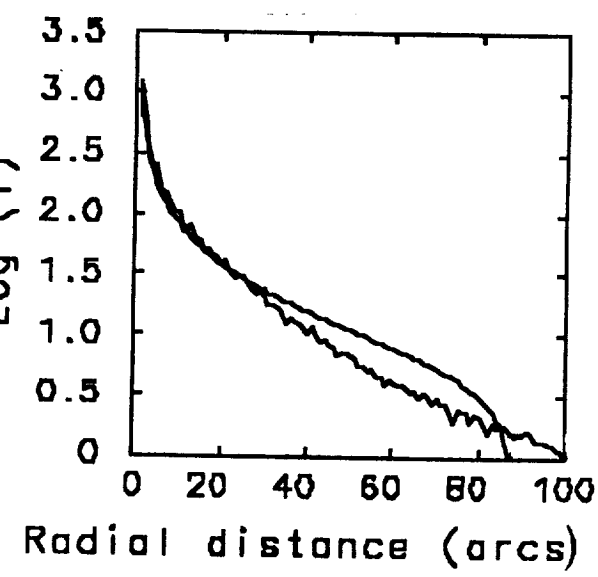

A COMPUTER SEARCH FOR ASTEROID FAMILIES; B.A. Lindblad, Lund Observatory, Box 43, S-221 00 Lund, Sweden

Various problems in the identification of asteroid families on the basis of the proper elements are discussed. Previous work in this area is briefly reviewed. Lindblad and Southworth (1971) proposed the use of the D-criterion for mathematically defining a clustering in three dimensional *a*, *e*, *i* proper element space. It was shown that, once the rejection level was defined, this method easily sorted out all the known families with practically the same membership as in previous studies by Hirayama and Brouwer.

Some twenty years has now ellapsed since the first study. The available data sample of numered asteroids has increased from 1697 to 4100, and new methods of computing the proper elements have been developed. A tape with improved proper elements of 4100 numbered asteroids was announced at the ACM III meeting in Uppsala (1989) by Milani and Knezević. It has recently been distributed to a number of scientists. In view of these improvements in the data base the author has found it appropriate to make a new study of the asteroid families. The study is based on the same selection criteria as in the previous study.

ACTIVITY AND ORBIT OF THE LYRID METEOR STREAM; B.A. Lindblad, Lund Observatory, Box 43, S-221 00 Lund, Sweden
V. Porubçan, Astronomical Institute, Slovak Academy of Sciences, 842 28 Bratislava, Czechoslovakia

The activity of the Lyrid meteor stream is in most years fairly low with a reported visual rate at maximum (21-22 April) of 5-10 meteors per hour. Short bursts of very high Lyrid activity, with visual hourly rates of 100 or more, have sometimes been reported. These observations generally refer to faint visual meteors. We find that the reported bursts of high activity have occurred at solar longitudes 31°.2 to 31°.4 (equinox 1950.0), while the recurrent or "normal" maximum for bright (visual and photographic) meteors occurs at solar longitudes 31°.5 to 31°.9. A mass separation of the meteors in the shower is thus indicated.

A precise determination of the mean Lyrid orbit is made based on 12 orbits photographed in the period 1941-85. The mean photographic orbit is compared with the orbit determined from Harvard radio data and with that of P/Comet Thatcher (1861 I). The present Lyrid orbit is almost identical to that of the parent comet. An interesting feature of the photographic Lyrids is the extremely small scatter around the mean orbit; the stand. dev. in the angular orbital elements being of the order of 1°.

Dynamical timescales in the Jupiter family

Mats Lindgren

Astronomiska observatoriet, Box 515, 751 20 Uppsala, Sweden

The dynamical lifetime of the comets in the Jupiter family have not yet been determined very accurately. And since the model for the apparent steady–state of this population basically consists of a balance between the dynamical infeed of comets from some source population, and a combination of dynamical and physical loss, one of the parameters we need to know is how long a comet on average spends in the Jupiter family. The calculation of this lifetime is not a trivial one, since we in this case are dealing with dynamics that include close encounters with Jupiter, and hence very large perturbations with corresponding "jumps" between orbits belonging to the Jupiter family and other orbits. The actual calculation of the dynamical lifetime then consists of adding, in some cases several, separate periods of time between returns and ejections into and out of the Jupiter family.

The method chosen for this investigation consists of a statistical analysis of the orbital evolution over 50000 years of a large number of fictitious cometary orbits evenly distributed in the Jupiter–Saturn region. The dynamical model used is the system: Sun–Jupiter–Comet with Jupiter in its present orbit.

COBE/Diffuse Infrared Background Experiment (DIRBE) Observations of Comet Austin (1989c1) , Comet Levy (1990c), and Comet Okazaki-Levy-Rudenko (1989r)

C.M. Lisse (STX), M.G. Hauser, T. Kelsall, S.H. Moseley, R.F. Silverberg (NASA/GSFC), H.T. Freudenreich (STX)

The Diffuse Infrared Background Experiment on the Cosmic Background Explorer (COBE*) observed Comets Austin, Levy, and Okazaki-Levy-Rudenko during its 10 months of cryogenic operations. The DIRBE is a 0.7^{o} FOV, superfluid-helium cooled, ten band absolute photometer covering the wavelength range 1-300 μm, that surveys half the sky each day in a helical scan pattern covering 64 -124^{o} elongation from the sun. DIRBE detected thermal emission from dust in the tails of these comets at 12 and 25 μm with high contrast against the sky background; detection at other wavelengths depended on the comet's activity and viewing geometry. Each comet is scanned at least once every 103-minute orbit while in the DIRBE viewing swath, over a period of weeks. Single comet scans are used to investigate the spatial spectral profile, and multiple comet scans are used to build a single-band image on the timescale of a day. We present our latest images, spectra, temporal trends, and interpretations of the DIRBE comet observations.

*COBE is supported by NASA's Astrophysics Division. Goddard Space Flight Center (GSFC), under the scientific guidance of the COBE Science Working Group, is responsible for the development and operation of COBE.

COSMOGONIC ASPECTS OF ASTEROID ROTATION. D.F.Lupishko and F.P.Velichko, Astronomical Observatory of Kharkov University Sumskaya str. 35, Kharkov 310022, USSR

The available data on asteroid rotation rates, sense of rotation and orientation of asteroid axes in space are analysed from the point of view of asteroid rotation origin and its connection with cosmogonic processes in asteroid belt. These data show that observable rotation and shape of overwhelming majority of asteroids were acquired by them in process of collisional evolution. At the same time the rotation of largest asteroids is primordial one, acquired in process of accumulation and following the collisional evolution did not change it considerably. And as primordial rotation of asteroids is preferentially prograde, it may be considered as observable argument in favour of accretion process of their origin.

Rotation peculiarities and shape of M-type asteroids are in agreement with higher strength (that is density) of their matter. V-like dependence of a part of asteroids with retrograde rotation versus asteroid diameters has been revealed, which has minimum near D=125 km (similar to dependences of rotation rates and lightcurve amplitudes on diameter). It is shown that there is a rather considerable unisotropy of distribution of asteroid axis orientation in space. There is no doubt that the explanation of the nature of "cosmogonic diameter" (D=125 km) phenomenon and other observable effects will provide the important information on the processes of dynamical evolution in asteroid belt.

A CCD Comparison of Outer Jovian Satellites and Trojan Asteroids

Jane X. Luu (Harvard-Smithsonian Center for Astrophysics)

The eight small outer Jovian satellites are little known compared to their brighter, more illustrious cousins, the Galilean satellites. They are divided into 2 groups, each containing 4 satellites; the inner group travels in prograde orbits while the outer group travels in retrograde orbits. From the distinct orbital characteristics of the two groups, most of the theories of their origin involve the capture and break-up of two planetesimals upon entry into the atmosphere of proto-Jupiter. Their proximity to the Trojan asteroids has led to conjectures of a link between them and the Trojans. However, Tholen and Zellner (1984, *Icarus* 58) found no red spectrum among six of the satellites and postulated that they were all C-type objects, therefore unlikely to have derived from the Trojan population.

We present new charge-coupled device (CCD) photometry and spectroscopy of the 8 outer Jovian satellites obtained from 1987 to 1989. The lightcurves of the satellites show that the rotational properties (lightcurve amplitude Δm and rotation period) of the satellites are similar to those of main belt asteroids (see Fig. 1). Fig. 1 also shows that the satellites have distinctly smaller Δm's than the known comet nuclei. In comparison with the Trojans, the satellites are similarly spectrally diverse, with reflectivity gradients ranging from neutral (0.4 ± 0.1 % / 10^3 Å) to red (12 ± 1 % / 10^3 Å) (see Fig. 2). The Δm's of the satellites fall within the range of Δm's observed in the Trojans, although the satellite Δm's are generally restricted to smaller values (≤ 0.27 mag) than the Trojan Δm's. The wide range of colors, plus the assumed low albedo for most of the satellites, indicate that the satellites resemble a mixture of both C-type and D-type asteroids, not just C-types, as had been suggested previously. Similarities between the satellites and the Trojans are also consistent with the hypothesis that these two groups of objects share a common origin (Kuiper 1956, *Vistas in Astronomy*, vol. 2). Physical properties of the satellites are generally consistent with, but do not prove, the capture origin theory (Pollack *et al.* 1979, *Icarus* 37).

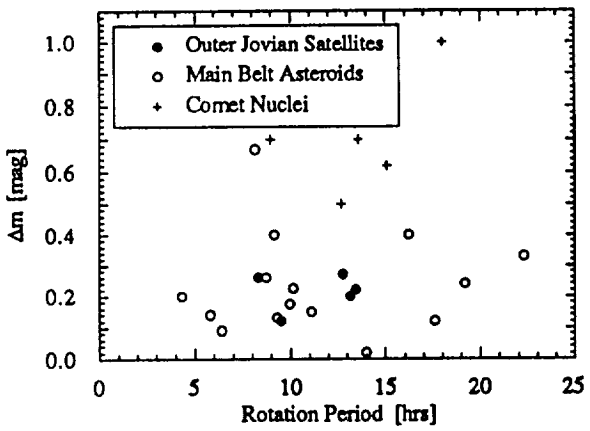

Fig. 1. Rotation period vs. lightcurve amplitude Δm for outer Jovian satellites, main belt asteroids and comet nuclei. All three groups of objects have similar rotation periods, but the nuclei have larger Δm's than both the satellites and the main belt asteroids.

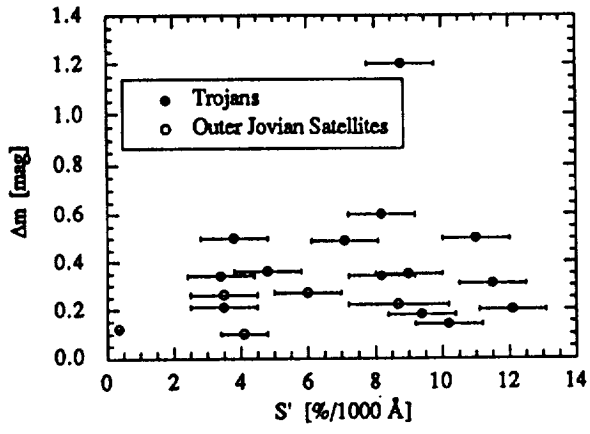

Fig. 2. S' vs. lightcurve amplitude Δm for outer Jovian satellites and Trojan asteroids. The satellites are statistically indistinguishable from the Trojans in both S' and Δm.

EVOLUTION OF THE ASTEROID SPIN VECTOR DISTRIBUTION

Per Magnusson Queen Mary and Westfield College, London

Collisions in the present asteroid belt tend to randomize the distribution of asteroid spin vector directions. Observations however, show that there is a tendency for large asteroids to spin predominantly in the prograde sense. Is this consistent with present ideas of the evolution of the asteroid belt ?

I will present new statistics on the distribution of asteroid spin vectors based on an enlarged sample of objects. This distribution may be compared with distributions resulting from pure 3–dimensional random walks in spin vector space. The influence on this idealized model from random collisional angular momentum "kicks" is estimated. Within this model I constrain the cumulative collisional flux that asteroids have been subject to since the end of the accretion phase. A lower limit on the original predominance of prograde rotators is also obtained. Future work along these lines may tell us more about the accretion process and give a unified model for the evolution of planetary and asteroidal spin.

COMETARY ORBITAL EVOLUTION IN THE OUTER PLANETARY REGION

A. Manara, Osservatorio Astronomico di Brera, Milano (I)
G.B. Valsecchi, I.A.S. - Planetologia, Roma (I)

We have made a numerical experiment consisting of the integration of the motion of 100 fictitious comets for 1000 revolutions each, starting from low eccentricity, low inclination orbits not far from those of the four giant planets. The purpose of this study is to get a reasonable understanding of the way in which the orbits of potential short-period comets evolve under the action of planetary perturbations. An essential role is of course played by close planetary encounters, which are found to govern the evolution of the majority of the comets that show substantial orbital changes at the end of the simulation. This finding casts doubts on the possibility to treat the multi-stage capture of comets into short-period orbits as a diffusion process, given the stochastic nature of a scattering process essentially dominated by close planetary encounters. The distribution of perturbations at close encounters shows distinct tail asymmetries that are related to the positions of the pre-encounter orbits in the phase space of orbital elements semimajor axis, eccentricity and inclination. Moreover, the majority of the strongest perturbations, i.e. of those contained in the asymmetric tails of the distribution, are experienced by comets in orbits nearly tangent to that of the planet encountered. This last result suggests that the regions of phase space corresponding to orbits nearly tangent to those of the planets should constitute a preferential path followed by comets on their way towards short-period orbits. We are also performing some additional integrations using planetary masses increased by a factor 10, as was made in recent numerical experiments aimed at reproducing the entire process of multi-stage capture from a trans-neptunian source. The aim of this computations is to compare them with those done with the realistic masses, in order to check if the effect of the increased masses is only that of shortening the multi-stage capture process, in terms of number of revolutions of the comets integrated, or if is also that of altering the phase space paths followed by the comets, and the efficiency of the transport process along those paths.

THE EIGHT OBSERVATIONS RECORDED IN THE ANGLO SAXON CHRONICLE OF COMETS; E. G. Mardon, A. A. Mardon, Red Deer College, Red Deer, Canada, Texas A & M University, College Station, Texas, USA.

This research paper is an examination of the eight cometary references [679AD, 729AD, 891AD, 905AD, 905AD, 975AD, 995AD, 1066AD, 1106AD] found in the various manuscripts of the Anglo Saxon Chronicle between 538 AD and 1140 AD with linguistic notes on the Old English text and scientific observations. This is an examination of astronomical phenomena and other climatic or natural events, that are described in the Anglo Saxon Chronicle, which is also referred to as the Old English Annals. The Anglo Saxon Chronicle is an Old English history of events begun under the direction of King Alfred the Great in the 9th Century and containing earlier material in adapted form. It was written from records kept by various English Monasteries. After the account of King Alfred's wars which started with the invading Danes, the Chronicle was officially kept up year by year until the last entry dated for 1154 AD. It survives in seven manuscripts, although the Anglo Saxon Chronicle contains non-factual material and legends, and references often verifiable through other contemporary or near contemporary sources, like the Bayeux Tapestry containing a panel of the 'long-haired comet', that appeared in 1066 AD, and few months prior to the invasion of England by William the Conqueror.

678 AD "Her ateowede cometa se steorra on Auguste. and scan iii monðas ælce morgen swilce sunne beam." "In this year appeared the comet or star in August and shone for three months. Like a morning sunbeam." **729 AD** "Her atewoden twegan cometan." "In this year appeared two comets." **891 AD** "] ſy ilcan geare ofer Eastron. ymbe 'gang' dagas oſſe ær, æt eowde se steorra ſe mon on boc læden hæt cometa, same men cweſaſ on Énglisc ſæt hit sie feaxede steorra. forſæm ſær stent lang leoma of hwilum on ane healfe, hwilum on ælce healfe." "And the same year after Easter during Rogation-tide or earlier appeared the star which in Latin is called'comet', likewise men say in English that a comet is a (flax) long-haired star, because long beams of light shine there forth, sometimes on one side, sometimes on every side." **905 AD** "Her cometa æt eowde ·xiii· k† Nouembris." "In this year the comet appeared thirteen days before the Kalendes of November." **975 AD** "And her Eadward Eadgares sunu feng to rice. and ſa sona on ſam ilcan geare on herfeste æteowde cometa se steorra. and com ſam eaftran geare swiðe mycel hungor." "And in this year Edward, Egar's son, succeeded to thed Kingdom, and soon at harvest time of the same year appeared that star known as Comet. And the next year came great hunger." **995 AD** "Her on ſissum geare ætewde cometa se steorra." "In this year appeared the comet or star." **1066 AD** "On ſisü geare cõ Harold kyng o Eoforic to Westmynstre. to ſã Eastran ſe wæron æft' ſã middan wintran ſa se kyng forðferde. and ſa Eastran on ſone dæig xvi kl' Mai. -Da wearð geond eall Englaland swylc tacen on heofenü gesewen swylce nan mann æ´r ne geseh. Sume menn cwædon ƒ hyt cométa se steorra wære. ſone sume menn hatað ſone fexedon steorran. and he æteowde ærest on ſone æfen LETANIA MAIOR. ƒ ys viii kl' Mai. and Swa scean ealle ſa vii niht." "In this year came King Harold from York to Westminster, the Easter following the Christmas of the King's death. Easter being on April 16. At that time throughout all England, a portent such as men had never seen before was seen in the heavens. Some declared that the star was a Comet, which was called the long-haired star it first appeared on the eve of the feast of Letania Minor, that is April 21st and shone every night for a week." **1106 AD** "In the first week of Lent, on Friday, the forteenth day before the Kalends of March a strange star appeared in the evening and for a long time afterwards was seen shining for a while each evening. The star made its appearance in the south west, and seemed to be small and dark, but the light that shone from it was very bright and appeared like an enormous beam of light shining in opposite direction to the star. Some said that they had seen other unknown stars about this time, but we cannot speak about these without reservation, because we did not ourselves see them. On the eve of Cena Domini, Thursday before Easter two moons were seen in the sky before day, one in the east and one in the west and both at the full, and that day the moon was 14 days old. The light from the tail of a comet seemed to be streaming towards instead of from the nucleus."

THE RECOVERY OF ASTEROIDS AFTER TWO OBSERVATIONS; B. G. Marsden, Harvard-Smithsonian Center for Astrophysics, Cambridge, MA 02138, U.S.A.

The most common procedure for arranging for additional observations of a newly-discovered asteroid for which there currently exist only two observations (or, conceivably, one observation and a motion) is to utilize representative "Väisälä orbits" fitted to the available data on the assumption that the object was observed exactly at perihelion--or, conceivably, aphelion (Väisälä 1939, Astron.-Optika Inst. Univ. Turku Informo No. 1). The procedure was generalized, at least in principle, by Bowell, Chernykh and Marsden (1989, Asteroids II, p. 21), who defined an appropriate search area surrounding these apsidal solutions. Other recent work tackles the problem by noting that, at least at opposition, there are constraints on semimajor axis and/or inclination (Bowell, Skiff, Wasserman and Russell 1990, ACM III, p. 19; Kristensen 1990, Astron. Nachr. 311, 133).

I consider here a process by which what amounts to the generalized Väisälä method can actually be put into practice. The method used is effectively an inverse of the Gauss-Encke-Merton (GEM) procedure in the rigorous yet in many respects simplified form I have discussed previously (Marsden 1985, Astron. J. 90, 1541). With the Cunningham (1946, Ph.D. thesis, Harvard University) choice of coordinate system the loci of prospective third observations are straightforwardly defined in terms of two parameters, namely, a first guess at the topocentric distance and a quantity describing the curvature of the apparent trajectory. Unlike the Väisälä approach to the problem, however, the inverse GEM process also handles Apollo objects, which by definition cannot be simultaneously both at opposition and at perihelion; the interesting case of 1990 MU is used as an example.

The new process has also proven very effective at selecting physically meaningful results in cases where the specified third observation leads to indeterminacy, and it also readily flags cases where at least one of the three observations must be erroneous.

COMET NONGRAVITATIONAL FORCES AND METEORITIC IMPACTS:

J. J. Matese, P. G. Whitman and D. P. Whitmire, Department of Physics
The University of Southwestern Louisiana, Lafayette, LA 70504-4210

The Oort effect (*Bull. Astr. Inst. Neth.* 11, 91 (1950)) is the tendency for near-parabolic comet energies to cluster in a narrow, bound range of values. When the orbits are corrected for planetary perturbations, the original values of reciprocal semimajor axes, 1/a, have a mean of 36 units (1 unit = 10^{-6} AU^{-1}) and a standard deviation about the mean of 14 units. This tight clustering diminishes for comets having the smallest range of perihelion distance, q, where the mean original orbit is hyperbolic and the standard deviation is five times as large (Marsden, B. G., et al., *Astron. J.* 83, 64 (1978)). We demonstrate here that small-q prograde comets have no significant difference in their energy distribution when compared to the large-q population. The non-Oort-like distribution of the small-q retrograde component could be due to observational selection effects, a different injection mechanism or larger nongravitational forces for this group of comets. Arguments suggesting that enhanced volatility is the explanation are given.

We have considered new comets (1/a < 100 units) in Marsden's 1989 catalogue. At a level 5x the formal measured error, δ, there are 4 class I and 3 class II comets that remain hyperbolic. All are retrograde and have small q. A statistical analysis is presented based on class I comets. We subdivide into prograde and retrograde sets the pairs of values (1/a, δ^2) sequenced in ascending q. Cumulative, weighted means (relative weights = δ^{-2}) are formed and standard deviations are determined. Confidence levels are discussed for the hypothesis that the distinctive distribution of the small-q retrograde population is not due to chance. Selection effects and alternative injection mechanisms are considered, but we argue that enhanced nongravitational forces are the cause. The dynamical parameter suggested is the energy of relative motion between a comet and a meteoroid in a prograde ecliptic circular orbit of radius r

$$U^2/2 = (3GM_\odot/2r)\,[1-(8q/9r)^{1/2}\cos(i)].$$

If r = q the energy for i = 180° comets is 34 times larger than for i = 0° comets. Mantle processing by an ecliptic population of meteoroids may be the cause of enhanced nongravitational forces with a concomitant deviation from the Oort clustering. The known meteoroid population would directly expose only a small portion of the volatiles underlying a mantle and crater growth need then be demonstrated. Alternatively, we suggest impacts of an as yet undiscovered population of larger objects (≈ 10 m) previously invoked as a cause of erratic behavior.

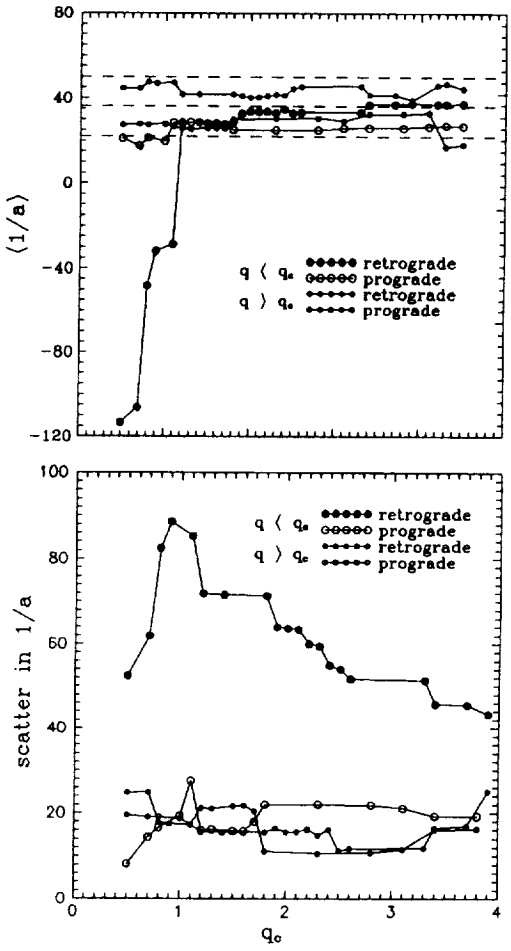

Dark Matter in the Solar System: HCN Polymers; Clifford N. Matthews, Dept. of Chemistry, University of Illinois at Chicago, Chicago, Illinois 60680, U.S.A.

In the presence of a base such as ammonia, liquid HCN polymerizes spontaneously at room temperature to a black solid from which a yellow-brown powder can be extracted by water and further hydrolyzed to yield α-amino acids. Our continuing research suggests that the yellow-orange-brown-black polymers are of two types: stable ladder structures with conjugated –C=N– bonds, and polyamidines readily converted by water to polypeptides.

These macromolecules, so easily formed in a reducing environment, could be major components of the dark matter observed on many solar system bodies. The non-volatile black crust of comet Halley may consist largely of such polymers, since the original presence on cometary nuclei of frozen volatiles such as methane, ammonia, and water makes them ideal sites for the formation and condensed-phase polymerization of hydrogen cyanide. Dust emanating from Halley's nucleus, contributing to the coma and tail, would also arise partly from these solids. Indeed, secondary species such as CN have been widely detected, as well as HCN itself and particles consisting only of H, C, and N. HCN polymerization could account, too, for the solid –C≡N bearing material detected by Cruikshank et al. on outer solar system bodies of low-albedo such as the comets Bowell and Panther, the surfaces of numerous asteriods of taxonomic type D, the rings of Uranus and the dark hemisphere of Saturn's satellite Iapetus.

Implications for prebiotic chemistry are profound. Primitive Earth may have been covered by HCN polymers through cometary bombardment or terrestrial synthesis, producing a proteinaceous matrix able to promote the molecular interactions leading to the emergence of life.

The Contribution of Interplanetary Particulates to the Near-Earth Satellite Impact Environment: Cometary or Asteroidal ?

J. A. M. McDonnell and P. R. Ratcliff

Unit for Space Sciences, University of Kent at Canterbury, Canterbury, CT2 7NR, United Kingdom

Characteristics of the near-Earth space particulate environment have been measured by experiments on NASA's Long Duration Exposure Facility (LDEF) over a period of 5.75 years. Data from numerous microparticle impacts have been collected and correlated to yield an average LDEF-referenced flux-size distribution as a function of the direction of exposure on LDEF. Comparison of results on the different faces offers a means of distinguishing between orbital and unbound particulates. Results so far suggest that for larger particles the flux seen is consistent with that predicted from the interplanetary flux, while for smaller masses there is evidence of an excess flux due to an orbital component, whether of natural or debris origin. The temporal stability over the space age measurement span since 1960 argues against this being entirely due to space debris.

Modelling of aerocapture of interplanetary particulates reveals a strong dependance of capture cross-section on particle mass and geocentric velocity. In consequence, capture strongly favours small particles in low eccentricity, low inclination orbits. Such orbits are more typical of material of asteroidal origin than of cometary particles. The excess of small orbital particles seen in low Earth orbit could reflect preferential capture of asteroidal, rather than of cometary, material.

Bias Correction Factors for Near Earth Asteroids

Lucy A. McFadden(California Space Institute, UCSD, La Jolla, CA 92093-0216)
Gretchen K. Benedix (Dept. of Physics, UCSC; California Space Institute 0216, UCSD, La Jolla, CA 92093-0216)
Esther Morrow(Math Dept., UCSD; California Space Institute 0216, UCSD, La Jolla CA 92093-0216)

Knowledge of the population size and physical characteristics (albedo, size, rotation rate) of near-Earth asteroids (NEAs) is biased by observational selection effects. Several approaches to evaluating these biases are under study in order to predict the size and physical characteristics of the entire population. The NEAs are a population of probably thousands of objects ranging in size from tens of meters to 40 kilometers and in orbits that cross or approach that of Earth's. Their proximity to Earth and potential for collision with Earth makes them intriguing. Over 160 NEAs are currently catalogued. Their true size distribution, albedo distribution and distribution of rotation rates are unknown.

Defining modeled NEA asteroid populations in terms of their orbital and physical elements; a, e, i, ω, Ω, M, albedo, and diameter (at a later point we will include rotation rates), we simulate an asteroid search program using the actual telescope pointings of right ascension, declination, date, and time to test for the presence of an asteroid in the field of view of the telescope. The computer search is done using an ephemeris program which calculates the position of each object in our model population at the date and time of each telescope pointing. The program then tests to see if that object is within the field of view of the telescope (FOV = 8.75°) and brighter than the limiting magnitude of the telescope (V=+18.0). The program tabulates the discoveries. The effect of the starting population on the outcome of the simulation's discoveries is compared to the results of the actual search program in order to define a most probable starting population.

Our first model population, called the Zeus objects, consists of 2000 orbits of randomly chosen orbital elements, albedos, and absolute magnitudes. Values for i, Ω, ω, and M were chosen randomly with the limits 0-90° for i and 0-360° for the rest. Values for e ($> 0, < 1$) and q (< 1.3 AU) were chosen randomly. From these values $a = q/(1-e)$ was computed and selected between 0.723 AU (Venus) and 5.2 AU (Jupiter). The ephemeris program was written in Fortran by David Tholen, for a PC-386 computer. The telescope pointings used to date are from Eugene and Carolyn Shoemaker's search program at the Mt. Palomar 48 cm Schmidt Telescope for the years 1984-1987.

The bias factor for each orbital and physical parameter is defined as the ratio of the discovered to the starting distribution. In order to determine the most likely bias factor we will use different starting populations to compute additional bias factors. The mean value will be the observational bias factor. We continue to model populations with different distributions and plan to incorporate telescope pointings from other search programs.

Near-Infrared Reflectance Spectra-Applications to Problems in Asteroid-Meteorite Relationships.

Lucy A. McFadden, Alan Chamberlin (California Space Institute, UCSD, La Jolla, CA 92093-0216), Faith Vilas (NASA/JSC, Houston, TX 77058)

Near-infrared spectral reflectance data were collected at the Infrared Telescope Facility (IRTF) at Mauna Kea Observatories in 1985 and 1986 for the purpose of searching the region near the 3:1 Kirkwood gap for asteroids with the spectral signatures of ordinary chondrite parent bodies. We are looking at 12 reflectance spectra.

The presence of ordinary chondrite parent bodies among this specific set of observed asteroids is not obvious. Though our sample is biased towards the larger asteroids in the region due to limitations imposed by detector sensitivity. Our data set, which was acquired with the same instrumentation used for the 52-color asteroid survey (Bell et al., 1987), also present some additional findings.

We note the range of spectral characteristics that exist among asteroids with the same taxonomic type. This is not a surprise but is a point that is worth illustrating. Tholen's taxonomic classification system designates an individual letter to a group of asteroids covering a specific range of photometric properties. With the single letter designation, we tend to think that all S-type or all P-type asteroids are alike. Our data remind us of the variability in the spectral properties and thus the mineralogy and/or surface texture or structure of the asteroid surfaces.

Another quickly drawn conclusion about the asteroids near the 3:1 Kirkwood gap is that they are all S-type asteroids, because this region of the asteroid belt is in the inner belt, where S-type asteroids predominate. However, when we look at the available data for this region, an equal number of asteroids are dark and not S-types.

One of the major differences between the reflectance spectra of ordinary chondrites and S-type asteroids is that the near-infrared reflectance of the S-asteroids has been believed to be significantly higher than the spectra of ordinary chondrites measured in the laboratory. It seems that with the availability of the 52-color asteroid survey, and the careful photometric calibration that has gone into that work and was used in reduction of the data presented here, that clearly not all S-type asteroids have a high IR reflectance. The availability of photometric data in the near-infrared of moderate spectral resolution may reduce some of the restrictions in finding asteroid analogues to the ordinary chondrites that were thought to exist with a less complete data set (Feierberg et al., 1982). Although the requirement that the positions of the 1- and 2-mm pyroxene and olivine bands be consistent with the chemistry of ordinary chondrite silicates remains the strictest requirement for finding ordinary chondrite analogues among the asteroids.

SPIN VECTORS OF ASTEROIDS 21 LUTETIA, 250 BETTINA, 337 DEVOSA, AND 694 EKARD; T.Michałowski, and T.Kwiatkowski, Astronomical Observatory, Adam Mickiewicz University, ul. Słoneczna 36, 60-286 Poznań, Poland

Lightcurve amplitudes, magnitudes and epochs of extrema of brightness are used in order to obtain the spin vectors of asteroids 21, 250, 337, and 694. There are no previous results for 250 and 337 - in cases of 21 and 694 we compare our poles with those already obtained by the others.

SECULAR RESONANCES AND ASTEROID FAMILIES

A. Milani, Univ. Pisa and Z. Knežević, Astron. Obs., Belgrade

We have developed a new analytical theory for secular resonance location. It is complete to degree four in the eccentricity and inclination of both the planets and the perturbed bodies, and to order two in the masses of the planets. The mixed effects resulting from the interactions of perturbations from different planets are accounted for. Not only the classical resonances associated with combinations of two secular frequencies, but also those associated with combinations of four frequencies can be studied. The algorithm can be applied to examine the regions with moderate eccentricity and inclination over the entire solar system.

We have applied this theory to the asteroid main belt, also to investigate how the distribution of the asteroids in the phase space is affected by the secular resonance surfaces. Apart from the well established fact that the classical resonances bound the densely populated portion of the main belt, and isolate smaller groups of asteroids, we discuss some interesting and somewhat puzzling features of the four frequencies resonances. As an example the secular resonance associated with the combination $g+s-g_6-s_6$ cuts across the large and well identifiable Eos family; apparently it does not result in long term dynamical erosion of the identifiable family, although the proper element theory has to be suitably adapted not to loose the accuracy. The theory for the Eos family accounting for this resonance allows to explain the uneven distribution of the argument $\varpi + \Omega$ among the family members, without assuming a recent formation; on the contrary, lower limit for the age can be derived.

GROUND-BASED OBSERVATIONS OF 951 GASPRA: CCD LIGHTCURVES AND SPECTROPHOTOMETRY WITH THE GALILEO FILTERS

S. Mottola ‡, M. Di Martino *, M. Gonano-Beurer ‡, H. Hoffmann ‡, and G. Neukum ‡;
‡DLR German Aerospace Research Establishment, D-8031 Oberpfaffenhofen,
*Osservatorio Astronomico di Torino, I-10025 Pino Torinese, Italy

CCD photometry and spectrophotometry of 951 Gaspra have been carried out by our group since the apparition of 1988 to characterize the physical and dynamical properties of this asteroid. The aim of this work is to provide a ground-based reference to be integrated and compared with the data which will be obtained during the Galileo encounter of October 1991.
In the frame of an international campaign (Di Martino et al., 1990) we observed 951 Gaspra during the apparitions of 1988 and 1990. As a result of these reconnaissance observations, which spanned over a long time interval and covered 20 deg. solar phase angle, we have determined for the first time the magnitude-phase and amplitude-phase relationships (Blanco et al., 1990; Barucci et al., 1990). From these measurements we could also derive the values of the parameters for the Bowell-Harris-Lumme photometric model: H= 11.788 $\pm$ 0.018 and G=0.217 $\pm$ 0.025 , the measured value of G being within the average for S asteroids (G=0.22 $\pm$ 0.03, Skoglöv et al., 1990). Data were achieved in the BVR filters, giving the following color indices B-V= 0.80 $\pm$ 0.05 and V-R= 0.50 $\pm$ 0.05.
Moreover from these observations it was possible to determine for the first time a sidereal period for this object, Psid= 7.0422 $\pm$ 0.0002 hr, and to obtain the indication of its prograde sense of rotation, applying the technique proposed by Taylor and Tedesco (1983).

During the apparition of 1991 of 951 Gaspra, we will carry out observations from the European Southern Observatory (La Silla,Chile), using the DLR CCD Camera equipped with a spare set of the Galileo SSI filters. These filters, which cover the wavelength range 0.4 - 1.0 μm, will be used for the first time to take measurements of this object.
The campaign will be mainly devoted to the study of the spectrophotometric properties of this small-sized and atypic S-type asteroid (Veverka et al., 1990) and will allow to obtain an homogeneous data set to be directly compared with the measurements returned by the spacecraft. The acquisition of high time-resolution, high SNR lightcurves in the different spectral channels will make it possible to search for the occurence of surface heterogeneities, linked most probably to a different content of metal and mafic silicates, and albedo spots (morphological/textural variegations) on hemispherical scale.
At present only a tentative solution for the orientation of the rotational axis has been derived on the base of the available data set for three oppositions (Chapman, 1990). The results of the 1991 apparition should also allow to give additional inputs for an accurate determination of the direction of the spin axis.

REFERENCES

Barucci M.A., C. Blanco, G. De Angelis, M. Di Martino, M. Fulchignoni, M. Gonano, J. Lecacheux, S. Mottola, G. Neukum, W. Wisniewski, *BAAS*, vol.22, n. 3, p. 1113 (1990).
Blanco C., M. Di Martino, W. Ferreri, M. Gonano, S. Mottola, G. Neukum, Photoelectric and CCD Photometry of 951 Gaspra, *Advances in Space Research*, in press, (1990)
Chapman C.R., private communication (1990).
Di Martino M., W. Ferreri, M. Fulchignoni, G. De Angelis, M.A. Barucci, J. Lecacheux, R. Burchi, A. Di Paolantonio, *Icarus* 87, 372-376 (1990).
Skoglöv E., C-I. Lagerkvist, P. Magnusson, in: *Asteroids Comets and Meteors III*, eds. C-I. Lagerkvist, H. Rickman, B.A. Lindblad, M. Lindgren, Univ. Uppsala 1990, p. 183.
Taylor R.C. and E.F. Tedesco, *Icarus* 54, 13-22 (1983).
Veverka J., Y. Langevin, R. Farquhar and M. Fulchignoni in: Spacecraft Exploration of Asteroids: the 1988 perspective, *Asteroids II* , eds. R.P. Binzel, T. Gehrels, M.S. Matthews, Univ. Arizona, Tucson 1989, p. 970

CCD-PHOTOMETRY OF COMETS AT LARGE HELIOCENTRIC DISTANCES;

B.E.A. Mueller, Kitt Peak National Observatory, Tucson AZ 85719

CCD imaging and time series photometry are used to determine the state of activity, nuclear properties and eventually the rotational motion of cometary nuclei. The rather surprising outburst of P/Halley at 14.3 AU (Hainaut, Smette & West, 1991, *IAU Circ.* **5189**; Meech 1991, *IAU Circ.* **5196**) proves that cometary activity and mantle evolution are not yet fully understood. On the other hand Tempel 2 had an activity onset during its last apparition at a heliocentric distance of only 1.9 AU (Boehnhardt et al. 1990, *Icarus* **86**, 58). It is thus very important to understand the temporal evolution of comets and therfore the differences between new and old comets and a possible realation to asteroids.

CCD-photometry of comets at large heliocentric distances is presented. The photometry contains mostly R-band data, however some data also exist in the V- and the I-bands. Preliminary results of this long-term program on activity status and rotational state of the objects are introduced. The objects observed include P/Giacobini-Zinner, P/Churyumov-Gerasimenko, P/Tempel 2, and 2060 Chiron.

ASTEROID ORBITAL ERROR ANALYSIS: THEORY AND APPLICATION

K. Muinonen and E. Bowell
Lowell Observatory, Flagstaff, Arizona, U.S.A.

We present a rigorous Bayesian theory for asteroid orbital error estimation in which the probability density of the orbital elements is derived from the noise statistics of the observations. For Gaussian noise in a linearized approximation, the probability density is also Gaussian, and the errors of the orbital elements at a given epoch are fully described by the covariance matrix. The law of error propagation can then be applied to calculate past and future positional uncertainty ellipsoids (cf. Yeomans *et al.* (1987), *Astron. J.* **94**, 189).

A number of analytical results can be derived from the covariance matrix in a two–body orbit approximation (with minor changes, the results are valid for integrated orbits). For example, as an observational arc is lengthened, the accuracy of the semimajor axis is improved much faster than that of the other orbital elements. Moreover, the variances of the mean, eccentric, and true anomalies have a quadratic time dependence. It is also worth noting that the correlations among the orbital elements are relatively insensitive to the arc length. This is due to the geometric restrictions of optical ground–based observations, and could be alleviated by radar or spacecraft observations. In ephemeris prediction, the error ellipse is usually very elongated and aligned with the line of variation.

Selected applications of orbital error analysis:

- In orbit computation, the behaviour of the covariance matrix serves as a guide for eliminating poor observations and suggests a way to automate the process.
- In the case of newly discovered asteroids, a strategy for follow–up or recovery can be devised. For example, one may decide whether an asteroid having a one–apparition orbit is recoverable using a narrow– or wide–field instrument and what the breadth of the search should reasonably be.
- A figure of merit is associated with each possible future observation, thereby suggesting an observational strategy that would optimize the orbit improvement and avoid making observations that would not contribute significantly.
- A criterion for numbering an asteroid can be established on the basis of the predicted ephemeris uncertainty over a suitable interval. For example, an ephemeris accuracy of 10 arcsec or better over 20 years might be required.
- Ephemeris uncertainty predictions can be used for observations made in the past, thus allowing the identification of images on archive plates.
- Knowledge of the accuracy of orbital elements can be used to decide whether it is appropriate to calculate proper elements.
- Uncertainties in occultation ground tracks can be determined.
- A linearized approximation has been applied to spacecraft trajectory error analysis (cf. Cappellari *et al.* (1976), Eds., GSFC Report X–582–76–77).

"Infrared Remote Sensing of Cometary Parent Volatiles from the Ground, Air, and Space"

Michael J. Mumma, Michael DiSanti, Susan Hoban, and Dennis C. Reuter
Laboratory for Extraterrestrial Physics
NASA Goddard Space Flight Center
Greenbelt, Maryland 20771

The last five years have seen an explosion in our ability to directly detect the parent species in comets, beginning with the first definitive detection of cometary water in December 1985, from the Kuiper Airborne Observatory. In March 1986, infrared spectroscopy from the Vega-1 spacecraft provided the first detections of CO_2 and of the carbonaceous feature (3.2-3.5 μm), a definite detection of H_2CO, and a tentative detection of CO. Since then, the carbonaceous feature has been detected in every comet searched, and spectroscopy from the ground and air has produced tentative detections of CH_4, CH_3OH, and CO, and significant upper limits for CH_4 and H_2CO. Meanwhile, advanced instruments promise routine detection of many species that at present are only marginally detectable in bright comets. Using these, we can expect to identify the volatile and refractory progenitors of the carbonaceous feature, and to provide routine study of the carbon chemistry (CH_3OH, H_2CO, CO, CH_4 ...), the nitrogen chemistry (NH_3, HCN ...), and the sulphur chemistry (e.g. H_2S). Airborne observations will provide studies of H_2O and CS_2, and spaceborne instruments (e.g. on ISO) will provide measurements of CO_2, and of strong terrestrial absorbers (H_2O, CH_4, CO, etc.) at arbitrary Doppler shift. Unambiguous determinations of the ortho-para ratios, and measurements of isotopic ratios in several key species should be possible.

Difficulties lie ahead, however, for investigations that rely on small pixel sizes, such as certain advanced ground-based instruments and the HRS instrument on HST. The reduction in background needed to take full advantage of the 2-D array detectors in ground-based instruments leads to their use at high spectral resolution and small optical throughput. The spectral grasp is shortened, and the fraction of molecules sampled by a single pixel is also reduced, and this makes the retrieval of production rates increasingly sensitive to coma models of uncertain provenance. However, certain other aspects, such as co-registration of different spectral precursors (e.g. gases and refractories), can enhance the study of short term variability (therefore of nuclear heterogeneity), and of the morphology of the near nucleus region.

In this paper, I will attempt to present a balanced view of the present generation of infrared instruments for cometary compositional studies. Ground-based instruments will be compared with airborne and spaceborne capabilities. I will attempt to give examples of the unique science achievable with each, and will place particular emphasis on the unique aspects of a dedicated Cometary Composition Telescope in Earth orbit for investigating the chemical and structural heterogeneity of the cometary nucleus.

COSMO-DICE: PROJECT OF DYNAMICAL INVESTIGATION OF COMETARY EVOLUTION

Tsuko NAKAMURA (NAO,Tokyo) & Makoto YOSHIKAWA (University of Tokyo)

The orbits of more than 150 periodic comets are integrated numerically in very high precision. The adopted integrator is a variable-step extraporation method in quadruple precision. This corresponds to a rounding-off error of 10^{-28} at the start of integration. We incorporate positions of 9 planets from DE102 ephemerides in the integration and the calculations are carried out for the full time span of DE102 (about 4400 years, from BC1411 through AD3002). Error tolerance for a single integration step is set to 10^{-22}. Accuracy of integration is checked by the round-trip error of closure test which covers about 3400 years, so that this allows us to estimate the reliable time interval of our integration for each comet. This can also be used to know, for a given number of significant digits of the observed orbital elements of a comet, how the orbital error grows with the elapse of time.

It is shown that the reliability interval is about 1000-1500 years for most of low-inclination short-period comets whereas that for high-inclination and longer-period comets is about 3000-4000 years or more. It is also found that growth rate of the round-trip error has intimate correlation with the chaotic nature of cometary orbits.

In this poster session we graphically present the time variations for 4400 years of all the comets in orbital elements, perihelion and aphelion distances, Tisserand's invariant, mutual distances between planets and a comet, the round-trip errors for orbital elements and position and velocity vectors. We are preparing a MT of about 50MB (nearly in double precision) in the standard FITS format to distribute to the interested researchers, which contains 64-day interval positions and velocities of all the comets. We also have a plan to develop a program which enables us to present and compare easily, in an interactive mode on a graphic terminal, orbital behavior of comets and other related dynamical quantities such as Tisserand's invariant, libration arguments and so on.

LONG-TERM ORBITAL BEHAVIOR OF SHORT-PERIOD COMETS FOUND IN PROJECT COSMO-DICE

Tsuko NAKAMURA (NAO, Tokyo) & Makoto YOSHIKAWA (University of Tokyo)

We have performed systematic numerical integrations of more than 150 periodic comets for 4400 years (3400 years toward the past and 1000 years to the future), based on the JPL planetary ephemerides DE102. Details of this project are descirbed in our another paper which will be presented at the poster session. One of the most remarkable results of our project is that comets entering the capture region by Jupiter are proved to evolve to short-period (SP) comets in the framework of realistic dynamical model. It is found that more than 90% of the observed comets whose Tisserand's invariant (J) is between 2.8 and 3.1 actually take this evolutionary path within the past 3400 years. This evolution is much more rapid than that expected from Monte Carlo simulations for simplified dynamical models based on symmetric distribution of perturbations. This suggests that asymmetry of perturbation distribution plays an important role in cometary evolution.

Some of SP comets are shown to evolve from the orbits of which perihelion distance is located near Saturn' orbit and then is handed over under the control of Jupiter. This seems to support the multiple stage capture mechanism first proposed by Everhart (1977). We also found a comet which is ejected out of the solar system by Jupiter in a fairly strong hyperbolic orbit around 2330 AD.

It is confirmed that captured low-inclination SP comets with the J in the range given above show more or less strong chaotic behavior of orbital evolution. On the other hand, comets with longer orbital period and/or of high inclination reveal slow and quasi-periodic nature of orbital evolution.

LUMINESCENT GRAINS IN THE ATMOSPHERE OF COMET HALLEY; G.K.Nazarchuk, The Main Astronomical Observatory of the Ukrainian Academy of Sciences, 252127, Kiev, USSR

The sufficiently high space and spectral resolution (4 arcsec and 2 A) of the Comet Halley spectra obtained by the 6-meter telescope gave the possibility to find luminescent dust particles in the atmosphere of this comet [1,2]. The hypothesis about the presence of these particles is based on the observed deficiency of the equivalent widths of the Fraunhofer lines in the spectral continuum of Comet Halley.

It means that eighther there was an unusually high level of parasite scattered light inside the spectrograph or there was the component of the continuum which was not the solar light scattered by cometary grains. The first supposition was checked by spectra of reference stars and was rejected. The partition of the continuum to the luminescent and the scattered ones gave the following results.

Distance from the nucleus		Fraction of luminescence in the P/Halley continuum in the range 3300-6000 A
arcsec	km	
-20	-10000	5.6 %
-4	-2000	18.4
0	0	21.5
20	10000	5.2
36	18000	2.8
40	20000	2.0

Minus corresponds to the sunward direction.

Thus, the luminescent particles (probably, CHON-grains) are short-living. They disappear at the distance less than 1 arcmin from the nucleus. Taking into consideration that a spectrum of the circumnuclear region within several arcseconds with the resolved profiles of the Fraunhofer lines is necessary to detect the luminescence, one can easy understand why the luminescence has never been seen previously.

REFERENCES

1. Nazarchuk, G.K. Comet Circular N. 372, 1987, P. 2-3 (in russian).
2. Nazarchuk, G.K. Comet Circular N. 377, 1987, P. 2-4 (in russian).

Delivery of Meteorites from the Asteroid Belt.

M. Nolan and R. Greenberg / University of Arizona

The study of asteroid formation and composition is of keen interest, since the processes that formed our own Earth and the other planets may have been similar in some important ways. Also, the numerous objects in the main asteroid belt and elsewhere help us avoid the "sample of one" problem so common in planetary science. Unfortunately, asteroids are very difficult to study directly: we have relatively noisy, low resolution optical spectra of their disk-averaged surfaces in reflected sunlight or thermal emission, and even then we see only their "dirty" surfaces. Meteorites, on the other hand, can be studied in great detail at high resolution by a wide array of techniques with much lower noise. Thus it would aid our understanding to know how asteroids and meteorites are connected, even if only statistically.

Transport processes for bringing asteroids from the asteroid belt to the Earth have been critically reviewed by Greenberg and Nolan [1989]. Wisdom [1983] and Froeschlé and Scholl [1986] have shown that asteroidal material may be transported to the Earth by way of Jovian and secular resonances. We do not know for certain how asteroids get into the resonances, which are now fairly clear of asteroids, probably due to the same processes that bring material to the Earth. We probably understand in general the dynamical delivery mechanisms, but not their relative efficacy, or what regions of space they sample.

The main belt size distribution is known for sizes $\gtrsim 30$ km in diameter by direct telescopic observation, with some extrapolation and bias corrections for albedo at the smaller sizes. However, collisions are most likely to occur with smaller bodies. Thus our estimates for the collisional lifetimes of the bodies we can see are very uncertain. The collisional lifetimes affect in turn the expected steady-state population of bodies at all sizes.

As an alternative to using a variety of poorly understood processes to analyze the meteorite delivery process from the main belt, we can look at the process from the other end: meteorites arriving at the Earth. Networks of cameras operating since the early 1950s (*cf.* Jacchia and Whipple [1961]) photographed several thousand meteor trails. From these photographs, it was possible to determine the orbits of the asteroids which fell as meteors. Wetherill and ReVelle [1981] chose 27 meteors which they believed to be of ordinary chondritic composition (including Lost City, a recovered meteorite). Their orbital elements in a, e space show clusters near several Jovian resonances zones. We have similarly examined the orbits of 42 496 meteors from the IAU Meteor Data Center. Clustering persists only weakly in the vast data. The low accuracy of many of the orbits (D. Steele, pers. comm.) is a critical factor. There is a strong clustering toward orbits with perihelia near 1 AU. The Öpik two-body treatment of the the gravitational attraction of the Earth may not be sufficient for these orbits. We are numerically integrating the orbits of these meteors, to determine how large a correction is required. These results will help constrain how many came to Earth-crossing by each of the possible routes.

15 Years of Comet Photometry : A Comparative Analysis of 80 Comets

David J. Osip, David G. Schleicher, Robert L. Millis

Lowell Observatory

Michael F. A'Hearn

University of Maryland

Peter V. Birch

Perth Observatory

In 1976 we began a program of narrowband photometry of comets that has encompassed well over 400 nights of observations. To date, the program has provided detailed information on 80 comets, 11 of which have been observed during multiple apparitions. The filters (initially isolating CN, C_2, and continuum and later including C_3, OH, and NH) as well as the detectors used for the observations were changed over time, and the parameters adopted in the reduction and modelling of the data have likewise evolved. Accordingly, we have re-reduced the entire database and have derived production rates using current values for scalelengths and fluorescence efficiencies. Having completed this task, the results for different comets can now be meaningfully compared. General characteristics we will discuss in this paper include ranges in composition (molecular production rate ratios) and dustiness (gas production compared with $Af\rho$). Additionally, we will present an analysis of trends focusing on how the production rates vary with heliocentric distance and on pre- and post-perihelion asymmetries in the production rates of individual comets. Possible taxonomic groupings will also be described.
This research is supported by a grant from the NASA Planetary Astronomy Program.

A NEW METHOD FOR ASTROMETRIC OBSERVATIONS OF ASTEROIDS

Th. Pauwels, *Koninklijke Sterrenwacht van België, Ringlaan 3, B-1180 Brussel, Belgium*

When no accurate positions are known, on astrographic plates asteroids reveal themselves among the stars by their motion only. Therefore astrographic observations of asteroids are always done in such a way that moving objects can easily be detected on the plates. Among the classical methods we may mention:

- Long exposures, such that moving objects show trails.
- Long exposures with interruptions, such that moving objects give several images. The interruptions can be symmetric or asymmetric.
- Several plates of the same field with a small separation in time. Moving objects are detected by blinking the plates.
- Several exposures on the same plate, shifted by a known amount. Moving objects reveal themselves by a different pattern formed by the different exposures.

The method we suggest here consists of several superimposed so-called Trepied-Metcalf exposures. Each of the exposures is guided with the average (or expected) motion of the target objects. By superimposing several exposures, stars will show only one (trailed) image, while moving objects will show several images (more or less trailed, depending from how much each object's motion differs from the introduced average motion).

This method has several advantages over the classical methods. Some of these are:

- Fainter limit magnitude thanks to the Trepied-Metcalf exposure.
- No overloading of the picture, since there is only one image per star.
- Very easy detection of moving objects, not requiring a blink comparator.
- More precision in the measurements of the moving objects by measuring all images. Yet there is no need to measure several images of the reference stars.
- No waste of time between the exposures (compared to the second described classical method).

A few disadvantages are:

- Accumulation of sky background because of several exposures on the same plate.
- Very large non-spherical reference stars.
- Although possible, finding the motion of an object for recovery on following nights is difficult.
- Only one astrometric position for several images, all to be measured, since the distance between the exposures is *not* the motion of the object, but the manually introduced motion in guiding.

All these advantages and disadvantages can also be found in one or more classical methods. The desired combination of advantages and disadvantages should guide the observer in choosing his favourite method.

THE IMPORTANCE OF GUIDING ON THE MOTION OF A COMET IN ASTROMETRIC OBSERVATIONS

Th. Pauwels, *Koninklijke Sterrenwacht van België, Ringlaan 3, B-1180 Brussel, Belgium*

When doing astrometric observations of a comet, one is not interested in a beautiful picture, nor in showing the tail of a comet. Often, it may seem unnecessary to guide on the motion of the comet. A plate guided on the motion of the stars and with a trailed image of the comet can look very acceptable to be measured for an astrometric position. However, the results obtained in this way will be wrong.

When observing for an astrometric position, one is interested in the nucleus of the comet. This one can never be observed. However, the central condensation gives a very good approximation of the position of this nucleus. One tries to find the maximum of the light distribution of the cometary image and to take that as the position of the comet (the images of the Giotto spacecraft have shown that this introduces an error of the order of 10-20 km, which is completely negligible). In reallity the eye will not point the maximum but the middle of some isophote surrounding this maximum closely.

If the comet has moved (say, perpendicularly to the direction of the tail) during the exposure, then it may look as if there is a trailed central condensation, which can be measured quite well. However, positions obtained in this way will be shifted towards the tail of the comet, thus introducing a systematic error in the positions. This is due to the fact that the light intensity at any point of the photographic plate will be the integral of the light intensity of the comet, integrated along a line parallel to its motion. This integral will be a function of only one coordinate (perpendicular to the motion of the object), and will have a maximum for a different value of that coordinate than the original function. Usually the light distribution along a line parallel to the motion will have a rather sharp maximum if the cut is through the central condensation, but more prominent wings if the cut is shifted towards the tail. These wings can contribute more to the total integrated light distribution and thus give a brighter image than at the real location of the central condensation.

On LAMs and SAMs for Halley's Rotation

S. J. Peale
Dept. of Physics
University of California
Santa Barbara, CA

Both Long axis modes (LAMs) and short axis modes (SAMs) have been proposed for Halley's comet, where the acronyms refer to non principal axis rotation with precession of the spin vector in the body frame of reference about the axes of minimum moment of inertia and maximum moment of inertia respectively. The non principal axis rotation is invoked to accommodate a dual periodicity in the light curves, jet shapes and other types of observations of the comet. A LAM is characterized by a rotation of the long axis of the nucleus about the spin angular momentum vector with period P_ϕ while the nucleus rotates about the long axis with period P_ψ, which is the period of precession of the rotation vector about the long axis in the body frame of reference. The long axis also nods with a period of $P_\psi/2$ but with small amplitude for Halley's shape. The rotation of the long axis about the angular momentum vector with period P_ϕ as the long axis nods also is characteristic of a SAM, but in this case the motion *about* the long axis is an oscillation with period P_ψ instead of a complete rotation. Both Belton *et al.* (1991) and Samarasinha and A'Hearn (1991) find that only a LAM with $P_\phi \approx 3.7$ days and $P_\psi \approx 7.1$ to 7.4 days can be consistent with an extensive list of observational constraints. On the other hand, there can be no "Springtime for Halley" for a LAM to account for the post perihelion brightening of the the comet without an additional degree of freedom such as activating a new jet at perihelion passage at each apparition. All parts of the nucleus receive full solar illumination during the rotation cycle at all parts of the orbit for a LAM. The maximum rate of emission of a jet source is then governed only by Halley's proximity to the Sun leading to a light curve that is symmetric about perihelion if thermal inertia effects are small. For a SAM, the motion of the nucleus about the long axis is limited to a relative small range of angles, so with an appropriate orientation of the spin angular momentum with significant obliquity to the orbit plane, an active source could remain more or less in shadow until after perihelion passage to account for the post perihelion brightening. Since the post perihelion brightening is a robust observation of every apparition, whereas some of the other constraints depend on uncertain model parameters, it would appear that any derived rotation state must first be able to account for the post perihelion brightening. Either the LAM must be embellished to account for the brightening by some effect perhaps involving thermal inertia, or a SAM must be found that will remain consistent with the observations that have so far eliminated it. Halley's persistent activity at large post perihelion distances and the recent outburst of its cold nucleus may provide clues to a means for storing solar energy in a LAM nucleus.

COMET CLOSE ENCOUNTERS AND HYPERBOLIC METEOROIDS;
E.M.Pittich, Astronomical Institute, Slovak Academy of Sciences, 842 28 Bratislava, Czechoslovakia.

Catalogues of meteor orbits contain some quantity of hyperbolic orbits. In spite of the large percentage of these orbits is evidence that hyperbolic orbits are the result of measuring errors, some of them are real nonperiodical orbits. Part of hyperbolic orbits can be originated from cometary meteoroids at close encounters to the giant planets. This result was obtained by the numerical integration of orbits of meteoroids, which were ejected from nuclei of comets P/Shajn-Schaldach, and P/Encke, respectively. The first of these comets represents comets with close encounters to the planets during their orbital evolution, the second comet is the typical example of a comet without close encounters.

CHARACTERISTICS OF THE 1969 LEONIDS AND 1982 LYRIDS BURSTS; V. Porubčan and J. Štohl, Astronomical Institute SAV, 84228 Bratislava, ČSFR

Radar observations of the last bursts of the Leonids (1969) and Lyrids (1982) carried out at the Springhill Meteor Observatory, Canada, have enabled a detailed study of the activity and mass distribution of meteoroids across the corresponding dense and relatively young filaments of the two meteor streams. A significant common feature of both bursts is their very short duration, with the rates exceeding a half-maximum rate within 15-20 minutes only, and those exceeding a quarter-maximum rate within 50-55 minutes. Mass distribution exponent of the meteoroids in the filaments largely differs from the values obtained for the older populations of the streams. The highest mass exponent s 2.2 - 2.4 is found around the peak of the activity, confirming high contribution of smaller meteoroids in the narrow filaments of recent origin. Origin of the filaments in both streams is discussed.

THE FLUX OF SMALL ASTEROIDS NEAR THE EARTH; D. L. Rabinowitz, Lunar and Planetary Laboratory, The University of Arizona, Tucson AZ 85721

Until recently, no asteroid smaller than 100m had ever been identified outside the Earth's atmosphere. Such objects had been observed only as bright meteors and fireballs, with estimated diameters rarely exceeding 10m. Since September of 1990, however, T. Gehrels, J. V. Scotti, and I have made astrometric observations of two objects, 1990 UN and 1991 BA, with estimated diameters of 90 and 9m, respectively. These were discovered in the course of a regular search for Earth-approaching asteroids which we conduct each month at the 0.91m Spacewatch Telescope on Kitt Peak. We use a TK2048 CCD in drift-scan mode to image the sky and a real-time computer to monitor, record, and analyze the data. Our average discovery rate is about two Earth approachers per month, with absolute magnitudes ranging from 14.5 to 28.5. In this paper, I use these observations and also a computer model of the asteroid population observable by the Spacewatch Telescope to determine the asteroid flux near the Earth as a function of absolute magnitude. The computer model is necessary in order to determine the efficiency of the Spacewatch Telescope for detecting Earth approachers as a function of their size, phase angle, angular rate, and distances to the sun and the Earth. Given an assumed magnitude distribution, the model allows me to compute the expected number of Spacewatch discoveries as a function of absolute magnitude. I find that for asteroids larger than 100m, the observed magnitude dependence is consistent with the cumulative magnitude-frequency relation established for the main belt asteroids. Assuming this relation extends to smaller sizes, however, the probabilities for discovering 1990 UN and 1991 BA are only 10% and 1%, respectively. Objects smaller than 100m are therefore increasingly overabundant compared to an extrapolation from larger objects, with this excess increasing with decreasing size. Near 10m, the most probable flux near the Earth is two orders of magnitude higher. This is in agreement with the fluxes estimated from observations of bright meteors and fireballs. It is likely that processes other than collisional breakup of asteroidal material begin to supply the population of small objects near the Earth at sizes near 100m.

The 16 March 1986 Disconnection Event in Comet Halley

C.E. Randall, J.C. Brandt and Y. Yi
(U. Colorado/LASP)

We present an analysis of a disconnection event (DE) in Comet Halley in mid-March of 1986. Although disconnection events are arguably the most spectacular of all dynamic comet phenomena, the mechanisms by which they occur are not fully understood. It is generally believed that the solar wind plays a major role in determining when disconnection events occur, but the details of the solar wind/cometary interactions responsible for initiating the tail disconnection are still under debate. The two most widely accepted models are (1) high speed streams in the solar wind cause the tail to disconnect through such mechanisms as increased ion production or pressure effects; and (2) the tail disconnects after frontside reconnection of the interplanetary magnetic field (IMF) as the comet crosses a magnetic field sector boundary.

In order to study these proposed mechanisms, we have analyzed photographs from the International Halley Watch (IHW) archive throughout the 1985-1986 Comet Halley appearance. Photos between 16 March 1986 and 19 March 1986 clearly show the occurrence of a disconnection event, which we discuss here. From the images we have determined the precise time of the DE, and have examined the solar wind conditions and interplanetary magnetic field at this time in order to ascertain whether any correlations were evident which would support one of the proposed mechanisms for DE occurrence.

From kinematic extrapolation of tail–nucleus distance measurements on the photographs, we calculated the disconnection time of the 16-19 March 1986 event to be 16.1 ($\pm$0.1) March. We inferred the solar wind conditions around Comet Halley by corotating data from the IMP-8 satellite to the comet. Using this data, we determined that at the time of the DE the solar wind speed at the comet was $\sim$ 600 km/sec; the solar wind density was $\sim$ 8 cm^{-3}; and the IMF magnitude was $\sim$ 8 nT. These conditions are not particularly unusual, and thus would *not* be expected to have caused the observed DE via mechanisms such as ion production or pressure effects.

We estimated the position of the IMF neutral sheet using two different methods. The times and positions of 180-degree phase shifts in the IMF direction were measured by the IMP-8, ICE and PVO satellites, and corotated to Comet Halley's orbit. Also, the neutral sheet calculated at the solar source surface was corotated out to the comet. Both methods are consistent with one another, and show that Comet Halley crossed a magnetic field sector boundary shortly before the 16 March DE. We therefore conclude that the most likely cause of this disconnection event was front-side reconnection of the IMF.

Laboratory Studies On Cometary Crust Formation: The Importance Of Sintering; L. Ratke, H. Kochan, H. Thomas, Institut für Raumsimulation, DLR-Köln, P.O. Box 906058, D-5000 Köln 90, FRG.

In laboratory simulations with porous water-ice-dust mixtures strong crusts are observed after insolation with an artificial sun. Within the KOSI project strength increases up to an order of magnitude were observed compared to the strength of the loosely packed ice-dust mixtures. In the KOSI-experiments it was found that the thickness of the crust depends on the insolation power, its duration, the temperature profile, and the composition of the ice-dust mixture [1].The mechanism of crust formation are still unknown in detail. One of the mechanisms under discussion is the recondensation of the inward diffusing volatiles. This would reduce the pore volume and thus strengthen the ice-dust body. We propose here two other mechanisms which maybe of general importance especially for real comets: sintering of loosely packed ice-dust particles either due to sublimation and condensation or due to surface diffusion. Solid state sintering of particles is a well known phenomenon in powder metallurgy [2,3]. Sintering - which means the densification of arbitrarily packed powder aggregates - occurs due to dependence of for instance the partial pressure of water on particle radius or more generally the dependence of the chemical potential of a species on the particle curvature. The sintering process within particle aggregates forms "sinter necks" at the contact points between the particles. These have lower partial pressure than adjacent spherical particles. The neck grows therefore by transport of sublimated water from points of higher to lower curvature. Applying the theories developed in powder metallurgy to ice aggregates it is possible to describe the crust formation and its increasing strength. At different homologous temperatures different transport mechanisms (sintering) may occur.
At temperatures above 200 K sintering due to sublimation and condensation is possible, whereas at lower temperatures surface diffusion gives a faster reduction of pore volume and thus an increase in strength. The theoretical discussion of the crust formation by sintering supplemented by laboratory investigations performed with pure ice at different temperatures.

[1] H.Kochan,K.Roessler,L.Ratke,M.Heyl,H.Hellmann, G.Schwehm, *Proc. Int.Workshop on Physics and Mechanics of Cometary Materials*, MÜnster,FRG 1989, ESA-SP-302, pp.115-119
[2] H.E.Exner, *Principles of Single Phase Sintering*, Rev. Powder Met. Phys.Ceram.,1979, Vol.1, pp.7-251
[3] G.C.Kuczynski, *Physics and Chemistry of Sintering*, Advanc. Colloid Interf.Sci.,1972, vol.3, pp.275-330

VELOCITIES IN THE H_2O^+-ION TAIL OF COMET LEVY 1990c

H. Rauer, K. Jockers, C. Debi-Prasad, Max-Planck-Institut für Aeronomie,
D-W-3411 Katlenburg-Lindau, Germany

E.H. Geyer, Observatorium Hoher List, D-W-5568 Daun, Germany

Comet Levy 1990c was observed at the Observatory Hoher List, FRG, from 16th to the 25th of August 1990. A focal reducer and the CCD-camera of the Max-Planck-Institut für Aeronomie were used. The field of view was approximately 25 arcmin. Images were taken through an interference filter at 615.8±1.8 nm, to observe the H_2O^+-ion tail. The dust continuum was observed through another filter of 3 nm FWHM centered at 642 nm. From these images column densities have been derived out to a distance of 1 10^6 km from the cometary nucleus. Interferograms, using a Fabry-Perot-etalon with a fixed gap of 0.9 mm and spectral resolution of 0.2 Å at 615.8 nm, were also taken. From these interferograms, the geocentric velocity component of the water ions in the plasma tail has been derived. 2-dimensional velocity maps will be presented. These were used, together with the column densities derived in the images taken before and after the interferograms, to calculate production rates.

Space Weathering of a Non-Spherical, Rotating Body, R. O. Redman, National Research Council of Canada

During cratering events on airless bodies, large numbers of small particles are blasted out of the surface, with small particles generally having higher speeds than large particles. If the parent body is non-spherical and rotating, it can exchange energy gravitationally with the ejected particles. Some low energy particles are boosted into escaping orbits, while other high energy particles are recaptured. This process has been modelled for a contact binary asteroid consisting of two touching spheres rotating about their centre of mass at a specified fraction of the breakup velocity. The domain of initial velocities for which an ejected particle is recaptured has a fractal structure. The author hopes to illustrate this using an interactive computer program which calculates the orbit corresponding to each initial velocity. The implications for the collection of dust and gravel in the regolith of a rotating, non-spherical asteroid will be discussed.

VISUAL DATA OF MINOR METEOR SHOWERS

J. Rendtel, Arbeitskreis Meteore, PSF 37, 1561 Potsdam, Germany
International Meteor Organization

There are different lists of meteor showers, partially containing hundreds of radiants. Even if these would represent real sources of meteoroids, an observer cannot associate meteors seen to all these radiants.

The Visual Commission of the *International Meteor Organization, IMO* formulated rules for the work of visual observers. Three essential information which can be obtained by well trained observers are considered for shower association of meteors:

(i) direction of the trail (tracing back the line must meet the radiant of a certain size)

(ii) apparent trail length must not be longer than half the distance from its (possible) radiant; exception: fireballs penetrating to lower end heights

(iii) the angular velocity in dependence on the meteor's elevation and its distance from the radiant

In order to distinguish shower meteors from different showers as well as from the sporadic background, the observer is forced to look not more than 40° away from the radiant(s) under study. Furthermore, a radiant should be situated at least 30° above horizon. Otherwise the correction to zenith position becomes too large and the result is then uncertain simply due to the reduced number of shower meteors visible.

A mathematical treatment of the pollution of shower rates only by accidentially aligned sporadic meteors by GYSSENS (1989) yields to a rate of about 2/hour.

Experimental data derived from observational material of end August led to a ZHR of about 2 ... 3 for arbitrary points at the sphere fulfilling the above mentioned criteria. More recent analyses of spring data at a lower meteor activity level confirm, that one may expect a rate of about 15 percent of the total rate from any assumed radiant of about 10° diameter. If a certain velocity is assumed, this rate decreases to less than 10 percent for experienced observers.

Consequently, an experienced observer considering all the three criteria mentioned in the beginning, may deliver useful ZHR-values as soon as the ZHR reaches 2.5 ... 3. All ZHR below this level must be regarded as insignificant and useless.

The IMO collects visual observations in its Visual Meteor DataBase (VMDB). It contains statistical data of about 100,000 meteors per year and allows calculations of ZHR as well as of the population index r (or the mass index s). Knowing these data, further quantities, such as the number density or the particle flux can be determined (RENDTEL and KOSCHACK, 1989 and 1990).

In the IMO working list of showers are included only showers

(i) reaching a certain level of activity, and

(ii) having known orbital elements (thus known geocentric velocity).

All other meteors are regarded to be sporadic. Since the meteor trails are plotted on gnomonic charts (except the periods of high activity near major shower maxima), searches for radiants being of interest later, can be done. Furthermore, IMO prepares a positional database (PosDat). It will contain positional data of visual and telescopic meteors and is connected with a radiant search program. This will allow an effective search for instance for a possible activity of asteroid related radiants.

OBSERVED SPATIAL PROFILES OF C_2, C_3, CH, CN, [OI] AND NH_2 IN COMETS HALLEY, WILSON AND NISHIKAWA-TAKAMIZAWA-TAGO

Terrence W. Rettig (University of Notre Dame and Arizona State University)
Susan Wyckoff, Rodney S. Heyd (Arizona State University) and Raylee Stathakis (Anglo-Australian Observatory) and D. A. Ramsay (Herzberg Institute of Astrophysics, NRCC)

Long-slit spectral observations of comets Halley (1986), Wilson (1987) and Nishikawa-Takamizawa-Tago (1987) were obtained with the 3.9 meter Anglo-Australian Telescope. The observations of P/Halley were obtained in April 1986 and observations for C/Wilson and Nishikawa-Takamizawa-Tago were obtained in May 1987. Spectra of comets Halley and Wilson were obtained with the IPCS at a spectral resolution of 0.5 A and a spatial resolution of 10^3 km. Also, spectra of comets Wilson and Nishikawa-Takamizawa-Tago were obtained with a CCD at a resolution of 1.5 A and a spatial resolution of approximately $3x10^3$ km. The measured surface brightness profiles extend to approximately $6x10^4$ km from the nucleus in both sunward and tailward directions. Spatial profiles for C/Wilson are compared at the two different spectral resolutions with the IPCS and CCD detectors. These three comets were at approximately the same heliocentric distances and the brightness profiles are shown to have the same shapes within the observed errors even though the gas/dust ratios vary appreciably. Hence, the scalelengths derived from spatial profiles are determined to be the same for identical molecules in each of the three comets suggesting these molecules are derived from common parents. Production rates for NH_2 are determined and NH_2/H_2O ratios are presented. With standard parameters, the NH_2 brightness profile fits the vectorial model, reaffirming the probable NH_3 parenthood.

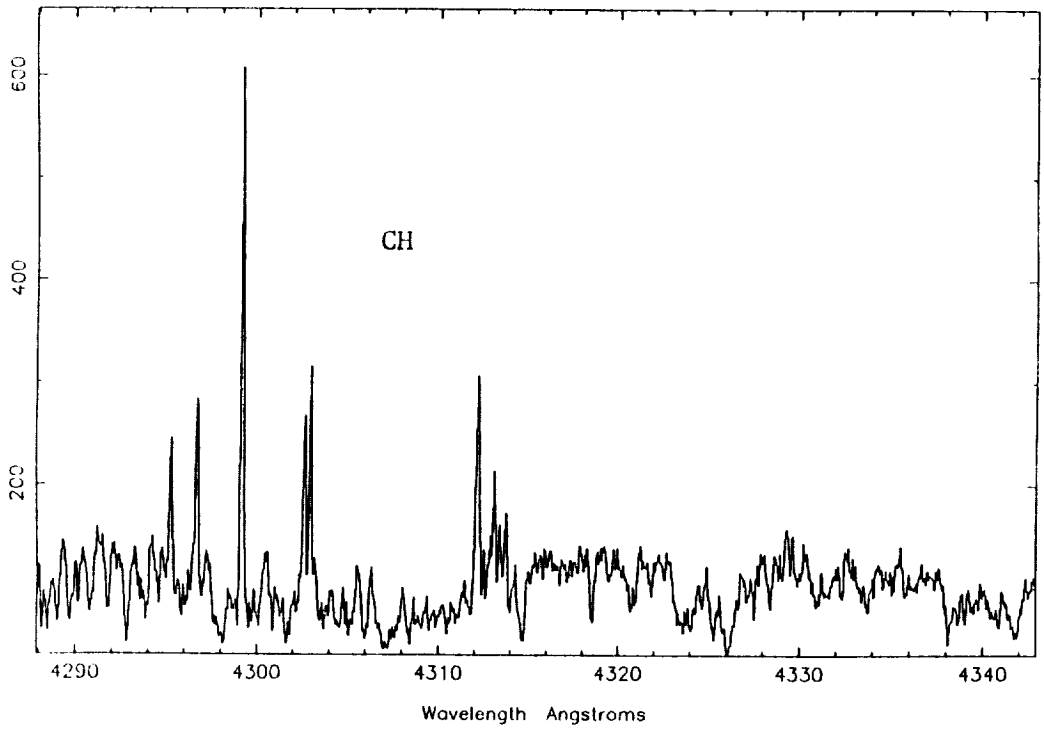

PARENT MOLECULAR SCALELENGTHS INFERRED FROM THE OBSERVED SURFACE BRIGHTNESS DISTRIBUTIONS OF C_2, C_3, NH_2, CH, CN, AND [OI] IN COMETS

Terrence W. Rettig (University of Notre Dame and Arizona State University),
Susan Wyckoff, Rodney S. Heyd, and Lisa Engel (Arizona State University)

Of the five molecules commonly observed in ground-based spectra of comets, the parent of only one species, NH_2, has been tentatively identified (NH_3). All radicals observed in the fluorescence spectra of comets are probably photodissociation fragments of parent molecules released directly from the comet nucleus. Thus with an appropriate coma outflow model and radical photodissociation timescale, the scalelength of a parent molecule can be inferred from the observed spatial distributions. Long-slit spectral observations of comets Halley, Wilson and Nishikawa-Takamizawa-Tago were obtained with the 3.9-m Anglo-Australian Telescope. The spectrograph slit in each case was centered on the comet nucleus and aligned with the comet tail axis. Spatially resolved surface brightness profiles of each molecular species were extracted from the long-slit spectra for each comet using IRAF routines. Empirical *vectorial* parent scale lengths were determined by matching the column densities predicted using the vectorial model (Festou 1981) to the observed spatial profiles. Photodissociation timescsales for candidate parent molecules of the observed species C_2, C_3, NH_2, CH, CN, and [OI] were calculated, and together with the model fits to the observed profiles, were used to infer possible parent identities.

RESONANCE FLUORESCENCE EXCITATION OF THE CN B-X(0,0) AND (0,1) P AND R BRANCHES IN COMET HALLEY

Terrence W. Rettig (University of Notre Dame and Arizona State University) and Marvin Kleine (Arizona State University) and D. A. Ramsay (Herzberg Institute of Astrophysics, NRCC)

High resolution spectra (0.5 A) of the P and R branches of the CN(0,0) violet system at 3883 A and the CN(0,1) band at 4216 A are presented. The spectra were obtained for comet P/Halley on 15 May 1986, when r = 1.38 A.U. and Δ = 0.43 A.U., using the 3.9-m Anglo-Australian Telescope. The P and R branch rotational lines in the two CN bands show the expected identical structure and internal relative intensities due to the fact that both bands originate from the same upper vibrational level in the B state. Spatial profiles are also presented for the CN(0,0) and CN(0,1) bands covering the sunward and tailward directions. These profiles show a noticeable variation in the log-log slope that cannot be explained or accounted for by stimulated emission, self-absorption, collisions or a contaminant. The rotational structure of the CN bands was modelled using a full fluorescence calculation of the lower three electronic states of the CN radical (A,B,X). The predicted rotational line intensities compare very well with the observations for both bands: CN(0,0) and CN(0,1).

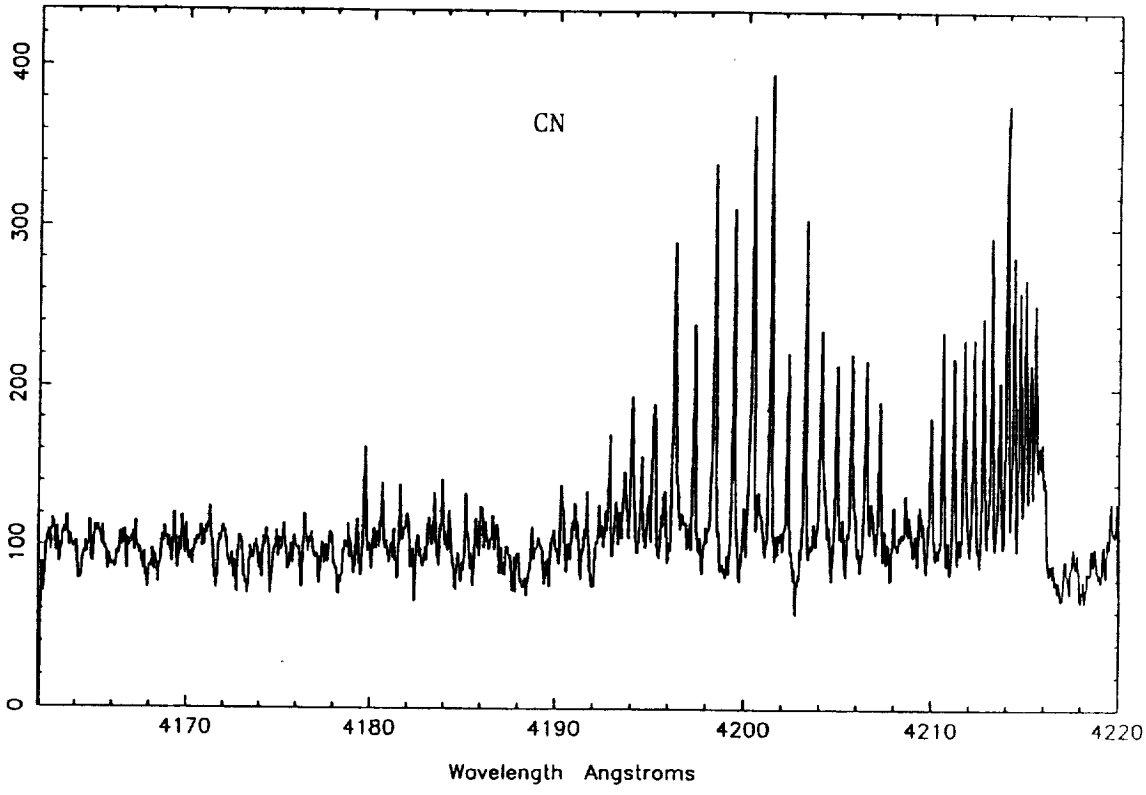

N91-26005

The Contribution of Methanol to the 3.4 μm Feature in Comets.

Dennis C. Reuter and Michael J. Mumma (NASA/GSFC)

With the advent of improved detectors and improved moderate resolution spectrometers (resolving powers ~100 to 1000) several interesting features have been seen in the infrared spectra of comets. In particular, an emission excess at 3.52 μm has been observed in several comets, and has recently been tentatively assigned to the ν_3 band of methanol (CH_3OH) (Hoban et al, 1991). Assuming this assignment is correct, there should be a factor of 3 to 4 more emission centered around 3.35 μm due to the ν_2 and ν_9 bands of this molecule. Using a model we have developed ,we can calculate the relative strengths of the CH_3OH features. This is illustrated in the figure below for a rotational temperature of 50 K assuming Haser outflow. Thus, part of the well known 3.4 μm "organic grain" feature may be attributable to methanol. In this paper we shall use the 3.52 μm emission strengths in a number of comets to retrieve methanol amounts, and then use our model to predict the fraction of the 3.4 μm flux which is contributed by the species. Implications for cometary formation shall be discussed.

References: Hoban et al., Icarus, 1991, *submitted*

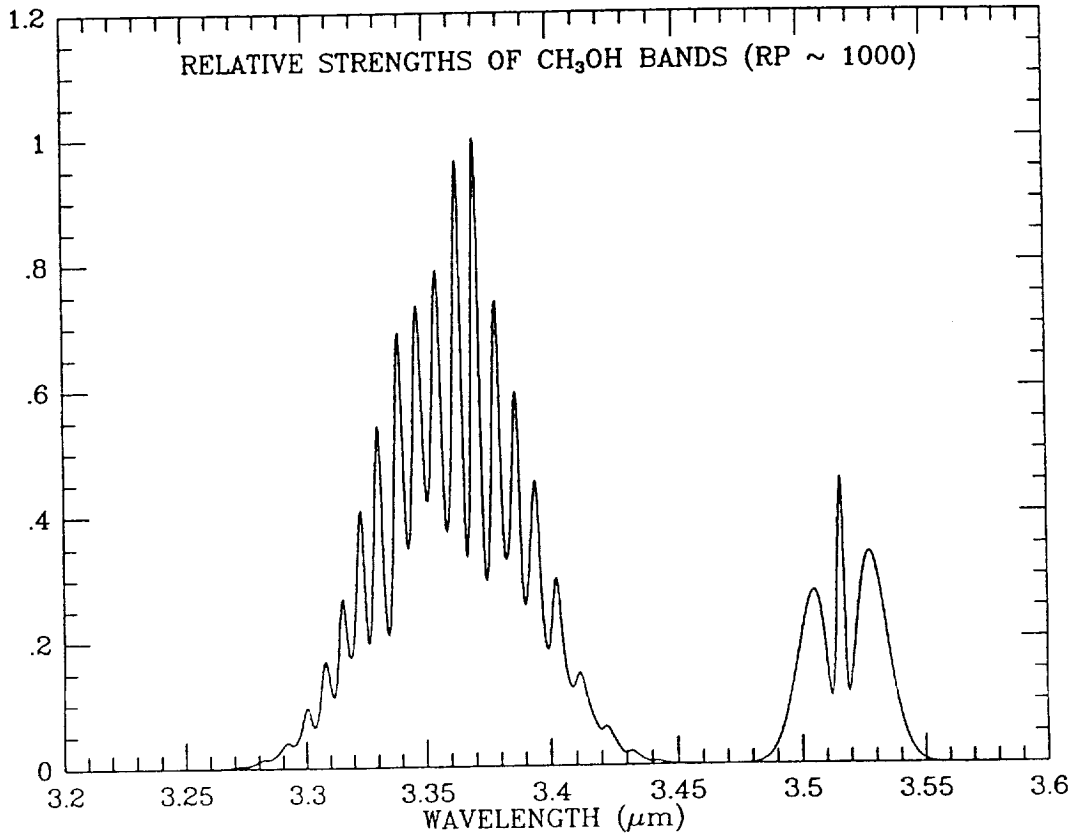

NONGRAVITATIONAL EFFECTS AND THE AGING OF PERIODIC COMETS

H. Rickman[1], C. Froeschlé[2], L. Kamél[1], M.C. Festou[3]

[1] Astronomiska Observatoriet, Box 515, S–75120 Uppsala, Sweden

[2] Observatoire de Nice, B.P. 139, F–06003 Nice Cedex, France

[3] Observatoire Midi-Pyrenées, URA 285 du CNRS, 14 av. E. Belin, F–31000 Toulouse, France

We present a statistical analysis of nongravitational parameters (A_2) looking for evidence relating to the evolution of cometary nuclei. Our sample is restricted to short-period comets but is otherwise essentially complete up to 1990. Several alternative representations of the advance or delay of the time of perihelion passage ($\Delta P'$, $\Delta P''$, ΔP_e) are also introduced on the basis of simple theory. A correlation with the perihelion asymmetry previously shown to exist for $\Delta P'$ (Festou *et al.* 1990) is interpreted as evidence for an increase of the mean free-sublimating fraction of the nuclear surface and/or a decrease of the mean nuclear radius with perihelion distance. Comparison with data on the dynamical histories (Belyaev *et al.* 1986) is done by assigning "dynamical ages" (i.e., number of revolutions since the last major decrease of the perihelion distance) to the various nongravitational parameters. A rapid decrease of the mean value of $|\Delta P''|$ with dynamical age is found and interpreted as evidence for rapid build-up of dust mantles on the nuclei. A picture of the long-term evolution of Jupiter-family comets is thus tentatively suggested, whereby sizeable nuclei become dust-mantled in successive spurts associated with the settling into new orbits with smaller perihelion distances. Their active lifetimes could hence be estimated as the time required to reach the overall minimum of the perihelion distance, i.e., as roughly half the dynamical lifetimes.

Belyaev, N.A., Kresák, L., Pittich, E.M., and Pushkarev, A.N. (1986). *Catalogue of Short-Period Comets*, Astron. Inst. Slovak Acad. Sci., 408 pages.

Festou, M., Rickman, H., and Kamél, L. (1990). Nature **345**, 235.

CARBON PETROLOGY IN COMETS.

Frans J.M. Rietmeijer, Department of Geology, University of New Mexico, Albuquerque, NM 87131, USA.

Chondritic porous [CP] interplanetary dust particles [IDPs] are the most likely candidates for cometary dust that we can study in our laboratories. Using the mineralogical, physical and chemical properties of CP IDPs, including CP particles that show evidence for incipient aqueous alteration[1-3], we can successfully interpret the data for dust in P/comet Halley[4,5]. The CP IDPs have higher bulk carbon contents than carbonaceous chondrites but lower carbon contents than silicate and mixed dust grains in P/comet Halley and the CP IDP intra-particle carbon contents are highly variable[6,7]. Cometary dust contains nebular material and preserved interstellar dust[8]. Thus, CP IDPs contain a record of conditions and processes that occurred in the outer regions of the solar nebula and they provide an opportunity to study the nature, production mechanisms and histories of carbon-rich materials in the evolving solar nebula and Solar System.

Carbon in CP IDPs is mostly reduced carbon but oxidised carbon is present [TABLE 1]. The arrows in the table indicate reaction paths linking carbon-rich materials in cometray dust as inferred from analytical electron microscope [AEM] analyses of CP IDPs. Important questions remain. What fraction of amorphous carbon and hydrocarbons is pristine nebular and interstellar dust and are the amorphous carbons and hydrocarbons forming the matrix of ultrafine-grained granular units (or tar balls) early accretion products[2] or the products of metamorphism of amorphous presolar dust[9]? The non-carbon mineralogy of CP IDP shows evidence for *in situ* aqueous alteration that also affected carbon-rich materials [TABLE 1] which provide data on the physico-chemical environments of neoformed carbon-rich materials. For example, turbostratic pre-graphitic carbons in CP IDPs (i.e., soft, mixed-layered carbons with C/[C+H+O+N] ratios similar to the groups D and E CHON paricles in P/comet Halley) formed via catalytically supported hydrous pyrolysis[10]. The soft carbons could be precursors of poorly graphitised carbons [PGCs] but the timing of PGC formation is uncertain [TABLE 1].

CONCLUSION. The AEM is an excellent tool to study the diversity of the carbon petrology in cometary dust that amply supports mineralogically active short-period comet nuclei. Some CP IDP carbon properties, inluding sulfur-bearing CHON particles, are comparable with P/comet Halley dust but the processes that produce the diverse carbon petrology are ill-understood.

REFERENCES. 1 Rietmeijer & Mackinnon, Rev. Geophys. 25, 1527, 1987; 2 Bradley et al, in MESS (Kerridge & Matthews, eds), 861, 1988; 3 Rietmeijer, EPSL 102, 148, 1991; 4 Jessberger et al, Nature 332, 691, 1988; 5 Rietmeijer et al, LPS 20, 904, 1989; 6 Schramm et al, Meteoritics 24, 99, 1989; 7 Blanford et al, Meteoritics 23, 113, 1988; 8 Brownlee, NASA Conf. Publ. 3061, 21, 1990; 9 Rietmeijer, Proc. 19LPSC, 513, 1989; 10 Rietmeijer, LPS 21, 1013, 1990.

TABLE 1: **CARBON MINERALS IN COMETARY DUST: A LITERATURE REVIEW**

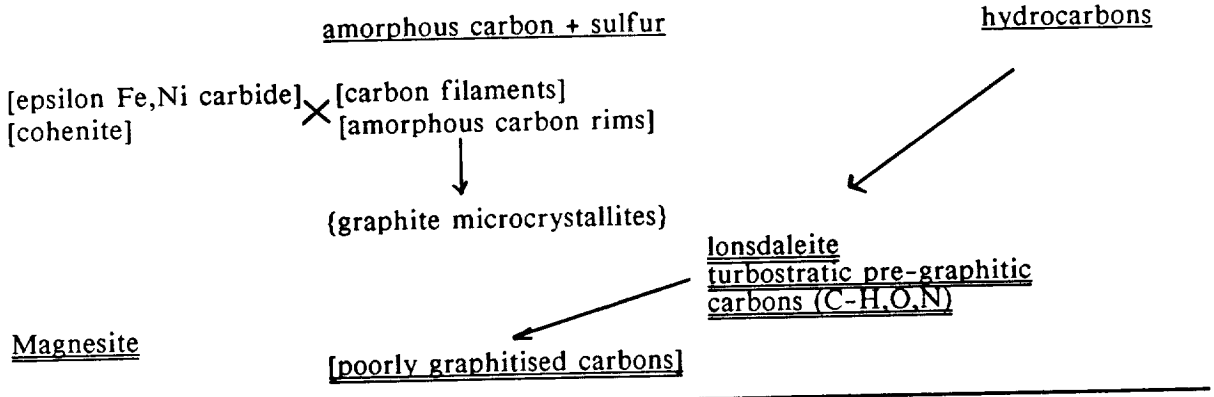

Carbon-rich materials are indigenous (underlined) and form during parent body alteration (double underlined). Heterogeneous catalysis, e.g. Fischer-Tropsch reactions, carbon production in the nebula and by pyrometamorphism on atmospheric entry (brackets). Rare graphite results from solid-state interface controlled nucleation (braces).

WAKE IN FAINT TELEVISION METEORS; **M.C. Robertson**[†] **and R.L. Hawkes**, ***Physics Department, Mount Allison University, Sackville, New Brunswick, Canada E0A 3C0***

The quantitative dustball meteor model of Hawkes & Jones (**MNRAS**, 1975, **173**, 339-356) was used as the basis for numerical lag computations involving grains of different mass (range 10^{-8} to 10^{-15} kg), velocity (15, 41, 60 and 66 km s^{-1}), zenith angle (cos z values of 0.4, 0.7 and 1.0), bulk density (700 and 3500 kg m^{-3}), and height of ejection (range 75 to 160 km). The assumption was made that wake involving faint meteors would be mainly due to differential aerodynamic lag of detached grains. The numerical work suggested that, for the parameters used, the lag of a detached grain is seldom more than a few km during times of significant luminosity. True wake in faint television meteors is masked by the presence of apparent wake due to the combined effects of detector persistence and image blooming. To partially circumvent this problem, we modified a dual MCP intensified CID video detector by addition of a rotating shutter in order to reduce the effective exposure times to about 2.0 ms (with one exposure per 1/60 s video field). Preliminary observations have been made, with the unexpected result that only 2 of the 29 analyzed meteors displayed statistically significant lag. It is unclear at this time whether this is due to a failure in the two component dustball model, a remarkable uniformity in grain sizes, or simply the lack of spatial resolution or intensity discrimination of the dual MCP system.

[†]current address Physics Department, Queen's University, Kingston, Ontario, Canada K7L 3N6

CHEMICAL AND PHYSICAL EFFECTS IN THE BULK OF COMETARY ANALOGS

K. Roessler, J. Bénit, G. Eich, M. Sauer

Institut für Chemie 1 (Nuklearchemie), Forschungszentrum Jülich, D-5170 Jülich, FRG

Cometary analogs of comet simulation experiments KOSI consist in essential of water ice, CO_2 ice, mineral dust and "organic components" such as CH_3OH ice, charcoal or kerogen. It could be shown by layerwise chemical analysis of the insolated samples by means of gas chromatography that the volatiles (CO_2, CH_3OH) diffused partly into the interior of the LN_2 cooled water ice - mineral dust matrices. They recondensed in colder layers, the more volatile the deeper, such as in a kind of "thermochromatography" leading to the formation of crystallites and to the occurrence of hard but permeable layers in some depth beneath the surface. The formation and strength of the crusts depends on the ratio of solid components and condensed gases. In particular CO_2 does not cocrystallize with H_2O ice, where it seems to bind together mineral grains. The ratios of the naturally occuring isotopes H/D, $^{12}C/^{13}C$, and $^{16}O/^{18}O$ were measured by mass spectrometry after melting and degassing of the samples in gas phase (CO_2) and remaining liquid (H_2O). A strong enrichment of the heavier isotopes was observed in the crustal regions. The results of visual inspection, test of material strength by drilling, and concentration profiles of chemical components in particular of experiments KOSI-6 and 7 are compared with the isotopic distribution. The analysis of the bulk of cometary analogs shows a high degree of differentiation of a formerly homogeneous body with its thermal history.

Sulfur-bearing species in comets

E. E. Roettger, S. A. Budzien, and P. D. Feldman (Johns Hopkins University)

The recent detection in cometary comae of H_2S (Colom *et al.* 1990) and upper limits on OCS, H_2CS (Bockelée-Morvan *et al.* 1990), SO, SO_2 (Kim and A'Hearn 1991), and S_2 (Feldman and Budzien 1989) permit a re-evaluation of the source of the atomic sulfur commonly detected in *IUE* spectra of comets. Photodissociation of CS_2, as inferred from the observed emission of CS, generally cannot provide all the observed atomic sulfur, as first pointed out by Azoulay and Festou (1985). The reported abundance of H_2S is found to be adequate to make up the difference in comet Austin ($1989c_1$), for which near-simultaneous ultraviolet and radio data are available. The relative S_2/H_2O production rate is found to be at least an order of magnitude lower in comet Austin ($1989c_1$) than was observed in comet IRAS-Araki-Alcock (1983 VII), the only comet to date in which S_2 was detected. Upper limits on SO and SO_2 are also derived for comet Austin. S_2, SO, and SO_2 do not contribute much of the atomic sulfur observed in comet Austin. Possible contributions from OCS and H_2CS are also evaluated.

References:

Azoulay, G., and Festou, M. C. 1986, In *Asteroids, Comets, Meteors II,* ed. C.-I. Lagerkvist, B. A. Lindblad, H. Lundstedt, and H. Rickman (Uppsala University, Uppsala), p. 273.

Bockelée-Morvan, D., Crovisier, J., Colom, P., Despois, D., and Paubert, G., 1991, in *Formation of Stars and Planets, and the Evolution of the Solar System* (ESA SP-315), p. 143.

Colom, P., Despois, D., Bockelée-Morvan, D., Crovisier, J., and Paubert, G. 1990, in *Workshop on Observations of Recent Comets,* ed. W. F. Huebner, P. A. Wehinger, J. Rahe, and I. Konno (Southwest Research Institute, San Antonio), p. 80.

Feldman, P., and Budzien, S. 1989, *Bull. AAS,* **21**, 937.

Kim, S., and A'Hearn, M. 1991, *Icarus,* (in press).

EVOLUTION OF NEAR UV HALLEY'S SPECTRUM IN THE INNER COMA

P.Rousselot, J.Clairemidi, F.Vernotte, G.Moreels, Observatoire de Besançon, BP 1615, 25010 Besançon Cedex, France

The near UV spectra obtained in the 280-330 nm with the three-channel spectrometer of Vega 2 show an intense solar-scattered continuum at distances smaller than 7 000 km. For instance, at a distance of 540 km, the dust-scattered continuum is comparable to the OH intensity at 309 nm. The solar type contribution to the spectra is substracted from the spectrometric data to obtain the component due to molecular emissions. In the inner coma, these spectra exhibit a progressive evolution with decreasing cometocentric distance.

Two spectra obtained when the projected distance to the optical axis was 3 631 and 538 km are compared. Their intensities are normalized to obtain a good superposition of the OH band profile. The longer wavelength band wing shows an emission excess between 315 and 325 nm. This additional intensity is interpreted as being probably due to prompt OH emission that results of water vapor photolysis at $\lambda < 136$nm following the process : $H_2O + h\nu \rightarrow H + OH\ (A_2\Sigma^+)$. The branching ratio is generally assumed equal to 7.5%, at the wavelength of Lyman α, where the major part of the OH $(A_2\Sigma^+)$ radicals are produced. New laboratory results are used to compute the prompt emission and compare the resulting synthetic spectrum with the Vega data.

At shorter wavelengths, the spectrum shows the presence of the OH (1,0) band. The CO_2^+ band at 289 nm generally is not present in the spectra. Two new features appear at 285 nm and as a broad band between 293 and 303 nm. The region around 290 nm is an intensity minimum. In an attempt to identify the S_2 fluorescence band system, the spectrum of comet IRAS obtained with IUE is plotted under the Vega spectra. It cannot be concluded that S_2 is present in these spectra because the minimum at 290 nm contradicts the presence of the intense $(B^3\Sigma_u \rightarrow X^3\Sigma_g)$ (7,0) and (9,1) bands of S_2. The spatial distribution of the 293-303 nm broad-band emission is displayed as a monochromatic chart of the field of view scanned by the spectrometer. It appears to be a mother-molecule distribution with a scalelength of 10 000 km. Many molecules show fluorescence bands in this spectral region. Among them are polycyclic hydrocarbons with two or three aromatic cycles or formaldehyde and its CHO photolysis product.

Mosaic CCD Method: A New Method for Observation of Dynamics of Cometary Magnetospheres

T. Saito[1], H. Takeuchi[1], Y. Kozuka[1], S. Okamura[2], I. Konno[3], M. Hamabe[2], T. Aoki[2], S. Minami[4], and S. Isobe[5]
1. Tohoku Univ., Japan 2. Kiso Obs., Univ. of Tokyo, Japan
3. SwRI, Texas, USA 4. Osaka City Univ., Japan
5. NAO, Japan

The plasma tail of comet Austin was observed at the Kiso Observatory of The University of Tokyo, with a new technique that is temporarily called "the mosaic CCD method". The comet was taken with a CCD (charge-coupled device) on the 105cmϕ Schmidt telescope. Two sets of seven photographs were taken each with 40-second exposure during about 50 minutes from 18h05m to 18h56mUT on April 29, 1990. The cometary magnetosphere about 1.6×10^6 km long was covered by each set of photographs. The figure shows the photographs. Six microstructures containing arcade structures were selected to examine the plasma velocity near the root of the plasma tail. It was found that the plasma had some finite velocity V_N at the apparent nucleus position and that thereafter it was accelerated as expected from the Minami and White theory. Dynamical characteristics of the arcade structure are well explained by the previous three-dimensional model of the cometary magnetosphere. A new concept is introduced on the plasma flow along the dayside plasmasphere surrounding the cometary nucleus; the plasma on the solar wind magnetic field must have some finite azimuthal speed at the stagnation point of the solar wind. The plasma is accelerated and carried along the plasmapause with the velocity reaching V_N when it crosses the earth-comet nucleus line.

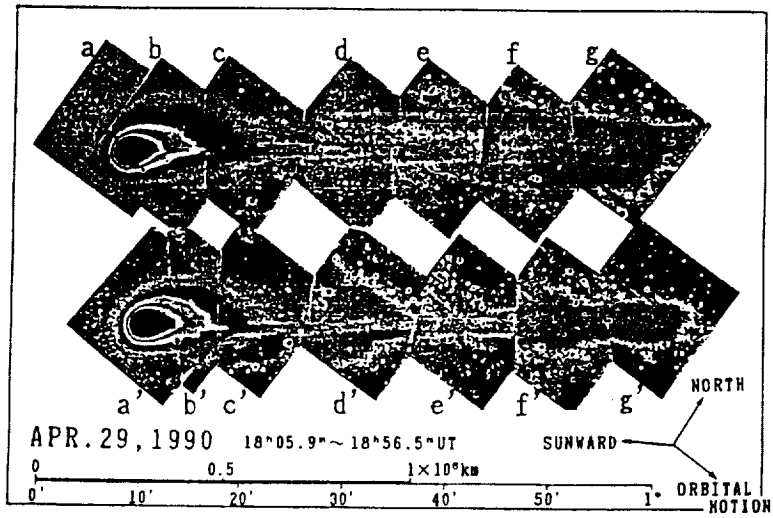

Determination of Time Dependent Production Rates in Comets

N. H. Samarasinha and M. F. A'Hearn (UMD)

Despite the variability of gas and dust production by comets, steady state models are normally used to analyze observations. Steady state models whether Haser, vectorial or even Monte Carlo models, are not capable of "recovering" the production rates as a function of time. Sometimes application of steady state models can give completely inappropriate results.

We have developed a model to "recover" the gas and dust production rates from a set of photometric observations taken over time. We have applied this model to determine the production rates for Comet Levy on a function of time. IUE Fine Error Sensor data as well as spectroscopic data were utilized for this purpose. The tentative conclusions indicate possible chemical inhomogeneities in the nucleus.

The free parameters involved in the model are production rates, life times and velocities of the species involved. If we know all except one of the parameters reasonably well, the model is capable of well determining the other parameter. A dense time series of observations are important for proper determination of production rates.

LIGHT SCATTERING BY TETRAHEDRAL PARTICLES WITH ROUGH SURFACES; T. Satoh, and K. Kawabata, Science University of Tokyo. H. Hasegawa, ASTEC Inc. M. Iwase, OLYMPUS Opt., Co.

Studying the light scattering processes by non-spherical (irregularly shaped) particles is very important for a wide range of astrophysical researches; it should be applicable to the photometrical and polarimetrical observations of asteroids, cometary dusts, interstellar dusts, and cloud particles of outer planets. However, practical methods to compute scattering properties of arbitrary shaped and oriented particles are not yet available today. We have tried to compute the scattering characteristics of tetrahedral particles which have rough surface.

The roughness of the tetrahedral surface is approximated by arranging small spheres on it. To simplify model computations, we have adopted following assumptions; (1) the size of sphere is comparable with the wavelength of light, and scattering by the sphere is according to Mie theory. (2) tetrahedron is large enough compared with the wavelength, so that the scattering by tetrahedron is represented by simple geometrical reflection and refraction law. (3) spheres and tetrahedron are composed of the same material, therefore refractive indices of them are identical. (4) scattering processes in the spheres and in the tetrahedron are separately computed and then synthesized. A FORTRAN program was generated and the computations were carried out on an EWS SPARC station 330.

Computational results and applications to several astrophysical observations will be reported.

REFERENCES

Bohren, C.F., and Huffman, D.R. 1983: *Absorption and Scattering of Light by Small Particles,* Wiley-Interscience, New York.

Draine, B.T. 1988: *Astrophys. J.* **333,** 848-872.

Hanner, M. 1987: *NASA CP-3004,* 22-49.

Martonchik, J.V., Orton, G.S., and Appleby, J.F. 1984: *Appl. Opt.* **23,** 541-547.

Van de Hulst, H.C. 1957 : *Light scattering by small particles,* Dover, New York.

West, R.A., Orton, G.S., Draine, B.T., and Hubbell, E.A. 1989: *Icarus* **80,** 220-223.

The Anomalous Molecular Abundances of Comet P/Wolf-Harrington

David G. Schleicher, Schelte J. Bus, and David J. Osip

Lowell Observatory

As part of an on–going program of comet photometry at Lowell Observatory, Comet P/Wolf–Harrington was observed on September 29, 1984. These data indicated that Wolf–Harrington had atypical abundance ratios, similar in sense yet more extreme than those previously reported for Comet P/Giacobini–Zinner (Schleicher, Millis, and Birch 1987). Narrowband filter photometry of Wolf-Harrington obtained on 4 additional nights this winter confirms that both the C_2 and C_3 abundances are anomalously low when compared either to OH or to CN. Moreover, the depletion of these pure carbon species – less than 1/20th normal – is the most extreme case observed in the current photometry database of 80 comets (cf. Millis *etal.* 1989). A spectrum obtained in February of this year using the MMT further verifies this conclusion. After subtraction of the continuum, only CN is clearly evident in the spectrum (shown below). In addition to final values for the C_2 and C_3 abundances, we will also present values for the relative abundances of NH and NH_2. This research is supported by a grant from the NASA Planetary Astronomy Program.

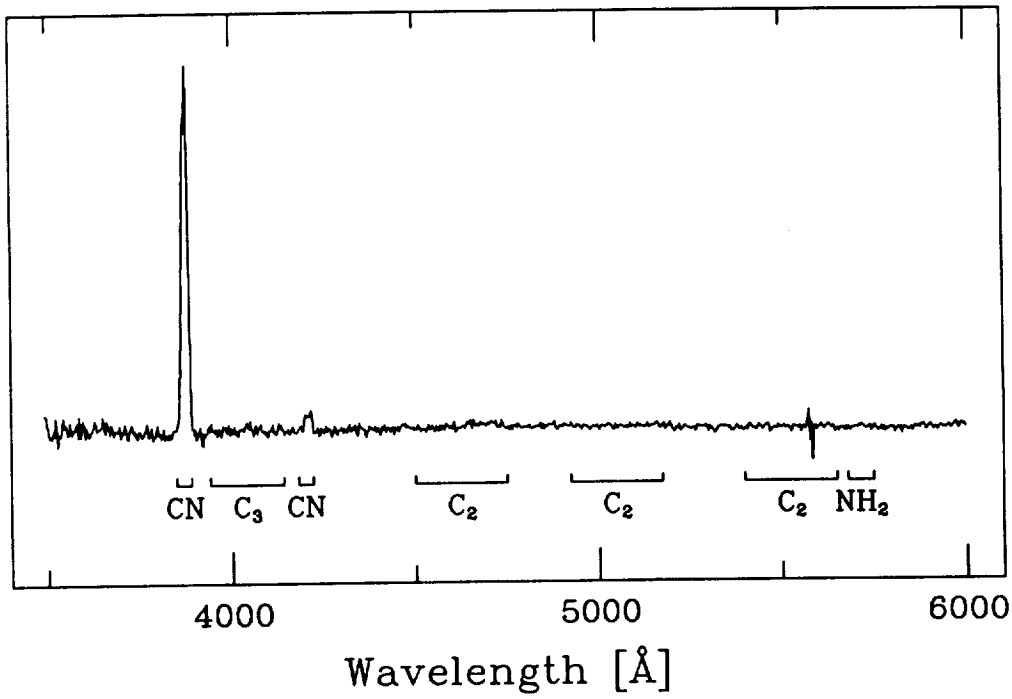

Comet Levy (1990c): Groundbased Photometric Results

David G. Schleicher, Robert L. Millis, David J. Osip

Lowell Observatory

and Peter V. Birch

Perth Observatory

Narrowband filter photometry of Comet Levy (1990c) has thus far been obtained on 27 nights at Lowell Observatory and 21 nights at Perth Observatory in the interval from 3 June 1990 to 17 March 1991. The emission bands of OH, NH, CN, C_3, and C_2 were isolated, along with continuum points at 3650 Å and 4845 Å. Relative abundances among the species were typical of most comets previously observed. All species showed pronounced asymmetry about perihelion, with production rates for most species being about twice as large before perihelion as after over the heliocentric distance range of 1.0–2.4 AU. The OH production rate's asymmetry was nearly double that observed for the other species, with maximum production occuring more than a month before other species. Periodic variations having a single–peaked lightcurve period of 18.9 hrs or a double–peaked lightcurve period of 37.8 hrs (see below) were observed in both the gas and dust during late–August 1990. Possible reasons for this behavior and their implications will be presented. This research is supported by a grant from the NASA Planetary Astronomy Program.

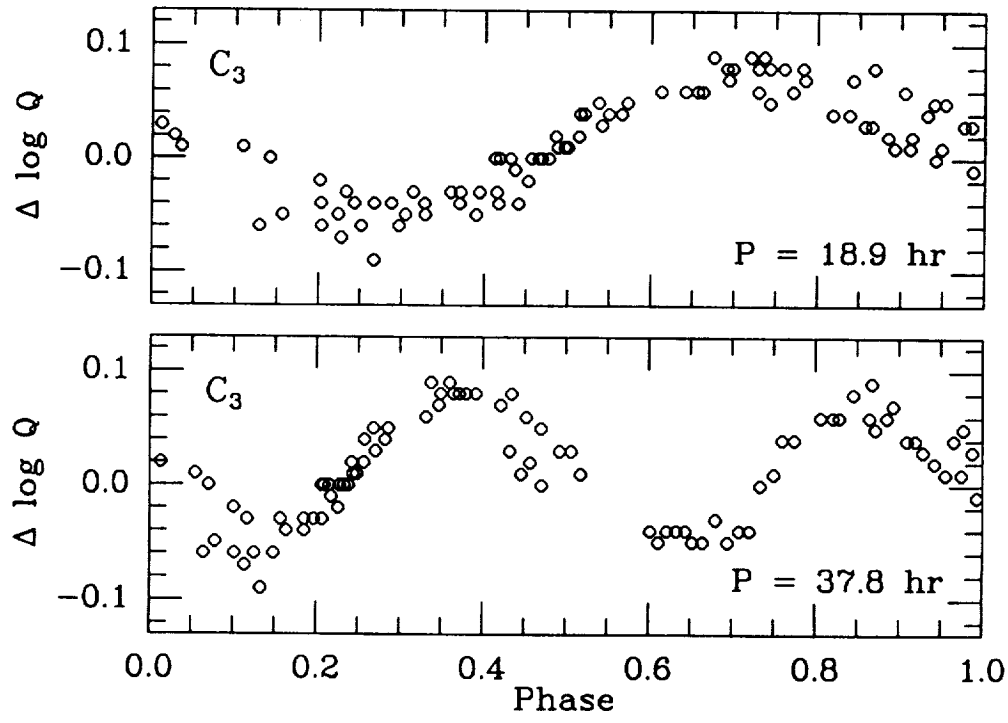

SUB-MILLIMETER MOLECULAR LINE OBSERVATIONS OF COMET LEVY

F. Peter Schloerb and Ge Weiguo

FCRAO, University of Massachusetts
Amherst, MA 01003

We present molecular line observations of HCN, H_2CO, and CH_3OH in Comet Levy. The comet was observed on 4 nights from 29 August - 1 September 1990 at the Caltech Submillimeter Observatory on Mauna Kea. Detections were made of the HCN J=3-2 transition at 265.886 GHz, the HCN J=4-3 transition at 354.505 GHz, the H_2CO 5_{15}-4_{14} transition at 351.769 GHz, and several transitions of the CH_3OH 5-4 band at 241.8 GHz. Of these transitions, only the HCN 3-2 line has been previously observed in a comet.

The HCN J=3-2 observations were carried out on 29 August, and a high (0.1 km s^{-1}) resolution spectrum is shown in the figure below. The HCN production rate is approximately 2 X 10^{26} s^{-1}, and given the overall gas production rates reported for Comet Levy, the abundance of HCN is consistent with that seen in other comets. The spectral line shape shown in the figure, is reasonably well fit by a model in which the HCN gas originates at the nucleus and flows radially outward at a velocity of 0.8 km s^{-1}, although some residual features remain. Further constraints on the distribution of HCN in the coma were obtained by mapping the HCN emission from the comet. The HCN map shows a large asymmetry in its emission with the strongest emission arising from the sunward side of the coma. Such an asymmetry is naturally consistent with the asymmetric outgassing from comet nucleii, observed indirectly from doppler shifts of spectral lines and directly from images of the coma. An analysis is underway to fit a model to the spectral line shape and the map in order to recover the 3D distribution of HCN in the coma.

The HCN J=4-3 and H_2CO 5_{15}-4_{14} transitions were observed simultaneously on the nights of 30 and 31 August. Once again, the lines were detected and small maps were made of the distribution of these molecules around the source. The strength of the HCN 4-3 line is consistent with the production rate derived for the HCN 3-2 line for a rotational temperature of approximately 30K. Some caution must be observed in this comparison, however, since both the HCN and H_2CO lines were observed to vary in intensity between the two nights that they were observed. The H_2CO line was detected 30 arcsec off of the nucleus position. Since H_2CO molecules that arise from the nucleus are expected to be photodestroyed by the time that they reach this position, we conclude that the observed extended emission must be due to an extended source for H_2CO in the coma. Therefore, we are presently fitting a vectorial model to the H_2CO data to determine its production rate and verify its origin in the coma.

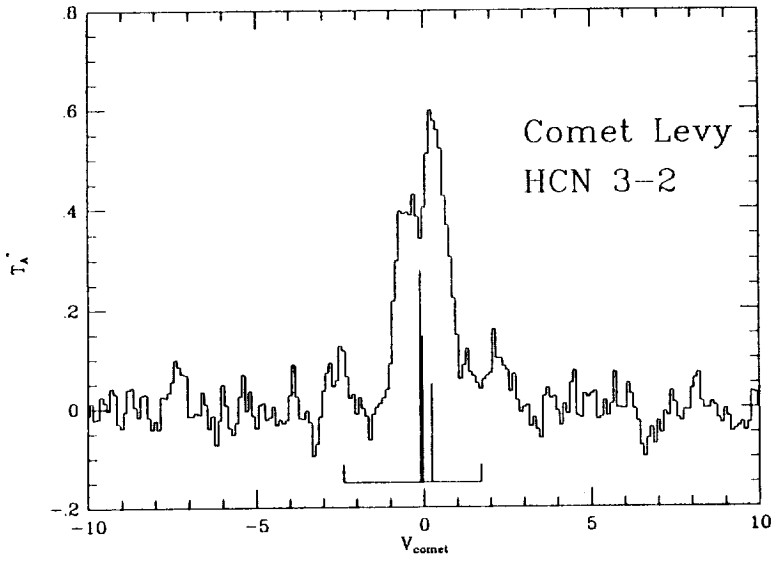

SPATIAL AND TEMPORAL VARIATIONS IN THE COLUMN DENSITY DISTRIBUTION OF COMET HALLEY'S CN COMA; R. Schulz, W. Schlosser, W. Meisser, P. Koczet, Astronomisches Institut, Ruhr-Universität Bochum, F.R.G., W.E. Celnik, Wilhelm-Foerster-Sternwarte, Berlin, F.R.G.

Mean radial column density profiles of comet Halley's CN coma have been derived from photographic observations obtained at ESO, La Silla (Chile) from 14 March to 16 March, 1986 and 1 April to 10 April, 1986. The CN photographs were digitized and sensitometric spots were used for relative intensity calibrations. The transformation into column densities was conducted by means of photoelectric measurements carried out simultaneously with the Bochum 61 cm Cassegrain telescope at ESO, La Silla. The resulting images correspond to two-dimensional column density profiles of the CN coma. From every image one mean radial column density profile was constructed by azimuthal averaging around the nucleus. Two examples for resulting profiles are shown in Fig. 1. The shapes of the profiles show continuously new formed 'bumps', which were shifted to outer coma regions as a function of time. It will be demonstrated, that these 'bumps' correspond to the CN shells found in the coma of Comet Halley (Schulz & Schlosser, 1989). The temporal changes of column density in the near-nucleus region will be compared to brightness variations in the inner coma of Comet Halley found by photoelectric measurements (Millis & Schleicher, 1986). The question of outbursts as a possible explanation for the 'bumps' in the radial column density profiles will be discussed with regard to the results of the analysis of intensity profiles from 4 December, 1985 (Festou et al., 1990).

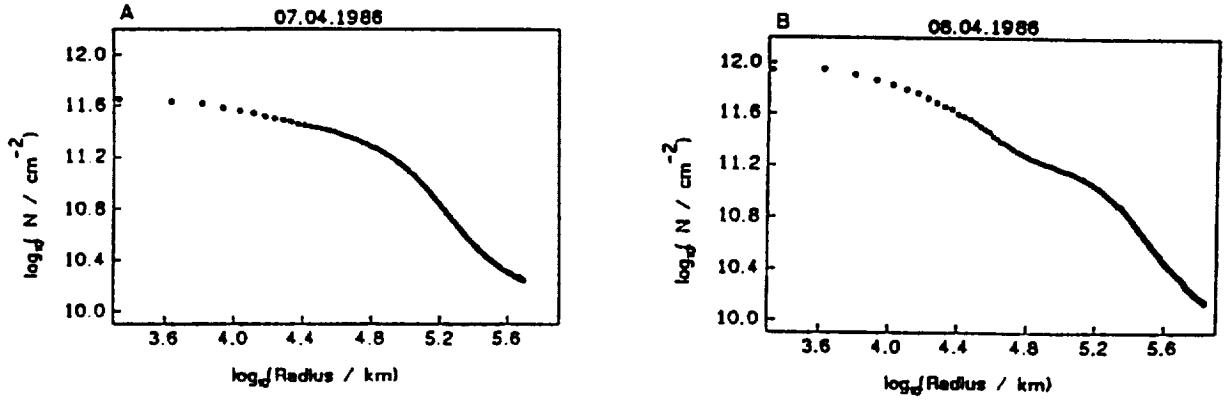

Fig. 1 Mean radial column density profiles from 7 April 1986, 2.31 UT (A) and 8 April 1986, 2.16 UT (B)

References

Millis, R.L., Schleicher, D.G., 1986, Nature **324**, 646
Schulz, R., Schlosser, W., 1989, Astron. Astrophys. **214**, 375
Festou, M.C., Tozzi, G.P., Smaldone, L.A., Felenbok, P., Faciani, R., Zucconi, J.-M., Astron. Astrophys. **227**, 609

ROSETTA - COMET NUCLEUS SAMPLE RETURN; G. Schwehm, ESA Rosetta Study Scientist for the ESA/NASA Rosetta Science Definition Team. Space Science Department of ESA, Noordwijk, The Netherlands

Research on comet-nucleus samples will carry the exploration of the solar system to its outer fringes. Rosetta - the Comet Nucleus Sample Return Mission - will begin to provide scientific study of the pre-solar environment and possibly sample materials from interstellar and galactic regimes. This study of the most primitive material in the solar system will provide an experimental approach to the determination of the chemical and physical processes that marked the beginning of that system 4.6 billion years ago.

The mission will address some of the most profound questions Space Science can ask, as it will provide information going back to our beginnings, the very roots from which everything has sprung, the planets, the sun, and life itself. Rosetta by its very nature is a generic new type of mission: its prime objective is to return a comet nucleus sample to Earth in a state as undisturbed as technically feasible so that it can be studied in Earth-based laboratories with the most sophisticated analytical techniques. However, by fulfilling its prime objective it will provide the opportunity for unique cometary science. The highest priority for in situ science will be given to those measurements that will make it possible to select and document the sampling site, to monitor the cometary environment for spacecraft hazards and contamination, and to support the near-nuclear navigation during the final approach and landing phase.

THE GIOTTO EXTENDED MISSION; G. Schwehm, Space Science Department of ESA, Noordwijk, The Netherlands
T. Morley, Orbit and Attitude Division, European Space Operations Centre, Darmstadt, Germany

The navigation of the ESA spacecraft Giotto to its encounter with comet P/Halley on 14 March 1986 required just 10% of the fuel available. Although the spacecraft was damaged by dust impacts during its close flyby of the nucleus of P/Halley it was retargeted to return close to Earth in order to maintain the option of extending the mission to encounter another comet, P/Grigg-Skjellerup on 10 July 1992.

On 2 April 1986 the spacecraft was put into hibernation configuration, orbiting the Sun in the ecliptic with an orbital period of 10 months. On 19 February 1990 it was reactivated and the spacecraft subsystems and payload were checked out to determine its health status.

On 2 July 1990 Giotto performed successfully the first-ever Earth gravity assist manoeuvre of a spacecraft approaching the Earth from deep space and was retargeted for comet P/Grigg-Skjellerup.

Despite the loss of four of its eleven instruments during the Halley encounter, it was concluded that the spacecraft is ready to provide valuable data during a potential encounter with a second comet.

Science investigations which can be performed with the remaining payload complement include:

- characterisation of the changing features of the solar-wind flow and observation of cometary pick-up ions and anomalous acceleration;
- determination of electron densities;
- observation of upstream waves, determination of the locations of the various boundaries (bow shock, ionopause, cometopause, etc.);
- observation of the magnetic pile-up region and cavity;
- determination of the dust spatial density and size distribution and the optical properties of the dust grains;
- study of discrete gaseous emissions;
- determination of combined dust and gas densities.

On 10th July 1992, ESA's GIOTTO spacecraft will encounter its second comet, P/Grigg-Skjellerup, at a relative speed of 14 km/s with closest approach occurring between 15:15 and 15:30 UT. Since the Halley Multi-colour Camera (HMC) is no longer functioning, it is likely that the spacecraft will be aimed directly at the nucleus. The final targeting does not need to be made until about two days before encounter, but whatever the choice, there is a requirement for the highest possible accuracy.

Giotto, in its encounter with P/Halley, benefitted from the two VEGA spacecraft acting as pathfinders to improve the knowledge of the orbit of Comet P/Halley. Such an opportunity does not exist for the Giotto Extended Mission, and the improvement of the cometary ephemeris will depend solely on the quantity and quality of ground-based astrometric measurements.

Observing conditions during the 1992 apparition of P/Grigg-Skjellerup are not very favourable. In particular, obtaining astrometric data during a few weeks immediately before encounter, which analysis has shown is the most useful period for improving the comet's orbit, will present a challenging task.

AUTOMATED DETECTION OF ASTEROIDS IN REAL-TIME WITH THE SPACEWATCH TELESCOPE; J. V. Scotti, D. L. Rabinowitz, and T. Gehrels, Lunar and Planetary Laboratory, University of Arizona, Tucson, Arizona, 85721

The Spacewatch 0.91-meter Newtonian telescope of the Steward Observatory on Kitt Peak is being used during the 18 nights centered on new moon to survey for Near-Earth asteroids using a TK2048 CCD in scanning mode. We hope to identify suitable low ΔV candidates amongst the Near-Earth asteroid population as possible exploration targets, as well as to study the physical properties of the objects in Near-Earth space. Between 1990 September and 1991 March, 12 Earth Approaching asteroids including 1 Aten, 9 Apollo, and 2 Amor type asteroids have been detected by automated software and discriminated by their angular rates from the rest of the detected asteroids in near-real-time by the observer. The average of about two Earth Approaching asteroids per month is comparable to the total number found by all other observatories combined. One other Apollo type asteroid was detected by the observer as a long trailed image. The positions of this last object were measured and the object was tracked by the observer in real-time. This object was determined to be a 6-12 meter object which passed within 170 000 kilometers of Earth. Of the 12 automatically detected Earth Approaching asteroids, 9 have been found at distances in excess of 0.6 AU from Earth. Approximate elements, the discovery brightness, the distance from Earth at discovery, the derived absolute magnitude, the estimated diameter, and the type for each discovery are shown in Table 1. Additionally, an average of more than 2000 other asteroids are detected each month. Positions, angular rates, and brightnesses are determined for each of these asteroids in real-time.

Table 1 – Spacewatch Near Earth Asteroid Discoveries

1989 October – 1991 March

Design.	a	e	i	V	Δ	H	D	class
				(1.0km – 10.0km)				
1990 TG1	2.48	.692	9.1	19.1	1.915	15.0	4.6	APO
1991 AM	1.63	.688	29.7	18.6	0.907	16.5	2.3	APO
1991 CB1	1.69	.622	15.8	21.1	1.157	18.0	1.3	APO
1991 EE	2.25	.624	9.8	19.4	0.904	17.5	1.5	APO
1991 FA	2.02	.466	3.2	18.7	0.830	17.5	1.5	AMO
1991 FE	2.31	.536	4.5	17.9	1.647	14.5	5.8	APO
				(0.1km – 1.0km)				
1989 UP	1.86	.473	3.9	15.8	0.061	20.7	0.3	APO
1990 SS	1.70	.475	19.4	18.9	0.623	19.0	0.9	APO
1990 UO	1.23	.758	29.3	20.5	0.604	20.5	0.4	APO
1990 UP	1.33	.169	28.1	18.1	0.210	20.5	0.4	AMO
1990 VA	0.99	.279	14.2	17.9	0.230	19.5	0.6	ATE
1991 BN	1.44	.398	3.4	20.9	0.672	20.0	0.5	APO
				(< 0.1km)				
1990 UN	1.71	.528	3.7	19.9	0.119	23.5	0.09	APO
1991 BA	2.24	.682	2.0	17.5	0.005	28.5	0.009	APO

NUCLEUS MODEL FOR PERIODIC COMET TEMPEL 2. *Zdenek Sekanina*, Jet Propulsion Laboratory, California Institute of Technology

Observational data obtained primarily during 1988 are analyzed and synthesized to develop a comprehensive physical model for the nucleus of Periodic Comet Tempel 2, one of the best studied members of Jupiter's family of short-period comets. It is confirmed that a previous investigation (Sekanina 1987, ESA SP–278, pp. 323–336) provided reliable information on the comet's spin-axis orientation, which implies an obliquity of 54° of the orbit plane to the equatorial plane and which appears to have varied little—if at all—with time. This conclusion is critical for fitting a triaxial ellipsoid to approximate the figure of the nucleus. Its dimensions are found to be $16.4 \times 9.8 \times 7.0$ km, if A'Hearn *et al.*'s (1989, Astrophys. J. **347**, pp. 1155–1166) visual geometric albedo of 0.022 is accepted. While the nucleus of P/Tempel 2 is similar to that of P/Halley in volume and surface area, it is distinctly more flattened in the polar direction. Forced precession, caused by torques from outgassing, is shown to be negligible, but there may be an effect on the nucleus spin rate. If this effect was insignificant in the period of February–June 1988, the remarkable invariability of the comet's sidereal rotation period, derived to be $8^h55^m55^s.2$ with a formal uncertainty of only $\pm 0^s.2$, would indicate general correctness of the employed spin-vector positional determination. Temporal variations in the production of water cannot be fitted on the assumption of outgassing from a *flat* region (or regions). An appreciable depth is implied, leading to the conclusion that the source is most probably a vent-like depression (or depressions). Assuming that outgassing is possible only from the depression's floor when it is sunlit and that there is no outgassing from the walls, the best match is found for an effective diameter-to-depth ratio of 1.6, a total floor area of 14 km^2, and a slope angle of the walls of 81°. The total loss rate of water is estimated at 10^{13} g per revolution about the Sun. Deconvolution of the observed optical and thermal infrared diurnal light curves consistently reveals the existence of three isolated vents on the nucleus within about 30° of the northern rotation pole. Modeling of a collimated flow of dust ejecta from a vent indicates the presence of disintegrating particles in the coma, whose typical lifetimes are 25–30 hr. The differential size distribution for large grains varies inversely as the cube of particle size, with a poorly defined cutoff radius of 1 mm. There is also some evidence for a population of very short-lived, perhaps water ice, grains. The dust production rate on 22–30 June is found to have amounted to 10^5 g/s, implying a dust-to-water production rate ratio of 0.7–1.0 by mass. The proposed model indicates that the calculated nucleus figure corresponds to one of the hydrostatic equilibrium configurations known as Jacobi ellipsoids. The derived sidereal rotation period suggests an "equilibrium" nucleus density of 0.54 g/cm^3 and implies that the comet's nucleus cannot be subjected to significant hydrostatic forces. To facilitate future testing of the nucleus model, predictions are provided for expected temporal variations (i) in the axial orientation of the fan-shaped coma, (ii) in the parameters of the optical and thermal infrared diurnal light curves of the nucleus, and (iii) in the water production rate. It is noted that the comet's return of 2005 is so extremely unfavorable to earth-based optical monitoring for several months on either side of perihelion that the choice of P/Tempel 2 as the target for the Comet Rendezvous Asteroid Flyby mission at this return would restrict active-phase supporting observations only to the infrared and radio wavelengths. The complete description of the present investigation is scheduled to appear in the July 1991 issue of *The Astronomical Journal*.

N91-26007

RANDOMIZATION OF PARTICLE MOTIONS AND THE OBSERVED MORPHOLOGY OF COMETARY HEADS. *Zdenek Sekanina*, Jet Propulsion Laboratory, California Institute of Technology

A great diversity is known to exist in the coma morphology of comets. In particular, some comets show much structural detail in their heads (such as jets, halos, fans, plumes, streamers), while others have completely structureless comas. Obvious questions arise as to why is this so and what does the presence or absence of features tell us about the emission processes on cometary nuclei. In an effort to investigate these problems, I have modified a computer code that generates synthetic images of dust comets by introducing random perturbations into motions of ejected particles. The perturbed rectangular cometocentric coordinates ξ', η', and ζ' of any dust grain in the coma have been written in the form

$$\begin{pmatrix} \xi' \\ \eta' \\ \zeta' \end{pmatrix} = \begin{pmatrix} \xi \\ \eta \\ \zeta \end{pmatrix} + \sum_{i=1}^{2} \alpha_i \, \rho^{i-1} c_i \, \mathcal{R}_{i\alpha} \begin{pmatrix} \cos(2\pi\mathcal{R}_{i\theta}) \, \sin(\pi\mathcal{R}_{i\phi}) \\ \sin(2\pi\mathcal{R}_{i\theta}) \, \sin(\pi\mathcal{R}_{i\phi}) \\ \cos(\pi\mathcal{R}_{i\phi}) \end{pmatrix},$$

where ξ, η, and ζ define the grain's unperturbed position, α_1 and α_2 are the parameters of random perturbations that, respectively, are independent of the grain's length of residence $\rho = (\xi^2 + \eta^2 + \zeta^2)^{1/2}$ and vary as ρ, c_i are normalizing constants, and $\mathcal{R}_{i\alpha}$, $\mathcal{R}_{i\theta}$, and $\mathcal{R}_{i\phi}$ are random numbers $[\mathcal{R}_{i\alpha} \in (0, \infty), \{\mathcal{R}_{i\theta}, \mathcal{R}_{i\phi}\} \in (0, 1)]$ that satisfy the following conditions:

$$\mathcal{R}_{i\alpha} = (\ln 2)^{-1} \ln \frac{1}{1 - \mathcal{R}}, \qquad \mathcal{R}_{i\theta} = \mathcal{R}, \qquad \mathcal{R}_{i\phi} = \arcsin(2\mathcal{R} - 1)/\pi + \tfrac{1}{2},$$

where $\mathcal{R}$ is a random number from a set arranged uniformly over the interval of (0,1). These formulas generate spherically symmetrical distributions of perturbation vectors centered on the unperturbed positions in such a manner that equal numbers of grains are located at distances smaller and greater than $\alpha_1 c_1$ or $\alpha_2 \rho c_2$. An example below illustrates expected effects of variable perturbations exerted on dust motions in the coma. The circumstances of ejection are identical for all five images, the image on the far left representing the grains' unperturbed positions. It is noted that the introduction of perturbations has made the computer generated images simulate the appearance of comets quite faithfully and that by increasing the perturbations beyond a certain limit it has been possible to "erase" the coma morphology diagnostic of the details of the ejection process. It is proposed that the degree of collimation of an ejecta flow from discrete active sources on the nucleus surface and possible emissions of dust from the rest of the nucleus directly affect the sharpness of features observed in the dust coma. Molecules of comet gases that radiate in the spectral region employed (and whose velocity distribution is much more chaotic than that of dust particles) and limited atmospheric seeing likewise contribute to blurring structural detail in ground-based imaging observations of comets. The absence of discrete features in the coma does by no means imply the absence of localized sources of activity on the nucleus.

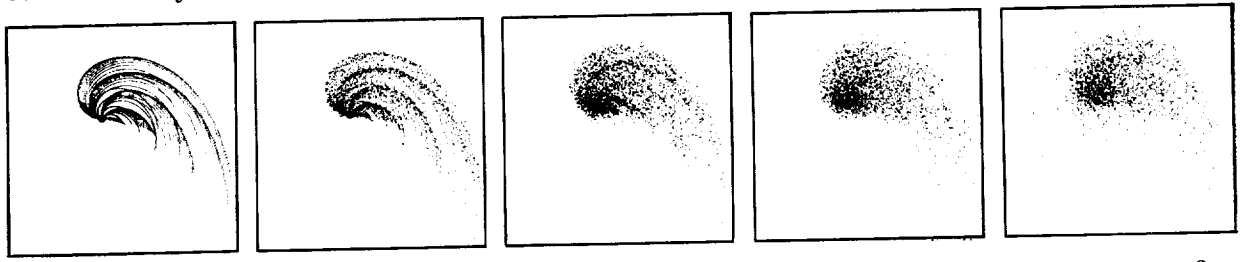

$\alpha_1 = 0$, $\alpha_2 = 0$ $\quad$ $\alpha_1 = \frac{1}{2}$, $\alpha_2 = \frac{1}{2}$ $\quad$ $\alpha_1 = 2$, $\alpha_2 = 2$ $\quad$ $\alpha_1 = 2$, $\alpha_2 = 10$ $\quad$ $\alpha_1 = 10$, $\alpha_2 = 2$

N91-26008

SUBLIMATION RATES OF CARBON MONOXIDE AND CARBON DIOXIDE FROM COMET NUCLEI AT LARGE DISTANCES FROM THE SUN.

Zdenek Sekanina, Jet Propulsion Laboratory, California Institute of Technology

One of the more attractive among the plausible scenarios for the major emission event recently observed in Comet Halley at a heliocentric distance of 14.3 AU is activation of a source of ejecta driven by an icy substance much more volatile than water. As a prerequisite for the forthcoming detailed analysis of the imaging observations of this event, a simple model is proposed that yields the sublimation rate versus time at any location on the surface of a rotating cometary nucleus for two candidate ices: carbon monoxide and carbon dioxide. The model's variable parameters are the comet's heliocentric distance r and the Sun's instantaneous zenith angle z. Following a technique developed for water ice (Sekanina 1988, *Astron. J.* **95**, pp. 911–924), the sublimation rate $Z(z,r)$ calculated from the equation of energy balance is approximated as follows

$$Z(z,r) = Z_0(r) \cdot \zeta(z,r),$$

where $Z_0(r)$ is the peak sublimation rate at r, which occurs at the subsolar point, and

$$\begin{aligned} \zeta(z,r) &= \cos z - f(r) \cdot \sin^2 z \qquad \text{for } 0 \le z \le z_c, \\ &= 0 \qquad\qquad\qquad\qquad\quad \text{for } z > z_c. \end{aligned}$$

Here $z_c = \arccos\{[1+(2f)^{-2}]^{1/2} - (2f)^{-1}\}$ is the Sun's critical zenith angle, beyond which the sublimation rate is negligible compared with that at the subsolar point. This approximation allows one to write the rotation-averaged sublimation rate $\langle Z \rangle$ at a given r as

$$\langle Z \rangle = (Z_0/\pi) \cdot (a\,\Theta_c + b \sin\Theta_c + c \sin 2\Theta_c),$$

where $\Theta_c(r)$ is a critical hour angle of the Sun that depends upon z_c and the cometocentric latitudes of the active source, $\phi_{\rm act}$, and the subsolar point, $\phi_{\rm ss}$,

$$\cos\Theta_c = \cos z_c \sec\phi_{\rm act} \sec\phi_{\rm ss} - \tan\phi_{\rm act} \tan\phi_{\rm ss},$$

and the coefficients a, b, and c are functions of $\phi_{\rm act}$, $\phi_{\rm ss}$, and $f(r)$. The calculated peak sublimation rate $Z_0(r)$ is for either ice expressed with high precision by

$$\log Z_0(r) = A + B \log(r/r_0) + C\,(r/r_0)^{\beta} + D \log\{1 + (r/r_0)^{\gamma}\},$$

where A, B, C, D, β, and γ are constants for the given ice and r_0 is a "normalizing" heliocentric distance that is related to the ice's sublimation heat L (crudely, $r_0 \propto 1/L^2$). For CO the function $f(r)$ is fitted empirically by

$$f(r) = E\,(r/r_0)^2 \left\{1 + F(r/r_0) + G\,(r/r_0)^2\right\}.$$

For CO_2 this expression yields a fit that is somewhat inferior to that offered by a law

$$f(r) = \tilde{E}\,(r/r_0)^{7/4} \exp\left\{\tilde{F}\,(r/r_0)^{\tilde{G}}\right\}.$$

With r in AU and $Z(r)$ in molecules/cm^2/s, the numerical values of the coefficients are listed in the table below for an assumed unit bolometric emissivity and an albedo of 4 percent. The coefficients A through γ provide an excellent fit up to $r \approx 500$ AU for CO and up to $r \approx 40$ AU for CO_2. The coefficients E through G offer a very good fit up to $r \approx 300$ AU for CO and the coefficients E through $\tilde{G}$ are applicable up to $r \approx 20$ AU for CO_2.

Ice	r_0 (AU)	A	B	C	D	β	γ	E	F	G	$\tilde{E}$	$\tilde{F}$	$\tilde{G}$
CO	285	14.184	−2.00	−0.74	−0.63	2.09	14.95	1.386	−1.337	1.343	...	...	...
CO_2	20.2	15.961	−1.95	−0.75	−1.74	1.50	8.55	1.882	−1.775	1.779	0.78	0.90	2.70

A COMPARATIVE EFFICIENCY OF NUMERICAL ALGORITHMS BASED ON KS-REGULARIZATION OF EQUATIONS OF MOTION OF UNUSUAL MINOR PLANETS AND COMETS; V.A.Shefer, Tomsk State University, Tomsk, USSR

This paper concentrates on application of regularizing and stabilizing KS-transformation in the problem of investigation of the motion of unusual minor planets and comets. The equations of motion of a minor body in KS-variables and the variational equations in heliocentric and planetocentric systems of coordinates are used. A short description of the peculiarities of software realizing developed algorithms is given. The original results of the investigation of efficiency of the algorithms and the application package are discussed on the example of motion of unusual minor planets Icarus and Geographos as well as comets Halley, Honda-Mrkos-Pajdusakova and Gehrels 3.

INTERPRETING ASTEROID PHOTOMETRY AND POLARIMETRY USING A MODEL OF SHADOWING AND COHERENT BACKSCATTERING

Yu. G. Shkuratov † and K. O. Muinonen ‡

† Astronomical Observatory of Kharkov State University,
Sumskaya Street 35, Kharkov 310022, U.S.S.R.
‡ Lowell Observatory,
1400 West Mars Hill Road, Flagstaff, AZ 86001, U.S.A.

Theoretical models of the opposition effect and of negative polarization (or polarization reversal) are usually based on geometric optics. However, such models do not explain some experimental findings; for example, the enhancement of both the opposition effect and negative polarization with decreasing particle size down to wavelength scales.

We have proposed a multiple–scattering interference explanation for these findings (Muinonen 1989, Shkuratov 1988 and 1989) and have outlined two different approaches. One was based on exact electromagnetic solutions for simple scattering systems that include dipole–dipole and dipole–surface coupling; surface–surface coupling was studied in the geometric optics approximation (including phase). The other approach was based on a point–scatterer approximation characterized by model photometric and polarimetric phase functions, and the shadowing effect was derived from the virtual volumes associated with the point–scatterers. Both approaches yielded qualitatively similar results, although neither was entirely satisfactory. We regard them as prototypes for a future unified model of shadowing and coherent backscattering.

Using the aforementioned calculations, two particular results for asteroids can be stated:
(a) The observed opposition effect and negative polarization require the existence of micron–scale fine structure in regolith particles. Although such small–scale structure has been widely assumed in the past, it is not predicted by previous theoretical models.
(b) Recently, a sharp and narrow opposition effect (the so–called opposition spike) has been observed for some bright asteroids. In contrast, weak or non–existent opposition effects are exhibited by some dark asteroids. Such observations are explained by the coherent multiple backscattering mechanism.

References.

Muinonen, K. (1989). Proc. 1989 URSI EM–Theory Symp. (Stockholm), 428–430.
Shkuratov, Yu. G. (1988). Kin. Phys. Neb. Tel **4**, 4, 33–39.
Shkuratov, Yu. G. (1989). Astron. Vestn. **23**, 2, 176–180.

HYDROTHERMAL PROCESSING OF COMETARY VOLATILES

Everett L. Shock and William B. McKinnon
Department of Earth and Planetary Sciences and McDonnell Center for the Space Sciences, Washington University, St. Louis, MO 63130 USA

Cometary volatiles can be processed through hydrothermal systems in several settings in the solar system. Molten cometary ices may circulate through hot rocks during the heating of larger comets, asteroids, or planetesimals caused by decay of radioactive elements or accompanying capture by still larger bodies. If so, the resulting aqueous solutions may be responsible for the aqueous alteration which is documented in carbonaceous meteorites and some interplanetary dust particles. In addition, hydrothermal processes may help explain differences between comets and other volatile-rich outer solar system objects like Triton. It is also possible that cometary volatiles were processed through hydrothermal systems subsequent to their arrival on the early Earth, which may have implications for the origin of life. The chemical consequences of this hydrothermal reprocessing of cometary volatiles can be assessed with speciation and mass transfer calculations which explicitly account for changes in temperature, pressure, and oxidation state. Temperature and pressure profiles can be predicted for various heating mechanisms, and redox conditions can be evaluated from reactions between hydrothermal fluids and various mineral assemblages. For example, subsequent to its capture by Neptune, Triton would have experienced an episode of tidal heating sufficient to melt its icy mantle and possibly its rocky core as well. This heating would have driven hydrothermal circulation at the core-rock/mantle-ocean boundary. By assuming an initial cometary composition for the icy mantle and evaluating the effects of changes in temperature and oxidation state, we find that hydrothermal processing helps to explain the presence of nitrogen and the lack of carbon monoxide in Triton's atmosphere. In addition, depending on the temperature and prevailing oxidation state, ammonia, as well as acetic acid, ethanol, urea, and ethanamine are possible components of Triton's resulting mantle material. A principal uncertainty that needs to be addressed is the range of cometary compositions, particularly with respect to overall carbon and nitrogen relative abundances, and the partitioning of carbon between relatively unreactive methane and other cometary species. Calculations of a similar nature can be used to examine the consequences of reactions between molten cometary ices and possible initial mineral assemblages of chondrite parent bodies. Temperature and compositional constraints imposed by the petrologic and isotopic evidence for aqueous alteration can then be used to test the possibility of organic compound synthesis during the aqueous alteration events.

SYSTEMATIC SURVEY FOR BRIGHT JUPITER TROJANS; C.S. Shoemaker, E.M. Shoemaker, R.F. Wolfe, U.S. Geological Survey, Flagstaff, AZ 86001, and E. Bowell, Lowell Observatory, Flagstaff, AZ 86001

A systematic survey for bright Jupiter Trojans using the Palomar 46-cm Schmidt was initiated in late 1985 [1,2]. Renewed work was begun on the L4 region in 1988, and an intensive examination of the L5 region was made in the fall of that year. The survey has been continued each subsequent year with the goal of finding all Trojans brighter than H=10.25 and of obtaining precise, multiple-opposition orbits for all known bright Trojans. Concurrently, surveys for faint Trojans are being carried out by L.M. French, S.J. Bus, and E. Bowell, using the Cerro Tololo 61-cm Schmidt, and by E. Bowell and K. Russell, using the U.K. 1.2-m Schmidt [3].

To date, 57 Trojans have been found with the 46-cm Schmidt, 30 in the L4 swarm and 27 in L5. In 12 cases, previously known Trojans with short-arc orbits were rediscovered; multiple opposition orbits were thus obtained. Five Trojans found independently at Palomar were discovered nearly simultaneously at other observatories. Eighteen of the Trojans found with the 46-cm Schmidt are now numbered; positions have been measured on multiple oppositions for all but 12 of the remaining objects.

A question of considerable interest has been the relative sizes of the L4 and L5 swarms [4]. Our new discoveries have increased the number of known L5 Tojans brighter than H=10.25 by about 60%. We conclude that discovery probably is now complete to H ≈ 9, the approximate magnitude of the brightest object that we found in 1988. At this magnitude, the cumulative numbers of objects in the L4 and L5 swarms are nearly the same. Although we have found roughly equal numbers of new L4 and L5 Trojans, the mean magnitude of our L4 Trojans is about 0.2 mag brighter than that of our L5's. This difference is the consequence of exceptionally good observing conditions in the fall of 1988. It is clear that L5 Trojans are less numerous than L4's at magnitudes fainter than H = 9.25, but the difference appears to be only about 30%, at least for Trojans brighter than H = 10.25. We suggest that, at fainter magnitudes, the magnitude-frequency distribution of the L5 population is parallel with the distribution estimated for L4 by Shoemaker et al. [1]. This suggested distribution for the L5 population is close to that estimated by van Houten et al. [5] for L4. By extrapolation, we infer that there are about 100 L5 Trojans brighter than H = 11.

The mean inclination of the Trojans found with the 46-cm Schmidt is 17.6 degrees in the L4 swarm and 16.0 degrees in L5. The value for the L5 swarm is slightly less than the mean of 17.7 degrees estimated by Shoemaker et al. [1] for the total Trojan population, probably because of lack of coverage of the L5 libration region at high southern ecliptic latitudes.

The large increase in multiple opposition orbits available for L5 Trojans has led to a successful search of the L5 swarm for dynamical pairs or groups of possible collisional origin. We calculated proper elements by analytical methods presented in [6] for 75 multiple opposition orbits of L5 Trojans. Libration amplitude (D), proper eccentricity (e_p), and proper inclination (i_p) obtained by analytical methods are similar to the proper elements obtained by Bien and Schubart by numerical integration for 21 numbered L5 Trojans [7]. Ten fairly closely matched dynamical pairs and one dynamical group of three Trojans were found. Calculated velocities of separation for the recognized pairs and within the group of three are comparable with separation velocities between members of main asteroid belt families.

References: [1] Shoemaker, E.M., Shoemaker, C.S., and Wolfe, R.F., 1989, in Binzel, R.P., Gehrels, T., and Matthews, M.S., eds., Asteroids II, Tucson, Univ. Ariz. Press, p. 487-524. [2] Shoemaker, C.S., and Shoemaker, E.M., 1988, Lunar and Planet. Sci. 19, p. 1077-1078. [3] French, L.M., Vilas, F., Hartmann, W.K., and Tholen, D.J., 1989, in Binzel, R.P., Gehrels, T., and Matthews, M.S., eds., Asteroids II, Tucson, Univ. Ariz. Press, p. 468-586. [4] Degewij, J., and van Houten, C.J., 1979, in Gehrels, T., ed., Asteroids, Tucson, Univ. Ariz. Press, p. 417-435. [5] van Houten, C.J., van Houten-Groeneveld, I., and Gehrels, T., 1970, Astron. J., v. 75, p. 659-662. [6] Levison, H.F., Shoemaker, E.M., and Wolfe, R.F., 1991, Lunar and Planet. Sci. 22, p. 803-804. [7] Bien, R., and Schubart, J., 1987, Astron. Astrophys., v. 175, p. 292-298.

GEOLOGICAL AND ASTRONOMICAL EVIDENCE FOR COMET IMPACT AND COMET SHOWERS DURING THE LAST 100 MILLION YEARS.
E. M. Shoemaker, U.S. Geological Survey, Flagstaff, AZ 86001.

The present near-Earth flux and magnitude distribution of asteroids and comets can be estimated from discovery rates in systematic surveys of the sky and from the total record of discoveries. These observations have been utilized to calculate the present rate of cratering on Earth by impact of asteroids and comets [1]. The cumulative magnitude-frequency distribution of Earth-crossing asteroids drops steeply, roughly as $\Sigma N \propto e^{2H}$, at magnitudes brighter than about H = 16 [1]. Systematic observations by Roemer, on the other hand, suggest that the distribution of nuclear magnitudes of Earth-crossing comets follows a flatter distribution, approximately of the form $\Sigma N \propto e^{0.9H}$, up to the brightest objects observed [2]. Because of this difference, Shoemaker et al. [1] estimated that asteroid impacts have dominated the production of craters <50 km in diameter over the last 100 Myr, but that comet impacts may have produced most craters >50 km in diameter. The largest known impacts, therefore, are the ones most likely to yield evidence of the collision of comets.

The impact event at the K/T boundary probably was the most energetic of the past 100 Myr. An impactor with a diameter of order 10 km has been suggested from the observed column abundance of siderophile elements at the boundary [3]. This size body would produce a crater about 150 km in diameter [4, 5]; if the object were a comet, the diameters of the projectile and the crater might have been somewhat greater. The abundance pattern of the siderophile elements at the boundary appears to be consistent with a primitive body. Three structures of known or possible impact origin may be associated with the boundary event: 1) the 35-km-diameter Manson structure in Iowa [6], 2) the ~100-km-diameter Popigai structure in Siberia [7], and 3) the ~180-km-diameter Chicxulub structure in Yucatan [8, 9]. The Popigai structure is the largest firmly identified Phanerozoic impact crater; Chicxulub, if confirmed as an impact crater, would be one of the largest known impact structures on Earth. If these structures are similar but not identical in age, they might have been formed by a comet shower. On the other hand, two impact events appear to be represented by two successive thin clay layers at the K/T boundary in western North America. Because the two clay layers are in contact, wherever they have been recognized, the two impact events must have been very closely spaced in time. The distribution and lithology of shocked grains in the upper clay layer suggest that the Manson structure is a likely source of these grains [10]. Stratigraphic relationships in the Gulf of Mexico-Caribbean region point strongly to a large crater in that region [11, 12]. Chicxulub is a likely source of the K/T boundary deposits in the surrounding region and also of the lower clay layer in western North America. Manson and Chicxulub may have been produced by fragments of a single very large comet that had been disrupted to form a compact comet stream, perhaps analogous to the present group of sun-grazing comets.

At least three separate large impact events fairly closely spaced in time were associated with a step-wise mass extinction in the late Eocene. These impacts are recorded in deep-sea sediments by two horizons of impact-glass spherules in the *Globorotalia cerroazulensis* foraminiferal zone and by a third spherule horizon in the underlying *Globigerapsis semiinvoluta* zone [13]. An Ir anomaly coincides with the lower spherule horizon of the *G. cerroazulensis* zone; an Ir anomaly recognized in the *G. semiinvoluta* zone in Italy probably is correlative with the *semiinvoluta* spherule horizon [14]. No craters related to the spherule horizons have yet been identified, although two craters of similar age are known. The time interval separating the deposition of the lowest and highest spherule horizons is about 1 to 2 Myr, consistent with the theoretical duration of a comet shower [15]. The upper two spherule horizons are separated by about 30 cm stratigraphically and probably by less than 100,000 years in time. It is unlikely that the close spacing in time of the three spherule-producing impacts and their association with extinction steps are due to chance [16]. The late Eocene extinction steps are coincident with episodes of cooling of the oceans, and the end of the Eocene is marked by abrupt cooling of the oceans [17] and by major glaciation in Antarctica. A mild comet shower evidently occurred in the late Eocene, and it appears to have triggered a shift in global climate.

The present flux of long-period comets may also correspond to a mild comet shower. If the flux of comets at the present level is extrapolated back over time, the estimated production of large craters by comet impact is about equal to the observed record on the Moon of large craters younger than 1.0 Gyr. But the lunar crater record must reflect comet showers as well as the background rate of comet impact. Hence the present comet flux is estimated to be not less than twice the background flux [1]. Furthermore, several surges in the flux of large Earth-crossing asteroids probably occurred during the last 1.0 Gyr, owing to catastrophic breakup of large bodies in the main asteroid belt [18]. If so, most large craters on the Moon younger than 1.0 Gyr are more likely to have been formed by impacts of asteroids than of comets. The present comet flux, in this case, must be several times higher than the mean flux over the last 1.0 Gyr (including the contribution from showers). Onset of the inferred present comet shower might be correlated with the beginning of strong advances of northern hemisphere continental icecaps in the Pleistocene. The great strewn field of Australasian tektites and microtektites may be a signature of one or more large comet impacts during this shower.

References: [1] Shoemaker, E.M., Shoemaker, C.S., and Wolfe, R.F., 1990, Geol. Soc. Amer. Spec. Paper 247, 155-170. [2] Shoemaker, E.M., and Wolfe, R.F., 1982, in Morrison, D., ed., The Satellites of Jupiter, Tucson, Univ. Arizona Press, 277-339. [3] Alvarez, L.W., et al., 1980, Science, 208, 1095-1108. [4] Emiliani, C., Kraus, E.B., and Shoemaker, E.M., 1981, Earth and Planet. Sci. Lett., 55, 317-334. [5] Roddy, D.J., et al., 1987, Internat. Jour. of Impact Engineering, 5, 525-541. [6] Kunk et al., 1989, Science, 244, 1565-1568. [7] Deino, A.L., Garvin, J.B., and Montanari, A., 1991, Lunar and Planet. Sci. Conf. XXII, 297-298. [8] Hildebrand, A.R., and Penfield, G.T.,1990, EOS, 71, 1425. [9] Kring, D.A., Hildebrand, A.R., and Boynton, W.V., 1991, Lunar and Planet. Sci. Conf. XXII, 755-756. [10] Izett, G.A., 1990, Geol. Soc. America Spec. Paper 249. [11] Hildebrand, A.R. and Boynton, W.V., 1990, Science, 248, 843-846. [12] Alvarez, W., et al., 1991, Lunar and Planet. Sci. Conf. XXII, 17-18. [13] Keller, et al., 1987, Meteoritics, 22, 25-60. [14] Montanari, A., 1990, EOS, 71, 1425. [15] Hut, et al., 1987, Nature, 329, 118-126. [16] Shoemaker, E.M., and Wolfe, R.F., 1986, in Smoluchowski, R., Bahcall, J.N., and Matthews, M., eds., The Galaxy and the Solar System, Tucson, Univ. Ariz. Press, 338-386. [17] Kennett, J.P., and Shackleton, N.J., 1976, Nature, 260, 513-515. [18] Shoemaker, E.M., 1984, in Holland, H.D., and Trendall, A.F., eds., Patterns of Change in Earth Evolution, Dahlem Konferenzen F.R.G., Springer-Verlag, 15-40.

ON THE DISTRIBUTION OF MINOR PLANET INCLINATIONS; V. A. Shor, Institute of Theoretical Astronomy, USSR Academy of Sciences, E. I. Yagudina, Institute of Applied Astronomy, USSR Academy of Sciences

The distributions of the asteroid orbits with inclination and the longitude of ascending node on the ecliptic plane have been studied. The position of the plane that can be considered as the mean plane of the asteroid belt has been determined. The distribution of inclinations of the asteroids with respect to this plane has been constructed and its distinctive features are discussed.

RECOVERY OF THE AVERAGED MODEL OF COMETARY GRAIN BY POLARIMETRIC DATA;
L.M.Shulman, The Main Astronomical Observatory of the Ukrainian Academy of Sciences, 252127, Kiev, USSR

The standard approach to interpretation of cometary polarimetric data is the numerical solution of a set of direct light scattering problems with the variation of parameters and subsequent comparison of the results with the observational data. One needs to take the definite shape, refraction index and the distribution of the grains on size in order to calculate the picture of the scattering of light.

The classic Mie's theory is not valid for irregular (shapeless or non-uniform) particles. In such cases the couple dipole method [1] was recently used to calculate the scattering by fluffy particles. Another approach to analyses of observational data is proposed here. It is based on the solution of the inverse problem of light scattering. No parameters of the dust particles should be presetted before the calculation. The input information for the analyses is the observed spacial distribution of the Stokes parameters [2]. Therefore, using appropriate hypothesis on symmetry and asymptotic behaviour of the Stokes parameters one can obtain the averaged size and shape of the comet dust particle as well as the distribution of refractivity inside it.

REFERENCES

1. Gustafson, B.A.S., Zerull, R.H., Corbach, E., and Schulz, K. in: Fluffy structures. II., ed. by P.M.M. Jenniskens and J.I.Hage, Leiden, 1989, P. 316.
2. Shulman, L.M., Comet Circular N. 414, Kiev, 1990, P. 7-8.

DIURNAL VARIATION OF OVERDENSE METEOR ECHO DURATION AND OZONE; Miloš Šimek, Astronomical Institute of the Czechoslovak Academy of Sciences, Ondřejov, Czechoslovakia.

Diurnal variation of median duration of overdense sporadic radar meteor echoes is examined. The meteors recorded in December, January and August by Ondřejov meteor radar for a period 1958-1990 have been used for the analysis. Maximum median echo duration located 1-3 hours after local sunrise at meteor height confirms already known sunrise effect. Minimum echo duration occuring at sunset-time seems to be an effectual point of diurnal variation of the echo duration, when ozone is no more dissociated by solar UV radiation. The effect of diurnal change of echo duration should be considered when mass-distribution of meteor showers is analysed.

Melting, Vaporization, and Energy Partitioning for Impacts on Asteroidal and Planetary Objects: Catherine L. Smither and Thomas J. Ahrens, Lindhurst Laboratory of Experimental Geophysics, Seismological Laboratory, California Institute of Technology, Pasadena CA 91125

Our study focuses on the effects of impacts of silicate projectiles on asteroidal and planetary-sized silicate targets, simulating these impacts using a 3-D Smoothed Particle Hydrodynamics (SPH) code [1,2]. Three target sizes are considered here: radii of 6400, 1700, and 100 km. For the two larger cases, the impactor velocity was varied from 10 to 20 km/sec, and the impactor was 60% of the radius of the 6400 km target, and 40% of the 1700 km target. For the smallest bodies, impactor and target were the same size. Both normal and oblique (60° offset between the centers of the target and impactor bodies) were modeled.

In the simulation of the larger bodies, the entire impactor was shocked to internal energies sufficient for complete melting. In addition, as much as 38% of the target (3.5 projectile masses) was melted in the case of a normal impact at 20 km/sec on the 6400 km radius target. Lower impact velocities produced less melt in the target; an impact at 10 km/sec on the 1700 km radius target melted only 15% or .5 projectile masses of the target material. The 10 km/sec impacts were not sufficient to vaporize more than 25% of the impactor and 1% of the target mass. Higher velocity impacts vaporized 6% of the target and 82% of the impacts in the case of a normal impact on the 6400 km body. Models of the 100 km impacts at 5 km/sec show a total of 1.4 projectile masses melted, of which 0.35 projectile masses vaporized. The effects of impact-induced rotation and the balance between accretion, co-orbiting ejecta and erosion versus impact velocity and encounter orientation will also be addressed.

Initially, the bulk of the energy in the system is in the kinetic energy of the impactor. After impact, this energy is partitioned into the kinetic and internal energies of the target and the impactor. Studies of impacts on a half-space [3] predict that little or none of the initial energy will remain in the kinetic energy of the impactor after the first stages of impact. The results of these simulations, however, show that the kinetic energy of the impactor particles can remain a significant amount of the initial energy of the system. The figure below show the energy budget for two simulations of impacts at 10 km/sec on the 1700 km radius planet. The energy is normalized to the initial energy; time is plotted as dimensionless time τ=Ut/a, where U is the impact velocity, t is the time after impact, and a is the radius of the impactor. The amount of the total energy remaining the the kinetic energy of the impactor is much greater in the case of a normal impact than for an oblique impact, since more of the impactor travels at a higher velocity away from the target. The same plot for the 20 km/sec impact shows a greater proportion of the total energy in the kinetic energies of both bodies. For the largest targets, the final internal energy as a percent of the total energy is higher than in the case of the 1700 km impacts; 38% as opposed to 29% for the targets in the 20 km/sec normal impacts and 41% vs 18% for the oblique 10 km/sec impacts.

References:

[1] Monaghan JJ and Gingold RA (1983) *J. Comput. Phys.*52 374-389.

[2] Benz W, Slattery, WL amd Cameron AGW (1986) *Icarus* 66 515-535.

[3] O'Keefe JD and Ahrens TJ (1977) *Proc. Lunar Sci Conf 8th*, 3357-3374.

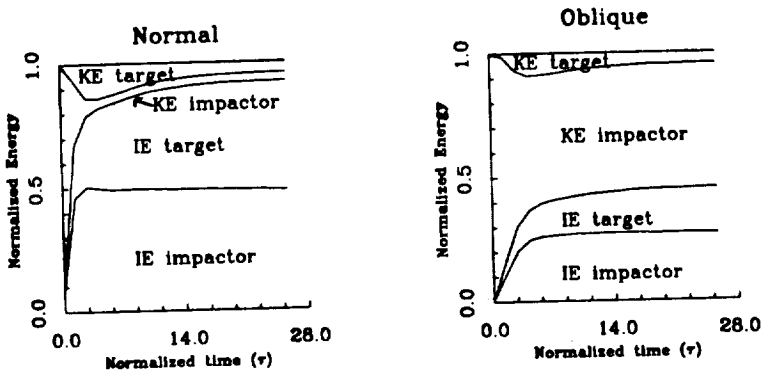

Impact budget for normal and oblique impacts on a 1700 km target at 10 km/sec.

PRELIMINARY ORBITS OF TROJAN ASTEROIDS; A.G.Sokolsky, Institute of Theoretical Astronomy of USSR Academy of Sciences

There are many attempts to construct the semi-analytical theories of Trojan asteroids which are based on the assumption of their proximity to the triangular libration points of Sun-Jupiter system within the framework of the restricted three-body problem. But as it was shown by Yu.Riabov [1] it is not possible to construct a Trojan theory with sufficient precision if the libration point itself is taken as the first approximation orbit. For this reason the idea to select preliminary orbit from other particular solutions of the three-body problem looks quite natural.

It is possible to take as such approximation the finite amplitude periodic orbit which is numerical extending (with respect to the constant of energy) small periodic motions in the vicinity of the triangular libration points of the three-body problem. The predictor-corrector method in the Hamiltonian modification [2] (about Lagrangian modification see [3]) was used for construction of the periodic orbits family. The concrete values of parameters which separate the preliminary orbit of each Trojan from three-body problem periodic solutions can be found as the result of processing of many year observations by least square method.

The preliminary orbit may be improved in future by KAM-theory taking into account the eccentricity of Jupiter orbit, Saturn gravitational action and other perturbation effects.

1. Riabov Yu.A. On the periodic solutions in the vicinity of the triangular libration points of plane restricted three-body problem.- Soviet Astron.J., 1952, v.29, N 5, pp.582-596.

2. Karimov S.R., Sokolsky A.G. A method of extending (with respect to the parameters) the natural families of periodic motions of Hamiltonian systems. - Preprint ITA Acad.Sci.USSR, 1990, N 9.

3. Karimov S.R., Sokolsky A.G. Periodic motions, generated by Lagrangian solutions of the circular restricted three-body problem. - Celestial Mechanics, 1989, v.46, N 4, pp.335-381.

ORBITAL EVOLUTION OF OUTER BELT ASTEROIDS IN SPACE CASE;

N.A.Solovaya, and I.A.Gerasimov, Celestial Mechanics Department, Sternberg State Astronomical Institute, 119 899 Moscow, U.S.S.R.

The evolution of minor planets of the outer part of the asteroidal belt for different inclinations of their orbits is investigated. It is considered in the framework of the semi-averaged elliptic restricted three body problem. The Jacobi's integral exists. Regions of the Hill's stability and unstability are defined. Numerical investigations showed that the regions of the stability are becoming smaller for increasing orbital inclinations. Some asteroids of the Hilda group can be in the unstable region, but their orbits are librators.

THE TAPANUI REGION OF NEW ZEALAND : A "TUNGUSKA" OF 800 YEARS AGO?

Duncan Steel, *Anglo-Australian Observatory, Private Bag, Coonabarabran, NSW 2357, Australia;* and
Peter Snow, *Suffolk Street, Tapanui, Otago, New Zealand.*

Near the town of Tapanui in the province of Otago in the south of New Zealand is a structure known as the Landslip Crater. Although there is some doubt that this is a scar formed by an impact upon the Earth's surface of a large solid body, there is much evidence that links this site to a major cataclysm around 800 years ago. The area apparently contains many peculiar gelogical features, and it has been claimed that the "images" of plants and avian materials on rock surfaces may have been formed by an intense high-temperature flash, like an ash glaze in pottery. There is much physical evidence for a widespread fire at about that time, possibly followed by a deluge, and this has usually been ascribed to the indigenous Maoris using fire to drive the now-extinct Moas (*Dinornis*: a giant terrestrial bird) from the forests. However, studies of tree falls and their distribution indicate a rather more coherent event. There is also the evidence of Maori myth, legend, poetry and song which speak of the falling of the skies, raging winds, upheaval of the Earth, and mysterious devastating fires from space. Many local place names may be translated in terms of a catastrophic event having occurred thereabouts, and Tapanui itself apparently means "The Big Explosion". One Maori lament states that:

> "Very calm and placid have become the raging billows,
> That caused the total destruction of the Moa,
> When the horns of the Moon fell from above down."

The purpose of this paper is to bring the site to the attention of scientists with expertise in the various areas which would be necessary for a rigorous study of the area, in order to show whether or not a Tunguska-type event did occur there around the twelfth century.

1991 DA : AN ASTEROID IN A BIZARRE ORBIT

Duncan Steel and Rob McNaught,
Anglo-Australian Observatory,
Private Bag, Coonabarabran, NSW 2357, Australia

David Asher,
Department of Physics, University of Oxford,
Keble Road, Oxford, OX1 3RH, England, U.K.

Asteroidal object 1991 DA was discovered by R.H.McNaught on a U.K. Schmidt Telescope plate taken on 1991 February 18 by P.McKenzie. Initial solutions were based on an Apollo-type motion (*IAU Circular 5193*) due to the asteroidal appearance of the object, but later observations have shown that it is on one of the most bizarre orbits known for any asteroid: at 61.9 degrees its inclination is the third highest of all known minor planets, and its eccentricity of 0.866 is also the third highest amongst asteroids. With a perihelion distance of 1.58 AU and aphelion at 22 AU, 1991 DA crosses the paths of Mars, Jupiter, Saturn and Uranus, and therefore must have a dynamical lifetime measured in units of only $\sim 10^5$ years. The two other "asteroids" which cross any of the giant planets apart from Jupiter (944 Hidalgo and 2060 Chiron) have much lower eccentricities and have long been suspected as being dormant comets; the detection of comet-like activity in Chiron beginning in 1989 (Hartmann *et al.*, *Icarus*, **83**, 1-15, 1990; Luu & Jewitt, *Astron. J.*, **100**, 913-932, 1990) has confirmed that this belief is well-founded. CCD imaging by English and Freeman (*IAU Circ. 5199*) and by West and by Ryder (*IAU Circ. 5208*) has shown no evidence of a coma despite the fact that 1991 DA is close to perihelion at this time, and spectral observations by Steel and McNaught with the Anglo-Australian Telescope have also shown no evidence of comet-like emissions: thus 1991 DA appears to be an inert asteroid. With regard to the past and future orbit of this body, it is clear that statistical-type numerical integrations like those of Hahn and Bailey for Chiron (*Nature*, **348**, 132-136, 1990) are to be recommended since these may elucidate the path by which the present orbit of 1991 DA has come about. One of us (D.A.) has performed preliminary integrations that show the perihelion distance to have changed from 1.3 AU 10 kyr ago through 1.6 AU at present to 1.8 AU 10 kyr in the future. Over this period the semi-major axis varies non-monotonically between 11.7 and 12.1 AU, the eccentricity drops from 0.89 to 0.85, and the inclination from 72 to 54 degrees. Longer-term integrations indicate that q was less than 1 AU about 20 kyr yr ago. The elements do not appear to be chaotic during ± 25 kyr integrations.

WATER MASERS, RED GIANTS, AND OORT CLOUDS AROUND OTHER STARS; S. Alan Stern (CASA/University of Colorado) and J. Michael Shull (CASA/University of Colorado).

In some 4-5$\times 10^9$ yrs the Sun will exhaust its hydrogen supply and begin its post main sequence evolution. This process is a common one for lower main sequence stars. During their luminous, post main sequence phase, solar-type stars typically attain luminosities of $6 \times 10^3 L_\odot$ for one-to-several hundred million years. The effects of such a luminosity increase on the Sun's comet reservoir will be dramatic. If comet clouds are common around solar-type stars, then prodigious cometary destruction should be a hallmark of post main sequence stellar evolution.

We suggest that destruction of orbiting comets and debris provides a natural mechanism to explain several attributes of giant star outflows. These include:

- The ubiquitous presence of H_2O and OH around post main sequence stars (Jones, et al. 1983; Bowers and Hagen 1984).
- Toroidal OH Outflow Geometries Observed in VLBI Experiments (Bowers, et al. 1989).
- The coexistence of both water-ice and water-vapor at distances of several hundred AU (Jura and Morris 1985). And
- Reports of dust (Stencel, et al. 1989) and complex organics (Geballe, et al. 1989) located at the water condensation radius of many M giants and supergiants.

The competing explanation for water emission around these stars is photochemistry in the stellar outflow (Goldreich and Scoville 1976).

We stress that our models of comet cloud destruction do not indicate that the bulk stellar mass loss itself, nor the high dust mass loss rates common to giant and supergiant stars are the result of comet cloud destruction. However, the source of water in these outflows is easily, and naturally explained by the destruction of orbiting, volatile rich bodies. If confirmed by observations, our work would imply the nearly-ubiquitous presence of comet clouds around other stars. We are untertaking such an observation program as a part of the NASA Origins of Solar Systems Program.

MEASUREMENT CONSTRAINTS ON NOBLE GASES IN A COMET: FAR-ULTRAVIOLET SPECTRA OF COMET AUSTIN (1988c1).

S.A. Stern, J.C. Green, W. Cash, and T.A. Cook (CASA/University of Colorado).

We employ a long-slit spectrum of comet Austin (1988c1) obtained during a 258 second observation by the University of Colorado imaging FUV rocket telescope/spectrometer on 28.4 April 1990 UT to derive meaningful upper limits on the abundance of Ar and He in comet Austin. This far-UV spectrum spans the wavelength range 910-1180 Å, with a resolution of 3 Å. The instrumental effective area is essentially flat across the bandpass, with a value of ~ 0.5 cm^2 in first order.

Comet Austin was a bright comet likely making its first apparition from the Oort Cloud at the time of our observation. The absence of both the 1048 and 1066 Å fluorescence emissions in comet Austin on the date of our observations allow us to place constraints on the formation temperature and subsequent thermal history of this comet. We will discuss the data set, describe how upper limits on Ar I (1048 and 1066 Å observed in first order) and He I (584 Å observed in second order) were obtained, compare these upper limits to an IUE-derived H_2O production rate in 1988c1 extrapolated to our observation date, and then discuss the implications of these results for the origin of comets in general, and comet Austin in particular.

These results constitute the first meaningful spectroscopic upper limits on noble gases in a cometary coma. They also demonstrate the important potential for FUSE satellite FUV spectroscopy of comets in the late 1990s.

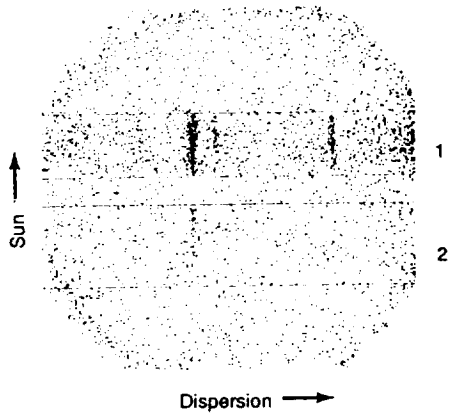

Fig. 1. A plot of all the events recorded during the observation of comet Austin. The numbers 1 and 2 indicate the locations of the primary and secondary slits, respectively. Wavelength increases toward the right. The brightest feature in the primary slit is the feature at 1026 Å. The higher level of background at the extreme right of the detector is due to scattered Lyman α.

CARTOGRAPHY OF ASTEROIDS AND COMET NUCLEI FROM LOW RESOLUTION DATA; Philip J. Stooke, Department of Geography, University of Western Ontario, London, Ontario, Canada N6A 5C2 (Stooke@vaxr.sscl.uwo.ca).

High resolution images of non-spherical objects, anticipated from Galileo, CRAF and Cassini and existing for Phobos and Deimos, lend themselves to conventional planetary cartographic procedures: control network analysis, stereophotogrammetry, image mosaicking in 2D or 3D and airbrush mapping (1). There remains the problem of a suitable map projection for bodies which are extremely elongated or irregular in shape. Where the available data are of very low resolution, as may be expected from speckle interferometry, Hubble Space Telescope images (even after its optics are modified), ground-based radar imaging, convex hull estimates, lightcurve modelling and distant spacecraft encounters, conventional methods of shape determination will be less useful or will fail altogether. This will leave limb and terminator topography as the principal sources of topographic information.

I have developed a method for shape determination based on limb and terminator topography. After initial development (2) and testing (3,4,5) it has been applied to the nucleus of Comet Halley (6) and the jovian satellite Amalthea. The Halley map will be repeated if a new concensus is reached on the rotation state. The Amalthea results, presented here, demonstrate the method itself and the range of cartographic products now available for such bodies.

Voyager images of Amalthea were decompressed from PDS CD-ROMs. Outlines were digitized from enlarged displays, and coordinates converted from display line and sample values to kilometres in the image plane. An initial triaxial ellipsoid model was registered with the digitized outlines and iteratively modified by locally increasing or decreasing radii until the model successfully duplicated all limbs and terminators in the eight images used for modelling. Topography of major craters and ridges was estimated but is very poorly constrained by the data. The model is illustrated with graticules depicting Voyager images (Figure 1), views from mutually perpendicular directions including the polar view not seen by Voyager (Figure 2), and as a Morphographic Conformal Projection (the non-spherical equivalent of the familiar Stereographic) graticule (Figure 3). These can be used as bases for shaded relief, albedo and geological maps of the body. Finally, contour maps of radii and elevations relative to a 280 by 150 by 140 km triaxial ellipsoid are given in cylindrical projections (Figure 4).

The origin of the planetocentric coordinate system is the assumed centre of mass, tested by comparing volumes on either side of three mutually perpendicular planes during modelling. The centre of mass is probably within about 5 km of the position assumed here, assuming uniform or radially symmetrical internal mass distribution. The model is found to have a volume of 2.5 $\pm$ 0.5 million cubic km. Radii are typically uncertain by about 2 pixels (10 to 20 km) near limbs and terminators (less where several intersect), but are very poorly constrained in regions where no limb or terminator traces occur in Voyager coverage. Although limbs can be located to within a pixel on most Voyager images, their geographic locations on the model are uncertain by many degrees, or even tens of degrees in some cases, resulting in lower reliability in the model.

The shape-modelling methods described here may be applied to any object for which low resolution data sets are acquired. The Morphographic map projections are suitable for all non-spherical bodies including those whose shapes are determined by more precise means. Particularly significant uses include registering data obtained from different instruments (e.g. HST images and a radar convex hull) or at different oppositions, and estimating local slopes for photometric studies. The results can be portrayed graphically as shown here, giving base maps for geological interpretation and aids to visualization of the object itself.

REFERENCES: (1) Greeley, R. and R.M. Batson, eds, 1990: **Planetary Mapping**, Cambridge University Press. (2) Stooke, P.J., 1986: **Proc. 2nd Internat. Symp. Spatial Data Handling**, pp. 523-536. (3) Stooke, P.J., 1988: Ph.D. Diss., Univ. of Victoria. (4) Stooke, P.J. and C.P. Keller, 1987: **Lunar Planet. Sci. XVIII**, pp. 956-957. (5) Stooke, P.J. and C.P. Keller, 1990: **Cartographica** 27 (2): 82-100. (6) Stooke, P.J. and A. Abergel, 1991: **Astron. Astrophys.** (in press).

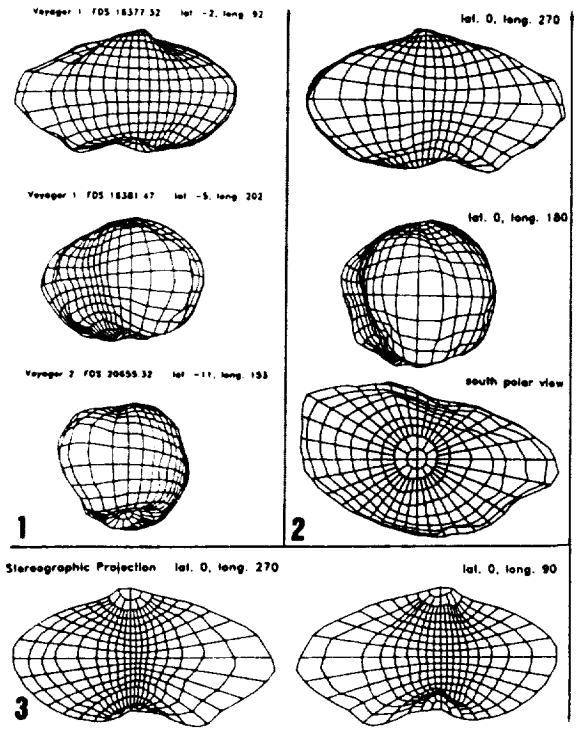

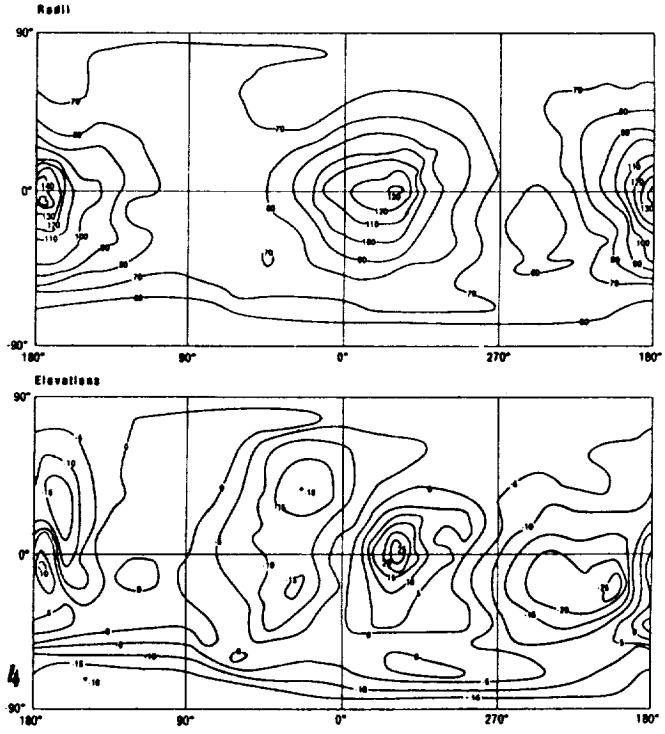

SPECTROPHOTOMETERY OF THE CONTINUUM IN 18 COMETS; A. D. Storrs, A. L. Cochran, and E. S. Barker, Univ. of Texas, McDonald Observatory

We have studied the continuum emission in spectra of 18 comets. We find that the gas-to-dust ratio increases with increasing activity (as measured by the production rate of CN). Approximately equal numbers of comets show changes in continuum brightness with distance from the optocenter equal to, or significantly slower than the canonical $(\text{distance})^{-1}$ falloff. All continuua were red compared to the solar spectrum, with an average reddening of 27 % per 1000 Å. There is some evidence for a change in the slope of the continuum with distance from the optocenter, in some comets. We will discuss trends throughout each comet's apparition as well as comparisons between comets.

C_2 JET IN RECENT COMETS

Bunji SUZUKI*1, Hiroshi KURIHARA*2, and Jun-ichi WATANABE*3
*1 Koshigaya Senior High School, 2788-1,Koshigaya,Koshigaya-shi, Saitama 343 Japan
*2 Kanagawa Industrial High School, 19,Hirakawa-chou Kanagawa-ku, Yokohama 221 Japan
*3 National Astronomical Observatory, Mitaka, Tokyo 181, Japan

We carried out CCD imaging observations of recent three comets (Comet P/Brorsen-Metcalf 1989o, Comet Austin 1989c1 and Comet Levy 1990c). Some jet structures were found out in C_2 images of Comet P/Brorsen-Metcalf and Comet Austin by applying a ring masking technique. The width of these jet structures is at least 45° or more, which is wider than C_2 jets detected in Comet P/Halley(Cosmovici et al. 1988, Clairemidi et al. 1990). The distinctive feature of the C_2 component in Comet Austin is a straight structure extending in the anti solar direction (Fig. 1). This structure reminds us two possible interpretations. One is an edge-on view of a C_2 spiral jet. The other interpretation is a "C_2 tail", which may be caused by the evaporation of the blown-off CHON grains in the invisible CHON tail(Suzuki et al. 1990).

On the other hand, we could not detect any asymmetry in the C_2 images of Comet Levy. The heliocentric distance of this comet during our observation was 1.4 AU which is larger than those of former two comets. This indicates that the production rate of the C_2 molecules in the jet structure depends on the heliocentric distance.

This paper will focus on some results of our C_2 imaging observations, and on discussions of the formation mechanism of C_2 jet structure.

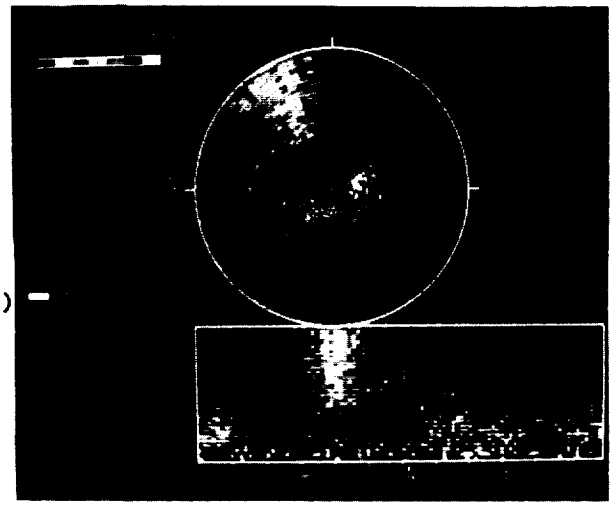

Figure 1
C_2 jets of Comet Austin

Date : 30 Apr. 1990
Time : 18:42:30
Exp. : 240 sec.
Telescope : 60-cm Reflector(f/4.7)

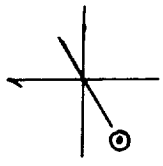

References

Clairemidi,J.,Moreels,G.,and Krasnopolsky,V.A.1990,Icarus,86,115
Cosmovici,C.B.,Schwarz,G.,Ip,W.H,and Mack,P.1988,Nature,332,705
Suzuki,B.,Kurihara,H.,and Watanabe,J.1990,Publ.Astron.Soc.Japan,42,L93

MODELS OF THE FLUX AND ORBITAL DISTRIBUTION OF METEOROIDS

N.T. Svetashkova. Tomsk State University, Tomsk, USSR

The computation method of distribution of flux density and orbital elements from observations of radiometeors rates described in [1] is used. Due to lesser selectivity it gives more exact results than observations of individual orbits of meteoroids, but uncertainty for the antapex area remains. By varying initial conditions and using the results for prognostication of meteor activity we have constructed three models of spatial distribution of meteoroids with masses greater 10^{-4}g , each of which describes observed rates of radio meteors rather precisely. It is shown that in various models heliocentric density of meteoroids for elongation angles from the apex of the Earth's motion $E>160^{\circ}$ at latitudes $|\beta|<20^{\circ}$ can change 20 times remaining practically constant for the other participant of the selestial sphere. Here the number of orbits increases approximately twice with a=1.6-2 AU, $i<20^{\circ}$,q'=2.5-3 AU. Distributions of elements of orbits agree with the results of other authors if they were also obtained from twenty-four-hour observations and cover the whole sky. According to our data the main part of meteoroids move along comet orbits (e>0.7), there is also an increase of their number with e=0.4-0.5, which is characteristic of asteroids of Apollo and Amor groups. The retrograde orbits make up from 5 to 17% in different models, which agrees with inclination orbits of comets, asteroids, bolides and particles of the zodiacal light. However, in contrast to enumerated object there is a considerably isotropic component with arbitrary inclinations $i>30^{\circ}$(~50%). The distribution of perihelion distances shows that about half of the orbits have q'>5 AU, but there is also a maximum of the order 20% in the region q'=2.5-3 AU.

[1] Svetashkova, N.T. and Sukhotin, A.A. 1990.IN Asteroids, Comets, Meteors III, Uppsala, 575.

METEORITE EVIDENCE FOR NOBLE GASES IN ANCIENT ASTEROIDAL ATMOSPHERES;
Timothy D. Swindle, Lunar and Planetary Laboratory, University of Arizona, Tucson AZ 85721

Asteroids are typically described as "atmosphereless" bodies. However, such a description is only relative. Although they clearly lack the thick, permanent atmospheres of planets like Earth, Moon and Mars, or even the dramatic temporary atmospheres of comets, there will be gas molecules in the vicinity of asteroids, and hence, like the Moon and Mercury (1), there will be atmospheric processes of some sort occurring, starting with neutral atoms in ballistic trajectories. In fact, asteroidal atmospheric processes may provide a method for determining when meteorite regolith breccias were exposed to the solar wind, a parameter that is currently largely unconstrained, although published assumptions range from 4.55 Ga ago (2) to just before ejection into an Earth-crossing orbit (3).

The primary loss mechanism for noble gases heavier than He in the lunar atmosphere is not Jeans escape, but photo-ionization by solar ultraviolet radiation followed by acceleration by the electromagnetic fields associated with the solar wind. Some of the ionization occurs at locations where the ion will be accelerated toward the lunar surface, so some atoms should be implanted (along with the impinging solar wind) into surficial grains. This effect is apparently observed for K-derived ^{40}Ar (4) and probably observed for I- and Pu-derived Xe (5), since variable amounts of the decay-produced noble gases are found intimately associated with solar wind. Since the rates at which these species are produced within the moon decrease with time as a result of decay, the ratio of implanted decay products to implanted solar wind may depend on the time of exposure (5,6).

A similar Xe effect has recently been observed in two gas-rich meteorites, although there is no evidence for any Ar effect (7). Since the two meteorites were both howardites, believed to be samples of the regolith of Vesta or a Vesta-like asteroid, it is important to consider whether a Vestal atmosphere could produce the effect believed to be responsible on the moon.

Calculations based on simplified analytical models (8) suggest that the lifetime against Jeans escape for Xe on Vesta is about an order of magnitude longer than for Ar. Furthermore, the threshhold for photoionization occurs at a longer wavelength for Xe than for Ar, and Xe photoionization cross-sections are higher (9), so a Xe effect is more likely than one for Ar. The details of how much Xe could be implanted depend sensitively on several factors, including the asteroid's size (which determines escape velocity), location (which determines temperature, and hence thermal velocity), and outgassing efficiency; the time of exposure (little decay-produced Xe should have been available more recently than 4 Ga ago); the exact photoionization cross-section rate (which depends on asteroid location, solar UV flux and solar UV spectrum); and the details of the interaction of a neutral Xe atom with the surface (in particular, how quickly it is thermalized). These factors have all been considered in more or less detail (e.g., by adjusting the input parameters in a Monte Carlo model), and the results suggest that photoionization and implantation of decay-produced noble gases might indeed be observable.

References: (1) Hunten et al. (1988) Mercury (U. Arizona), p. 562; (2) e.g., Caffee et al. (1987) Astrophys. J. 313, L31; (3) e.g., Housen et al. (1979) Icarus 39, 317; (4) Manka and Michel (1970) Science 169, 278; (5) Swindle et al. (1985) Origin of the Moon (LPI), p. 331; (6) e.g., Eugster et al. (1983) Lunar Planet. Sci. XIV, 177; (7) Swindle et al. (1990) Geochim. Cosmochim. Acta 54, 2183; (8) Spitzer (1952) Atmospheres of the Earth and Planets (U. Chicago), p. 211; (9) Samson (1982) Handbuch der Physik 31, 123.

DUST TRAILS AND THE NATURE OF COMETS; M. V. Sykes, University of Arizona, and R. G. Walker, Jamieson Science and Engineering

Cometary dust trails were first observed by the Infrared Astronomical Satellite and consist of large refractory particles ejected from short-period comets at low velocities. Comets observed to have trails by IRAS tend to lose the bulk of their mass in the large refractory trail particles, and are found to have a median refractory/volatile mass ratio of ~ 3. An examination of IRAS observation selection effects in a survey of dust trails indicates that trails are common to all short-period comets. We suggest that comets in general may be more like "frozen mudballs" than "dirty snowballs".

FORCED PRECESSION OF THE COMETARY NUCLEUS WITH RANDOMLY PLACED ACTIVE REGIONS; Slawomira Szutowicz, Space Research Centre, Bartycka 18, 00-716 Warszawa, Poland

A cometary nucleus is modelled as a rotating, triaxial and axisymmetric ellipsoid that is forced to precess due to jets of ejected material. Precession of the nucleus is followed numerically using Euler's equations. Randomly placed regions of exposed ice on the surface of the nucleus are assumed to produce gas and dust. The solution of the heat conduction equation for each active region is used to find the gas sublimation rate, the jet acceleration and the torque. The effect of distribution of active regions across the nucleus surface, of the shape of cometary nucleus and of its spin period on the total gas production curve and on the precession of the spin axis during the orbital motion of the comet is discussed.

VELOCITY DISTRIBUTION OF FRAGMENTS OF CATASTROPHIC IMPACTS AND ORIGIN OF ASTEROID FAMILIES; Yasuhiko Takagi, Toho Gakuen Junior College, 3–11 Heiwagaoka, Meito-ku, Nagoya 465, Japan; Manabu Kato, Department of Earth Sciences, Nagoya University, Chikusa-ku, Nagoya 464-01, Japan; Hitoshi Mizutani, Institute of Space and Astronautical Science, Yoshinodai 3–1–1, Sagamihara 229, Japan

Velocity distribution of fragments produced by catastrophic disruption of parent bodies significantly affect the asteroid family formation. Although the experimental approach to this problem was not sufficient due to some technical difficulties, our new series of impact experiments (1) determined three-dimensional velocities of some tens of fragments. In this paper we report some results of our new experiments on three-dimensional velocities of fragments and the implication to the origin of asteroid families.

Experiments were performed in the impact velocity range of 140 to 650 m/sec. Targets were basalt and pyrophyllite. Projectiles were aluminum. Motions of fragments were recorded by a high-speed camera with a stereographic device in 1500–3000 frames/sec. The initial position and three-dimensional velocity of each fragment were determined from the analysis of the films. Each recovered fragment was weighed and identified with the image on the film. The total mass of fragments of which velocities could be determined is 75 to 98 percent of the initial target mass.

The main results obtained by the experiments are:

[1] The velocity range of fragments except fine particles in jetting is rather narrow, at most within a factor of 3. The mass dependence of velocity suggested by Nakamura and Fujiwara (3) is not very evident.

[2] The nondimensional impact stress (2) is an appropriate scaling parameter to describe the overall fragment velocity as well as the antipodal velocity. This result shows that the energy partition to kinetic energy of basalt fragments is an order of magnitude larger than that of pyrophyllite fragments, because the normalizing velocity of basalt is four times larger than that of pyrophyllite.

These results suggest the fragment velocity is not simply controlled by the surface energy, but by the shock wave strength and target properties which may yield complicated consequence of the shock wave generation, expansion, and decay (2). The results also support the conclusion on asteroid families that family members are single fragments, rather than rubble pile remnants (4).

REFERENCES: (1) Takagi, Y., M. Kato, and H. Mizutani (1991) *Lunar Planet. Sci. XXII*, 1371–1372 (2) Mizutani, H., Y. Takagi, and S. Kawakami (1990) *Icarus*, **87**, 307–326; (3) Nakamura, A. and A. Fujiwara (1990) Velocity distribution of fragments formed in simulated collisional disruption, submitted to *Icarus*; (4) Takagi, Y. and H. Mizutani (1990) *Asteroids, Comets, Meteors III*, 191–194

The Vicinity of Jupiter: A Region to Look for Comets

G. Tancredi [1,2] **and M. Lindgren** [1]
[1] *Astronomiska Observatoriet, Box 515, S-75120 Uppsala, Sweden*
[2] *Dept. Astronomía, Fac. de Ciencias, Montevideo, Uruguay*

Low-relative velocity and long-lasting encounters can dramatically change the orbital elements of a comet; the object could be temporarily bound to Jupiter for a period of several years.

It is well stated that most of the discoveries of comets ocurred just after a close encounter with the planet and a decrease of the perihelion distance of the comet.

So, why don't we look for comets during its close encounters with Jupiter rather than wait to find it afterwards ?

To estimate the feasibility of this proposal we have made dynamical computations and observational analysis of the Jupiter family of comets. We estimated the number of comets we should expect to find by integrating all observed Jupiter family comets and recording the time spent captured by the planet. The resultant numbers can increase if we consider that the Jupiter family population is far from being complete.

A criterion to distinguish the captured comets from other moving objects in the field is discussed.

A survey of comets during its close encounters with Jupiter could have important consequences in several aspects dealing with the dynamical evolution of minor bodies of the Solar System; e.g. :

* the origin of comets and the effects of encounters with Jupiter in the transfer of comets from the outer to the inner region of the Solar System
* the captured-hypothesis for the origin of the outer satellites of the outer planets.

N91-26009

A CENSUS OF THE ASTEROID BELT; E.F. Tedesco and G.J. Veeder, Jet Propulsion Laboratory, California Institute of Technology

Observations obtained by the Infrared Astronomical Satellite (IRAS) during its ten month mission in 1983 were originally processed by the Asteroid Data Analysis System (ADAS) to search for 3453 asteroids with known orbital elements as of September 1985. A total of 1811 had one or more observations of sufficient reliability to be accepted. These results were released in October 1986. Recently we have been reprocessing IRAS data to increase both the number of recognized asteroid observations and their reliability. As input we used 7311 asteroids with known orbital elements as of December 1990. We refer to this processor as the IRAS Minor Planet Survey (IMPS). As of April 1991 approximately 3000 asteroids had been identified with one or more acceptable observations.

We will use these results to derive the total number of asteroids with diameters greater than 1 km. In addition to being an interesting piece of information in itself these size-frequency distributions produce bias-correction factors which, for example, will be used in investigations of the physical properties of asteroid dynamical families and to estimate the distribution of the taxonomic classes as a function of heliocentric distance.

The research described in this abstract was carried out at the Jet Propulsion Laboratory, California Institute of Technology, under the sponsorship of the Air Force Geophysics Laboratory through agreement with the National Aeronautics and Space Administration.

THE NH_2 COMAE OF COMETS BRORSEN-METCALF AND AUSTIN

Stephen C. Tegler and Luke Burke
Dept. of Astronomy, University of Florida

Susan Wyckoff
Physics and Astronomy Dept., Arizona State University

Uwe Fink
Lunar and Planetary Lab., University of Arizona

We have obtained images of comets Brorsen-Metcalf (7 August 1989 UT) and Austin (25 May 1990 UT) using the Steward Observatory 1.5-m telescope, the Lunar and Planetary Laboratory CCD camera, and narrowband interference filters (central wavelength = 6338 Å, fwhm = 20 Å and central wavelength = 6250 Å, fwhm = 20 Å). Images taken with the 6338 Å filter isolate the NH_2 (8-0) emission band and include a contribution from continuum emission. Images taken with the 6250 Å filter isolate continuum emission and have been used to remove the continuum contribution from the 6338 Å images. We present images of the NH_2 comae of these comets.

We describe Monte Carlo simulations of the NH_2 comae of comets Brorsen-Metcalf and Austin that assume

$$NH_3 + h\nu \rightarrow NH_2 + H$$

and

$$NH_2 + h\nu \rightarrow NH + H$$

are responsible for the creation and destruction of NH_2 molecules. The rates for these reactions are calculated from photodissociation cross sections and satellite observed solar ultraviolet fluxes. In the simulation we account for the distribution of excess energy from photodissociation of NH_3 molecules into internal and kinetic energy of NH_2 molecules. We present a comparison between the observed and simulated NH_2 surface brightness distributions and conclude that an NH_3 source is consistent with the observed NH_2 surface brightness distributions of both comets.

Pre-Encounter Observations of 951 Gaspra

D. J. Tholen, *Institute for Astronomy, University of Hawaii*
J. D. Goldader, *Institute for Astronomy, University of Hawaii*
D. P. Cruikshank, *NASA Ames Research Center*
W. K. Hartmann, *Planetary Science Institute*

We obtained photometry and colorimetry of 951 Gaspra on nine nights during the 1990 opposition. A composite lightcurve constructed using data from eight of those nights yielded a synodic rotational period of 7.04246 ± 0.00006 hours, a mean absolute V magnitude of 11.8026 ± 0.0025, and a slope parameter of 0.285 ± 0.005. Barucci *et al.* (1990, BAAS **22**, 1113) found a comparable rotational period, but their slope parameter of 0.217 is significantly less than the value we determined from our data. The apparent discrepancy can be easily resolved by realizing that their determination is based primarily on data obtained prior to opposition, whereas our determination is based primarily on data obtained after opposition. Different phase functions pre- and post-opposition are a natural consequence of a changing aspect during an opposition. If the sub-Earth latitude on Gaspra is at a less equatorial aspect after opposition than it was before opposition, then we would expect to see a shallower phase function (corresponding to a larger numerical value of the slope parameter). Adding weight to this hypothesis is our last observation of the opposition, made in May after Gaspra had passed postopposition quadrature, which is displaced toward brighter absolute magnitudes relative to the rest of our data, indicating an even more poleward sub-Earth latitude than earlier in the opposition. Because the orbits of Earth and Gaspra are nearly coplanar, a substantial change in sub-Earth latitude during the opposition would not have been possible unless the obliquity of the asteroid's rotational axis is not small.

Rotationally resolved colorimetry of Gaspra shows a very slight variation in color with rotation, perhaps as much as 5 percent, but the precision of our data makes this variation significant at only the one standard deviation level.

To supplement the 0.3 to 1.1 micron reflectance spectrum of Gaspra obtained during the course of the Eight-Color Asteroid Survey by Zellner *et al.* (1985, Icarus **61**, 355), we obtained a spectrum of Gaspra from 0.8 to 2.5 microns using the double CVF at the Infrared Telescope Facility. A shallow absorption feature at 1 micron is obvious in the data. Although the data are noisier than we had expected, the band center appears to be slightly longward of 1 micron, which suggests than olivine dominates over pyroxene. An independent estimate of the pyroxene content can be obtained by examining the 2 micron region of the spectrum. The data hint at a slight depression in signal level relative to the continuum near 1.6 microns, but the noise level also allows the possibility of no absorption feature. It is worth noting that the redder than average visible colors are more reminiscent of the A-type asteroids, whose spectra are dominated by olivine, than the V-type asteroids, whose spectra are dominated by pyroxene. Gaspra would appear to be have a fairly high olivine to pyroxene ratio.

A comparison of our composite spectrum of Gaspra with one for 8 Flora obtained by Gaffey (1984, Icarus **60**, 83) shows reasonable agreement. According to Williams (1979, Asteroids, 1040), both 8 Flora and 951 Gaspra are members of his dynamical family 189, thus such spectral agreement hints at the compositional homogeneity of the parent body, if indeed these objects are fragments of the same parent body.

DETERMINATION OF ORBITS OF COMETS: P/KEARNS-KWEE, P/GUNN, INCLUDING NONGRAVITATIONAL EFFECTS IN THE COMETS' MOTION; B. Todorovic-Juchniewicz, G. Sitarski, Space Research Centre, Bartycka 18, 00-716 Warszawa, Poland

To improve the cometary orbits, 252 positional observations made in the period 1963-1991 for comet P/Kearns-Kwee and 200 positional observations made in the period 1954-1990 for comet P/Gunn were used. The correction of orbital elements were determined in two ways: - Model I - together with Marsden's nongravitational parameters A1, A2, A3; - Model II- together with angular parameters of a rotating cometary nucleus: the lag angle, the equatorial obliquity and the cometocentric solar longitude at perihelion , and with the parameter A. It was found that for comet P/Kearns-Kwee Model I with the constant values of the nongravitational parameters became incorrect and inconsistent with the real motion of the comet. On the contrary, the solution with Model II was very good, however, taking into account the time dependence of the nongravitational parameter A=A0*exp(-B*t). In the case of comet P/Kearns-Kwee, a parameter D of a displacement of the photometric center from the center of mass of the comet was also determined along with the parameters of motion. For the comet P/Gunn, the mathematical Model I may be acceptable whereas Model II taking into consideration the change of the nongravitational parameter A with time represent very well the real motion of this comet.

MINOR SATELLITES AND THE GASPRA ENCOUNTER; T.C. Van Flandern, Meta Research

On October 29, 1991, the Galileo spacecraft will encounter the minor planet 951 Gaspra. Pictures of the object and its environment will reveal immediately whether or not the minor planet has numerous moons ("minor satellites") in stable, bound orbits.

In 1977 predictions of occultations of stars by minor planets became widely available through the efforts of D.W. Dunham. At about the same time occultations of the same stars by secondary bodies, apparently in the vicinity of the associated minor planet, also started to be reported. To date there are a few dozen reports of secondary occultation events, two of which have been confirmed by a second, independent observer. In the best case to date, the Herculina occultation event in 1978, a secondary occultation of four seconds duration reported by a visual observer in California was confirmed in a photoelectric record made at the Lowell Observatory. Additional evidence for secondary bodies in the vicinity of minor planets was found by Binzel[1], and by Tedesco[2]. For example, lightcurves of some minor planets show multiple-body phenomena, such as eclipses and transits. Also, radar ranging to minor planets which approach the Earth quite closely have shown similar phenomena. Ostro et al.[3] report that 1989 PB had at least a double-peaked radar echo which appeared to be separated at certain elongation angles, with possible additional echoes present.

Since the target asteroids were essentially randomly selected, and minor satellite evidence occurs relatively frequently, it would appear that the presence of minor satellites is commonplace for asteroids smaller than the largest four. Moreover, given how few observers were involved, and how large the volume of space within a minor planet's own sphere of influence is, yet how often one or more secondary events were seen, it would seem that such minor satellites are numerous. This would lead to the expectation that at the upcoming encounter, Gaspra will also be found to have minor satellites. The only qualifier is that Gaspra is a "peculiar S-type" asteroid. S-types are believed to have been involved in collisions, which would tend to remove most of their satellites. And a peculiar asteroid is not a good basis for establishing that any particular phenomenon is normal for most asteroids.

Nonetheless, because of the apparent generality of this phenomenon, we predict that Gaspra will exhibit minor satellites during the encounter. Even if Gaspra was involved in a collision, tidally-decayed satellites should be found on its surface.

1. R.P. Binzel and T.C. Van Flandern, Science **203**, 903 (1979).

2. T. C. Van Flandern, E. F. Tedesco, R. P. Binzel, Asteroids, T. Gehrels, Ed. (U. of Ariz. Press, Tucson, 1979) pp. 443-465.

3. S. J. Ostro et al., Science **248**, 1523 (1990).

The role of organic polymers in structure and fragmentation of the cometary dust

V. Vanysek, Department of Astronomy and Astrophysics, Charles University 150 00 Prague 5 Czechoslovakia

In situ obtained data concerning the size and composition of the dust in Comet Halley indicate that a high percentage of the dust particles are composite grains containing organic species among the may be also polymerized molecules. One of the very first proposed candidate for polymers in cometary material was formaldehyde in form of polyoxymethylene or POM (Vanysek and Wickramasinghe 1975). After the discovery of repeating mass spectral pattern at 45, 61, 75, 91 and 105 *amu* in inner coma of comet Halley, the possible presence of POM or similar compounds in comets was widely discussed (see for instance Huebner 1987, Huebner *et al.* 1989, Moore and Tanabé 1990). Also within the frame of the model of agglomerated grains for cometary dust the possible role of organic polymers as gluing material between the individual building blocks of submicron size was outlined (Boehnhardt *et al.* 1990, Vanysek 1989). In he preset study this problem is newly revieved and confronted with new laboratory results. For fragile dust aggregates, where are only few bridges between individual particles the tensile strength should be in range 10^4 to 10^5 dyn cm^{-1}. Such a relatively stable "bridges" may be formed by polymerized formaldehyde as a natural "cosmic glue". It is shown that formation of such structures is possible even in dense interstellar molecular clouds.

References

Boehnhardt H. Fechtig H. and Vanysek V. 1990: Astron. Astrophys., 231, 543

Huebner W.F. 1987: *Science* 237, 628

Huebner W.F.Boice D.C. and Korth A. 1989: *Adv. Space Res.* 9(2), 29

Moore M.H. and Tanabé T. 1990: *Astrophys. J.* 365, L39

Vanysek V. and Wickramasinghe N.C. 1975: *Ap. Space Sci.* 33. L19

Vanysek V. 1989: in *Fluffy Structures II*, eds. P.M.M. Jenniskens and J.I. Hage , Leiden, p.18.

QUALITATIVE AND NUMERICAL-ANALYTIC METHODS FOR INVESTIGATION OF THE EVOLUTION OF ASTEROID ORBITS; M. A. Vaschkov'yak.

The present paper contains the short survay of the works, executed by author at the Keldysh Institute of Applied Mathematics, the USSR Academy of Sciences in 80-th years.

The qualitative investigation of the orbit evolution in restricted circular three-body problem [1a,b] is founded on the integrability of twice-averaged scheme or Gauss problem. In these works the analysis of the orbit crossing conditions is carried out, the typical families of the integral curves are constructed for different values of the parameters, the extreme characteristics of the evaluating orbits are calculated. The generalization of the method on the concentric coplanar system of N perturbing bodies has permited to reveal the same qualitative pecularities of the orbit evolution of the asteroids not belonging to the main belt [1c].

More exact numerical-analytic method for investigation of the asteroid orbits evolution [2] was created taking into account eccentricities, inclinations and the secular perturbations of the planet orbits. By use this method, in particular, the posibility of qualitative change of the evolution of perihelion argument for the orbit of asteroid 2335 (James) was discovered [3]. It reduses to the transition from libration regime in circulation one and back over interval of $\sim 10^5$-10^6 years and gives the clear example of the motion in the vicinity of the secular resonance.

REFERENCES.

1. Vashkov'yak M. A. Cosmic Research, 1981, Vol. 19;
   a) No 1, pp. 1-10; b) No 2, pp. 99-109; c) No 4, pp. 357-365;
   (Translated from Kosmicheskie Issledovaniya).
2. Vashkov'yak M. A. Cosmic Research, 1985, Vol. 23, No 3, pp. 277-287
   (Translated from Kosmicheskie Issledovaniya).
3. Vashkov'yak M. A. Cosmic research, 1986, Vol. 24, No 3. pp. 255-267
   (Translated from Kosmicheskie Issledovaniya).

N91-26011

IRAS ASTEROID FAMILIES; G.J. Veeder, J.G. Williams, E.F. Tedesco and D.L. Matson, Jet Propulsion Laboratory, California Institute of Technology

The Infrared Astronomical Satellite (IRAS) sampled the entire asteroid population at wavelengths from 12 to 100 microns during its 1983 all sky survey. The IRAS Minor Planet Survey (IMPS) includes updated results for more recently numbered as well as other additional asteroids with reliable orbital elements. Albedos and diameters have been derived from the observed thermal emission and assumed absolute visual magnitudes and then entered into the IMPS database at the Infrared Processing and Analysis Center (IPAC) for members of the Themis, Eos, Koronis and Maria asteroid families and compared with their visual colors. The IMPS results for the small (down to about 20 km) asteroids within these major families confirm trends previously noted for their larger members. Each of these dynamical families which are defined by their similar proper elements appears to have homogeneous physical properties. For example, small members of the large Themis family are also dark. The Eos family has intermediate albedos and B-V colors between the ranges observed for main belt C and S class asteroids. In particular, the centroid of the range of albedos for the Eos family near a value of 0.1 is at a relative minimum for the albedo distribution observed for the general main belt asteroid population. The homogeneity observed within each major asteroid family implies that even if the two parent bodies of the S class asteroids in the Koronis and Maria families were differentiated they had relatively uniform interiors and did not have large distinct (metallic) cores.

The research described in this abstract was carried out at the Jet Propulsion Laboratory, California Institute of Technology, sponsored by the Air Force Geophysics Laboratory through agreement with the National Aeronautics and Space Administration.

High Resolution Images of P/Tempel 1 and P/Tempel 2 Constructed from IRAS Survey Data

Russell G. Walker (Jamieson Science & Engineering, Inc), Humberto Campins (University of Florida), and Martin F. Schlapfer (Jamieson Science and Engineering, Inc).

Infrared images of P/Tempel 1 and P/Tempel 2 have been constructed from IRAS survey data using a computer algorithm based on the Maximum Correlation Method for Image Construction (MCM) (Aumann, H.H., Fowler, J.W., and Melnyk, M., Astron. J. **99**, no.5, pp 1674-1681, 1990). Image construction was performed in a moving Sun-referenced coordinate system with the comet at the origin. Motion of the comet relative to the IRAS scans determines the number of scans within the image, and thus limits the effective spatial resolution achievable by the MCM to about 40 arcsec at 12 μm and 25 μm, 57 arcsec at 60 μm, and 80 arcsec at 100 μm. The five sets of images of Tempel 1 at 12, 25, 60 and 100 μm span the period from 4.6 days to 81 days after perihelion passage. The four sets of images of P/Tempel 2 were taken from 46 to 97 days past perihelion. Figures 1 and 2 show a typical pair of 12 μm images of Tempel 1 and Tempel 2. Solar illumination is from the left. The heliocentric and geocentric distances are 1.50 AU and 1.08 AU respectively for both comets, and the phase is 42°. Tempel 1 is 19 days past perihelion, while Tempel 2 is 56 days past perihelion. The peak radiance of Tempel 1 is 126 MJy/sr, while that of Tempel 2 is 67 MJy/sr. Contours start at 3 times the mean noise of the map and are increasing by $\sqrt{2}$. The prominent linear feature in the Tempel 2 image is the dust trail which is observed both ahead and behind the comet along its orbit. Direct comparisons of post perihelion comet dust activity are made at comparable heliocentric distances, and the relative production of large grains is determined.

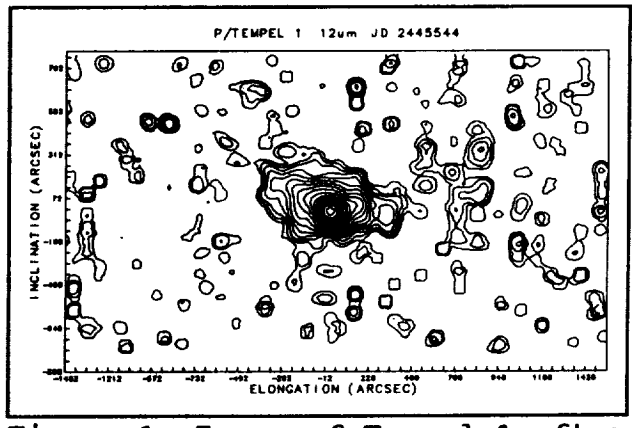

Figure 1. Image of Tempel 1 after 12 iterations of the MCM.

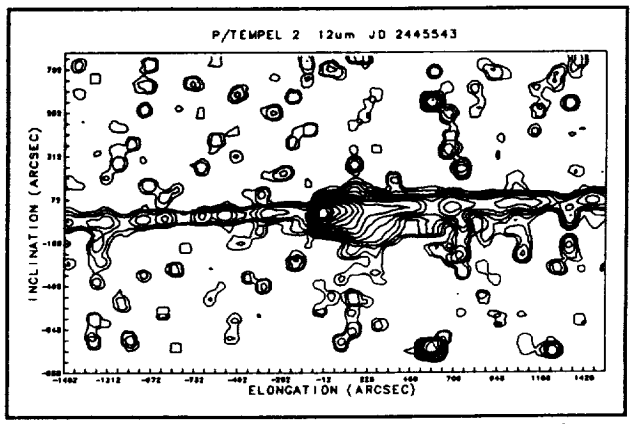

Figure 2. Image of Tempel 2 after 12 iterations of the MCM.

DISCOVERY OF COMETARY DUST FROM GRANITE Wang Erkang, Hu Zhong wei, Wan Yuqiu.
Nanjing University, 210008, Nanjing China*

A large number of dark magnetic microspherules were extracted from granite near Suzhou, Jiangsu province, China. Most of them range in diameter from 0.1-0.3mm. They can be divided into three types: Iron, Stony and Glassy. The analyzed results prove that these spherules are of extraterrestrial origin (1) (2). Further studies show the microspherules are of cometary dust.

The main chemical compositions of the spherules(for example:SiO2-45.39, TiO2-0.95, Al2O3-32.32, FeO-7.07, MnO-0.02, MgO-1.98, CaO-4.49, Na2O-0.25, K2O-0.90) are similar to those of Tunguska spherules. Some dusts are mainly composed of Fe, C, Ni, with the maximum content of C up to 9.21%. As M.E Lawler et al(1989) found that about 1% of Halley's comet dust are almost completely composed of Fe and C, auther belives these two kinds of dusts are quite similar to each other. Under HREM, special microscrystals, such as whiskers and platelets, can be observed in some samples, which reveals the characteristic of gas to particle. The INAA results demonstrate that contents of Al, Ca, Ti, V, Sc,, Hf, W are enriched, while Mg, Mn, Co, Cr, Zn seriously depleted. Besides, Content of REE is much more than that of CI chondrite. The REE distribution partten displays that it has not been differentiated obviously. In contrast to the results of K. Notsu (1978), main element and trace element of some samples are very similar to that of vaporized residual fraction of Allende meteorite.

These general characteristics mentioned above indicate that: Being riched in pre-solar system component features these dusts, and is exactly similar to cometary dust known so far. That shows the dusts are cometary origin. They took part in the evolution of the Earth and were captured by granite magma during the Mesozoic era.

References:

(1) Wang Erkang, et al., 1990,15th IMA. abstracts, 670-671.
(2) Wang Erkang, et al., 1990, 126th IAU. abstracts, 124.

* This project is supported by NNSFC.

ROTATION OF SPLIT COMETARY NUCLEI

Jun-ichi WATANABE
National Astronomical Observatory of Japan
Institute for Astronomy, University of Hawaii

The rotational motion of split cometary nuclei is studied. A large-amplitude precession in each fragment is easily excited by the splitting. Some simulation cases show the excitation of higher energy state for rotation with given angular momentum. The rotational state strongly depends on the mass-volume partition of the nuclei at the splitting, and on the original rotation.

This characteristic of the cometary nuclei survived after the splitting gives us a clue to study the internal structure of the nuclei. The damping of the precession needs long time(>10 Myr) if the internal dissipation is similar to that of asteroid(Burns and Safronov 1973). Hence, if most of the nuclei which were remnants of splitting have no large precession, then the internal structure of the cometary nuclei would be extremely fragile.

The excitation of the precession also gives us an important information on the origin of the short period comets. It is proposed that the short period comets are supplied from the larger bodies of long period comets by splitting. This idea solves the unbalance problem of number flux between the short and long period comets. There may be evidences for supporting this idea, for example, many splitting events, sun-grazing comets, and Chiron. This idea can be tested by observing rotational state of the short period comets if the internal dissipation in the nuclei is small. If they have precession with large amplitude, then these comets may be split origin.

On these view points, it is important to observe the split nuclei. We also show the result of CCD imaging observation of comet P/Taylor, which is a survived nucleus of splitting in 1916.

METEOR RADIANT MAPPING WITH MU RADAR

J. WATANABE(1), T. NAKAMURA(2), T. TSUDA(2),
M. TSUTSUMI(2), A. MIYASHITA(1), and M. YOSHIKAWA(3)
1:National Astronomical Observatory of Japan
2:Radio Atmospheric Science Center, Kyoto University
3:Communications Research Laboratory

We carried out mapping of radiant point of the meteor shower with the MU radar located at Shigaraki, Japan(34.85° N, 136.10° E). This radar is characterized by an active phased array system, and mainly used for atmospheric observations. The frequency is 46.5 MHz, which is also appropriate for meteor echo observations. As same as other radar systems, the MU radar can be interferometric use for determining the position of the meteors.

Our mapping method is similar to that originally proposed by Morton and Jones(1982). The modification is that we weighted each meteor by using the beam pattern. We present some preliminary results of the radiant point mapping of several meteor shows.

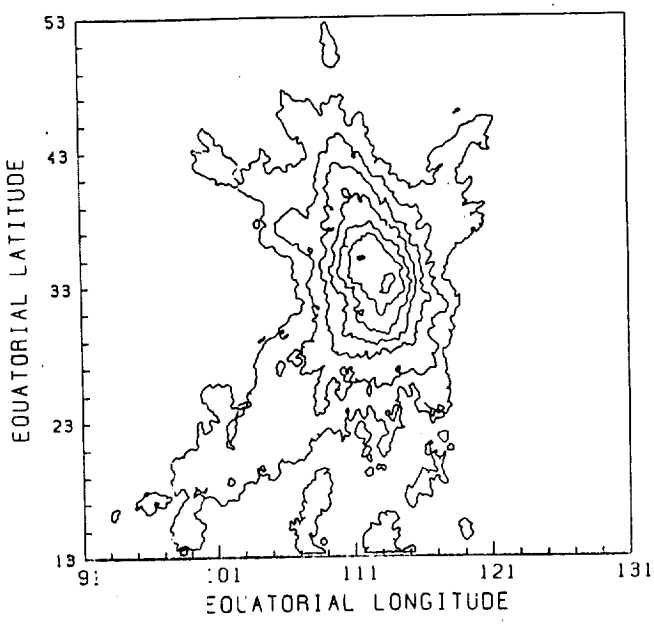

Fig. Radiant point map of the Geminids in 1989.

NEAR-IR IMAGING OBSERVATION OF COMET AUSTIN 1989C1

J. Watanabe(1), T.e. Aoki(2), N. Hiromoto(2), H. Takami(2)

1:National Astronomical Observatory of Japan

2:Communications Research Laboratory

Imaging observations of comet Austin 1989c1 were carried out with an array detector attached to the Nasmyth focus of the 1.5-m telescope. We obtained 36 images of J, H, K bands in total on April 29, 30, May 9, 26, and 27. A featureless, round shape of the comet was revealed in all images of 4.2' field of view. The asymmetry of the coma was not recognized even if we applied an image enhancement technique. The intensity distribution is well fitted by d^-2 density distribution of scattering dust in the coma, where d is the radial distance from the nucleus. The flux of the comet decreased as r^-5, where r is the heliocentric distance. This decreasing rate is steeper than that of comet P/Halley.

Photometry of comet Austin 1989c1 in K band. The open squares, circles, triangles, and crosses represents magnitude data of 4200km, 8400km, 12600km, and 16800km apertures at the comet.

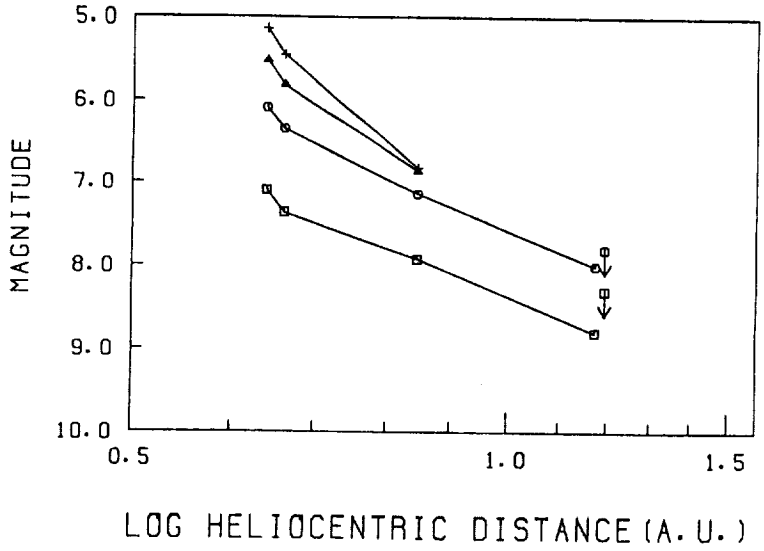

Comets, Image Deconvolution, and Second-Generation Instruments

Harold A. Weaver, Space Telescope Science Institute, 3700 San Martin Drive, Baltimore MD 20771

NO ABSTRACT AVAILABLE

Inner Coma Imaging of Comet Levy (1990c) with the Hubble Space Telescope

H. A. Weaver
Space Telescope Science Institute

M. F. A'Hearn
University of Maryland

P. D. Feldman
Johns Hopkins University

C. Arpigny
Université de Liège

W. A. Baum
University of Washington

J. C. Brandt
University of Colorado

R. M. Light
University of California, Santa Cruz

J. A. Westphal
California Institute of Technology

Observations of comet Levy (1990c) were carried out with the *Hubble Space Telescope (HST)* on UT 27 Sep 1990. At that time, both the heliocentric and geocentric distances were ~1 AU. The comet was imaged with the *Wide Field Camera (WFC)* through both red and blue filters, which were selected to isolate continuum emission peaking sharply at the nucleus. Each *WFC* pixel is 0.″1 on a side, corresponding to 78 km at the comet. The longest exposures (4 sec) through the red filter had sufficient signal to noise that image deconvolution could be used to recover virtually the full spatial resolution of *HST*. These images reveal a fan-shaped inner coma in which the sunward-facing hemisphere is significantly brighter (by a factor of ~2.5) than the tailward hemisphere, consistent with volatile sublimation occurring primarily on the dayside of the nucleus. Spatial brightness profiles perpendicular to the sun-comet line are very symmetric about the nucleus and follow a ρ^{-1} brightness distribution (where ρ is the projected distance to the nucleus) to within 100 km of the nucleus. By taking the difference between two images taken 6.5 hrs apart, we have been able to investigate quantitatively the temporal variability of the comet. These difference images show a hemispherical arc of dust propagating through the coma, which might explain the light curve variations observed during ground-based and *IUE* observations. The velocity (projected along the direction perpendicular to the line of sight) of the dust in the arc is ~0.16 km s^{-1}.

Limit on the CH_4/CO Ratio in Comet Levy (1990c) and Comparisons with other Comets

H. A. Weaver
Space Telescope Science Institute

G. Chin
NASA Goddard

T. Y. Brooke
University of Hawaii

A. T. Tokunaga
University of Hawaii

T. R. Geballe
Joint Astronomy Centre

Near-infrared observations of comet Levy (1990c) were made on UT 4.3 and 5.3 Sep 1990 from the United Kingdom Infrared Telescope on Mauna Kea. A scanning Fabry-Perot interferometer in combination with a cooled grating spectrometer was used to make a sensitive search for fluorescent emission from the ν_3 band of CH_4 near $\lambda \sim 3.3$ μm. If CH_4 is a parent molecule released directly from the nucleus, then the 3σ limit on its abundance is $CH_4/H_2O \leq 0.0031$, assuming that the kinetic temperature of the inner coma is $\sim$50 K and that the CH_4 spin species are equilibrated at a temperature $\geq$50 K. Since *IUE* observations of CO in Levy indicate that $CO/H_2O \sim 0.04$ (Feldman *et al.*), we find that $CH_4/CO \leq 0.1$. Infrared spectroscopic searches for CH_4 in Comet Halley also yielded no positive detections (Drapatz *et al.*; Kawara *et al.*); the more sensitive upper limit from the latter observations is $CH_4/H_2O \leq 0.003$. Since $CO/H_2O \sim 0.05$ in Halley (not including the extended source of CO), the upper limits on the CH_4/CO ratios are almost identical for comets Levy and Halley. A marginal infrared detection of the CH_4 ν_3 band in comet Wilson yielded $CH_4/H_2O \sim 0.01 - 0.05$ (Larson *et al.*), but there was no positive detection of CO (Roettger *et al.*; an upper limit $CO/H_2O \leq 0.07$ was derived). If the identification of the feature in the infrared spectrum of comet Wilson is correct, then that would indicate a very high CH_4/CO ratio in this comet. Recent detections of CH_4 in three interstellar sources yields $CH_4/CO = 0.01 - 0.04$, when both gaseous and solid components are included (Lacy *et al.*). Thus, the limits obtained on CH_4/CO in comets Halley and Levy are consistent with an interstellar origin for these species, while the data on comet Wilson appear to be inconsistent with the idea that this comet is composed of relatively unmodified interstellar material. Recent models of the solar nebula (*e.g.*, Fegley and Prinn; Lunine *et al.*) can account for any of the CH_4/CO ratios derived above, if the various parameters that determine the molecular abundances are adjusted appropriately. However, it appears that a single formation site for all comets is excluded by the observations.

SPECTRA OF COMET P/HALLEY AT R = 4 - 8 AU

Peter A. Wehinger, Marvin Kleine, and Susan Wyckoff, Arizona State University
Stephen Tegler, University of Florida
Michael S. J. Belton, Kitt Peak National Observatory

Spectra of Comet Halley ($\lambda\lambda$ = 3400-6500 Å) were acquired at pre- and post-perihelion distances of 4.8 AU on 1985 Feb 17 (coma V = 18.9 mag) and 1987 Feb 01 (coma V = 15.9 mag) using the 4.5-m Multiple-Mirror Telescope and the CTIO 4.0-m telescope, respectively. The CN(0,0) violet system band flux at 4.8 AU was $\sim$ 15 times greater at the post-perhelion phase compared to pre-perihelion. Additional post-perihelion spectra, obtained on 1986 Nov 28-30 with the MMT, showed CN(0,0) and very weak C_3 4040 Å emission. The MMT data are one-dimensional spectra (aperture: 5 arc sec diameter) obtained with an intensified Reticon while the CTIO data are two-dimensional spectra (slit length = 280 arc sec) obtained with a 2D-Frutti photon counting system. Extended CN(0,0) emission was detected in the 1987 Feb 1 (at 4.8 AU) spectra to a distance of at least 70 arc sec in the solar and anti-solar directions. Additional CCD spectra obtained with the KPNO 2.2-meter telescope on 1988 Feb. 20 (at 7.9 AU) show scattered solar continuum $\sim$ 32 arc sec diameter. However, no emission features were detected at 7.9 AU.

This research is supported in part by NASA Grant NAGW-547. The MMT is part of the F. L. Whipple Observatory which is operated by the Smithsonian Institution and the University of Arizona. CTIO and KPNO are operated by NOAO under contract with the NSF.

THE COMET RENDEZVOUS ASTEROID FLYBY MISSION: A STATUS REPORT; Paul Weissman and Marcia Neugebauer, Jet Propulsion Laboratory, Pasadena, CA 91109.

The Comet Rendezvous Asteroid Flyby mission received a New Start in fiscal year 1990. CRAF will match orbits with an active short-period comet and follow it around the Sun, making scientific measurements of the nucleus, coma, and tail. The Imaging system will map the nucleus surface at a resolution of 1 meter/line-pair or better, while VIMS and TIREX will produce spectral and thermal maps of the surface. Onboard instruments will collect cometary dust, ice, and gases and perform elemental and molecular analyses. A suite of fields and particles instruments will observe the solar wind interaction with the cometary atmosphere and tail. Radio tracking of the spacecraft will provide an accurate measure of the nucleus mass and higher harmonics in the comet's gravity field. En route to the comet, the spacecraft will make a close flyby of a large asteroid, preferably a primitive type from the outer main belt. Observations at the asteroid include remote sensing mapping of the surface, detection of any solar wind interaction observable at the flyby distance, and measurement of the asteroid mass to better than 10% accuracy.

Detailed design of the CRAF spacecraft is currently underway at JPL. Recent mass growth has necessitated a switch to Venus-Earth gravity assist type trajectories, similar to that used by the Galileo spacecraft. These trajectories require longer flight times from launch to rendezvous with the target comet. The details of the current baseline mission, spacecraft design, and instrument payload will be reviewed. CRAF is a joint project of the space agencies of the United States, Germany, and Italy.

Reference: Neugebauer, M., and Weissman, P. R., The CRAF Mission, *EOS* **70**, 633, 1989.

RUNAWAY PLANETESIMAL GROWTH SUGGESTS A NEW MODEL FOR THE FORMATION AND ACCELERATION OF THE ASTEROIDS. G.W. Wetherill, DTM, Carnegie Institution of Washington, Washington, D.C. 20015 U.S.A.

Quantitative models of the growth of planets from 1 to 10 km planetesimals predict a first stage of runaway growth to form $\sim 10^{26}$g planetary embryos on a time scale of 10^4–10^5 years in the terrestrial planet region (1,2). A decrease in surface density with semi-major axis (a) proportional to $1/a$ then also predicts growth of larger (3 to 6 $\times$ 10^{26}g) embryos at the distance of the present asteroid belt on a time scale of 10^5 to 10^6 years. In the absence of any other assumed effects, these embryos will coalesce to form at least one Earth-size planet in the asteroid belt, contrary to observation.

It is commonly proposed that this problem can be avoided by preemptive complete formation of Jupiter on a similar $<10^6$ year time scale, suppression of asteroidal runaways by long range Jovian perturbations and subsequent acceleration and collisional destruction of asteroid-size bodies (e.g. 3,4). As yet, no quantitative calculations have been presented that support all the required features of this hypothesis. It appears, in fact, that severe problems arise in extending this hypothesis to deplete the region between 1 and 2.3 A.U., because of both the shorter time scale and the relative weakness of Jupiter perturbations in this region. A quantitative attempt to remove the problems in this intermediate distance region has had only moderate success (5).

The present calculations support a suggestion that this difficulty can be eliminated by assuming that runaway embryos actually formed in the asteroid belt, at least out to 3.3 A.U., followed by relatively leisurely formation of Jupiter on a 5 to 10 m.y. time scale. It is found that following the formation of Jupiter, mutual perturbations between embryos random walk them into Jovian commensurability resonances, leading to large chaotic fluctuations in eccentricity. In this way material is removed from the asteroid belt by ejection into Jupiter-crossing orbits or into collisions with growing terrestrial planets, i.e. by the same mechanisms responsible for the removal of asteroids and meteorites from the present asteroid belt. Acceleration of the residual asteroidal material to its present velocity distribution is a natural byproduct of the same gravitational processes. The final configurations of terrestrial planets are at least as satisfactory as those found when the initial distribution is much more narrowly confined.

In this scheme, the present asteroids would represent the residual fragmented collision debris from both embryos and from primordial planetesimals that did not accumulate into embryos. This speculation introduces a wide range of possibilities for the formation of metamorphosed, unmetamorphosed, and igneous asteroids and meteorites.

REFERENCES

(1) Wetherill G.W., Stewart G.R. (1989) *Icarus 77*, 350–357.

(2) Ohtsuki K., Nakagawa Y., Nakazawa K. (1988) *Icarus 75*, 552–565.

(3) Lissauer J.J. (1987) *Icarus 69*, 249–265.

(4) Wetherill G.W. (1989) *In:* Asteroids II (R. Binzel, Ed.), 661–680, University of Arizona Press.

(5) Wetherill G.W. (1990) *Proc. US-USSR Workshop on Planet. Sci.*, 98–115, National Academy of Science Press.

N91-26016

A NEW ACTIVITY INDEX FOR COMETS

by Fred L. Whipple
Smithsonian Astrophysical Observatory

An activity index, AI, is derived from observational data to measure the increase of activity in magnitudes for comets when brightest near perihelion as compared to their inactive reflective brightnesses at great solar distances. Because the observational data are still instrumentally limited in the latter case and because many comets carry particulate clouds about them at great solar distances, the application of the activity index is still limited. A tentative application is made for the comets observed by Max Beyer over a period of nearly 40 years, providing a uniform magnitude system for the near-perihelion observations. At maximum solar distance observations were mostly by H.M. Jeffers, E. Roemer, and G. van Biesbroek.

In all, AI determinations are made for 32 long-period (L-P) comets and for 14 short-period (S-P). The range of values of AI is the order of 3 to 10 magnitudes with a median about 6. An expected strong correlation with perihelion distance, q, was found to vary as $\sim q^{-2.3}$. Residuals from a least-square solution, ΔAI, were used for comparing comets of different orbital classes, the standard deviation of a single value of ΔAI was only $\pm 1^m.1$ for L-P comets and $\pm 1^m.2$ for S-P comets

Among the L-P comets, 19 of Period, P$> 10^4$ yr yielded $< \Delta AI >= -0^m.27$ compared to $+0^m.39$ for 13 of $10^4 > P > 10^2$ yr. This denies any effect of aging among the L-P comets. The 14 S-P comets yielded $< \Delta AI >$ less $0^m.3 \pm 0^m.3$ than the 32 L-P comets.

The results suggest a common activity level, nature and probably origin for comets of all orbits, sizes and ages.

This study was supported by a NASA Grant.

N91-26017

PLANETOLOGICAL IMPLICATIONS OF MASS LOSS FROM THE EARLY SUN

D.P. Whitmire and J.J. Matese, Department of Physics, The University of Southwestern Louisiana, Lafayette, LA 70504; L.R. Doyle, SETI Institute, NASA-Ames, Moffett Field, CA 94035; R.T. Reynolds, Theoretical Studies Branch, NASA-Ames, Moffett Field, CA 94035

The element lithium is observed to be underabundant in the Sun by a factor of ≈ 100. To account for this depletion, Boothroyd et al. (Ap. J., in press 1991) have proposed a model in which the Sun's zero-age-main-sequence mass was $\approx 1.1\ M_\odot$. If this is the explanation for the lithium depletion, then astronomical observations of F/G dwarfs in clusters suggest that the timescale for mass loss is ≈ 0.6 Gyr. Assuming this approximate timescale, we have investigated several planetological implications of the astrophysical model.

Since solar wind drag is unimportant for planets, conservation of angular momentum would require that they migrate outward by $\approx 10\%$ during the hypothesized mass loss phase. Dynamical drag due to the enhanced solar wind would be important for any unaccreted residual planetesimals in orbits between the planets. Depending on size and location, the planetesimals could even migrate inward. We assume that the specific angular momentum of the wind is much less than that of the planetesimal. In this case a planetesimal of radius r, density ρ, and original semimajor axis a_o would migrate to a final semimajor axis given by

$$a^2 = a_o^2(M_o/M)^2 + (M/4\pi\rho r)[1 - (M_o/M)^3]$$

where $M_o(M)$ is the original (final) solar mass. As an example, consider rocky planetesimals of density = 3 g cm^{-3} and radii < 1 km lying between the original orbits of Earth and Mars. These hypothetical planetesimals would enter the Earth/Moon sphere of influence during the mass loss phase, resulting in an enhanced impact rate in the inner Solar System. A similar effect would have occurred for any remaining low density icy planetesimals at locations within ≈ 7 AU. Other assumptions about the angular momentum content of the wind will give different migration formulae. However, in general there will be differential migration between planets and planetesimals. This would result in an enhanced impact rate during the postulated mass loss phase, assuming the existence of a sufficient supply of unaccreted planetesimals. Thus, in the context of the astronomical model and the assumption of residual planetesimals, a phenomenon similar to that of the late heavy bombardment would have occurred during the Sun's mass loss phase.

Climatically, the proposed astronomical model is consistent with the Earth not having undergone a moist or runaway greenhouse, even though the solar flux is extremely sensitive to mass ($\propto M^{6.75}$). The model is also consistent with the existence of liquid water on early Mars without postulating a massive CO_2 atmosphere plus (as yet) unmodeled effects (Kasting, Icarus, submitted 1991). Finally, the model is consistent with the approximate coincidence between the loss of liquid water on early Mars and the end of the late heavy bombardment.

C-4

GAPRA AND IDA IN FAMILIES

James G. Williams
Jet Propulsion Laboratory, Calif. Institute of Technology,
Pasadena, CA 91109

The Galileo flyby candidates 951 Gaspra and 243 Ida are both in families. The figure shows part of the Flora region near 8 Flora, a 141 km S. The remaining asteroids are all small, small enough to be cratering ejecta from Flora. The Flora region is the most complex region of the belt, consisting of adjacent and overlapping families. The cluster to the lower left of 8 Flora is family 189 which results from a cratering event, the cluster to the upper right is family 183, probably another cratering event. Gaspra has been assigned to family 189, but as can be seen it is not in the dense portion of the family and, due to the complexity of the region, cannot be guaranteed to have arisen from the same event. Because the spectrum of Gaspra is similar to Flora and because Gaspra is near to Flora, Gaspra is almost certainly a piece of 8 Flora, probably ejecta from a cratering event. 243 Ida belongs to the Koronis family and is located in the dense core of that family. The Koronis family results from a total breakup. The Galileo spacecraft will have the opportunity to sample fragments from two types of impact events.

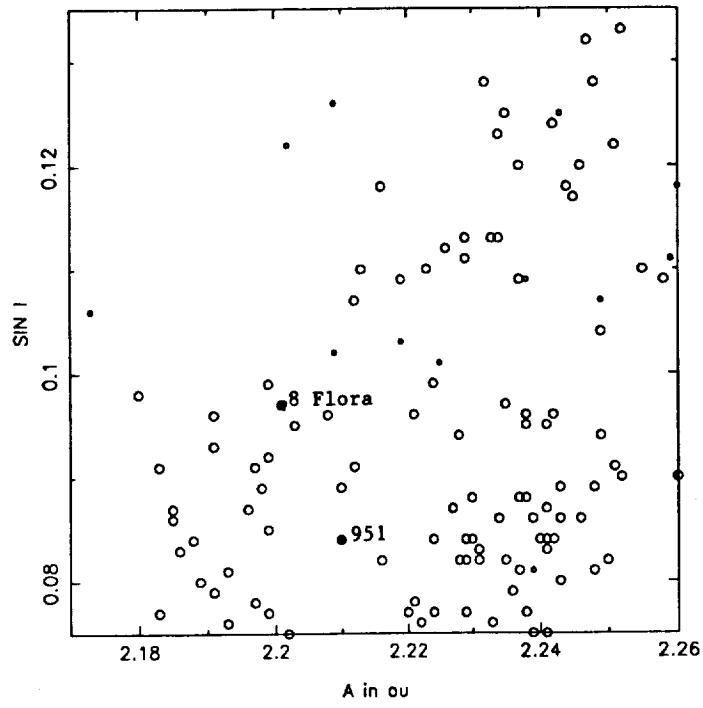

WHAT MAKES A FAMILY RELIABLE?

James G. Williams
Jet Propulsion Laboratory, Calif. Institute of Technology,
Pasadena, CA 91109

Several factors contribute to the perception of a family's reliability. Included are high population, a compact size in proper element space, high density, a low background of neighboring objects, neighboring families clearly separate, and reasonable geometry (no pretzels). If available, albedos, colors, spectra, and taxonomic classifications are important, particulary if the family's properties are in contrast to the background. The addition of newly discovered, higher numbered asteroids is an indicator of reliability. Seldom is a family lucky enough to satisfy all of the above properties. There are more families of low population than high population. Some families have larger extent than others and if they are not well populated they will be less evident. There are examples of crowded or overlapping families. Examples of multiple families from a single parent body are known. The background density of asteroids is different in different parts of the belt. The taxonomy may not be homogeneous in some families. Some considerations are more detailed. A family with a steep size distribution has more members to discover, but there appear to be genuine families with shallow size distributions which do not add many high numbered objects. The background asteroids may not be isolated, they may form low population clumps (unrecognized families) so that it is possible to mistakenly combine disparate clumps into one "family". Structure is common in the well populated families (commonly asymmetries) and it cannot be assumed that the less populated families lack structure. Among the less certain families, additional data will establish reliability or require reconsideration, but some cases (e. g., overlapping families) will always prove difficult.

The Unusual Lightcurve of 1990 TR

Wieslaw Z. Wisniewski
Space Sciences Bld.
Lunar and Planetary Laboratory
University of Arizona
Tucson, Arizona 85721

Amor asteroids 1990 TR was monitored during 3 nights shortly after discovery. Obtained lightcurves did not reveal repetable two maxima and two minima. However, some features suggest periodicity and P = 6h 25m is determined. Individual and composite lightcurves are presented.

NEW FAMILIES OF ASTEROIDS; R.F. Wolfe, U.S. Geol. Survey, Flagstaff, AZ 86001

Since early in this century, many and often conflicting divisions of asteroids into families have been advanced (Hirayama, 1928; Brouwer, 1951; Arnold, 1969; Linblad and Southworth, 1971; Williams, 1979, 1989). The present study extends the work of J. G. Williams. Williams has linked asteroids into more than 100 families, using his proper elements, for about the first 2100 numbered asteroids and for Palomar-Leiden Survey (PLS) asteroids with one-month-arc orbits (Williams and Hierath, 1987).

The goal of the present study was to determine family membership of faint asteroids discovered by S. J. Bus in 1981 during the United Kingdom-Caltech Asteroid Survey (UCAS). This survey led to the determination of relatively precise orbits for about 1200 new faint asteroids. It was expected that examination of such a population of faint asteroids for family membership would shed considerable light on relative ages of families and on the collisional breakup process.

At present, multiple-opposition orbits have been calculated for about 6500 asteroids. The availability of this large number of precise orbits makes it possible to recognize and to study details of family structure more readily than ever before. Using osculating orbital elements from B.G. Marsden of the Minor Planet Center for numbered asteroids through number 4559 and for all multiple-opposition unnumbered objects, I calculated proper elements by the method of Williams (1969). In addition, I calculated proper elements from osculating elements of the UCAS asteroids. After removing all asteroids falling within Williams' family boundaries in semi-major axis, eccentricity, and inclination, I combined the remainder with all other non-family members for which proper elements had been calculated. From this sample, using both graphics and computer analysis, I have found over 30 new candidate families. Some of these families consist solely of faint PLS and UCAS asteroids.

The formation of a family in the asteroid belt by impact is the equivalent of the formation on a planet of an impact crater. Each family is the result of a discrete impact event. Collision of a small asteroid with a larger asteroid commonly breaks up the larger object into several smaller bodies that are moderately dispersed in orbital element phase space by the impulses acquired during the impact.

The Tiflis Family was the first group of Mars crossers found in this study. (753) Tiflis itself is a shallow, Mars-crossing asteroid with a crossing depth of -.015. From impulses acquired in the collisional breakup of the parent, most of the smaller fragments have become deeper Mars crossers. Their orbital elements, as would be expected, appear to have been further dispersed by Mars encounter. Thus, there is a greater spread in proper elements, particularly inclination, than in non-planet-crossing families. The fact that we can still recognize this family indicates that it must be fairly young, because encounter with Mars should lead to still larger dispersion of orbital elements in a period of on the order of a few hundred million years.

Asteroids such as Tiflis, which just graze the orbit of Mars, are an important source of deep Mars crossers. Most of these very shallow Mars crossers are found in a relatively stable region of proper-element space remote from resonances. They have very long dynamical lifetimes, and they may have occupied shallow crossing orbits since the time of heavy bombardment. Collisions with these shallow-crossing asteroids probably are a significant source not only of deeper Mars crossers but also of Earth-crossing asteroids, because further Mars encounters can deliver asteroids to Earth-crossing orbits. In the Tiflis Family, we see evidence for the first stages of injection of collision fragments into deeper crossing orbits. Because of the importance of this Mars-crossing family, emphasis has been placed on locating others. One of the groups subsequently discovered is composed of high-inclination asteroids.

References: Arnold, J. (1969) Astron J. 74, 1235-1242; Brouwer, D. (1951) Astron. J., 56, 9-32; Hirayama, K. (1928) Jap. J. Astron. Geophys. 5, 137-162; Linblad, B.A., and Southworth, R.B. (1971) in Physical Studies of Minor Planets, T. Gehrels, ed., NASA SP-267, 337-352; Williams, J.G. (1969) Ph.D. Thesis, Univ. of Calif. Los Angeles; Williams, J.G. (1979) in T. Gehrels, Ed., Asteroids (Univ. of Ariz. Press) 1040-1063; Williams, J.G. (1989) in R. Binzel, T. Gehrels, and M. Matthews, eds., Asteroids II (Univ. of Ariz. Press) 1034-1075; Williams, J.G., and Hierath, J. (1987) Icarus 72, 276-303.

VELOCITY DISTRIBUTIONS OF H AND OH PRODUCED THROUGH SOLAR PHOTODISSOCIATION OF H_2O, C. Y. Robert Wu, F. Z. Chen, and D. L. Judge, Space Sciences Center and Department of Physics, University of Southern California, Los Angeles, CA 90089-1341

This paper presents the calculated velocity distributions of atomic hydrogen and hydroxyl radical produced through solar photodissociation of gaseous H_2O molecules. The relevant processes that produce H and OH photofragments in the ground and excited states are:

$$H_2O + h\nu \rightarrow H + OH \quad (1)$$
$$\rightarrow 2H + O \quad (2)$$
$$\rightarrow H + OH^+ + e \quad (3)$$
$$\rightarrow H^+ + OH + e \quad (4)$$

In his pioneering work, Festou[1] only treated process (1) and only considered the first absorption band of H_2O in the 1360-1860Å region and the absorption at the H Ly-α line. Recently, Crovisier[2] improved the model calculation by including the vibrational energy distributions of the ground state OH fragment.

In the present work we have extended the wavelength region of the photodissociation precesses and have also included processes (2) through (4). The calculation has been carried out using (a) the most recent available absolute partial cross sections for the production of H and OH through photodissociation of H_2O from its absorption onset throughout the EUV region[3], (b) the newly available vibrational[2] and rotational[4] energy distributions of both the excited[4] and ground[2,4] state OH photofragments, and (c) the integrated solar flux in 10Å increments from 500 to 1860Å in the "continuum" regions and the specific wavelength and flux at the bright solar lines, e.g., the H Ly-α, -β, -γ, O VI, C III, He I, etc. Since there are undetected neutral products with quantum yield as high as 0.4 in the 600-830Å region[3] that have not yet been included in the calculation, our present work represents a lower bound. The results, however, show that the hydrogen atoms produced exhibit multiple velocity groups centered at 14, 18, 30, 35, 37, 40 km/s and higher. Since most of the current cometary modeling uses a single velocity of 20 km/s associated with the photodissociation of H_2O. The present results may be useful in interpreting the "many peaks" observed in the velocity distributions of the H Ly-α[5] and Hα[6] of comet Halley.

1. M.C. Festou, Astron. Astrophys. 96, 52 (1981).
2. J. Crovisier, Astron. Astrophys. 213, 459 (1989).
3. C.Y.R. Wu and D.L. Judge, J. Chem. Phys. 89, 6275 (1988).
4. C.Y.R. Wu and D.L. Judge, Trends in Chem. Phys. (in press, 1991).
5. R.P. McCoy, R.R. Meier, G.R. Carruthers, H.U. Keller, and C.B. Opal, EOS 69, 1289 (1988).
6. R.B. Kerr, C.A. Tepley, R.P. Cageao, S.K. Atreya, T.M. Donahue, and I.M. Cherchneff, Geophys Res. Lett. 14, 53 (1987).

Formation of the Leonid Meteor Stream and Storm

Zidian Wu and I. P. Williams

Astronomy Unit, Queen Mary and Westfield College, University of London,
Mile End Road, London E1 4NS, UK

It is well known that some meteor showers display a very high level of activity at certain times, the most famous being the Leonid shower with very spectacular displays at roughly 33 year intervals. This period being also the period of the parent comet of the stream, Comet Tempel-Tuttle. An investigation of the geometry of the comet and the Earth at the time of each high activity occurrence by Yeomans (1981) suggests that most of the meteoroids are found outside the cometary orbit and lagging the comet.

In this paper we simulate the formation process of such a stream by numerically integrating the orbits of dust particles ejected from the comet and moving under the influence of gravity and radiation pressure. The intersection of these dust particles with the Earth is also considered and it is concluded that about 12% of the ejected particles may be observed and that of those observable, 60% will be outside the cometary orbit and behind the comet.

Reference

Yeomans, D.K., 1981, Comet Tempel-Tuttle and the Leonid Meteors, *ICARUS*. **47**, 492-499

NITROGEN CONSTRAINTS ON SOLAR NEBULA CHEMISTRY

Susan Wyckoff, Department of Physics and Astronomy, Arizona State University

The isotopic, elemental and molecular abundances observed in comets potentially contain vital information about the prevailing conditions in the outermost parts of the early solar nebula. Ammonia abundances have been inferred from NH_2 production rates derived for a small sample of comets (Wyckoff, Tegler, Engel 1991b). The N_2/NH_3 ratio has been estimated for comet Halley. An inventory of nitrogen compounds in comet Halley indicates a large depletion of elemental nitrogen in the cometary volatiles, and that most of the nitrogen is carried by NH_2 and CN containing compounds (Wyckoff, Tegler and Engel 1991a). The nitrogen deficiency can probably be explained by fractionation during condensation of volatiles in the outer solar nebula or by subsequent thermal diffusion as the comet nucleus orbits the sun, or both. The elemental nitrogen depletion in comet Halley can be used to correct the observed N_2/NH_3 coma abundance ratio to the gas-phase value in the comet-forming region of the solar nebula. This ratio is found to be significantly *smaller* than the initial N_2/NH_3 abundance generally assumed in models of solar nebula chemistry. On the other hand, this corrected N_2/NH_3 ratio is *comparable* to that observed in star-forming regions in dense molecular clouds (Womack, Wyckoff and Ziurys 1991). Thus contrary to general belief, $N_2 \sim NH_3$ in both the early solar nebula and the present-day star-forming regions.

References

Womack, M., Wyckoff, S., Ziurys, L. 1991, *Ap. J.*, in press.

Wyckoff, S., Tegler, S. C. , Engel, L. 1991a, *Ap. J.* **367**, 641.

Wyckoff, S., Tegler, S. C., Engel, L. 1991b, *Ap. J.* **368**, 279.

The Effect of Electron Collisions on Rotational Excitation of Cometary Water

Xingfa Xie* and Michael J. Mumma†
Laboratory for Extraterrestial Physics
Code 693
NASA Goddard Space Flight Center
Greenbelt, MD 20771

March 28, 1991

The e-H_2O collisional rate for exciting rotational transitions in cometary water is evaluated for conditions found in Comet Halley. The e-H_2O collisional rate exceeds that for excitation by neutral-neutral collisions at distances exceeding 3000 km from the cometary nucleus, in the case of the $0_{00} \rightarrow 1_{11}$ transition. The estimates are based on theoretical and experimental studies of e-H_2O collisions, on ion and electron parameters acquired in-situ by instruments on the Giotto and Vega spacecraft, and on results obtained from models of the cometary ionosphere. The contribution of electron collisions may explain the need for large water-water cross-sections in models which neglect the effect of electrons. The importance of electron collisions is enhanced for populations of water molecules in regions where their rotational lines are optically thick.

*Astronomy Department, University of Pennsylvania, Philadelphia, PA 19104.
†Chief Scientist, Planetary and Astrophysical Sciences.

The Ephemeris Development Effort for Asteroid 951 Gaspra

D.K. Yeomans (JPL/Caltech)

En route to its encounter with Jupiter, the Galileo spacecraft will fly closely past asteroid 951 Gaspra on October 29, 1991. While the pre-encounter spacecraft images of the asteroid on the star background will be used to dramatically improve the knowledge of its position in the spacecraft - asteroid target plane, the component of its position uncertainty in the spacecraft - asteroid direction will remain relatively unchanged. The spacecraft's close approach time will remain relatively large and can only be improved using ground-based astrometric measurements of the asteroid. Thus, the extent to which the onboard camera must mosaic to successfully image Gaspra will depend upon the accuracy with which its ephemeris can be improved using ground-based astrometric observations. These data now extend back to 1913.

Additional efforts are being made to improve the accuracy of recent astrometric observations including those that will be made throughout the spring and summer of 1991 and end just a few weeks prior to the spacecraft encounter itself. Arnold Klemola (Lick Observatory) and William Owen (JPL) have developed special Lick Observatory reference star catalogs for Gaspra whereby the positions of stars within one degree on either side of its apparent celestial path have been re-determined using either the new PPM catalog (northern hemisphere) or the Perth 70 catalog (southern hemisphere). Within 2' of the asteroid's path, all stars (9-16 mag.) were included in the catalogs while out to 1^{o} on either side of the paths, an approximate density of 27 stars per square degree has been achieved. These special reference star catalogs have been distributed to a group of experienced observers for reducing their astrometric data. As a result of these special star catalog efforts, and the dedication of a small group of astrometric observers, the Gaspra position uncertainty at the time of the Galileo encounter is expected to be less than 200 km.

Using Radar Data to Improve the Orbits of Asteroids and Comets

D.K. Yeomans (JPL/Caltech)

Since the time of the first radar observations of asteroid 1566 Icarus in June 1968, there have been successful radar experiments involving over 60 different mainbelt and near-Earth asteroids (Ostro 1989, *Asteroids II*; Ostro et al. 1991, AJ, submitted). Although the focus of these radar experiments has been to infer the asteroids' physical characteristics from the echoes and properties of the returned signals, corrections to the predicted Doppler and/or time delay ephemerides are also obtained. The measured differences between the transmitted and received frequencies (Doppler shifts) and the round trip time delays can provide extremely powerful data types for the orbit determination of asteroids and comets (Yeomans et al. 1987, AJ, **94**,189).

Radar observation residuals can be typically 1 Hz in Doppler and about a microsecond in round-trip delay time. At the Arecibo transmitter frequency (2380 MHz), these errors correspond to range and velocity errors of 150 m and 6.5 cm/sec. For the Goldstone frequency (8495 MHz), the corresponding velocity error is less than 2 cm/s. The power of the radar data becomes evident when one realizes that radar measurement errors are orders of magnitude smaller than the position and velocity uncertainties inherent in orbits based only upon optical data over short time intervals.

Astrometric radar data effectively measures the object's distance and velocity along the observer's line-of-sight and hence these data are complementary to optical, plane-of-sky measurements. Radar data taken during an object's close approach to the Earth are most powerful, and the orbit refinement most dramatic, if the object has only a short optical astrometric history. A case in point is the recovery of minor planet 1989 PB by M. Hartley, S.M. Hughes and R. McNaught at the Anglo-Australian Observatory on May 3, 1990. Using an ephemeris based upon the 65 available optical position measurements over the interval from 1989 August 1 - 24, the predicted and observed positions of the object on May 3, 1990 differed by 37" in right ascension and 23" in declination. Had an orbit been available that included the 6 Doppler and 6 delay measurements, in addition to the optical observations, the predicted and observed positions differences would have been reduced to 1.4" and 0.8."

For the 30 asteroids and 2 periodic comets for which radar astrometric data was given by Ostro et al. (1991, AJ, submitted), Yeomans et al. (1991, AJ, submitted) computed orbits using both the radar and the existing optical measurements. Ten of these objects were considered by Weissman et al. (1989, *Asteroids II*, 880) to be extinct comets and Yeomans (1991, AJ, in press) found that for at least one of them, 1566 Icarus, the inclusion of a cometlike, outgassing acceleration model was required to successfully fit the observations.

With the relatively recent realization that a large population of near-Earth asteroids are on Earth approaching orbits, there is a critical need to accurately monitor their future motions. For the majority of these objects that lack a long history of optical astrometric data, accurate extrapolations of their motions will require the use of radar data in future orbital solutions.

230 ATHAMANTIS: ROTATION PERIOD AMBIGUITY

Young, James W. and Harris, Alan W.

Jet Propulsion Laboratory - California Institute of Technology

Partial photometric lightcurves of the asteroid 230 Athamantis over a 28-year span of time are presented. An original estimated 8 hour rotational rate by the Chinese (Purple Mountain) has been found incorrect, but the remaining two period ambiguities of 12 hours or 24 hours has yet to be determined.

ON DYNAMICAL STRUCTURE OF THE TROJAN GROUP OF ASTEROIDS;
R.V.Zagretdinov and I.P.Williams, Queen Mary and Westfield College, London, U.K.
M.Yoshikawa, Tokyo Astronomical Observatory, Japan

Using a semi-analytical model, the motions of Trojan asteroids in the three-dimensional elliptic restricted three body problem is considered. Regions where changes of semimajor axes and critical argument (mean longitude of Jupiter minus that of asteroids) occur for various sets of proper eccentricity, proper inclination and longitude of perihelion of asteroids minus that of Jupiter are plotted.

Using an analytical theory, amplitudes and periods of libration, for 70 Trojans has been calculated. Comparison with the results of Shoemaker et.al.(Asteroids II,1989) and of Bien and Schubart (Astron. Astroph.,175,292,1987) have been made, and in most cases good agreement was found. In addition, the possible presence of second order resonance among the real Trojan asteroids had been investigated.

A COMPARISON BETWEEN FAMILIES OBTAINED FROM DIFFERENT PROPER ELEMENTS

V. Zappala'(1), A. Cellino(1) and P. Farinella(2)

(1) Osservatorio Astronomico di Torino
strada Osservatorio 20
I-10025 Pino Torinese (TO) - ITALY

(2) Dipartimento di Matematica
Universita' di Pisa
via Buonarroti 2
I-56127 Pisa - ITALY

Using the hierarchical method of family identification developed by Zappala' et al. (Astron.J.,100, 2030, 1990) we compare the results coming from the data set of proper elements computed by Williams (about 2100 numbered + about 1200 PLS II asteroids) and by Milani and Knezevic (5.7 version, about 4200 asteroids). Apart from some expected discrepancies due to the different datasets and/or low accuracy of proper elements computed in peculiar dynamical zones, a good agreement was found in several cases. It follows that these high reliability families represent a sample which can be considered independent on the methods used for their proper elements computation. Therefore, they should be considered as the best candidates for detailed physical studies.

Introduction: The Science Instruments of HST

Benjamin H. Zellner, Computer Sciences Corporation, Space Telescope Science Institute, 3700 San Martin Drive, Baltimore MD 20771

NO ABSTRACT AVAILABLE

Some Interesting Targets for Future Work

Benjamin H. Zellner, Computer Sciences Corporation, Space Telescope Science Institute, 3700 San Martin Drive, Baltimore MD 20771

NO ABSTRACT AVAILABLE

A CANDIDATE FOR THE PARENT BODY OF THE TAURID COMPLEX AND ITS SEARCH EPHEMERIS; K. Ziolkowski, Space Research Centre, Bartycka 18, 00-716 Warszawa, Poland

Untypical asteroid 5025 P-L, which has its perihelion close to the orbit of Mercury and its aphelion between the orbits of Jupiter and Saturn, seems to be a good candidate for the parent body of the Taurid complex of small interplanetary objects. Evidences that this asteroid is a major source of meteoroids as well as an analysis of the orbits of asteroidal and cometary members of the Taurid complex presented in the paper, lead to conclusion that 5025 P-L might be regarded as a remnant of a giant comet which was a progenitor of the overall complex according to the hypothesis of Clube and Napier. Unfortunately, the orbit of 5025 P-L is very poorly determined because the computations were based upon only three positional observations over an arc of only four days in October 1960. Any further research on the problem of origin and evolution of the Taurid complex needs better determined orbit of this key asteroid. Therefore its new positions are necessary. In order to enable the search of eventual trails of 5025 P-L on the plates which can be found in archives, its ephemeris for the opposition in 1960, when the asteroid passed about 0.5 AU from the Earth, is presented.

CoMA - a high resolution time-of-flight secondary ion mass spectrometer (TOF-SIMS) for in situ analysis of cometary matter

H. Zscheeg, J. Kissel, Gh. Natour

Introduction

To shed some light on the origin and history of comets and thus on the formation of the solar system, a detailed in situ analysis of the elemental, isotopic and molecular composition of solid and gaseous cometary - and therefore pristine - matter is highly desirable. The cometary matter analyzer CoMA being developed for the NASA 9 year cometary rendezvous and asteroid flyby mission (CRAF), will meet this desire by examining dust grains and gas originating from a comet, probably Tempel 2. CoMA is a contribution of the FRG.

The goals

CoMA will perform the analysis of cometary samples with an unprecedented mass resolution for a space instrument. Thus it will be able to separate the isotopes of a number of light elements (H, Li, C, Mg) and also to minimize the effects of molecular interferences. This translates to a resolution >3000 at 13 da and >13000 at 350 da. CoMA will comprise a mass range up to 3000 da.

To achieve this, the instrument consists of three basic units: the dust collector subsystem, the primary ion gun and the time-of-flight mass spectrometer.

The dust collector subsystem accommodates about 120 target devices of different structures . It will mechanically move the targets from the collect- to the store-, sputter- and analyze-positions and also add to the electric scan capability of the ion source a mechanical one.

The high brightness liquid metal primary ion gun /2/ produces 10 keV 1 ns pulses of isotopically pure ^{115}In ions and forwards them into a 20 um spot on the sample. A DC mode is used for erosion purposes.

The time-of-flight mass spectrometer is able to compensate for second order flight time variations originating in the energy spread of the secondary ions by using a two staged ion reflector /1/. Folding of the ion flight path by implementing an additional ion mirror reduces geometric dimensions.

Status of CoMA

The feasibility of the basic design was verified by a first model, using components of standard mechanical precision and a 3 ns pulse UV-laser for secondary ion production.

Measurements with a second model basically resembling the flight unit were successful. A similar model underwent first vibration tests.

The primary ion gun in its present state can deliver 2.8 ns ion pulses generated by a combination of scanning the DC-beam across an aperture and subsequently bunching the emerging pulses.

Also under way is the development of an efficient secondary ion detector, a chevron type channelplate assembly with integrated amplifier.

Time measurement electronics evolve on a digital and an analog track. The digital version is centered around a delay line and the analog one around ramp generators. Presently both versions are capable of flight time measurements of 1ns accuracy.

/1/ B. A. Mamyrin, V. I. Karataev, D. V. Shmikk, and V.A. Zagulin: "The mass-reflectron, a new nonmagnetic time-of-flight mass spectrometer with high resolution" Sov.Phys.-JETP, Vol.37, No. 1, July 1973

/2/ J. Kissel, H. Zscheeg and F. G. Ruedenauer: "Pulsed Operation of a Liquid Metal Ion Source" Appl. Phys. A 47, 167-169, (1988)

Author Index